Phenotypic and functional analysis of organ-specific endothelial cells

By Sophie Hidden

A thesis submitted to the University of Birmingham for the degree of
DOCTOR OF PHILOSOPHY

Centre for Liver Research
Division of Immunity and Infection
Medical School
University of Birmingham
April 2010

Abstract

All classes of leukocytes must be able to move from the circulation into tissue to carry out their protective functions. To achieve this transfer, the flowing cells must adhere to the endothelium and migrate through the vessel wall. Though this process follows common stages during recruitment in different organs, there is also specialisation in underlying molecular mechanisms. The main aim was to further elucidate these organ specific phenotypic differences and relate them to the functional ability of EC to recruit subsets and total leukocytes from flow. Murine models of human disease are an incredibly useful experimental tool allowing investigation of whole diseases to the effect of one gene on a disease outcome. Isolation of primary human endothelial cell populations is well-defined (hLSEC/HUVEC) however obtaining and culturing the murine counterparts is more challenging. Primary mLSEC were isolated from murine livers using α-CD146 magnetic beads and the phenotype compared to immortalised cell lines from heart (mUCEC-1), skin (s.END) and brain (b.End.5). The expression of a number of adhesion molecules and endothelial markers varied within cell type in response to pro-inflammatory insult (Endoglin, CD34, CD31). Some artefacts of immortalisation were also apparent (VCAM-1 expression in mUCEC-1 and LYVE-1 in s.END). Functional assays indicated small differences in cell types and further microarray analysis elucidated further candidates, including chemokines, which could be involved in regulating leukocyte recruitment processes in the different organs examined.

To my parents, Lesley and Jeremy and my sister Lucy.

In loving memory of Jane Hannah.

Acknowledgements

I would like to thank Dr. Trish Lalor for guidance and support throughout my PhD and for the opportunity to work in her group. I also owe a great deal to those in the Liver Labs both old and new. I would like to thank the Post-Doctoral staff, in particular Dr Chris Weston, Dr Victoria Aldridge, Dr Emma Haughton and Dr Stuart Curbishley for all their help and answering all my questions even the stupid ones! They provide immeasurable support to all the students and for that I am very grateful.

In addition I would like to thank Prof. Graeme Anderson and all of the Thymus Development Labs for their constant supply of surplus mouse livers, brains and spleens without which I could not have carried out my research.

I would like to thank Dr Bard Smedsrod for allowing me to visit his laboratory in Tromso and learn the perfusion method under the excellent guidance of his staff.

Last but not least I would also like to thank my parents for their undivided support over the last three years, both financially and emotionally and all my friends for putting up with me through the stresses and strains of a PhD.

This work was supported by the MRC and the Department of Immunity and Infection, University of Birmingham.

Table of Contents

1. GENERAL INTRODUCTION 1

1.1 Inflammation and inflammatory mediators 2
1.2 Role of Lymphocytes 5
1.2.1 T-Cell Development: CD4+/CD8+ 7
1.2.2 Role of neutrophils 7
1.2.3 Development and fate of neutrophils 8
1.3 The role of endothelium 9
1.3.1 Vascular endothelial cells and their function 9
1.4 Leukocyte Recruitment 10
1.5 Tissue specific recruitment 16
1.5.1 Skin 17
1.5.2 The Brain 18
1.5.3 The Liver 21
1.5.4 Heart 22
1.6 Modulation of EC responses by their environment 22
1.6.1 Modulation of EC responses by shear stress 23
1.7 The use of mouse models in research of human disease 24
1.8 Isolating primary murine endothelial cells 28
1.9 Isolating human endothelial cells 29
1.10 The Human Liver 31
1.11 Immortalisation of cells 35
1.12 Genomic Analysis: Gene Array Technologies 36
1.13 Endothelial cell markers 38
1.13.1 CD34 38
1.13.2 Endoglin 39
1.14 Adhesion molecules involved in leukocyte binding to endothelial cells 39
1.14.1 The Selectins 40
1.14.2 The Integrins 41
1.14.2.1 ICAM-2 41
1.14.2.2 VCAM-1 42
1.14.3 Junctional Molecules 42
1.14.3.1 CD31 42
1.14.3.2 JAM-2 44
1.14.3.3 CD99 45
1.15 Markers of mLSEC 45
1.15.1 LYVE-1 46
1.15.2 VAP-1 47
1.16 Outlines of project 49

2. METHODS 50

2.1 Isolation and maintenance of primary endothelial cells 51
2.1.1 Isolation of mLSEC via in situ perfusion of murine liver 53
2.1.2 Isolation of mLSEC using Miltenyi αLSEC microbeads. 54
2.1.3 Isolation of mLSEC in the absence of selection method. 55
2.1.4 Isolation of mLSEC with Miltenyi αCD146 MACS kit. 56
2.2 Culture and maintenance of cell lines 57
2.3 FACS Analysis using a murine anti LSEC-FITC conjugated monoclonal antibody. 58
2.4 Immunohistochemical staining of murine tissue sections 59
2.4.1 Preparation of tissue sections 59
2.4.2 Demonstration of molecule expression by Immunohistochemical staining (IHC) 60
2.4.3 Demonstration of molecule expression by Immunofluorescent staining (IF) 63
2.6 ELISA protocol for endothelial cells in 96-well plates 65
2.7 Collection of liver and/or spleen from murine samples 67
2.8 Isolation and fluorescent labelling of murine splenocytes 68

2.8.1 Leukocyte subset isolation using MoFlo 68
2.9 Isolation of murine neutrophils from bone marrow 69
2.9.1 Morphological determination of neutrophil purity in bone marrow fractions 74
2.10 Culture of murine endothelial cells for flow based adhesion assays 76
2.10.1 Microslide System 76
2.10.2 Culture of EC in IBIDI VI Chambers 79
2.10.3 Assessment of leukocyte adhesion to endothelial cells under flow using the microslide system. 82
2.10.4 Assessment of leukocyte adhesion to endothelial cells under flow using the IBIDI VI System. 85
2.11 Static Adhesion Assays 87
2.12 RNA extraction using Qiagen RNeasy columns 87
2.13 Analysis of differential gene expression in resting and stimulated endothelial cells using DNA microarrays. 88
2.13.1 Labelling 88
2.13.2 Hybridisation and Scanning 89
2.13.3 Bioinformatics Analysis 89
2.13.4 Quantitative Real-Time PCR 90

3. ISOLATION AND CULTURE OF PRIMARY MURINE MICROVASCULAR ENDOTHELIAL CELLS. 91

3.1 INTRODUCTION 92

3.1.1 Liver sinusoidal endothelial cells (LSEC) 93
3.1.2 Culturing liver sinusoidal endothelial cells. 94
3.1.3 Brain microvascular endothelial cells 96
3.1.4 Current methodologies to isolate primary endothelial cells 97

3.2 RESULTS 101

3.2.1 Isolation of mLSEC via in situ perfusion of murine liver 101
3.2.1.1 Isolation of mLSEC using immunomagnetic bead selection with Miltenyi αLSEC microbeads. 106
3.2.1.2 Use of cytometry in conjunction with LSEC-FITC to optimise isolation procedure 110
3.2.1.3 Isolation of mLSEC using Easy Sep MACS beads 114
3.2.1.5 Optimal protocol for LSEC isolation 120

3.3 DISCUSSION 124

3.3.1 Use of perfusion to isolate rodent sinusoidal endothelium 125
3.3.1.1 Use of magnetic selection to isolate rodent sinusoidal endothelium 126
3.3.2 Isolation of Brain microvascular EC 130
3.3.3 Primary cells vs. Immortalised Cell Lines. 132

4. PHENOTYPIC CHARACTERISATION OF ORGAN SPECIFIC ENDOTHELIAL CELLS. 135

4.1 INTRODUCTION 136

4.1.1 Structure and Function of EC 138
4.1.2 Markers of endothelial cells 138
4.1.3 Endothelium in disease 139
4.1.4 Use of cell lines to study in vitro endothelial cell systems 140
4.1.5 Recruitment in Kidney and Lung Tissue 141

4.2 RESULTS 142

4.2 1 Optimisation of methodology for comparison of endothelial cell marker expression.....142
4.2.2 Expression of classical endothelial cell markers is maintained in culture.....151
4.2.3 Induction of adhesion molecules in response to cytokine treatment. 163
4.2.4 Expression of VAP-1 and LYVE-1 is minimally altered by cytokine treatment....172

4.3 DISCUSSION 178

4.3.1 Contribution of immortalised cell lines to research.....178
4.3.2 Expression of endothelial markers and adhesion molecules by IHC and response of EC to pro-inflammatory insult.....179

5. FUNCTIONAL ANALYSIS OF LEUKOCYTE RECRUITMENT TO ORGAN SPECIFIC ENDOTHELIAL CELLS IN RESPONSE TO CYTOKINE STIMULATION. 187

5.1 INTRODUCTION 188

5.1.1 Leukocyte Recruitment via endothelial cells.....188
5.1.1.1 STEP ONE: Capture on the endothelium. 189
5.1.1.2 STEP TWO: Leukocyte Activation or 'triggering' 190
5.1.1.3 STEP THREE: Firm adhesion 192
5.1.1.4 STEP FOUR: Transmigration.....193
5.1.2 Modulation of EC responses by their environment 195
5.1.2.1 Modulation of EC responses by shear stress.....196

5.2 RESULTS.....198

5.2.1 Optimisation of the flow assay using murine neutrophils 198
5.2.2 Optimisation of the lymphocyte flow assay using murine endothelial monolayers 204
5.2.3 Comparison of the ability of endothelium from different organs to support leukocyte adhesion under different conditions.....210
5.2.3.1 A: The effects of cytokine treatment on lymphocyte adhesion to murine endothelium under flow. 210
5.2.3.2 B: The ability of murine endothelial cell lines to recruit leukocyte subsets from flow 214
5.2.3.3 C: The effects of cytokine treatment on lymphocyte adhesion to primary murine hepatic endothelium under flow 218
5.2.3.4 D: The ability of primary murine hepatic endothelium to recruit leukocyte subsets from flow and under static conditions.....221
5.2.4 Modulation of the ability of endothelium to recruit leukocytes by shear conditioning.....225

5. DISCUSSION 229

5.1 Optimisation of leukocyte isolation.....230
5.2 Neutrophil adherence to purified E-Selectin.....231
5.3 Effect of TNF-α on neutrophil recruitment.....232
5.4 Characterisation of murine lymphocyte adhesion to immortalised cell lines under flow. 233
5.5 Characterisation of murine lymphocyte adhesion to primary EC under flow. 237
5.6 Isolation and recruitment of lymphocyte subsets.....238
5.7 Static adhesion 240
5.8 Continuous Flow 241

6. DNA MICROARRAY ANALYSIS OF ENDOTHELIAL POPULATIONS. 246

6.1 INTRODUCTION 247

6.1.2 How do arrays work? 248

6.1.3 Microarray analysis procedure 249
6.1.4 Data Acquisition 250
6.1.5 Applications of DNA microarrays in research. 251

6.2 RESULTS 252

6.2.1 Analysis of expression of key genes of interest using microarrays. 259
6.2.2 Ingenuity Analysis: Pathways 271
6.2.3 Validation of gene expression using qPCR 276

6.3 DISCUSSION 280

6.3.1 Gene Expression Patterns in mUCEC-1 Cells 280
6.3.2 Gene Expression Patterns in s.END Cells 281
6.3.3 Further investigations of EC phenotype with microarray technologies 283

7. DISCUSSION 286

7.1 Isolation of primary murine endothelial cells. 287
7.1.1 Characterisation of mLSEC. 290
7.1.2 Functional analysis of mLSEC behaviour in vitro 292
7.2 Use of immortalised endothelial cell lines 293
7.2.1 Characterisation of mUCEC-1 cells. 296
7.2.2 Characterisation of s.END cells. 299
7.2.3 Characterisation of b.End.5 cells. 302
7.3 Variation in endothelial gene expression 304
7.4 Summary and Future Work 307

8. APPENDICES 311

8.1 Solutions for in situ perfusion of murine liver 311
8.2 Gene lists for DNA Microarray Analysis 312

TABLE OF FIGURES

Figure 1. 1: The role of T and B Cells in specific immunity (Parkin et al. 2001)..... 6
Figure 1. 2: Diagram of the leukocyte recruitment paradigm (Ley et al. 2007). 15
Figure 1. 3: Schematic of hepatic microvascular subunits and the portal triads. 33
Figure 2. 1: Schematic of general endothelial cell isolation protocols including details of isolation methods used in this thesis. 52
Table 2. 1: Table of samples extracted, monoclonal antibodies with which they were labelled and total volumes from which they were extracted. 59
Table 2. 2: Source and working concentration of monoclonal antibodies (MAbs) used in immunohistochemical staining of experimental samples. 61
Table 2. 3: Cytokine treatments for ELISA. 65
Table 2. 4: Antibodies used for MoFlo sorting of T-Cell subsets CD4+ and CD8+ 69
Figure 2. 2: Coulter Counter spectra of typical bone marrow isolates before and after red blood cell lysis step. 72
Figure 2. 3: Coulter Counter spectra of typical bone marrow cell samples collected from the Percoll gradient at various interfaces. 73
Figure 2. 4: Light microscope image (LM) of a typical cytospin sample from the middle fraction of the differential Percoll gradient used in the isolation of bone marrow derived neutrophils. 75
Figure 2.5 Diagram of special culture dish for microslides constructed by the Glassware Workshop, School of Engineering, University of Birmingham, UK and culture system set-up for 'static' experiments. 78
Figure 2. 5: IBIDI VI flow chambers. 81
Figure 2. 6: Outline of apparatus used to carry out functional experiments using murine leukocytes. . 84
Figure 2. 7: Comparative images of endothelial cell lines and primary cultures in normal tissue culture compared to two methods used for functional flow assays; microslides and IBIDI VI chambers..... 86
Table 3. 1: Summary of sample of methods for isolating primary endothelial cell populations. Evidence for the variety of methods available for isolation from various organs and markers used to identify endothelial cell populations. 99
Figure 3. 1: Detail of perfusion method for isolating mLSEC. 102
Figure 3. 2: Immunohistochemical staining of mLSEC. 103
Figure 3. 3: Representative images of results of initial perfusion experiments. 105
Figure 3. 4: Schematic isolation of mLSEC using Miltenyi LSEC microbeads. 107
Figure 3. 5: Light micrograph of cellular matter obtained from LSEC immunomagnetic bead selection. 108
Figure 3. 6: Image of cryosectioned murine liver stained by immunofluoresence methods..... 109
Figure 3. 7: Schematic diagram summarising the location of LSEC throughout the isolation procedure. 111
Figure 3. 8: Flowcytograms depicting cells contained within post collagenase digest sample. 112
Figure 3. 9: Flowcytograms depicting cells contained within post collagenase digest sample stained with (A) Rat IgG and (B) α mouse LSEC-FITC at 1/30 dilution of manufacturers stock. 113
Table 3. 2: Representative Data of FACS experiment determining at which stage of isolation endothelial cells were being lost. 114
Figure 3. 10: Schematic showing the principle behind the Easy-Sep method. 115
Figure 3. 11: Diagram of mLSEC isolation using MACS αCD146 kit. 117
Figure 3. 12: Light micrograph images of LSEC cell populations resulting liver endothelial cell isolation protocol. 118
Figure 3. 13: Light micrograph and confocal images of primary mLSEC. 119
Table 3. 3: Typical results of the various mLSEC isolation methods used. 120
Figure 3. 14: Schematic of mBMEC isolation method. 122
Figure 3. 15:Light micrograph images of varying cell populations resulting from brain microvascular endothelial cell isolation protocol. 123
Figure 4. 1: Control stained murine tissues. 144
Figure 4. 2: Images of immortalised EC lines and mLSEC. 146
Figure 4. 3: Control stained immortalised EC lines and mLSEC. 147
Figure 4. 4: Rat IgG control samples for cell-based ELISA. 149
Figure 4. 5: Rab IgG control samples for cell-based ELISA. 150
Figure 4. 6: Expression profile of CD31 by IHC 152
Figure 4. 7: Expression profile of CD31 in response to stimuli demonstrated by ELISA. 153
Figure 4. 8: Expression profile of Endoglin by IHC 155
Figure 4. 9: Expression profile of Endoglin in response to stimuli demonstrated by ELISA. 156

Figure 4. 10: Expression profile of JAM-2 by IHC *158*
Figure 4. 11: Expression profile of JAM-2 in response to stimuli demonstrated by ELISA. *159*
Figure 4. 12: Expression profile of CD34 by IHC *161*
Figure 4. 13: Expression profile of CD34 in response to stimuli demonstrated by ELISA. *162*
Figure 4. 14: Expression profile of E-Selectin by IHC *164*
Figure 4. 15: Expression profile of E-Selectin in response to stimuli demonstrated by ELISA. *165*
Figure 4. 16: Expression profile of ICAM-2 by IHC *167*
Figure 4. 17: Expression profile of ICAM-2 in response to stimuli demonstrated by ELISA. *168*
Figure 4. 18: Expression profile of VCAM-1 by IHC *170*
Figure 4. 19: Expression profile of VCAM-1 in response to stimuli demonstrated by ELISA. *171*
Figure 4. 20: Expression profile of VAP-1 by IHC *173*
Figure 4. 21: Expression profile of VAP-1 in response to stimuli demonstrated by ELISA. *174*
Figure 4. 22: Expression profile of LYVE-1 by IHC *176*
Figure 4. 23: Expression profile of CD31 in response to stimuli demonstrated by ELISA. *177*
Figure 5. 1 Effect of E-Selectin concentration on the number of adherent neutrophils (A), velocity of rolling neutrophils (B). *200*
Figure 5. 2: The effect of increasing shear stress and E-Selectin concentration on the number of adherent neutrophils (A), percentage rolling of adhered (B) and rolling velocities (C). *201*
Figure 5. 3: Effect of TNF-α concentration on the number of adherent neutrophils (A), the percentage of adherent cells that were rolling (B) and the velocity of rolling neutrophils (C). *203*
Figure 5. 4: Effect of increasing shear stress and cell tracker green on the ability of lymphocytes to adhere to a TNF-α stimulated EC monolayers in microslides. *205*
Figure 5. 5: Effect of tissue culture vessel on the ability of CTG labelled lymphocytes to adhere to endothelial monolayers mUCEC-1 (A), s.END (B) and b.End.5 (C) stimulated with TNF-α+IFN-γ. *207*
Figure 5. 6: Effect of TNF-α and pertussis toxin (PTX) treated lymphocytes on the number of lymphocytes adhering to mUCEC-1 monolayer (A) and the number of shape-changed lymphocytes (B). *209*
Figure 5. 7: Effect of pro-inflammatory stimuli on the number of adherent lymphocytes for 4 hours. *211*
Figure 5. 8: Effect of pro-inflammatory stimuli on the number of adherent lymphocytes for 24 hours. *212*
Figure 5. 9: Isolation of CD4+/CD8+ single positive cells from whole murine spleen using the MoFlo Cell Sorter. *215*
Figure 5. 10: Effect of pro-inflammatory stimuli on the adherence of lymphocyte subsets. *217*
Figure 5. 11: Effect of pro-inflammatory stimuli on the number of lymphocytes adhering to mLSEC. *220*
Figure 5. 12: Effect of LPS and TNF-α+IFN-γ on the adherence of total lymphocytes and subsets. *222*
Figure 5. 13: Effect of LPS and TNF-α+IFN-γ on the lymphocyte recruitment in static assays. *224*
Figure 5. 14: The effect of shear conditioning on the total number of adherent neutrophils (A), the percentage of adherent neutrophils that adhered (B) and the velocities of rolling neutrophils (C). *226*
Figure 5. 15: The effect of increasing concentrations of TNF-α on the number of adherent lymphocytes. *228*
Figure 6. 1: Sample of Bioanalyzer data. Representative images of RNA sample purity obtained from Bioanalyzer. *253*
Figure 6.2: Heatmap of all genes present or marginal (50%) in mUCEC-1 and s.END cells in all treatments examined. *255*
Figure 6.3: Heatmap of gene variation. Graph representing genes present in mUCEC-1 and s.END cells. *256*
Figure 6.4: Baseline gene expression. Image represents genes expressed in mUCEC-1 and s.END cells treated with control media. *257*
Figure 6.5: Expression of endothelial cell markers. *260*
Figure 6.6: Expression of adhesion molecules. *262*
Figure 6.7: Expression of CCL Chemokines. *264*
Figure 6.8: Expression of CXCL Chemokines. *266*
Figure 6.9: Expression of chemokine receptors. *268*
Figure 6.10: Expression of interleukins and Receptors. *269*
Figure 6.12: Canonical pathways in s.END Cells. *272*
Figure 6.13: Core pathway analysis in s.END Cells. *273*
Figure 6.14: Canonical pathways in mUCEC-1 Cells. *274*
Figure 6.15: Core pathway analysis in mUCEC-1 Cells. *275*
Figure 6.16: qPCR Validation in mUCEC-1 cells. *278*
Figure 6.17: qPCR Validation in s.END cells. *279*
Table 7. 1: Table summarising expression profile of endothelial markers and adhesion molecules of primary mLSEC cells. *290*

Table 7. 2: Table summarising expression profile of endothelial markers and adhesion molecules of mUCEC-1 cells.....297
Table 7. 3: Table summarising expression profile of endothelial markers and adhesion molecules of s.END cells.....300
Table 7. 4: Table summarising expression profile of endothelial markers and adhesion molecules of b.End.5 cells.....303

ABBREVIATIONS

AA	Arachidonic Acid
Ac-LDL	Acetylated Low Density Lipoprotein
AJ	Adherens Junction
ALPS	Autoimmune Lymphoproliferative Syndrome
APC	Antigen Presenting Cell
b.End.5	Brain Endothelioma
BBB	Blood Brain Barrier
BEC	Biliary Epithelial Cells
BMEC	Brain microvascular endothelial cells
BMP-2	Bone Morphogenetic Protein-2
CCl_4	Carbon Tetrachloride
cDNA	complementary DNA
CDR	Complimentarity Determining Regions
CLA	Cutaneous Lymphocyte Antigen
CLEVER-1	Common Lymphatic Endothelial and Vascular Endothelial Receptor-1
CNS	Central Nervous System
CR	Consensus Repeats
CTG	Cell Tracker Green
CYP450	Cytochrome P450
DAPI	4',6-diamidino-2-phenylindol
DARC	Duffy Antigen Receptor for Chemokines
DC	Dendritic Cells
DMEM	Dulbecco's Modified Eagles Medium
DNA	Deoxyribonucleic Acid
EAE	Experimental Autoimmune Encephalomyelitis
EC	Endothelial Cells
ECGS	Endothelial Cell Growth Supplement
EDTA	Ethylenediaminetetraacetic Acid
EGF	Epidermal Growth Factor
EGFR	Epidermal Growth Factor Receptor
ELAM-1	Endothelial Leukocyte Adhesion Molecule-1
ELISA	Enzyme Linked Immuno-Sorbant Assay
ELR	Glutamic Acid Arginine Motif
EM	Electron Microscopy
ESM-1	Endothelial Cell Specific Molecule-1
EST	Expressed Sequence Tag
FACS	Fluorescently Activated Cell Sorting
FCS	Foetal Calf Serum
FGF	Fibroblast Growth Factor
FITC	Fluorescein isothiocyanate
GAG	Glycosominoglycans
Gld	Lymphadenopathy
GM-CSF	Granulocyte Monocyte-Colony

	Stimulating Factor
GPCR	G-Protein Coupled Receptor
HA	Hyaluronic Acid
HCC	Hepatocellular Carcinoma
HEV	High Endothelial Venule
HGF	Hepatocyte Growth Factor
hLSEC	human Liver Sinusoidal Endothelial Cells
HRP	Horse Radish Peroxidase
HSC	Hepatic Stellate Cells
HUVEC	Human Umbilical Vein Endothelial Cells
IB4	Isolectin B4
ICAM-1	Inter-Cellular Adhesion Molecule-1
ICAM-2	Inter-Cellular Adhesion Molecule-2
IF	Immunofluorescence
IFN-γ	Interferon-Gamma
IgG	Immunoglobulin
IHC	Immunohistochemistry
IL-10	Interleukin-10
IL-1β	Interleukin-1-Beta
IL-6	Interleukin-6
IL-8	Interleukin-8
IMC	Isotype Matched Control
IMS	Industrial Methylated Spirits
ITAC	Interferon Inducible T-Cell Alpha Chemoattractant Protein
ITIM	Immunotyrosine Based Motif
IU	Infective Units
IVC	Inferior Vena Cava
JAM-2	Junctional Adhesion Molecule-2
KC	Kupffer Cells
LAD-1	Lymphocyte Adhesion Deficiency-1
LF	Laminar Flow
LFA-1	Lymphocyte Function Associated Antigen-1
LM	Light Microscopy
Lpr	Lymphoproliferative
LPS	Lipopolysaccharide
LYVE-1	Lymphatic Vessel Hyaluronan Receptor-1
mAb	Monoclonal Antibody
MACS	Magnetically Activated Cell Sorting
MadCAM-1	Mucosal Addressin cell adhesion molecule-1
MAPK	Mitogen Activated Protein Kinase
mBMEC	murine Brain Microvascular Endothelial Cells
MCP-1	Monocyte Chemoattractant Protein
MCP-1	Monocyte Chemoattractant Protein-1
MCP-2	Monocyte Chemoattractant Protein-2

mES	Murine Embryonic Stem Cells
MHC	Major histocompatibility complex
MIG	Monokine Induced by Gamma Interferon
MIP	Macrophage Inflammatory Protein
MIP-1β	Macrophage Inflammatory Protein-1β
mLSEC	murine Liver Sinusoidal Endothelial Cells
MS	Multiple Sclerosis
mUCEC-1	Cardiac EC Line
NaCl	Sodium Chloride
NK/NKT	Natural Killer/Natural Killer T-Cells
NO	Nitric Oxide
NPC	Non Parenchymal Cells
ORF	Open Reading Frame
Pa	Pascal
PAF	Platelet Activating Factor
PBS	Phosphate Buffered Saline
PCR	Polymerase Chain Reaction
PCV	Post-capillary Venule
PDGF	Platelet Derived Growth Factor
PE	Phycoerythrin
PECAM-1	Platelet-Endothelial Adhesion Molecule-1
PFA	Paraformaldehyde
PMN	Polymorphonuclear Leukocyte
PRR	Pattern Recognition Receptor
PSGL-1	P-Selectin Glycoprotein Ligand-1
PTX	Pertussis Toxin
PV	Portal Vein
QLT	Quantitative Trait Loci
qPCR	Quantitative PCR
RA	Rheumatoid Arthritis
RANTES	CCL5
RIN	RNA Integrity Number
RNA	Ribonucleic Acid
ROS	Reactive Oxygen Species
RPMI	Roswell Park Memorial Institute
RT	Room Temperature
RTC	Rat Tail Collagen
s.END	Skin Endothelioma
SAGE	Serial Analysis of Gene Expression
SDF	Stromal Cell Derived Factor
sLE^x	Sialyl Lewis
SSAO	Semicarbazide sensitive amine oxidase
TCM	Tissue Culture Media
TCR	T-Cell Receptor
TEM	Transendothelial Migration
TGF-β	Transforming Growth Factor-Beta
TJ	Tight Junction

TLR	Toll Like Receptor
TNF-α	Tumour Necrosis Factor-Alpha
TNFR6	TNF Receptor 6
VAP-1	Vascular Adhesion Protein-1
VCAM-1	Vascular Cellular Adhesion Molecule-1
VEGF	Vascular Endothelial Growth Factor
VEGFR2	Vascular Endothelial Growth Factor Receptor 2
VLA-4	Very Late Antigen-4
VVO	Vesiculo-Vascular Organelle
vWF	Von Willebrand Factor

1. GENERAL INTRODUCTION

1.1 Inflammation and inflammatory mediators

The Romans originally defined inflammation in the first century as heat (calor), pain (dolor), redness (rubor) and swelling (tumour). It is the response of the immune system to physical tissue damage or the presence of a pathogen or foreign antigen. Inflammation occurs in three distinct phases. Almost immediately, a physical barrier is formed by clots of fibrinogen, minimising the movement of fluids and spread of infection. Acute inflammation is transient, blood flow in the effected area is increased as vessels dilate, reducing velocity resulting in heat and redness. Endothelial cells (EC) aid vascular permeability by altering the properties of cellular junctions allowing fluid and proteins to exit the general circulation and accumulate in the tissue leading to swelling and pain. In the sub-acute phase the pattern of EC adhesion molecule expression changes to recruit circulating leukocytes. Initial neutrophilic infiltration is followed by monocytes, eosinophils and lymphocytes. Additional effector molecules and cells are delivered to the site of infection enhancing the eradication of invading pathogens by tissue resident macrophages. This then progresses to a chronic proliferative stage leading to fibrosis and tissue degeneration (Parkin *et al.* 2001).

Inflammation is mediated by a number of different substances both exogenous and endogenous including nitric oxide (NO), interleukins, serotonin and endotoxins. In acute inflammation macrophages produce prostaglandins, leukotrienes, eicosanoids and platelet activating factor (PAF), in response to the identification of pathogens. These lipid-derived mediators are generated by the metabolism of phospholipid membranes. Complement is also involved here; products from dying cells contribute to this enzymatic cascade system attracting neutrophils, leading to mast cell degranulation and release of histamine and opsonisation of bacteria. In addition, pro-

inflammatory cytokines such as TNF-α (Tumour necrosis factor-alpha), IL-1 (Interleukin-1) and IL-6 (Interleukin-6) are produced to perpetuate inflammation (Parkin *et al.* 2001).

Cytokines are produced by almost all cells of the body and have a wide range of functions including cell activation, proliferation and apoptosis. These small molecular weight molecules act in an autocrine, paracrine and endocrine manner sending signals by binding to specific cell surface receptors. Their role is to regulate the direction, amplitude and duration of the inflammatory response (Moser *et al.* 2004). Chemokines are chemotactic cytokines; produced in response to pro-inflammatory stimuli, and they play an important role in leukocyte migration. Grouped according to the location of two cysteine (C) residues within a number of different amino acids (X) there are CXC (α-chemokines) and CC (β-chemokines). Exceptions exist, such as CXXXC (Fractalkine) and C (Lymphotactin). Chemokines can cause prolonged effects as they bind to glycosaminoglycans (GAG's) on the surface of cells and extra-cellular matrix leading to leukocyte activation and migration (Murdoch *et al.* 2000).

Inflammation is mediated by several substances, in this project I used a number of different pro-inflammatory stimuli to activate endothelial cell populations, including the cytokines TNF-α, IFN-γ (Interferon-gamma), IL-1β and bacterial product LPS (Lipopolysaccharide). Cytokines are small molecular substances allowing cells to communicate. These messengers send signals by binding specific cell-surface receptors leading to changes in cellular behaviour (Parkin *et al.* 2001). TNF-α is produced rapidly by all inflammatory cells, particularly activated mast cells. TNF-α is a member of a group of cytokines that stimulate the acute phase reaction produced

in response to LPS and IL-1. The TNF-receptor is expressed on all inflammatory cells which when stimulated are activated to synthesise more TNF-α, amplifying the response via a positive feedback loop.

IFN-γ originally called macrophage-activating factor, is produced by T-Cells and Natural Killer Cells, activating macrophage and neutrophil intracellular killing, enhancing NKT (Natural Killer Cell) function and antigen presentation by upregulating MHC II (Major Histocompatibility Complex) receptor expression on Antigen Presenting Cells (APC's) via a different receptor to class 1 interferons. γ-interferon is used therapeutically in patients with congenital neutrophil defects, macrophage based infections and those with defects in the production of the cytokine itself or receptor (Parkin *et al.* 2001).

Interleukins are cytokines produced by leukocytes, in particular macrophages and monocytes. IL-1 was one of the first cytokines to be described, also known as lymphocyte activating factor, it was only in 1984-85 that it was discovered to be composed of two subunits (α andβ), which act in a similar fashion. IL-1 is an endogenous pyrogen inducing fever (via prostaglandins), lowering blood pressure, activating T-Cells and producing additional interleukins.

LPS or Lipopolysaccharide is an endotoxin and a component of the outer membrane of gram-negative bacteria. Essential for bacterial structural integrity it protects the membrane from chemical attack. Endotoxins mediate acute inflammation via Toll Like Receptor 4 (TLR 4) (Ley *et al.* 2007;Parkin *et al.* 2001).

1.2 Role of Lymphocytes

Adaptive immunity depends on lymphocytes, providing life-long protection following disease or vaccination. This immunological memory enables familiar pathogens to be overcome if the innate immune system is ineffective (Delves *et al.* 2000). Lymphocytes arise from a common lymphoid progenitor in the bone marrow, which can develop into either B-Cells, which have the capacity to differentiate into antibody producing plasma cells when activated, or T-Cells. Lymphocytes are housed in the lymphatic system and lymphoid tissues. These organs can be broadly categorised into primary (thymus) or secondary lymphoid organs (Spleen, Peyers Patches), where lymphocytes are generated or maintained respectively. Both groups of lymphocytes originate in the bone marrow but only B-Cells mature there, whereas T-Cells migrate to the thymus as thymocytes. Post maturation both cell types enter the general circulation before migrating to secondary lymphoid organs. In order to contribute to a fully functioning immune system, T-Cells need to acquire antigen specificity. This rearrangement and splicing of random DNA segments coding for antigen binding areas of receptors (complimentarity determining sequences) produces over 10^8 T-Cell receptors, enough to accommodate all the antigens encountered in a lifetime (Arstila *et al.* 1999). After gene rearrangement these cells are still considered ‘naïve’ as they have not yet encountered their specific antigen as part of an immune response. These cells then go on to populate secondary lymphoid organs such as the spleen, tonsils, lymph nodes and mucosa associated lymphatic tissues (e.g. Peyers Patches). Cells of the lymphatics can move throughout the lymphatic system as tissues provide an ordered expression of adhesion molecules allowing T and B cells to review various tissues searching for antigens in immune surveillance.

Figure 1. 1: The role of T and B Cells in specific immunity (Parkin et al. 2001)

Representative schematic diagram of T and B-Cell development in the bone marrow and thymus.

1.2.1 T-Cell Development: CD4+/CD8+

As mentioned previously naïve cells are primed to respond to their defined antigen inducing an immune response. However, this process needs to be tightly regulated in order to prevent responses to self-antigens. To combat this T-Cells undergo a process of positive and negative selection in the thymus (Fig.1.1). When T-Cells enter the thymus they are double negative expressing neither CD4+ nor CD8+. Cells that have a high avidity for self-peptides presented by MHC are negatively selected and deleted (clonal deletion). Those with low avidity are positively selected and become double positives. In the final stages, remaining single positive T-cells are selected for as they either bind self peptide/antigen via MHC class I (CD8+) or MHC class II (CD4+). Antigen can be presented to T-cells in one of two ways depending on their phenotype. MHC Class I displays endogenous antigens such as viral or tumour proteins, whereas, exogenous antigens which can be taken up by professional antigen presenting cells such as dendritic cells (DC's) are presented via MHC Class II. This specificity allows targeted cytotoxic attack by CD8+ cells expressing viral proteins on their surface and induction of cytokine production by CD4+ cells in response to a local infection activating surrounding cells of the immune system. The two types of effector T-Cells are T-helper cells and T-cytotoxic cells expressing either CD4 or CD8 surface markers. Both are co-receptors acting in addition to the T-Cell Receptor (TCR) with corresponding MHC complexes.

1.2.2 Role of neutrophils

Neutrophils are an essential component of the protective innate immune response. To fulfil this crucial role they must be able to rapidly move from the circulation,

migrate through the endothelium lining the vasculature and phagocytose any invading pathogens. The recruitment of neutrophils must be highly regulated however, as neutrophils are double-edged swords. They utilise proteinases and reactive oxygen species (ROS) to neutralise the pathogen, but these substances can inflict tissue damage (Morgan *et al.* 2005). It is thought that neutrophils have a relatively short life span to avoid this possibility. If these harmful cells are allowed to accumulate in tissues as a result of unresolved inflammation or deregulated recruitment they could potentially cause damage for example in the synovium in Rheumatoid Arthritis (RA) (Bostan *et al.* 2002).

1.2.3 Development and fate of neutrophils

Neutrophil development begins in the bone marrow where pluripotent myeloid stem cells are directed down the myeloblastic cell lineage by a number of specific growth factors and cytokines. The myeloid stem cell differentiates into granulocyte-monocyte progenitor in response to granulocyte-monocyte colony stimulating factor (GM-CSF), IL-3 and IL-6. Exposure to additional GM-CSF and G-CSF results in the production of fully functional segmented neutrophils (Pallister. 1998). The resulting mature neutrophils exit the bone marrow and enter the peripheral bloodstream. Here they either circulate freely in the blood, the circulating pool or enter the marginated pool. The marginated pool of neutrophils circulates slowly through the lungs and microcirculation and can be mobilised rapidly in response to stimuli, such as exercise (Adams *et al.* 2005).

In the absence of a pro-inflammatory stimulus, neutrophils circulate through the peripheral blood for 6-12 hours, after which they are thought to die by apoptosis and are removed by macrophages of the reticuloendothelial system (Brown *et al.* 1999). When neutrophils encounter pro-inflammatory cytokines, growth factors (Homburg et *al.* 1996) or signals transduced during migration they have been shown to survive for up to 48 hours (McGettrick *et al.* 2006). This increased lifespan is thought to allow neutrophils to carry out their protective functions in tissue.

1.3 The role of endothelium

1.3.1 Vascular endothelial cells and their function

Endothelial cells line the whole of the vasculature and are highly heterogeneous. EC play a major role in leukocyte recruitment as well as haemostasis, regulation of vascular tone, angiogenesis and the control of movement of solutes between the vascular system and tissues (Johnson-Leger *et al.* 2000;Matharu *et al.* 2006;Springer 1995). Endothelial phenotype has been shown to vary in both structure and function from organ to organ and throughout the vascular tree. EC are notoriously difficult to define, as no specific marker of EC exists. In addition any ‘endothelial-like’ markers such as CD31 or VE-Cadherin, or structural characteristics for example Weibel-Palade bodies or fenestrations vary between subsets of EC and can also be present on additional cell types. For example fenestrated epithelial cells are found around the fenestrated capillaries of the glomerulus. In addition CD31 is also expressed on platelets, macrophages and subsets of T-Cells.

The structure of EC varies throughout the vasculature, although conventionally flat in vessels they are cuboidal in shape in high endothelial venules and their thickness varies from 0.1µm in capillaries to 1µm in the aorta (Girard *et al.* 1995). Vascular endothelium is either continuous or discontinuous and can be further categorised by the presence or absence of fenestrations respectively. Fenestrations are transcellular pores of approximately 70nm with a thin diaphragm across their opening in some cases, providing size selective filtration. Non-fenestrated continuous endothelium is present in the brain, skin, heart and lungs. Fenestrated endothelium occurs in exo and endocrine glands, gastrointestinal mucosa and glomeruli where substances are filtered or transported across the endothelium into tissues. Discontinuous endothelium is found in sinusoidal beds such as the liver, which lack a basement membrane and possess an increased number of larger fenestrations up to 100-200nm in diameter (Aird 2007b;Braet *et al.* 2002). Vascular Endothelial Growth Factor (VEGF) is thought to play an important role in the presence and maintenance of intercellular gaps and fenestrations. The presence of exogenous VEGF has been shown to induce fenestrations in vascular beds of the skin and cremaster, where they are normally absent (Roberts *et al.* 1995).

1.4 Leukocyte Recruitment

The recruitment of leukocytes into tissues is highly regulated process involving complex interactions between leukocytes and endothelial cells. By modifying the expression of adhesion receptors and chemokines on their surface, EC can control the recruitment of leukocytes in response to locally produced inflammatory

substances, including TNF-α and IL-1β (Bahra *et al.* 1998;Mantovani *et al.* 1992). However, their location leads to the involvement of these cells in the pathology of several diseases due to deregulated or inappropriate leukocyte recruitment. The most relevant diseases in this context are chronic inflammatory diseases including atherosclerosis and acute diseases such as ischemia/reperfusion injury and early transplant rejection. The location of endothelial cells means they are ideally situated to interact with passing leukocytes in the circulation. There are thought to be differences in leukocyte recruitment due to variation of EC phenotype in different levels of the vascular tree and in different organs of the body (Berlin *et al.* 1993;Picker 1992). For example CCL25 is thought to be important in attracting CCR9 expressing CD8+ effector cells to the gut associated lymphoid tissues in the small intestine (Campbell *et al.* 2002). The homing receptor pair or addressing of L-Selectin and Peripheral Lymph Node Addressin (PNAd) is also thought to mediate lymphocyte adhesion to peripheral lymph node HEV (Garrood *et al.* 2006)

Each tissue may provide a diverse cellular, physiological and rheological environment under which endothelial cells and leukocytes may respond differently. Study of these localised phenotypic differences may yield data, which could increase the level of understanding of mechanisms of inflammatory diseases in different organs.

Leukocyte recruitment can be separated into two main types: (1) constitutive recruitment which takes place in high endothelial venules (HEV) for immune surveillance and (2), recruitment in response to trauma and infection, *i.e.* inflammation, which occurs mostly in post-capillary venules (PCV). Both of these processes are thought to be similar but utilise different specific adhesion molecules

and chemokines. $\alpha 4\beta 7$ integrins and L-Selectin in particular have been shown to play a role in immune surveillance directing lymphocytes to peyers patches and mesenteric lymph nodes (Stoolman 1993). Chemokines also play an in important part here. They can be split into two categories, inflammatory and homeostatic, directing leukocytes in infection and tissue injury or to the bone marrow and thymus during haematopoiesis and initiation of the adaptive immune response respectively (Moser *et al.* 2004). In both types of recruitment, leukocytes must migrate into surrounding tissues from the bloodstream via a process known as extravasation. This highly regulated process occurs in the low shear stress environment of post-capillary and high endothelial venules (Anderson *et al.* 1993).

A specific sequence of events has to occur in order for the leukocytes to migrate from the bloodstream into the surrounding tissues. Specialised adhesion molecules are essential in this capture process. These molecules are constitutively expressed on the endothelial cells present in high endothelial venules of lymph nodes, allowing continuous trafficking of lymphocytes into the lymphatics. In non-lymphoid tissue the endothelial cells in PCV are able to upregulate expression of such molecules in response to pro-inflammatory stimuli as a result of infection, directing leukocytes to the affected tissue (Parkin *et al.* 2001).

In normal conditions leukocytes localise to the centre of venules where the flow is fastest; under inflammatory conditions the blood vessels dilate decreasing the rate of flow, increasing the frequency of complex interactions between the vascular endothelium and lymphocytes in the circulation. Immune surveillance differs, as

lymphocytes are constantly recruited from the bloodstream and home to their predisposed site.

A number of cell surface receptors and adhesion molecules expressed on the both cell types are involved in regulating specific interactions between the lymphocytes and endothelial cells required for recruitment. A general paradigm of leukocyte recruitment exists (Fig. 1.2) and involves a defined sequence of events divided into several steps (Adams *et al.* 1994;Buckley *et al.* 2000;Springer 1994). Flowing leukocytes must make contact with the vessel wall. This comes about as a result of margination. The leukocytes are pushed towards the vessel wall by the central flow of red blood cells (Goldsmith *et al.* 1984). As a result of inflammation, substances such as histamine and prostaglandins trigger an increase in local blood flow and permeability. Protein rich fluids move from the general circulation into the surrounding tissues increasing the blood haematocrit and viscosity, resulting in slower blood flow. The increasing numbers of erythrocytes in post capillary venules gravitate towards the centre of the vein pushing circulating leukocytes outwards, thus facilitating more leukocyte endothelial interactions. On contact with the endothelium, weak, rapidly-reversible interactions are formed with Selectin receptors (Lawrence *et al,* 1991), leading to tethering and rolling along the vascular wall (Alon *et al.* 2002;Bahra *et al.* 1998). Chemokines present on the surface of vascular endothelial cells initiate activation of the leukocyte leading to tight adhesion to the vascular surface via integrins and their receptors (Springer 1993). In the final stages, the leukocyte migrates through the endothelium to the surrounding tissue in response to a chemotactic gradient generated by endothelial or resident inflammatory cells. This multi-step process involving defined independent steps generates opportunities for regulation. Each step is mediated by distinct interactions between specific sets of

adhesion molecules, allowing targeted recruitment of different leukocyte subsets to specific tissues if the tissues provide the unique combination of receptors and chemokines (Springer 1994).

Figure 1. 2: Diagram of the leukocyte recruitment paradigm (Ley *et al.* 2007).

Schematic of current outline of the leukocyte recruitment cascade from the circulation into surrounding tissues. Includes rolling, firm adhesion and transmigration through the endothelium.

1.5 Tissue specific recruitment

An increasing amount of literature illustrates the use of unique adhesion molecules and chemokines, differentially expressed in a variety of tissues, to drive tissue-specific leukocyte recruitment (Mackay 1993). This variation accommodates the different functions required by diverse tissues and systems.

Mucosal addressin adhesion molecule-1 (MAdCAM-1) is expressed predominantly by intestinal lymphatic EC (Berlin *et al.* 1993). This binds to α4β7 and α4β1 integrins, which are expressed uniquely by a specific subset of T-lymphocytes displaying tissue tropism (Berg *et al.* 1993). A similar mechanism operates in the skin, where cutaneous lymphocyte antigen (CLA) mediates lymphocyte binding to dermal endothelium via its interactions with E-selectin (Picker 1992). Tissue specific endothelial cells produce these address codes. These EC are exposed to different stromal and haemodynamic environments depending on which organ they reside in. This unique location conditions the EC, which can result in varied phenotype, gene expression and signalling producing these unique address codes, leading to differential recruitment of leukocytes from the circulation.

I have looked at several organs in this project, from the microvasculature of the skin, brain, heart and hepatic sinusoids. Each of these endothelial populations performs different functions and in particular play certain roles in the immune system. I will highlight in particular how these EC regulate leukocyte recruitment in the specific tissues.

In general the process of recruitment is the same in most tissue beds; however there are some differences, which I will highlight here. It must also be considered that much research was conducted *in vitro* to examine disease processes in the effected tissues and 'normal' conditions may not be directly physiologically relevant. In addition, in order to recapitulate certain *in vivo* systems in the absence of primary cells, immortalised cell lines have been used.

1.5.1 Skin

The skin acts as protective barrier for the internal organs from the external environment, combating toxins, pathogens and physical stresses. In order to protect the body the skin acts as an efficient immune organ containing a wide array of immune-competent cells and inflammatory mediators supplied by the circulation and lymphatics. Intercellular adhesion molecule-1 (ICAM-1) has many different effects in skin; it is constitutively expressed at low levels on EC, which increase in response to pro-inflammatory stimuli, IL-1, TNF-α and IFN-γ in particular. T-Cells can utilise ICAM-1: LFA-1 (Lymphocyte function antigen) interactions to adhere to EC's and keratinocytes and migrate into the epidermis, in addition these interactions are essential for inducing T-Cell activation as a co-stimulatory signal. In B-Cells LFA-1 binding to ICAM-1 is thought to reduce the amount of antigen needed to form the immunological synapse and activate B-Cells (Carrasco *et al.* 2004). Expression has been found in a number of diseases including cutaneous cancers. In a disease model of dermatitis, increased ICAM-1 expression on keratinocytes correlated with a mononuclear infiltration. IL-1 and TNF-α produced by keratinocytes can increase

ICAM-1 and MHC II expression on Langerhans cells (specialised dermal APC's) having a positive effect on antigen presentation (Kupper 1990). In addition E-Selectin and CLA have been proposed as candidates for a 'skin vascular addressin' important for trafficking leukocytes to the skin (Picker 1992). E-Selectin is expressed on EC in inflamed tissues, but in particular in the skin where it is constitutively expressed allowing continuous surveillance and increasing in the presence of TNF-α. In addition the epithelial-expressed chemokine CCL27 is thought to be involved in homeostatic leukocyte recruitment (Kunkel *et al.* 2002). Neutrophils express the sLEx ligand for E-Selectin (ELAM-1) and CLA is the suggested candidate on T-Cells. Expression of these receptor ligand pairs allows targeted recruitment or homing of specific subsets of cells (Henseleit *et al.* 1999).

1.5.2 The Brain

The human brain contains almost 98% of the body's neural tissue and weighs approximately 1.4kg. Brain size varies between individuals and male brains are on average 10% larger compared to females. The brain is an extremely active organ requiring large amounts of glucose and oxygen continuously. Blood reaches the brain through the internal carotid arteries and vertebral arteries and leaves through the internal jugular veins. The most important structure of the brain in the context of the report is the BBB, which biochemical isolates the neural tissue from the general circulation. Composed of brain parenchymal microvascular endothelial cells, ensheathed by astrocytes, foot processes and pericytes, the endothelium of the cerebral vasculature contains a large number of tight junctions preventing the transport of materials between juxtaposed endothelial cells (Greenwood *et al.* 2002). Only lipid soluble substances such as oxygen and prostaglandins can diffuse across

the endothelium into the interstitial fluid of the central nervous system (CNS). Other water-soluble compounds and ions are either transported through channels in endothelial cell membranes or through active or passive transport. The selective permeability characteristic of the BBB is somewhat controlled by astrocytes which are in close contact with brain microvascular endothelial cells (BMEC). The substances they produce help regulate the functions of the BBB and if destroyed as a consequence of brain damage the integrity of the BBB is compromised. The cerebrospinal fluid that is responsible for transporting nutrients, chemical messengers and disposing of waste products is separate from the blood. In addition the ion concentrations and pH can differ vastly from that of the bloodstream. The properties of the brain can however be manipulated to administer drugs to treat brain disorders or trauma.

Much research is being carried out to shed more light on the role of the BBB. In order to study its function many groups isolate cerebral cells including astrocytes and BMEC to study the system *in vitro*. Many methods involve isolating the small capillaries and microvasculature of the brain out of which endothelial cells are cultured. This has been attempted primarily using bovine brain. Most methods involve the removal of the meninges, homogenisation of the tissue, enzymatic digestion, followed by either gradient centrifugation or antibody selection/depletion (Audus *et al.* 1996). BMEC appear to retain many morphological and biochemical properties present *in vivo* including cobblestone morphology and the permeability properties of the BBB such as the transcellular passage of glucose (Audus *et al.* 1996). However it must be considered that once isolated primary cells can begin to dedifferentiate in culture due to the absence of external stimuli or direct contact with additional cell types present in the physiological environment.

The brain is of interest in this context as the physiochemical environment of the brain microvasculature, like the liver sinusoid, differs in comparison to most organs. In contrast to the sinusoids, brain endothelial cells are exposed to high shear stress and are in close contact with surrounding astrocytes (Lui *et al.* 2003). Due to the varied microenvironment the recruitment of leukocytes to cerebral tissues, and the molecules involved in subsequent processes are different. In addition circulating leukocytes have to overcome the blood-brain barrier (BBB) in order to combat inflammation in the brain (Williams *et al.* 1995). A number of different adhesion molecules, ICAM-1, Vascular Cell Adhesion Molecule-1 (VCAM-1) and CD31 are involved in the recruitment and transport of leukocytes into the brain parenchyma. The function of ICAM-1/VCAM-2 has demonstrated on cytokine stimulated primary mouse, rat and human brain microvascular endothelial cells (BMEC) (Xiaoyan *et al.* 2001) and inflammatory conditions such as Multiple Sclerosis (MS) including the experimental model Experimental Autoimmune Encephalomyelitis (EAE) (Lee *et al.* 1999). In particular ICAM-1, CD31 and ICAM-2 are thought to be involved in downstream signalling events, via G-protein coupled receptors perpetuating further recruitment, due to the induction of cytoskeletal changes creating transmigratory cups (Greenwood *et al.* 2002). In addition experiments examining the effect of adenoviral vectors in naïve brain tissue, an issue to be considered in gene therapy, found that injection of $1x10^8$ infective units (IU) into brain increased the levels of mRNA coding for IP-10, MCP-1 and RANTES, which play a role in the innate immune response (Zirger *et al.* 2006).

1.5.3 The Liver

The liver receives blood from two sources, the hepatic artery and the hepatic portal vein. Portal blood contains numerous nutrients, waste products and metabolites absorbed and produced during digestion. The presence of nutrient-rich portal blood means that the liver is constantly exposed to gut derived antigens and particles of food and is in a favourable position to metabolise protein, ignore harmless food antigens and clear any harmful pathogens, which may enter the system. The liver is also an important immunological organ with a large resident population of rapidly responsive immune cells providing essential immune surveillance (Lalor and Adams 2002;Lalor *et al.* 2002a;Lalor and Adams 1999). The liver contains a large number of resident lymphocytes, up to 10^8 (Racanelli *et al.* 2006) consisting of CD4+, CD8+, B-Cells, NK and NKT cells.

Hepatic sinusoidal endothelial cells (LSEC) are a variety of specialised endothelial cells that populate the low shear vascular bed of the liver. The most noted phenotypic differences are observed between the vascular endothelium in the portal vessels and the sinusoidal endothelial cells (Lalor & Adams 2002;Lalor *et al.* 2002b). In terms of leukocyte recruitment, adhesion in LSEC lacks an important rolling step required in all other organs. Selectins are not essential for recruitment, leukocytes were initially thought to become physically trapped in the small sinusoids but further studies have found ICAM-1 and VCAM-1 to be important. In addition adhesion can occur via integrin dependent or independent mechanisms such as the non-classical pathway involving Common Lymphatic Endothelial and Vascular Endothelial Receptor-1 (CLEVER-1), the mannose receptor or CD44 and Vascular Adhesion Protein-1 (VAP-

1) (Lee *et al.* 2008). Recruitment in portal and central venules of liver is similar to the standard paradigm.

1.5.4 Heart

The endothelium plays an important role in cardiac health, protecting the heart from infection and resolving inflammation (Hillis *et al.* 1998). However, EC also contribute to inflammatory disorders and atherosclerosis having adverse effects on the heart. In bacterial endocarditis, plasma levels of E-Selectin, VCAM-1 and ICAM-1 are elevated (B.Soderquist *et al.* 1999). It has been postulated that the increased levels of E-Selectin released are related to the degree of vascular injury caused by sepsis. Increased levels of ICAM-1, VCAM-1, E-Selectin, CD34 and CD31 were found on inflamed, degenerated and florid heart valves suggesting adhesion molecule mediated leukocyte recruitment and activated endothelium implicating EC in disease pathogenesis and complications such as thromboembolism (Muller *et al.* 2000). However it cannot be distinguished whether this is a result of local adhesion molecule release at the site of disease or systemic infection. ICAM-1 and VCAM-1 were also implicated in the infiltration of CD8+ T-Cells in the cardiac tissue of patients with severe cardiomyopathy (Haverslag *et al*. 2008).

1.6 Modulation of EC responses by their environment

There is growing evidence that functional responses of endothelial cells can be modulated by the local physiochemical environment (Nash *et al.* 2004). One aspect briefly considered in the current project is to examine the effect of haemodynamic

forces on the ability of EC to recruit leukocytes. These forces affect intra-cellular signalling, secretion, and protein and gene expression (Chien *et al.* 1998;Jalali *et al.* 1998). In addition, underlying stromal cells and substrate can modify EC phenotype and their ability to recruit leukocytes (Aird 2003;Nash *et al.* 2004). In particular EC cultured with smooth muscle cells were shown to have an augmented response to oxidised LDL judged by the ability to bind monocytic cells (Kinard *et al.* 2001). In addition EC cultured with alveolar epithelium showed increased recruitment of leukocytes upon cytokine stimulation (Eghtesad *et al.* 2001). Interestingly the specific phenotype of endothelial cells isolated from different tissues may be retained *in vitro* for extended periods (Nash *et al.* 2004). For instance, isolated murine cardiac and lung EC, both supported adhesion of flowing T-cells, but were shown to use different mechanisms. Cardiac EC after stimulation with TNF-α were found to used VCAM-1:VLA-4 and RANTES:CCR5 induced mechanisms, whereas in lung EC, ICAM-1, MIP-2 and MIP-1β were thought to be important (Lim *et al.* 2003).

1.6.1 Modulation of EC responses by shear stress

Vascular endothelium is exposed to a number of different haemodynamic forces. These include the frictional shear stress imposed by the bloodstream and hydrostatic pressure acting perpendicular to the vessel wall, which exerts compression and circumferential strain (Matharu *et al.* 2006). The most widely studied of these forces is shear stress (Lelkes 1999). Shear stress varies in different organs and throughout the vasculature, with arterial stress in the range of 1 to 4 Pa in comparison to 0.05 to 2 Pa in the microcirculation, where leukocyte recruitment takes place. Variation in shear stress is dependent on local pressure gradients, flow rate and the diameter of the vessels (Matharu *et al.* 2006). The type of blood flow is also variable, with

undisturbed laminar flow (LF) present within the microcirculation and some straight larger vessels. Arterial blood flow is not only pulsatile as a result of the cardiac cycle but there are also some areas of disturbed flow due to curvature of the arteries or bifurcations (Caro *et al.* 1969;Cunningham *et al.* 2005;Libby *et al.* 2005).

Endothelium responds to changes in haemodynamic forces by rapidly releasing a number of vasoactive substances including NO. Over time shear stress can also modify levels of expression of genes, a number of which are involved in leukocyte recruitment (Matharu *et al.* 2006). The altered expressions of some of these genes are too short lived to have a prolonged effect on leukocyte recruitment. The above supports the theory that initial exposure to shear or changes in shear cause transient responses, while prolonged exposure establishes a new phenotype with, for instance, altered response to pro-inflammatory cytokines. Studies have found that long-term exposure to shear inhibited TNF-α induced activation of NFkB and the associated upregulation of adhesion molecules and chemokines (IL-8 and Gro-α) in HUVEC (Sheikh *et al.* 2005). This is important because the ability of EC's to alter their phenotype under varying shear stresses could be important in situations where blood flow is disturbed such as ischemia/reperfusion and altered flow as a result of surgery (Nash *et al.* 2004).

1.7 The use of mouse models in research of human disease

One of the main aims of this project was to create an effective murine flow model to examine leukocyte recruitment as a useful standard to which comparisons could be made to the behaviour of isolated primary cells *in vitro*. The question is, why use

mice, when the ultimate aim is to apply any data obtained to the human situation? Murine models are a useful experimental research tool. They provide a great amount of flexibility and allow you to model tissues that are difficult to access in humans or are not freely available for experimental analysis. Models also provide a controlled environment in which you can test various reagents and knockdown genes *i.e.* knockout mice. In addition *in vitro* culture systems can be exposed to conditions not subject to manipulation in a whole animal systems in for example, intra-vital microscopy.

Several mouse models of human disease have been developed including cancer, neurodegenerative, neuromuscular, hearing and sight disorders and immunological and haematological disorders (Bedell *et al.* 1997b). Comparisons have been made between human and mouse genetic maps. These genetic and physical linkage maps enable identification of homologous genes and generation of mutants that closely resemble the human disease phenotype (Bedell *et al.* 1997a). In addition, the location of disease-associated genes discovered in mice can predict the location of the human locus. There are several different methods of creating mouse models including inbred, congenic and recombinant inbred strains allowing manipulation of several different parameters (Frankel *et al.* 1995). Transgenic mice were first developed in the 80's by injecting foreign DNA into the germline of mice. The animals containing this human disease gene could be studied to track disease pathogenesis and effectiveness of treatment regimes. Scientists could examine the response of different strains and examine interactions of genes. However there are issues with transgenic strains as the gene may be located within introns, misexpressed or integrate into other genes disrupting function (Wilson *et al.* 2003). Knockout mice are a result of the introduction of specific mutations in endogenous genes that can

transmit through the germ line (Melton *et al.* 1994). Mutations are created via homologous recombination in embryonic stem cells (mES), which contribute to all cell lineages when injected into blastocyts, although many are embryonically lethal (Bedell *et al.* 1997a). Strain specificity can impact on disease phenotype as unlinked genes can have a dramatic effect on disease outcome. For example, null mutations in the epidermal growth factor receptor (EGFR) gene were found to cause defects including peri-implantation and juvenile lethality in mice from CF-1, 129/SvJ and C57BL/6 background (Threadgill *et al.* 1995).

Although it is possible to create models where single specific genes are altered a number of the most important diseases such as cancer, diabetes and obesity are caused by the combination of several mutations in different loci. In addition some are genetically inherited but can be affected by somatically acquired mutations or environmental factors, called quantitative trait loci (QLT's). Several QLT's of human disease have been identified in mice, including atherosclerosis (Hyman *et al.* 1994), epilepsy (Frankel *et al*. 1994) and obesity (West *et al.* 1994). In the context of this research inflammatory and immune disorders are of particular relevance. Models of autoimmunity have helped to model diseases such as lupus, arthritis and diabetes (Bedell *et al.* 1997b). Studies on lymphoproliferation (lpr) and generalised lymphadenopathy (gld) have shown the importance of apoptosis in the maintenance of immune self-tolerance. Sufferers of autoimmune lymphoproliferative syndrome (ALPS) have been found to have mutations in the Fas gene. Fas Ligand was found to be mutated in gld mice (Fisher *et al.* 1995;Singer *et al.* 1994). In addition several models have been created to examine the role of *Apoe* and *Ldlr* in atherosclerosis. Homozygotes for the *Apoe* null mutations develop severe hypercholesterolemia and

atherosclerotic lesions at a young age, even when fed a low fat diet (Knecht *et al.* 1995).

Knockout mice can be used to examine the process of leukocyte recruitment and the role of each step in successful adhesion and migration. If functioning correctly, the recruitment of leukocytes is an essential mechanism for combating invading pathogens. If however, this process is modified or malfunctions in some way, as is the case in some autoimmune diseases, it can lead to undesirable consequences. If recruitment is ineffective it can increase the host's susceptibility to infection leading to recurrent or persistent infections, which are never resolved effectively. In leukocyte adhesion deficiencies for example, functional defects in neutrophil adhesion molecules such P-selectin or β2 integrins lead to poor recruitment to the site of infection due to impaired neutrophil adherence (Resenzweig *et al.* 2002). Smith *et al* (Smith *et al.* 1988) showed that polymorphonuclear lymphocytes (PMN) from LAD-1 patients could bind to activated human umbilical vein endothelial cells (HUVEC), but they couldn't transmigrate. On the other hand if recruitment is uncontrolled it can result in adherent neutrophils releasing their lysosomal enzymes inappropriately for example in vasculitis (Calderwood *et al.* 2005). If clearance of tissue resident apoptosing neutrophils is deregulated it can lead to chronic inflammation and organ damage (Morgan *et al.* 2005).

The advent of intravital microscopy has enabled researchers to examine leukocyte recruitment in real time *in vivo*. Although a remarkably useful experimental tool, it is difficult to examine tissue specific recruitment, as whole tissues are difficult to visualise microscopically. The majority of experiments manipulate parameters of recruitment in the mesentery and cremaster muscle as they are easily

transilluminated. Recruitment and transmigration can be investigated in liver (Zarbock *et al.* 2009). Due to the multi-lobular structure of rodent livers it is only possible to visualise recruitment in the edges of liver lobes and it is difficult to observe post-sinusoidal events. Multi-photon microscopy allows deeper tissue penetration and higher resolution.

Intra vital systems are physiologically relevant as they are performed *in vivo*, however there are drawbacks as discussed above, for example factors affecting the physiochemical environment cannot be easily manipulated. Primary isolated endothelium and immortalised cell lines can be cultured *in vitro* easily treated and exposed to biological and physical stimuli.

1.8 Isolating primary murine endothelial cells

Tissue specific variation in leukocyte recruitment is a widely accepted idea. However direct comparisons and extrapolation linking phenotypic variations to functional differences has not been made. One of the ultimate aims of this research was to highlight tissue specific phenotypic and functional variations by examining endothelial cells from heart, skin, brain and liver sinusoids. Details of specialised recruitment have been discussed in previous sections. However, attempts were made to isolate primary endothelial cell populations from murine brain and liver discussed in more detail here.

Several groups have published data detailing the isolation of primary murine endothelial cells from a number of different tissues, including, lung, heart, fat pad,

aortic rings (Marelli-Berg *et al.* 2000), liver (Katz *et al.* 2004) and brain (Wu *et al.* 2003). These EC populations are used to study endocytosis (Smedsrod *et al.* 1985), immunological function (Knolle *et al.* 1999), EC marker expression, angiogenesis, metastasis and endothelial specific roles in complex pathologies such as atherosclerosis among others. Most methods involve dissociation of the tissue in question using physical or enzymatic techniques. Cells can be separated on the basis of size or buoyant density and further purified using negative or positive antibody selection methods.

1.9 Isolating human endothelial cells

Unlike isolating murine endothelium, there are well-defined methods for isolating primary human endothelial cells, in particular human umbilical vein endothelial cells (HUVEC) and human sinusoidal endothelial cells (hLSEC). Much research examining endothelial cell behaviour has been done using HUVEC due to availability of tissue and ease of isolation (Jaffe *et al.* 1973). The umbilical veins are cannulated and digested using proteolytic enzymes (collagenase) to release the endothelial layer, which is then washed out and cultured on collagen-coated tissue plastic in medium 199 in the presence of human serum (Cooke *et al.* 1993). The isolation of hLSEC is more complicated, the tissue is dissociated and digested using collagenase, non-parenchymal cells are separated on the basis of buoyant density on a Percoll gradient. Contaminating biliary epithelial cells are removed by negative magnetic bead selection using HEA-125 followed by positive endothelial cell selection using CD31. hLSEC are cultured in human basal endothelial cell medium, with PSG, human serum, Hepatocyte growth factor (HGF) and vascular endothelial cell growth factor (VEGF) (Lalor *et al.* 2000b;Lalor & Adams 1999).

Although research involving macrovascular endothelium has provided useful insights, more interest lies in the microvasculature as this is where disease processes tend to occur. Isolation methods here prove more challenging as it is not possible to use cannulation. The majority of methods use physical dissociation of whole tissue followed by enzymatic digestion. Initial isolation methods involved allowing isolated cells to adhere and identifying cells with cobblestone morphology. In addition to endothelial cells, there were also contaminating adherent cells including fibroblasts, which tend to outgrow other cell populations. EC also have the propensity to differentiate in culture in response to the composition of culture medium. In order to minimise contamination a variety of purification methods can be used, cell preparations can be separated by size with meshes or filters of varying pore sizes and/or buoyant density via density gradient purification (Percoll, Optiprep). The desired endothelial population can then be positively/negatively selected using endothelial markers such as acetylated low-density lipoprotein (AcLDL) with flow cytometry or magnetic bead selection with CD31/CD146.

When the desired population of cells is obtained the challenge is then to maintain the phenotype of freshly isolated cells *in vitro*. Human cells require the presence of human serum in culture, whereas the inclusion of autologous serum in murine cultures is controversial, as serum has been shown to be toxic (Martinez *et al.* 2008). In both cases it is important however, to provide an artificial matrix to for the cells to adhere to, be it gelatin, collagen, fibronectin, vitronectin *etc*.

It is crucial to be able to phenotype and identify primary isolated cell populations. There are a number of characteristic endothelial cell features including CD31, CD34, and vWF (von Willebrand Factor) expression, uptake of ac-LDL, binding of lectins, ‘cobblestone’ morphology and the propensity to form tubes in matrigel. Although largely present on populations of endothelial cells these features are not universal and are more than likely to vary temporally and spatially *in vitro* and *in vivo* and between cultures accounting for their marked heterogeneity. vWF has been reported in sections of human liver, whereas expression is variable in cultured hLSEC. Studies using rat LSEC found that shortly after isolation CD31 is expressed intracellularly but after prolonged culture when LSEC dedifferentiate and lose characteristic fenestrations CD31 is found on the surface as with most other endothelium. As I previously mentioned EC are highly endocytic a number of scavenger receptors can be used to identify LSEC including stabilin-2 and Lymphatic Vessel Hyaluronan Receptor-1 (LYVE-1).

1.10 The Human Liver

The liver is the one of the largest organs in the human body, weighing approximately 1.4kg in women and 1.6 kg in men. Second in size only to the skin it is located in the right upper portion of the abdomen sitting underneath the diaphragm and protected by the rib cage. Consisting of two lobes, the larger right is separated from the left by the falciform ligament. The gall bladder, a pear shaped organ around 7-10 cm in length stores bile produced by hepatocytes is situated in a depression on the posterior surface of the liver. Bile is required to assist the digestion of fats by

emulsifying the fat into droplets, increasing the surface area upon which various lipases can hydrolyse the fat.

Figure 1. 3: Schematic of hepatic microvascular subunits and the portal triads.

Schematic diagram demonstrating the finer structure of human liver. Each of the hexagonal microvascular subunits consists of plates of hepatocytes. At each corner are the portal triads made up of branches of the hepatic artery, hepatic portal vein and bile duct. Blood flows from here through the fine sinusoids and drains through the central vein.

The liver receives blood from two sources, the hepatic artery provides around one third, delivering oxygenated arterial blood from the general circulation. The remaining blood flow is supplied by the hepatic portal vein, which supplies deoxygenated blood directly from various points along the gastrointestinal tract. Portal blood contains numerous nutrients, waste products and metabolites absorbed and produced during digestion. Blood from both sources then flows through the liver tissue and out through branches of the central vein.

Each of the liver lobes consists of many lobules or ‘hepatic microvascular’ subunits (Matsumoto *et al.* 1982). These lobules are the main functional unit of the liver (Fig. 1.3) Separated by various blood vessels and connective tissues they have a characteristic hexagonal shape consisting of rows of hepatocytes radiating out from the central hepatic vein. Located at the corners of each lobule are portal triads, comprising of branches of the hepatic artery, hepatic portal vein and bile duct. Radiating out from the portal triad, forming an irregular vascular network throughout the hepatocytes are the blood filled liver sinusoids that create a connection to the central vein. Blood entering the liver flows through the sinusoids and over the rows of hepatocytes before collecting in the central vein (Sherlock *et al.* 1993).

This characteristic dual blood supply enables the liver to perform its biological functions absorbing, metabolising, storing and detoxifying macromolecules and clearing foreign antigens from the blood. The presence of nutrient-rich portal blood means that the liver is constantly exposed to gut derived antigens and particles of food and is in a favourable position to metabolise protein, ignore harmless food antigens and clear any harmful pathogens, which may enter the system. The liver is also an important immunological organ with a large resident population of rapidly

responsive immune cells providing essential immune surveillance (Lalor & Adams 2002;Lalor *et al.* 2002b;Lalor & Adams 1999).

1.11 Immortalisation of cells

Due to the difficulty of isolating primary cell populations immortalised cell lines have been developed to allow further research and understanding of endothelial cell function. Two methods of immortalisation have been developed utilising viral mechanisms to prevent senescence. Care must be taken when utilising cell lines as the immortalisation process can result in phenotypic changes or an altered response to cytokines. H-2KB-tsA58 transgenic mice express a thermolabile strain (tsA58) of the simian virus (SV40) large T-Antigen linked to an inducible major histocompatibility complex H-2K promoter. T-Ag expression is only apparent when cells are cultured at the lower temperature of 33°C and promoter activity can be up regulated by the addition of IFN-γ. I have utilised a cardiac endothelial cell population using this method. mUCEC-1 have been shown to rapidly expand in culture, respond to growth factors and cytokines (TNF-α, IL-1β and LPS) and express appropriate adhesion molecules involved in leukocyte recruitment including CD31, Endoglin, ICAM-1/2, and VCAM-1 (Lidington *et al.* 2002). In addition cells can be isolated from hemangiomas (vascular tumours) generated by a retroviral construct encoding polyoma middle-sized T-Ag from skin, heart, brain and whole embryos. The remaining s.End (Bussolino *et al.* 1991) and b.End.5 (Rohnelt *et al.* 1997) cells used in my project were immortalised using this method (Bussolino *et al.* 1992).

1.12 Genomic Analysis: Gene Array Technologies

The use of array analysis in scientific research is ever increasing allowing the study of whole organism biology and how proteins, genes and other molecules interact to alter the behaviour of organisms. Several types of arrays exist from macro to micro investigating areas associated with proteomics, metabolomics and genomics (Hobman *et al.* 2007).

DNA microarrays in particular allow genomic analysis of cells or organisms. This technology relies on detecting interactions between molecules immobilised to a solid substrate with a complex mix of nucleic acids in solution. Nucleic acids (DNA/RNA) bind to complimentary sequences under optimal salt concentrations in solution and temperatures. Comparisons can be made between treatment groups independently or in competition with each other to examine differentially expressed genes (transcriptional profiles) (Zheng *et al.* 2007).

RNA samples are run on 'in house' or commercially available arrays, most of which consist of immobilised oligonucleotides. Fluorescently labelled nucleotides (cDNA) bind to the probes, images of which are obtained by scanning the array producing a map of spots to which opposing sequences have bound representing the level of transcription of that gene. Data is subjected to stringent statistical analysis to remove outliers and are then further selected on the basis of a fixed fold-change (Loos *et al.* 2001). Gene lists can be used to generate graphical representations of expression to highlight differences between populations or treatment groups. Further pathway analysis can generate data indicating which biological pathways or processes

differentially expressed genes are involved in providing an interesting insight into the data obtained.

A large amount of DNA microarray data is available, and some concerns mouse models of disease, in particular in this context inflammatory diseases such as atherosclerosis (Yuan *et al.* 2009) and psoriasis (Wolfram *et al.* 2009). Studies on endothelial cells from murine aortic walls in mice susceptible to atherosclerotic lesion formation showed between 590 and 1514 differentially expressed genes (Kobayashi *et al.* 2005). Subsequent pathway analysis suggested a role for calcium signalling in regulating atherosclerosis (Yuan *et al.* 2009). In addition genome wide analysis on skin from a murine model of scleroderma discovered differences in chemokine (CCL2, MIG etc), growth factor (VEGF-α, FGF-1) and adhesion molecule (VCAM-1 and Selectins) expression consistent with inflammatory conditions (Zhou *et al.* 2006). The use of this experimental tool may expose useful therapeutic targets and provide insights into disease pathology allowing the progression of research.

In the current study, broad phenotypic analysis was carried out using whole genome murine oligo gene arrays. However we selected specific genes from the whole array, in order to compare the phenotypes of the specific endothelial cells. We included a panel of common ‘endothelial phenotypic markers and adhesion markers which are described below.

1.13 Endothelial cell markers

The expression patterns of a number of different endothelial cell markers were examined on endothelium from all organs.

1.13.1 CD34

CD34 is a 105-120 kDa type 1 transmembrane sialomucin protein expressed of haematopoietic precursors and on the vascular endothelium of several organs (Baumhueter *et al.* 1994). It has been discovered that peripheral blood cells positive for CD34 can differentiate into ECs. In humans this molecule is not normally found on the sinusoidal endothelium (Couvelard *et al.* 1993;Daneker *et al.* 1998), except during disease in a process known as ‘capillarisation’ (Cui *et al.* 1996;Frachon *et al.* 2001). Although CD34 can be used as marker for sinusoidal neoangiogenesis in hepatocellular carcinoma in conjunction with VEGF (Ohmori *et al.* 2003). The expression of this molecule in rodent models has been studied by Baumhueter *et al* (Baumhueter *et al.* 1994) and was found that the global expression of murine CD34 on vascular tissues and its ability to act as a ligand for L–selectin was dependent on various posttranslational carbohydrate modifications and that an appropriately glycosylated form of CD34 could mediate leukocyte trafficking to both lymphoid and non-lymphoid tissue.

1.13.2 Endoglin

Endoglin or CD105 is a transmembrane glycoprotein of 658 amino acids residues that contains an extracellular domain, a single transmembrane domain and a short intracellular domain. Acting as a TGF-β type 3 auxiliary receptor (Cheifetz *et al.* 1992), endoglin is normally expressed as homodimers on the cell surface linked by disulfide bridges, which has been observed on the surface of microvascular endothelial cells (ten Dijke *et al.* 2008). Endoglin is thought to be expressed on most endothelial cells to some extent with levels increasing in activated vascular endothelial cells at sites of angiogenesis, inflammation and wound healing (Goumans *et al.* 2008). Its involvement in vascular development, remodelling and angiogenesis (Duff *et al.* 2003;Fonsatti *et al.* 2004) and elevated levels of expression in cancerous tumours make it attractive as a potential therapeutic target (Carmeliet *et al.* 2000).

1.14 Adhesion molecules involved in leukocyte binding to endothelial cells

The pattern of adhesion molecule expression varies in the presence or absence of inflammation. This allows targeted recruitment and infiltration of specific leukocyte subsets to tissues providing the correct combination of molecules. These adhesion molecules can be grouped according to not only structure and function but also the stage of recruitment they are involved in.

1.14.1 The Selectins

Selectins are a group of adhesion molecules involved in the intial tethering and rolling stages of leukocyte recruitment of which there are 3 types L, P and E-Selectin. These calcium dependent type 1 transmembrane glycoproteins are classified by the cell type in which they were discovered, leukocytes, platelets and endothelium respectively. Selectins consist of a common N-terminal lectin domain, an epidermal growth factor domain, a variable number of concensus repeats (CR), a single transmembrane domain and a short cytoplasmic tail. Variation in the number of CR's and within the N-terminal domain accounts for differences in adhesion molecule function. If the number of CR's is altered it can alter the ability of selectins to tether leukocytes (Patel *et al.* 1995). Both E and P-Selectin have been shown to be critical for leukocyte recruitment in intravital studies (Lawrence *et al.* 1991;Zimmerman *et al*. 1991;Zimmerman *et al.* 1992), however more recent studies have shown that they are not essential as CD44, CD34 and VAP-1 can replace them. E-Selectin (CD62E/ELAM-1) is expressed rapidly and synthesised *de novo* in activated endothelium in response to inflammatory mediators. During an inflammatory response P-Selectin is immediately trafficked to the cell surface from Weibel-Palade bodies, followed closely by E-Selectin leading to enhanced leukocyte recruitment and decreasing rolling velocity, increasing the chances of firm adhesion to the endothelium. Selectins bind to heavily glycosylated carbohydrate or mucin ligands including sialyl lewis and P-Selectin glycoprotein ligand (PSGL-1). E-Selectin binds both of these ligands, in addition to CD43, CD44 and E-Selectin ligand-1.

1.14.2 The Integrins

Integrins are involved in tight adhesion of the leukocyte to the endothelium. Chemokines present on the vascular surface activated the leukocytes leading to high affinity adhesion through integrins and their receptors.

1.14.2.1 ICAM-2

ICAM-2 (intracellular adhesion molecule-2) is a member of the Ig gene superfamily which share a limited sequence similarity which conserves their tertiary structure. Intracellular adhesion molecule 2 is a critical player in lymphocyte recruitment and extravasation (Li *et al.* 1993). ICAM-2 or CD102 is constitutively expressed on endothelial cells even in their resting state and is essential for interaction of lymphocytes and endothelial cells through integrins in particular for ICAM-2, LFA-1 (lymphocyte function-associated antigen 1; αL β2) expressed on circulating leukocytes (Oppenheimer-Marks *et al.* 1991) (Reiss *et al.* 1998), This expression in unstimulated endothelial cells implicates ICAM-2 in the process of immune surveillance where leukocytes traffic through uninflamed tissues. It has been shown by Reiss *et al* that if ICAM-2-deficient mouse endothelioma cells are used in a transmigration assay the migration of T-cells across the endothelial surface was greatly inhibited compared to the migration across wild type cells treated with anti-ICAM-2 functional blocking antibodies (Reiss *et al.* 1998).

1.14.2.2 VCAM-1

Vascular cell adhesion molecule or CD106 is another member of the large Ig gene superfamily expressed on activated endothelium and a ligand for VLA-4 (very late antigen α4 β1) (Steinhoff *et al.* 1993;Scoazec *et al.* 1991;Worthylake *et al.* 2001). VCAM-1 is involved in the initial step of the leukocyte recruitment cascade 'tethering and rolling' of the leukocyte in conjunction with the E and P- Selectins, although under flow conditions VCAM-1 supports the capture of leukocytes at lower shear stresses than the selectins and is thought to effectively capture eosinophils. Expression of VCAM-1 is required *de novo* and synthesis peaks 24 hours after stimulation (Reinhardt *et al.* 1998).

1.14.3 Junctional Molecules

Following tight adhesion to the endothelial surface the leukocytes must then enter the surrounding tissues to home to the site of inflammation. In order to do this they must traverse the endothelial cell barrier and underlying basement membrane and stromal cells. A number of different adhesion molecules are expressed at endothelial cell junctions aiding the process of transmigration and extravasation.

1.14.3.1 CD31

CD31 or PECAM-1 (platelet/endothelial cell adhesion molecule) can be used as a pan-endothelial marker. It is a transmembrane glycoprotein of ~ 130 kDa (Schenkel

et al. 2004;Newman *et al.* 1990). A member of the immunoglobulin superfamily (Newton *et al.* 1999) it has been shown to be important in mediating both homo and heterophilic cellular interactions (Delisser *et al.* 1993;Piali *et al.* 1995;Zocchi *et al.* 1996) and be involved in signalling events accredited to two ITIM (Immunoreceptor tyrosine-based) motifs on the cytoplasmic tail (Schenkel *et al.* 2004). This cell adhesion molecule has six Ig-like domains and is abundantly expressed on endothelial cell borders and diffusely over the surface of platelets, monocytes, neutrophils and subsets of T-Cells. CD31 is widely used, as a marker of 'continuous' or classic vascular endothelium but the presence of this marker on LSEC remains controversial. CD31 has been shown to be expressed on liver sinusoidal endothelial cells in primary biliary cirrhosis liver biopsies. The tubule like expression pattern of CD31 in conjunction with VCAM-1 is an indicator of neovessel development in an attempt to repair liver damage (Medina *et al*. 2005). It has however been shown in rodent studies to be present in normal sinusoidal endothelium (Neubauer *et al.* 2000a) (Do *et al.* 1999). It has been suggested however that in disease CD31 is down regulated on LSEC after treatment with pro-inflammatory factors such as Carbon tetrachloride (CCl_4) and TNF-α as observed in cultured rat endothelium (Neubauer *et al.* 2000b). Conversely CD31 expression has also shown to be absent in normal tissue and this expression profile along with CD4 expression can be used as a method of isolating rodent LSEC cells (Knolle *et al.* 1999). CD31 has shown to be very important in influencing several aspects of leukocyte migration and is thought to create a haptotactic (surface bound) gradient directed toward the intercellular junctions guiding leukocytes through their migratory route (Neubauer *et al.* 2000a).

1.14.3.2 JAM-2

JAM-2 or junctional adhesion molecule 2 is a member of the JAM family of which there are three members (Luscinskas *et al.* 2002b). The JAM's are also members of the Ig superfamily, and one of three transmembrane proteins present in intercellular tight junctions along with occludin and claudin (Johnson-Leger *et al.* 2003;Muller 2003). JAM-2 has been shown to localise to newly formed cell-cell junctions within minutes (Johnson-Leger *et al.* 2000). It has been postulated that JAM-2 may interact with JAM-3 to mediate lymphocyte homing (Luscinskas *et al.* 2002b). Although JAM-2 may bind to JAM-3 it may also interact with many other molecules including GM-CSF (Granulocyte Macrophage- Colony Stimulating Factor), several subsets of circulating NK (Natural Killer) cells and T-cell lines. The role of JAM-2 in transendothelial migration of lymphocytes has also been investigated. JAM-2 is highly expressed during embryogenesis (Aurrand-Lions *et al.* 2002b;Johnson-Leger, *et al.* 2000;Michel Aurrand-Lions *et al.* 2001) and then in adult populations it becomes restricted to the endothelium of HEV's present in secondary lymphoid tissue such as the spleen and Peyer's patches (Johnson-Leger *et al.* 2002; Aurrand-Lions *et al.* 2001). In murine cases JAM-2 has shown to greatly increase the proportion of lymphocytes migrating across endothelioma cells in monolayer culture (Johnson-Leger *et al.* 2002). Also in a human experimental system using HUVEC cultured on transwell inserts when abrogated using anti-JAM antibodies or soluble JAM, the transmigration of peripheral blood leukocytes across the HUVEC, which express JAM-2 was blocked. The same group obtained results that suggest this is also true in the murine system (Johnson-Leger *et al.* 2002).

1.14.3.3 CD99

CD99 is a heavily glycosylated transmembrane protein around 32 kDa and is another member of the Ig superfamily of adhesion molecules (Luscinskas *et al.* 2002a;Luscinskas *et al.* 2002b). Present on a broad range of haematopoietic cells it is thought by Schenkel *et al* (Schenkel *et al.* 2002) to be localised to the endothelial cell to cell borders and in addition on the surface of peripheral blood monocytes (Schenkel *et al.* 2002). It has been postulated that CD99 plays an important role in monocyte transmigration mediating the interaction between CD99 present on the two opposing cell types, although it is not known as yet whether CD99 plays the same role in the migration of other lymphocyte subsets (Luscinskas *et al.* 2002a;Luscinskas *et al.* 2002b). When blocked, diapedesis of monocytes was reduced by 90% distal to the point of action mediated by CD31, when both these molecules were blocked transmigration was almost completely abolished (Schenkel, *et al.* 2002).

1.15 Markers of mLSEC

In addition to traditional endothelial cell markers and adhesion molecules involved in the recruitment cascade, the expression of sinusoidal associated molecules was assessed in this study. LYVE-1 and VAP-1 expression is not limited to LSEC however the presence of these molecules in addition to other physical sinusoidal characteristics such as fenestrations can be used to identify LSEC. As mentioned previously, no one marker can be used to identify mLSEC populations rather a set of characteristic properties.

1.15.1 LYVE-1

LYVE -1 is one of a number of receptors for hyaluronic acid (HA) an extracellular matrix mucopolysaccharide. It has been suggested that the ability of LYVE-1 to bind hyaluronic acid (HA) in liver sinusoidal endothelial cells could be a process that is tightly regulated *in vivo* (Jackson *et al.* 2001;Jackson 2003). In diseased livers, in particular cirrhosis and primary liver cancer or HCC (hepatocellular carcinoma), the expression of LYVE-1 is unusual as it is absent in tumour blood vessels and regenerative hepatic nodules which develop in cirrhotic livers, this absence however is not seen in the lymphatics of diseased patients. There is a difference in the vascular structures of normal and diseased livers, in diseased livers the sinusoids resemble capillaries, identified by decreasing number and diameter of the characteristic fenestrae and the appearance of a basement membrane and increased serum HA (Fausto *et al.* 1991)**.** In cirrhosis these characteristic symptoms of capillarisation could be due to TGF-β (transforming growth factor beta) having adverse effects on the fenestrae and increasing HA synthesis by Ito cells and hepatic stellate cells involved in liver fibrosis. HA is a key molecule involved in cell migration during inflammatory responses, wound repair and embryogenesis (*Reed et al.* 1992) it is turned over rapidly with a half life of ~24 hrs (Prevo *et al.* 2001;Reed *et al.* 1992). The majority of these HA-binding proteins contain a HA-binding domain called the 'Link' module, only one of these receptors is a cell surface receptor, CD44 an 80-95 kDa protein expressed on leukocytes and erythrocytes to which LYVE-1 has significant homology (Jackson *et al.* 2003;Kohda *et al.* 1996). In CD44 knockout mice it is thought that LYVE-1 may compensate for its function in binding HA in response to pro-inflammatory cytokines and directing extravasation of leukocytes. LYVE-1 was also discovered to be an important molecule in the lymphatics as expression is high

on human, mouse and rat endothelial cells (Banerji *et al.* 1999). It has also been found in distinct cohorts of activated tissue macrophages and on LSEC and endothelial cells of the spleen, sites where HA is taken up and degraded (Carreira *et al.* 2001;Grant *et al.* 2002).

1.15.2 VAP-1

Vascular adhesion protein 1 is a homodimeric 170 kDa sialylglycoprotein (Kirton *et al.* 2005) which possesses dual functionality as both a semicarbazide sensitive amine oxidase (SSAO) which catalyse oxidative deamination of primary amines and an adhesion molecule regulating leukocyte transmigration (Salmi *et al,* 2001). Identified in the late 1980's VAP-1 was first characterised as an endothelial molecule acting as an 'address code' for lymphocyte homing to inflamed joints. Expression of VAP-1 however is not solely isolated to the synovial vessels it was first discovered in. Staining with monoclonal antibodies directed against VAP-1 indicated that it is expressed in high endothelial venules (HEV's) in lymphatic organs, LSEC and the small vessels of other tissues (Salmi *et al,* 2001) but unusually absent from all leukocytes. Another form of VAP-1 with different oligosaccharide modifications is however expressed in other cells such as adipocytes, pericytes and smooth muscle cells suggesting that these two forms may have differential functions (Jaakkola *et al.* 1999).

The level of VAP-1 expression seems to be tightly controlled. VAP-1 is stored in intra-cellular granules and expression has been shown to be induced in pigs and dogs only in inflammatory situations, indicated by examining the distribution of

intravenous anti VAP-1 monoclonal antibodies (MAbs) throughout the whole experimental animal (Salmi *et al.* 2001). This expression pattern is similar to P-selectin, which is selectively expressed upon inflammation. In flow systems designed to mimic the shear stresses of *in vivo* situations, VAP-1 expressed on hLSEC, rabbit endothelium and transfected rat endothelium has shown to bind flowing lymphocytes, but knockout models indicated that the absence of VAP-1 leads to increased rolling velocity and decreased rate of leukocyte transmigration (Kirton *et al.* 2005). VAP-1 is an essential part of the process of lymphocyte transmigration under non-static conditions.

1.16 Outlines of project

The liver is an important immunological organ inducing tolerance and combating pathogens. A large amount of leukocyte recruitment occurs in this tissue and the unique environment of the liver sinusoids provides intriguing insights into recruitment during inflammatory disorders. We are interested in how recruitment in liver compares to mechanisms controlling recruitment in other organs, which differ not only physiochemically but immunologically. The aim was to investigate the phenotypic differences in EC from different locations and examine how these relate to the functional ability of the endothelium to regulate adhesion and transmigration in immune surveillance and inflammation. Phenotypic variation was assessed using whole gene arrays, cell-based Enzyme linked immunosorbant assay (ELISA) and immunohistochemical techniques. Functional capabilities of endothelial cell populations were tested using flow-based and static adhesion assays developed at the University of Birmingham. These experiments allow the investigator to not only examine the effect of various treatments and manipulate parameters of the physiochemical environment under physiological conditions but also assess all stages of the leukocyte recruitment cascade in real time.

2. METHODS

2.1 Isolation and maintenance of primary endothelial cells

Much of this thesis was concerned with reviewing and developing methods used to isolate primary murine endothelial cells. Liver sinusoidal and brain microvascular endothelial cells were of particular interest due to the unusual phenotype. The majority of this research and method development is outlined in Results Chapter 1. Here I will briefly touch on generic methods for isolating and culturing primary endothelial cells. When reviewing the literature regarding endothelial cell isolation methods, there are several stages in common, outlined in Figure 2.1 below. Each isolation method is broadly split into three stages, dissociation of the tissue, and separation of component cell populations and selection of endothelial cell type of interest. We tried several different isolation protocols using a number of different methods of dissociation, separation and selection. In addition cells were cultured under a number of different conditions. We used several basal mediums RPMI, DMEM, EBM, growth factors EGF, HGF, VEGF, ECGF cultured on gelatin or collagen substrates.

Figure 2. 1: Schematic of general endothelial cell isolation protocols including details of isolation methods used in this thesis.

Each method can be broken down into three distinct steps, dissociation of the tissue, separation and selection. All isolations follow a similar pattern.

A single celled suspension of the tissue of interest is obtained using a combination of proteolytic enzymes and physical dissociation. Cells are then separated on the basis of size and relative buoyancy using density centrifugation materials to remove debris and contaminating cell populations. Cells at the desired gradient interface are then further positively or negatively selected using an antibody bead step and are plated out onto tissue culture plastic coated with basement membrane proteins to aid cell adherence.

In the case of primary cell populations used in this research primary endothelial cells were pelleted and gelatin coated tissue culture vessels. Livers sinusoidal EC were cultured in Roswell Park Memorial Institiute (RPMI) with 100U/ml penicillin, 100ng/ml streptomycin and 2mM glutamine, whereas brain microvascular EC were cultured in complete BMEC medium consisting of Dulbecco's Modified Eagles Medium (DMEM) (Gibco, UK), 20% Foetal Calf Serum (FCS) (Sigma, UK), 10ng/ml EGF, 10ng/ml VEGF (Peprotech, UK), 100U/ml penicillin, 100ng/ml streptomycin and 20mM HEPES (Sigma, UK) both at 37°C in a humidified 5% CO_2 incubator.

2.1.1 Isolation of mLSEC via in situ perfusion of murine liver

Male C57BL/6 mice were obtained from Biomedical Services Unit, Birmingham UK and Schedule 1 was performed by cerviacal dislocation prior to procedure. The mouse was stretched out and pinned in place on a platform. A wedge of tissue was placed underneath the lower thoracic region to elevate the abdomen and expose the liver. All buffers (Appendix) were heated to ~40°C in a water bath and used to prime all tubing to remove bubbles. The peritoneum was cut and the portal vein (PV)

visualised using a dissecting microscope. The PV was incised above the branch of the vein and rapidly cannulated. The inferior vena cava (IVC) was cut to allow buffers to wash through the liver and flow rate was increased from 3ml/min to 7ml/min. Enzyme buffer was then perfused through the liver until the edges of liver lobes became transluscent. The cannula was removed and perfusion stopped. The liver was carefully removed from the abdomen and transferred to a petri dish in perfusion buffer. The gall bladder and glissons capsule was removed and the remaining liver tissue was disaggregated with forceps. The resulting cell suspension was stored at 4°C until transferred to the laboratory. Cells were spun 54G/2min/4°C to pellet hepatocytes which were discarded. The remaining supernatant was pelleted at 1349G/10min/4°C and resuspended in 5mls of preservation buffer. The cell suspension was layered onto a Percoll gradient (23/50% 10mls of each) and centrifuged at 1349G/30mins/4°C with no brake. The cells at the interface of 23% and 50% containing the non-parenchymal fraction were removed with a Pasteur pipette and washed in an excess of PBS at 1349G/10min/4°C. The resulting pellet was resuspended in ~2mls of RPMI, seeded into a petri dish and cultured at 37°C for 10 mins to allow Kuppfer cells to adhere. Adherent cells were washed vigorously to remove non-adherent LSEC that were then seeded into collagen coated culture vessels in basal RPMI and cultured at 37°C/5% CO2.

2.1.2 Isolation of mLSEC using Miltenyi αLSEC microbeads.

Murine livers were obtained from adult female Balb/c mice in BMSU, University of Birmingham. In initial experiments the number of livers used in each isolation varied, but it was found that multiples of 3 livers per prep was optimal. Livers were washed in phosphate buffered saline (PBS) to remove excess blood and diced using scalpels.

Collagenase Type 2 (Sigma, UK) was reconstituted to 0.25% in DMEM/10% FCS and filter sterilised, 5mls of which was added to homogenised tissue for ~5mins. An excess of RPMI/10% FCS was added to quench enzyme activity; the tissue suspension was then sieved through a fine mesh (60µm) and washed through with sterile PBS to give a final volume of 200mls. The tissue suspension was centrifuged at 30G/10min three times to remove hepatocytes pellets. Non-parenchymal cells were pelleted at 300G/10mins and resuspended in ~6ml RPMI/10% FCS. Three ml of 60% Optiprep (diluted with 0.85% Sodium Chloride-NaCl) was added to 1.5ml of cell suspension and mixed well to which 4ml of DMEM was layered on top and centrifuged at 400G/15 mins. The cells at the interface were collected and washed in an excess of PBS to remove Optiprep at 400G/5mins. The pellet was resuspended in ~100µl of PBS to which 15-20µl of α-LSEC microbeads were added (per 2-3 livers) and made up to 1 ml with DMEM before incubating at 15-20 mins on ice. Selection columns were placed within a magnetic field and washed with 500µl of PBS. Cells were washed 400G/5mins and resuspended in 300µl of PBS and passed through columns to which labelled cells attached. Columns were washed with three 500µl volumes of PBS, labelled cells were eluted in 1ml of PBS by removing the column from the magnetic field. Selected cells were pelleted at 400G/5mins and distributed between collagen coated vessels and cultured at 37°C/5% CO2 in DMEM containing 10% FCS, mEGF, HGF and VEGF (all 10ng/ml).

2.1.3 Isolation of mLSEC in the absence of selection method.

Murine livers were obtained from adult female Balb/c mice from 4th floor Thymus Development group, University of Birmingham. Livers were washed in PBS to remove excess blood and minced with scalpels. Tissue was incubated in 5ml/liver of

filter sterilised Collagenase Type 4 (Sigma, UK) reconstituted to 0.05mg/ml in DMEM/10% FCS for 40 mins at 37°C. Tissue suspension was mechanically digested in Seward Stomacher® 400 Circulator at 250rpm for 30 secs and passed through a fine tissue sieve (60µm) in an excess of PBS to a final volume of 200ml. Cells were pelleted at 400G/5min, resuspended in PBS and spun several times 40G/3min to remove hepatocyte pellets. The remaining supernatant was centrifuged at 400G/5min and resuspended in a combined volume of 5ml PBS/liver. Two ml of pure Optiprep per liver was added, mixed well and split between several 15ml Falcon tubes onto which 1ml of PBS was layered. Gradient was centrifuged at 400G/20min, cells at the interface were collected and washed in PBS at 800G/5min. Resulting cell pellets were resuspended in complete endothelial basal medium (1% FCS/10ng/ml VEGF) and plated out into collagen coated vessels and cultured at 37°C/5% CO2.

2.1.4 Isolation of mLSEC with Miltenyi αCD146 MACS kit.

Murine livers were obtained from adult female Balb/c mice in BMSU, University of Birmingham. Livers were washed in PBS to remove excess blood. Collagenase Type 4 (Sigma, UK) was reconstituted to 2mg/ml in DMEM/10% FCS and filter sterilised. Approximately 5 mls of collagenase was injected into liver tissue with a 21G needle prior to dicing the tissue with two scalpels. The remaining collagenase solution (5ml/liver) was added, transferred to a sterile beaker and incubated at 37°C for 40mins, agitating every 5-10 mins. Digested liver tissue was sieved through a coarse (200µm) then fine (60µm) mesh in an excess of PBS using a syringe bung. The resultant cell suspension was centrifuged at 1349G/7min/4°C, pellets were resuspended in PBS (10ml/3 livers) and layered over a Percoll gradient (23 over 50%

20mls of each) and spun at 1349/30min/4°C. Cells were removed from the gradient interface and washed in an excess of PBS and pelleted 1349G/7min/4°C. The pellet was resuspended in an appropriate volume of PBS and αLSEC (CD146) microbeads (Miltenyi), 90µl buffer to 10µl beads per 107 cells. Sample was incubated shaking on ice for 15-20 mins, washed in an excess of PBS, spun 1349G/7min/4°C and resuspended in ~1ml PBS. Magneticall activated cell sorting (MACS) magnets and MS columns were prepared and primed with 500µl of PBS/column. A 500µl aliquot of cells was passed through each column and then washed with three 500µl volumes of PBS. MS columns were then removed from the magnetic field and flushed through with 1ml of buffer. Both the 'waste' and 'cellular' fractions were pelleted and plated out onto gelatin coated tissue culture vessels in RPMI with 100U/ml penicillin, 100ng/ml streptomycin and 2mM glutamine and cultured at 37°C. This method produced a reproducible yield of primary cells, which were used in further experiments.

2.2 Culture and maintenance of cell lines

Three immortalised murine endothelial cell lines were used in this investigation. mUCEC-1 (mouse cardiac endothelial cells) were cultured in complete media composed of DMEM (Gibco, UK), 10% FCS (Sigma, UK), 10ng/ml mEGF, (Preprotech, UK) 100U/ml penicillin, 100ng/ml streptomycin and 2mM glutamine (Sigma, UK). The skin endothelioma cell line (s.END, gift from Roy Bicknell) and Brain endothelioma (b.End.5) were cultured in complete media composed of DMEM (Gibco, UK) and 10% Foetal Calf Serum (Sigma, UK). In addition b.End cells required DMEM containing 1mM sodium pyruvate and antibiotic and glutamine

supplementation (as above, Sigma, UK). Cells were plated in various different tissue culture vessels and maintained at 37ºC, in a humidified 5% CO2 incubator until confluent. To passage, cells were dissociated using 5 mls of Sigma TrypLe Express and re-plated at a ratio of 1:3. When confluent, cells cultured in chamberslides and multiwell tissue culture plates were fixed by removing growth media and replacing it with 500µl of cold methanol (Fisher Scientific, UK) for 5 mins. Fixed cells were washed 3 times in PBS and stored at 4°C until use.

2.3 FACS Analysis using a murine anti LSEC-FITC conjugated monoclonal antibody.

Here, the LSEC isolation protocol was carried out as outlined in Section 2.1.2 but only 2 slow spins at 30G for 10 mins were carried out. A 200µl aliquot of cells was removed at various stages throughout the isolation protocol as outlined below.

(1, 2) Post collagenase digest and fine mesh (x2)

(3) Post slow spin 1, supernatant

(4) Post slow spin 1, pellet

(5) Post slow spin 2, supernatant

(6) Post slow spin 2, pellet

(7) Pelleted NPC's

(8) Post OptiPrep gradient centrifugation

(9) MACS column waste

All samples were stored in 1.5ml Eppendorfs pre-coated in FCS and stored on ice. Samples were pelleted by centrifugation at 2500 rpm for 5 mins and washed in PBS + 1% FCS. Samples were resuspended in 50µl of antibody solutions summarised below and incubated in the dark, on ice for 30 mins. Rat IgG was used as the isotype control at 5µg/ml and the test antibody murine α LSEC-FITC (Miltenyi, UK) was used at 1/30 dilution of manufacturers stock. Dilutions were in PBS + 1% FCS.

Monoclonal Abs	Sample	Total Volume from which aliquot was extracted.
Rat IgG	1	20
αmLSEC-FITC	2	20
αmLSEC-FITC	3	180
αmLSEC-FITC	4	10
αmLSEC-FITC	5	180
αmLSEC-FITC	6	10
αmLSEC-FITC	7	8
αmLSEC-FITC	8	1
αmLSEC-FITC	9	4

Table 2. 1: Table of samples extracted, monoclonal antibodies with which they were labelled and total volumes from which they were extracted.

Samples were diluted in and additional 1ml of PBS-FCS and pelleted and finally resuspended in 500µl of PBS-FCS and analysed on Coulter Epics XL FACS machine to visualise distinct cell populations and analyse expression levels of FITC fluorophore.

2.4 Immunohistochemical staining of murine tissue sections

2.4.1 Preparation of tissue sections

In order to visualise localisation of molecules of interest in murine tissues we used Immunohistochemical and immunofluorescent staining. Murine tissue was obtained from Balb/c and C57BL/6 mice that were surplus to requirements. Fresh brain, liver,

lung and kidney were snap frozen in liquid N2 and stored at –70ºC prior to sectioning. Frozen organs were embedded in OCT mountant (TissueTek Thermo Shandon) and 5 or 10µM sections were cut using a cryostat (Bright OTF) and mounted on glass microscope slides (BDH UK) coated with 0.01% Poly-L-Lysine (Sigma, UK). Once mounted, sections were fixed in acetone (Fisher Scientific, UK) for 2 mins, wrapped in foil and stored at –20ºC.

2.4.2 Demonstration of molecule expression by Immunohistochemical staining (IHC)

Sections from murine organs, chamberslides (Nalge Nunc International, USA) containing cell lines at various passages and primary murine endothelial cells were all stained using the following method. All the monoclonal antibodies used for Immunohistochemical staining are summarised in Table 2.2

Monoclonal Abs	Source	Final Concentration (IHC)	Final Concentration (ELISA)
Rat IgG Control	Sigma, UK	25µg ml^{-1}	5µg ml^{-1}
Rabbit IgG Control	Sigma, UK	5 µg ml^{-1}	5µg ml^{-1}
RαM CD31	Serotec, UK	25µg ml^{-1}	5µg ml^{-1}
RαM VAP-1	Gift of David Smith*	25µg ml^{-1}	5µg ml^{-1}
RαM VCAM-1	Serotec, UK	25µg ml^{-1}	5µg ml^{-1}
RαM CD99	Gift of Gabi Bixel	25µg ml^{-1}	5µg ml^{-1}
RαM ICAM-2	BD Biosciences, UK	25 µg ml^{-1}	5µg ml^{-1}
RabαM LYVE-1	Abcam, UK	1,5 µg ml^{-1}	1,5 µg ml^{-1}
RαM CD34	Serotec, UK	25 µg ml^{-1}	5µg ml^{-1}
RαM JAM-2	Serotec, UK	25 µg ml^{-1}	5µg ml^{-1}
RαM Endoglin	BD Biosciences, UK	1.5 µg ml^{-1}	1.5 µg ml^{-1}
RαM E-Selectin	Abcam, UK	25 µg ml^{-1}	5µg ml^{-1}
Gt α Rat HRP	Sigma, UK	1/1000 of stock	1/500 of stock
GtαRab-HRP	Serotec, UK	1/2000 of stock	1/2000 of stock
Gt α Rat-Alexa Fluor 633	Invitrogen, UK	1/1000 of stock	N/A

Table 2. 2: Source and working concentration of monoclonal antibodies (MAbs) used in immunohistochemical staining of experimental samples.

All antibodies were diluted in PBS. VAP-1 kind gift of David Smith, University of Oxford.

Prior to staining, all samples were equilibrated to room temperature before being re-fixed in acetone for 10 mins. After air-drying, samples were labelled and a wax pen was used to draw a line round the tissue section to create a small well to retain antibody solutions. Slides were pre-wetted with PBS wash buffer before staining, to prevent desiccation of samples.

Tissue sections were incubated for 20 mins in blocking solution (1% Goat serum in PBS) to abrogate non-specific binding of antibodies. Samples were incubated in a humidified chamber and placed on a rocker to ensure complete coverage of samples in the antibody solutions. Sections were washed (3x in PBS) and incubated with 150µl of relevant primary mAbs (monoclonal antibodies) directed against the molecules of interest for 1 hour. Purified immunoglobulins (IgG's) were used as negative control antibodies at equivalent concentrations and assessment of non-

specific staining of the 2° MAb was permitted by omission of the primary mAb step in some wells. Post primary antibody incubation, slides were washed and quenched in 0.5% w/w H_2O_2 in methanol with sodium azide for 5 mins. After washing three times in PBS the Horseradish Peroxidase (HRP)-conjugated secondary antibodies were added for a further hour.

Following a final wash in an excess of PBS positive staining was visualised by the addition of DAB (DAKO EnVision Detection System) substrate prepared according to manufacturers instructions. Sections were incubated for ~5 mins to permit development of a HRP-catalysed colour reaction in the substrate resulting in the formation of a brown-black precipitate. Staining was normalised against 5 minute staining time. Samples were quenched by immersion in distilled H_2O and incubated with haematoxylin counterstain (Sigma, UK) for ~30 seconds before being rinsed in tap water. Sections were dehydrated in increasing concentrations of Industrial Methylated Spirits (IMS) (50/70/90/100%) for 2 mins in each followed by a final 2 mins in Xylene before mounting with glass coverslips and Immunomount (Shandon, USA). Sections were examined using an Axioskop 40 microscope and images captured using a digital camera and Axiovision software (Karl Zeiss, UK). Samples were assessed according to staining intensity compared to negative isotype matched control and positive CD31.

Cells cultured in chamberslides were stained in a similar fashion to that described above for sections. Here antibodies and substrates were added into each well of the 8-welled chamberslides and the chambers were removed from the cells after the addition of the DAB substrate prior to haematoxylin counterstain.

2.4.3 Demonstration of molecule expression by Immunofluorescent staining (IF)

Primary mLSEC cultured on glass coverslips were stained using immunofluorescent methods to visualise the location of markers of interest using confocal microscopy. Prior to staining mLSEC were fixed with 4% paraformaldehyde (PFA) (Sigma, UK) for 10 mins and washed three times in PBS. Cells were permeabilised by the addition of ice-cold methanol for 10 mins at -20°C and then incubated for 20 mins in blocking solution (1% Goat Serum in PBS). Cells were washed (3x in PBS) and incubated with 150µl of primary antibodies in 1% Goat Serum in PBS (Table 2.2) for 1 hour. Isotype matched control and no primary were used as negative controls. Post-primary incubation the fluorescently conjugated secondary antibody (Goat α Rat- Alexa Fluor 633) was added for a further hour in the dark. Cells were washed to remove unbound antibodies, after the final wash, 200µl of DAPI (Fluka, UK) solution was added as a counterstain to each sample and incubated in the dark for 5 minutes. Samples were washed and dried and mounted on glass coverslips in non-fluorescent mounting media (Dako) to retard fading. Coverslips were examined on Axiovert 100M Confocal Microscope (Leica, Germany), images captured at x63 magnification using Axiovision software (Karl Zeiss, UK) and processed using LSM Image Browser.

2.5 Testing the specificity of α-mouse LSEC MAb using immunofluorescent methods.

In addition to IF of primary cells a modified immunofluoresence method was also used to localise the distribution of certain molecules of interest throughout murine liver tissue and also to examine the adherence of antibody conjugated MACS beads,

which were used in certain stages of this project. This method was adapted from the immunohistochemical technique outlined above. All washes as in the IHC were carried out in PBS and sections were fixed using the sodium azide method to reduce quenching of the fluorophores. Sections were stained with either Rat anti mouse (RαM) LSEC-FITC at 1/50 or 1/100 of manufacturers stock, an isotype match control (Rat IgG at 5µg/ml) or a no primary control (omission of the primary antibody). When examining the adherence of the α LSEC microbeads (MACS) a 200µl aliquot containing 10µl of beads (Miltenyi Biotech, UK), 10µl BSA (Sigma, UK) and 180µl of PBS was added to the tissue section in place of the primary antibody. A Rabbit α Rat-FITC secondary was used at 1/50 dilution of manufacturers stock for Rat IgG, beads and No Pri samples. In the case of sections stained with Rat anti mouse (RαM) LSEC-FITC antibody there was no need to use a primary as the antibody was already conjugated to the fluoroscein isothiocyanate (FITC) fluorophore. All incubations were carried out in a foil-wrapped tray to protect samples from light.

After the final wash in PBS, 200µl of DAPI (4'-6'-Diamidino-2phenylindole) (Fluka, UK) solution was added as a counterstain to each sample and incubated in the foil tray for 5 minutes. Samples were washed and dried and mounted on glass coverslips in non-fluorescent mounting media (Dako) to retard fading. Sections were then examined for staining using an Axiovert fluorescence microscope (Karl Zeiss, UK). Images were captured using a digital camera and Axiovision software (Karl Zeiss, UK)

2.6 ELISA protocol for endothelial cells in 96-well plates

Enzyme linked immuno-sorbent assays (ELISA) were used to quantify protein expression levels on cells cultured in 96-well tissue culture plates, and to assess the effects of cytokines on expression. The monoclonal antibodies used in this assay are outlined above in Table 2.3.

Cytokine	Stock Conc. (U/ml)	Dilution	Final Conc.
TNF-α	$1x10^5$	1/1000	100U
IL-1β	$5x10^6$	1/100,000	50U
IL-1β	$5x10^6$	1/50,000	100U
LPS	1mg/ml	1/1000	1µg/ml
IFN-γ	$1x10^5$	1/1000	100U
TNF-α + IFN-γ	$1x10^5$	1/1000	100U

Table 2. 3: Cytokine treatments for ELISA.
Cytokines (Peprotech, UK) were diluted in complete TCM and 100µl was added to appropriate wells for 4 or 24 hours before fixing the cells in methanol.

A confluent T75 flask of cell lines were passaged using TrypLE Express a third of which was resuspended in 10 mls of complete media (varied depending on cell line). 100µl aliquots were plated out into a 96 well tissue culture plate and incubated overnight in a 37°C/5% CO_2 constant temperature incubator to allow cells to adhere and spread. Semi-confluent, cells were stimulated with a combination of pro-inflammatory mediators (Table 2.3) in tissue culture medium (TCM) for 4 or 24 hours at 37°C. Stimulation was carried out at this stage to prevent rapidly dividing cells becoming overconfluent. After ensuring that the cells were confluent by light microscopy the media was removed and the cells were fixed in methanol (Fisher Scientific, UK). Plates were stored at 4°C for up to 2 weeks until ELISA development.

All wells were washed twice with 1% BSA (Sigma, UK) in PBS and incubated with 50-100µl of blocking buffer (PBS containing 1% goat serum) for ~1 hour. Wells were washed three times with PBS before addition of primary antibodies of interest (initial experiments were performed to optimise the concentrations at which primary and secondary monoclonal antibodies were used to obtain the most reliable results, outlined in Table 2.2) at various concentrations and incubated for 45 minutes. Isotype matched controls were used as negative controls with the addition of CD31 as a positive control at 2.5µg/ml. All tests were performed in triplicate. Wells were washed thrice with PBS and 50µl of the secondary antibody conjugated to horse radish peroxidase (HRP) was added and incubated at RT (room temperature) for a further 45 minutes.

The ELISA plate was developed using a substrate buffer that contained 1 OPD tablet dissolved in 3mls of distilled water and 1.25µl of 30% H_2O_2 solution (all Sigma, UK). After washing thoroughly with PBS, 50µl of freshly made substrate buffer was added to each well and incubated for ~5 mins. The ELISA plate was closely observed for appearance of brown chromagen yielded by the catalytic action of HRP and OPD. The reaction was quenched after 5 mins with 50µl of 0.5M sulphuric acid (H_2SO_4) and the plate was read at an absorbance of OD 490nm on a Synergy HT plate reader. Corrected values were obtained by taking the mean value of triplicate wells minus IgG control values.

2.7 Collection of liver and/or spleen from murine samples

Samples for lymphocyte isolation, generation of tissue sections and endothelial isolation were collected from freshly culled mice. Frequently tissue was extracted from mice that were excess to the experimental requirements or our laboratory or of other groups and would have otherwise been discarded. The source of tissue changed depending on what strain of mouse was available at the time tissue was needed. Thus we used carcasses of Balb/c weaners, adults and C57BL/6 adult mice obtained from Birmingham University Medical School Biomedical Services Unit (BMSU), the Thymus Development Laboratory, Institute of Biomedical Research and Dean Kavanagh, Institute of Biomedical Research, (all in Birmingham, UK).

To collect liver tissue samples, the mouse was stretched out on a polystyrene platform and fixed in place with several needles. The abdomen was liberally sprayed with alcohol to wet fur and prevent contamination of cells with fur or dander. The abdominal skin and peritoneum were cut exposing the internal organs. The multilobular liver was located and the ligaments holding liver in place were cut. The liver was removed and placed in plain RPMI-1640 /DMEM (Gibco, UK). This process was repeated several times depending on the number of animals used per isolation.

The spleen was removed in a similar fashion for use as a source of lymphocytes. The organ was isolated and any excess adipose tissue was removed before storing the spleens in RPMI-1640/DMEM.

2.8 Isolation and fluorescent labelling of murine splenocytes

The spleen was dissociated by gently pushing through a cell strainer in an excess of PBS. The resulting cell suspension was pelleted by centrifugation at 2000rpm/5 min and resuspended in ~2mls of RBC Lysis buffer (Sigma, UK). Cells were lysed for 5-10 mins before an excess of sterile PBS was added and cells were pelleted again. Cells were resuspended in RPMI+10%FCS, plated out in a T75 tissue culture flask and incubated overnight at 37°C for use in adhesion experiments.

After overnight incubation, the flask was agitated to aid detachment of the splenocytes from the tissue culture plastic and the cells were centrifuged at 2000rpm for 5min. Splenocytes were counted using Trypan blue exclusion and resuspended to a final density of 1x10-6/ml. Cell tracker green (CTG), a fluorescent dye was added to the cell suspension at a final concentration of 2.5µM and incubated at 37°C for 40 mins in RPMI 10% FCS. Cells were washed in an excess of medium and left to rest for 30 mins before use in functional assays.

2.8.1 Leukocyte subset isolation using MoFlo

In order to isolate CD4+/CD8+ cells from murine spleen, a mixed lymphocyte population was obtained, as outlined above. Cells were resuspended in 1ml PBS and a 50µl aliquot was removed for isotype matched control and FITC/PE single colour controls. The remaining sample was labelled with a combination of CD4+/CD8+ fluorescently conjugated antibodies (See Table 2.5). All samples were labelled for 20 mins at 4°, washed in PBS and filtered before running on MoFlo Cell sorter to isolate

single positive populations of >99% purity. Single positive lymphocytes were washed in PBS before labelling with cell tracker green.

Antibody	Manufacturer	Dilution
Rat IgG2a IMC-FITC	eBioscience	1/500
Rat IgG2b IMC-PE	eBioscience	1/1000
RαM CD8a-FITC	eBioscience	1/500
RαM CD4-PE	eBioscience	1/1000

Table 2. 4: Antibodies used for MoFlo sorting of T-Cell subsets CD4+ and CD8+

2.9 Isolation of murine neutrophils from bone marrow

Carcasses of adult male C57BL/6 or Balb/c mice were obtained and prepared as described previously. Bones were isolated from the legs and used as a source of bone marrow neutrophils. The skin was removed from both legs to expose the bone and muscle. Each leg was pulled at an angle to dislocate the hip from the pelvis so that the femoral head appeared. An incision was made past the head of the bone to allow the leg's removal. The remaining skin and muscle was removed to expose the leg bones. Bending the leg separated the upper and lower leg bones and an incision was made just past the patella. The foot was also removed at the ankle joint and any remaining skin and muscle was removed by scraping along the length of the bones with the scalpel. In the case of the lower tibia and fibula, the smaller fibula was separated from the tibia and discarded. All bones were kept on ice until required.

Incisions were made at the top and bottom of each bone to expose the red marrow. In the case of the fibula an incision was made where the marrow became red in colour. Approximately 2ml of calcium and magnesium free PBS **(**PBSA -Ca^{2+}/Mg^{2+}, Sigma, UK/Oxoid, UK) was flushed through the bore of each bone using a 21 gauge

needle, and collected into a 15ml Falcon tube, until the bones appeared white in colour. Eluted bone marrow cells were gently resuspended using a 25-gauge needle. This cell suspension was left for 5 min to allow the debris to settle out. The supernatant was collected and centrifuged at 200g for 5min. The supernatant was discarded and the pellet resuspended in 1ml 1% PBSA (PBS+BSA -Ca^{2+}/Mg^{2+}) to prevent clotting. Contaminating red blood cells (RBC) were lysed by the addition of 6ml of ice-cold distilled water to the sample. This was mixed for 30 seconds before adding 2ml of 4x concentrated PBS (-Ca^{2+}/Mg^{2+}) to the sample and centrifuging at 200g for 5min. The subsequent supernatant was removed and the pellet resuspended in 1ml PBSA (PBSA -Ca^{2+}/Mg^{2+}). A Percoll (Sigma, UK) density gradient was prepared by first mixing 9 parts Percoll with 1 part 10x PBS (Oxoid, UK). This 100% solution was diluted to several desired concentrations with PBS (52, 64 and 72%). In general, 2.5ml of each percentage was layered on top of one another in a 15ml tube, followed by 1ml of cell suspension and centrifuged at 1500g for 30min at 20°C. Each layer of Percoll, including the appropriate interfaces, was removed and transferred into 10ml round bottomed tubes. Each fraction was made up to 10ml with PBS (-Ca^{2+}/Mg^{2+}) and washed by centrifugation at 200g for 5min. The supernatant was removed and each fraction was resuspended in 1ml of PBSA (PBSA +Ca^{2+}/Mg^{2+}).

Bone marrow isolates, both before and after RBC lysis, and all Percoll fractions were counted using a Coulter Multisizer II (Coulter Electronics Ltd., Essex, UK) or a Neubauer haemocytometer to determine the number and size of the cells present in each sample. The Multisizer gave a frequency distribution of cell diameter, as an illustrated in Figs 2.2 and 2.3. This allowed cells in a given peak to be counted and aided assessment of RBC and debris. After counting, the middle Percoll fraction,

which contained the highest number of neutrophils and the least cellular debris, was diluted in PBSA (+Ca^{2+}/Mg^{2+}) to a final concentration of 10^6 cells/ml.

Figure 2. 2: Coulter Counter spectra of typical bone marrow isolates before and after red blood cell lysis step.

Each peak accounts for a distinct population of cells. The indistinct slope on the left accounts for cellular debris present in the sample. From this data you can estimate the total cell number, the size and the number of cells in each peak.

Figure 2. 3: **Coulter Counter spectra of typical bone marrow cell samples collected from the Percoll gradient at various interfaces.**

Each peak accounts for a distinct population of cells. The indistinct slope on the left accounts for cellular debris present in the sample. From this data you can estimate the total cell number, the size and the number of cells in each peak.

2.9.1 Morphological determination of neutrophil purity in bone marrow fractions

To assess what cell types were present in each bone marrow fraction, samples were centrifuged onto microscope slides using a Shandon Cytospin II (Scientific Instruments, South Trentham, UK). The slides were air dried for 15 mins and stained using DiffQuik (Dade Behring), fixed and viewed using light microscopy (LM). A differential count was carried out to determine the proportion of neutrophils present in each sample based on nuclear morphology. Murine neutrophils possess a characteristic doughnut shaped nucleus (apparent in Fig 2.4) as apposed to the segmented nuclei of human neutrophils

Figure 2. 4: Light microscope image (LM) of a typical cytospin sample from the middle fraction of the differential Percoll gradient used in the isolation of bone marrow derived neutrophils.

A 100ul aliquot of each gradient post counting was spun onto glass microscope slides using a Shandon Cytospin. Samples were spun at 500rpm for 5 min. Slides were then dried, stained with Diff Quik and mounted. Neutrophils can be identified by ring shaped nuclei. In this sample about 70% of cells are neutrophils. Images were captured using an Axiovert microscope at x10 magnification on Image ProPlus software.

2.10 Culture of murine endothelial cells for flow based adhesion assays

2.10.1 Microslide System

Microslides are glass capillaries with rectangular cross-section and internal length (L), width (W) and depth (D) = 50 x 3 x 0.3 mm (Camlab, Cambridge, UK). Microslides were pre-coated with APES (4-aminopropyl-triethoxysliane) as described (Cooke, Usami, Perry, & Nash 1993), to aid cell attachment to the surface. Briefly, microslides were soaked overnight in concentrated nitric acid and then rinsed first with water followed by acetone. They were immersed in APES (4% v/v in anhydrous acetone, Sigma, UK), for 30 seconds, rinsed with acetone and several changes of water, and finally autoclaved.

In preliminary experiments, microslides were also coated with 1% or 5% gelatin (Type B from Bovine Skin, Sigma, UK) solution in distilled water. Sterile gelatin solution (50µl) was injected into the microslides and incubated at 37°C for 30 min, after which slides were washed three times with 1ml of PBS before the addition of cells. However, it was discovered that collagen coating was more favourable. Sterile rat tail collagen (RTC) solution (50µl, in house preparation), diluted 1:1 with sterile PBS was injected into the microslides and incubated at 37°C for 1hr and 30 min, after which slides were washed three times with 1ml of PBS before the addition of cells.

In experiments using purified murine E-Selectin (gift of Dietmar Vestweber) instead of endothelial cells, the E-Selectin was diluted to the desired concentration in PBS and 50µl was injected into microslides and incubated at 37°C for 2 hours. The slide was then blocked with 1% PBSA for 1 hour before use.

For endothelial coating, one confluent 75cm^2 (T75) flask of the appropriate cell line was trypsinised and cells centrifuged at 2000rpm for 5min. The pellet was resuspended in 1ml of complete medium, 300µl of which was used to seed microslides. 50µl of cell suspension was injected into each of 6 microslides. The microslides were placed in a Petri dish on a sterile microscope slide and incubated at 37°C for 3h to allow the cells to settle and attach. Slides were then washed with 50µl of fresh medium to check a sufficient number of cells had attached to the surface to reach confluency within the desired time period. The microslides were placed in specially constructed culture dishes, which had been autoclaved. Microslides were attached to glass tubing ports, which had been fused into the wall of the dishes, using a short piece of silicone rubber tubing (2mm bore, 1mm wall thickness) and sterile forceps. Silicone rubber tubing was connected to each external arm. The dish was filled with culture medium and placed in a humidified CO_2 incubator. The tubing was passed though a port in the incubator wall (manufactured to order; either model GA2000, LEEC, Nottingham, UK or Nuaire DH; Triple Red, Thames, UK) and attached to a multichannel, 8-roller pump (Watson-Marlow 500 series pump with 308MC pumpheads; Watson-Marlow Bredel Pumps, Falmouth, UK), which pumped to waste. The pump was set to generate a flow rate (Q)=0.2ml/min for 30sec every 2 hours. Thus, medium contained in the microslide (~50µl) was changed regularly in order to permit prolonged growth and avoid hypoxia and media exhaustion. All of the above is outlined in Fig 2.5 below. Wall shear stress in the microslide was 0.05Pa during perfusion. Original seeding was at a density that yielded confluent monolayers in 24-48 hours.

Figure 2.5 Diagram of special culture dish for microslides constructed by the Glassware Workshop, School of Engineering, University of Birmingham, UK and culture system set-up for 'static' experiments.

The dish consists of a glass Petri dish with 6 glass adaptors fused into the wall, which seeded microslides are connected. The 6 adaptors are connected at the other end to lengths of tubing, which connect the microslides to a pump (Watson Marlow 5025). The system is designed to generate flow of medium across cultured cells every 2h to maintain viability. (Sheikh *et al.* 2004)

After 24 hours of culture under intermittent flow, the microslides were removed from the dish and stimulated with the pro-inflammatory stimulant at the desired concentrations. Cytokines were diluted in complete medium in the flow assay dish and reconnected for a further 24hrs of culture or 50µl of cytokine-containing medium was pipetted into each microslide every hour for 4 hours and microslides were returned to the incubator depending on the experimental requirements.

2.10.2 Culture of EC in IBIDI VI Chambers

Problems were encountered when attempting to examine the functional responses of primary LSEC under flow conditions using the microslide system due to the low cell yield. LSEC were seeded into gelatin-coated microslides but did not attach efficiently and those that did were of poor quality and appeared stressed. Fortunately a new system for culturing endothelial cells for flow assays became commercially available during my investigation. IBIDI VI chambers are made of gas permeable plastic negating the need for flow pumps and exchange of acidic medium during cell culture. The manufacturer supplies details of internal dimensions of the chambers and flow rates necessary to generate the required wall shear stress (Figure 2.6). Endothelial cells (lines and primaries) were rapidly seeded into each channel (30µl/chamber) to avoid air bubbles. The reservoirs were covered with the supplied lid and incubated at 37°C/5%CO2 to allow cells to attach on the accompanying rack, allowing sufficient gas exchange and air flow. Afterwards each reservoir was filled with ~60µl of cell free medium. For functional flow experiments the endothelium was stimulated with pro-inflammatory mediators. Control tissue culture medium was carefully removed from the reservoirs and replaced by capillary action with stimulating medium for 4 or

24hrs. At this point any non-adherent cells (primary cultures) can be removed by vigorous pipetting of PBS or culture medium through the channels.

Figure 2. 5: IBIDI VI flow chambers.

IBIDI VI chambers are made of gas permeable plastic allowing cells to be cultured in small chambers in ~30-50µl of medium. Cells can be subject to flow-based adhesion assays or fixed and stained to visualise molecules of interest.

2.10.3 Assessment of leukocyte adhesion to endothelial cells under flow using the microslide system.

Microslides containing confluent endothelial cells were glued to a glass microscope slide, mounted on a microscope stage, and viewed by phase-contrast videomicroscopy (Fig 9). One end of the microslide was attached via silicone rubber tubing to a Harvard syringe pump (Harvard Apparatus, South Natic, MA), allowing control of the flow rate through the microslide. The other end of the microslide was attached by silicon rubber tubing to an electronic valve (Lee Products, Gerards Cross, UK), permitting smooth switching between the leukocyte suspension and cell free buffer. Following insertion of the microslide into the flow system, EC's were washed with flow media (basal medium + BSA) to remove residual cytokines for 2 min. A 4-min bolus of leukocytes was perfused through the microslide, followed by a 2 min wash out with flow medium. The flow rate was chosen to yield wall shear stresses in the range of 0.05-0.2Pa as desired. Fluorescent videomicroscopic recordings were taken at various stages throughout the experiments (Fig. 2.7). During the last minute of the bolus and after 2 min of washout 5-10sec of video recordings were made of a series of fields, to visualise leukocytes interacting with the endothelium. The recordings were analysed off line using a computerised image analysis system (ImagePro; DataCell, Finchampstead, UK) or by manual counting. The numbers of adherent leukocytes were counted in the series of fields and corrected /mm2 /106 leukocytes perfused using the calibrated field size and known perfusion rate. Adherent cells were easily distinguished from non-adherent cells, which were visible only as faint streaks. The number of rolling cells was also determined by digitising several 5-sec fields during washout. The leading edge of the adherent leukocyte was marked and tracked over time. Rolling velocities were

calculated by taking the mean of the distance moved over the 5sec to give a value in μm/sec.

-

Figure 2. 6: Outline of apparatus used to carry out functional experiments using murine leukocytes.

The microslide or IBIDI VI chamber is secured onto the microscope stage and attached to the syringe pump outflow, which regulates the shear stress, and to the sample/wash reservoir. All tubing is primed before connection to allow a smooth transition between wash buffer and the murine leukocytes using an electronic valve. The microscope and the majority of the experimental apparatus are enclosed in a 37°C chamber. Video images are captured and analysed offline.

2.10.4 Assessment of leukocyte adhesion to endothelial cells under flow using the IBIDI VI System.

IBIDI VI chambers containing confluent endothelial cells were mounted on a microscope stage, and viewed by phase-contrast videomicroscopy, in a similar fashion to microslides. Male adaptors were attached to the standard flow assay tubing to fit neatly onto the corresponding female adaptors on IBIDI VI flow chambers allowing smooth perfusion of cell free buffer and sample over the endothelium. The assessment of cell adhesion under flow was then carried out as outlined in Section 2.10.3.

Figure 2. 7: Comparative images of endothelial cell lines and primary cultures in normal tissue culture compared to two methods used for functional flow assays; microslides and IBIDI VI chambers.

All images captured at x10 magnification on Light Microscope.

2.11 Static Adhesion Assays

In addition to flow based adhesion assays, static assays were carried out on all cell lines and primary cell populations. Endothelium was cultured in 24-well plates to semi-confluency before adding pro-inflammatory mediator containing medium (LPS 1µg/ml or TNF-α+IFN-γ 100U/ml) for 24 hours. Primary LSEC were allowed to settle for 2-3hrs before stimulation. Post incubation, medium was removed and replaced with 1ml of cell tracker green labelled lymphocytes at 0.5x106/ml in RPMI for 2 hours before fixation with methanol. The number of adherent lymphocytes in 10 fields per sample was counted using a fluorescent microscope and normalised to give number adherent/mm2.

2.12 RNA extraction using Qiagen RNeasy columns

Samples of RNA were extracted from samples of all cell lines and primary cells stimulated with a panel of cytokines for 24 hours using a quiagen RNeasy Mini kit according to manufacturers instructions. Post-stimulation cells were trypsinised (in the case of cell lines) or removed from tissue culture plastic surface with a cell scraper (primary isolates). The resulting cell pellets were disrupted with 350µl of RLT buffer containing β-mercaptoethanol (1µl βME/100µl RLT) and the DNA was sheared with a 21G needle. An equal volume of 70% ethanol was added to the DNA suspension before transferring to a Qiagen column, which was then spun at 10,000rpm for 15sec. RNA present on the membrane was then washed with 700µl of RLT buffer in each column and spun at 10,000rpm for 15sec, followed by 500µl of RPE and spun again. An additional 500µl of RPE was added and then spun for

2min/10,000rpm to dry the membrane. The RNA was then eluted by the addition of 2 x 40µl of RNAse free water to the column and spinning at 10,000rpm/15sec. The amount and purity of RNA was read using a Bio-Tek Synergy HT plate reader. Samples were diluted in RNAse free PCR water (5µl RNA: 95µl water) and read at 260/280nm, values were compared to a blank well containing only water and purity and concentration calculated accordingly. The integrity of the RNA was confirmed with analysis by the Agilent 2100 Bioanalyser (Palo Alto, CA, USA) using the RNA 600 LabChip^{TM} kit.

2.13 Analysis of differential gene expression in resting and stimulated endothelial cells using DNA microarrays.

All products were purchased from Agilent Technologies Ltd (Wokingham, Berkshire, UK) unless otherwise noted.

2.13.1 Labelling

400ng RNA from each sample and 3µl (1:2500 dilution) Agilent One-Colour RNA Spike-In RNA were labelled with the Agilent Low RNA Input Linear Amplification Kit PLUS, One-Colour according to manufacturers instructions as follows: 1.2µl T7 Promoter Primer was added to 400ng RNA and 3µl spike in control (in a 11.5µl volume and denatured at 65°C. First strand buffer (to 1x), DTT (to 10mM), dNTP (to 0.5mM), MMLV (1µl of stock provided in the kit in a 20µl reaction) and RNaseOut (0.5µl of stock provided in the kit in a 20µl reaction) was added. The cDNA was

synthesised during the following incubation step (2h at 40°C). After 10 min denaturation at 65°C and the addition of Cy-labelled CTP (to 0.3mM), Transcription Buffer (to 1x), DTT (to 10mM), NTP (8µl of stock provided in the kit in an 80µl reaction), PEG (to 4%), RNaseOut (0.5µl of stock provided in the kit in an 80µl reaction), Inorganic Phosphatase (0.6µl of stock provided in the kit in an 80µl reaction) and T7 RNA Polymerase (0.8µl of stock provided in the kit in an 80µl reaction) the synthesis of the fluorescent labelled cRNA was performed during the second incubation step (2h at 40°C). The labelled cRNA was purified with the RNeasy Mini Kit (Qiagen Ltd, Crawley, UK) according to the manufacturers' protocol.

2.13.2 Hybridisation and Scanning

The Agilent Hybridisation Kit was used in conjunction with Agilent Mouse Oligo Arrays. 2µg of the labelled sample RNA were used for hybridisation according to the Agilent One-Colour Microarray-Based Gene Expression Analysis Protocol. The hybridisation was performed for 17h at 65°C at 10rpm. Slides were then washed for 1 min at 22°C in Wash Solution 1 and 1 min at 22°C in Wash Solution 2, pre-warmed to 37°C. Slides were incubated for 30s in Agilent Stabilisation and Drying Solution. The slides were scanned with the Agilent G2565BA Microarray Scanner System.

2.13.3 Bioinformatics Analysis

Extracted data were analysed using GeneSpring GX 7.3.1 (Silicon Genetics, CA, USA). Agilent standard scenario normalisations for FE-1 colour arrays were applied to all data sets. A subset of genes for data interrogation was generated that excluded

controls, spots of poor quality and gene probes that were present in less than 50% of samples. From these selected probes, relative expression was determined between each treatment and control for each cell line. Heatmaps could be generated from genes 50% present or marginal from which more specific gene lists could be generated for each treatment group and cell line. Genes differentially regulated by greater than 2-fold were selected. One-way parametric, ANOVA tests were performed followed by Benjamini and Hochberg multiple test correction with a false discovery rate of 0.05. Microsoft Excel templates were prepared containing genes that were differentially regulated. Ingenuity™ Pathway Analysis 3.0 (Ingenuity™ Systems, CA, USA) was utilised to assemble functional networks and pathways.

2.13.4 Quantitative Real-Time PCR

RNA was prepared as before and in vitro transcription was performed on 1µg total RNA using the first strand cDNA synthesis kit (Roche). Real-time PCR was performed using a Bio-Rad iCYCLER. QuantiTect® probes (Qiagen) were used for real time RT-PCR together with iQ™ SYBR® Green supermix (BioRad). The Bio-Rad iCYCLER with SYBR Green detection was used for real time RT-PCR. PCR thermocycler conditions were 95°C for 2 min, followed by 45 cycles of 95°C for 20s and 60°C for 30s. Samples were run in triplicate with test probes using B-Actin as a housekeeping gene to control for differences in amount of starting material. Fold-changes (compared to baseline control) were calculated by normalising the test-crossing threshold (Ct) with the amplified control Ct.

3. ISOLATION AND CULTURE OF PRIMARY MURINE MICROVASCULAR ENDOTHELIAL CELLS.

3.1 Introduction

Endothelial cells are a highly heterogeneous cell type, which line the vasculature and the lymphatic system. They have major roles in leukocyte recruitment as well as in haemostasis, regulation of vascular tone, angiogenesis and the control of movement of solutes between the vascular system and tissues (Johnson-Leger *et al.* 2000;Matharu *et al.* 2006;Springer 1995). The location of endothelial cells means they are ideally situated to interact with passing leukocytes in the circulation. By modifying the expression of adhesion receptors and chemokines on their surface, EC can control the recruitment of leukocytes in response to locally produced inflammatory substances, including TNF-α and IL-1β (Bahra *et al.* 1998;Mantovani *et al.* 1992). There are thought to be differences in leukocyte recruitment due to variation of EC phenotype in different levels of the vascular tree and in different organs of the body (Berlin *et al.* 1993;Picker 1992). These phenotypic differences may also alter EC morphology, permeability, secretory potential and gene expression (Aird 2003;Chi *et al.* 2003). Whilst tightly regulated under normal circumstances, inappropriate leukocyte recruitment underlies chronic inflammatory diseases including atherosclerosis, or acute diseases such as ischemia/reperfusion injury and early transplant rejection. This pivotal role in a wide variety of fundamental biological and physiological processes makes endothelial cells an obvious therapeutic target for much research and of particular interest to our research group. Whilst our laboratory has much experience isolating human cell populations, before this project began we lacked the technological expertise to isolate murine endothelium. Murine endothelial cells are widely used for *in vitro* experiments as a model of human systems. In addition to tissue being more readily available than human samples, genetically modified mouse models can be generated to examine disease processes, which is

not possible in humans. In particular our lab was interested in isolating mLSEC as a comparison to human counterparts being routinely isolated.

3.1.1 Liver sinusoidal endothelial cells (LSEC)

LSEC are a variety of specialised endothelial cells that populate the 'capillary' vascular bed of the liver, with the most noted phenotypic differences observed between the vascular endothelium in the portal vessels and the sinusoidal endothelial cells (Lalor & Adams 2002;Lalor *et al.* 2002b). The lining of the sinusoids consists of a monolayer of these specialised endothelial cells as well as a Kupffer cells (liver-resident tissue macrophages) which phagocytose bacteria, cell debris and various other deleterious particles from the bloodstream as well as playing a role in immune surveillance. In addition hepatic stellate cells (HSC), pericytes in the perisinusoidal space, which are involved in fibrosis in response to liver damage, exist in close contact with the LSEC. The thin sinusoidal lining allows rapid exchange of nutrients, oxygen and other substances between hepatocytes and the bloodstream through the space of Disse separating the two distinct cell types as it flows though the liver (Scoazec *et al.* 1994). The location of LSEC and their low shear environment facilitates their specific functions, as LSEC are one of the first cell populations to come into contact with blood components flowing slowly through the liver.

Thus LSEC form a barrier controlling the exchange of substances into the parenchyma of the liver, in addition they are highly specialised endothelial cells which regulate inflammation and subsequent leukocyte recruitment into the tissue, the hosts' immune response during infection and receptor mediated clearance of harmful

pathogens. LSEC have a unique morphology characterised by the absence of tight junctions between cells or basal lamina, and most characteristically the presence of a number of open fenestrations forming sieve plates (Smedsrod *et al.* 1994;DeLeve *et al.* 2004). These sieve plates are a highly evolved structure acting as a 'dynamic filter' aiding the transportation of macromolecules including pathogens and viruses into the liver parenchyma.

3.1.2 Culturing liver sinusoidal endothelial cells.

In the field of sinusoidal endothelial cell research there has been much controversy over the optimal isolation and culture conditions for LSEC. There are two schools of thought regarding culture of LSEC. One claims that LSEC attributes are only apparent in short-term culture (Martinez *et al.* 2008) whereas the other claims LSEC can proliferate and be passaged in long-term culture (Gerlach *et al.* 2001;Karrar *et al*. 2007). Sinusoidal endothelium have a propensity to dedifferentiate in prolonged culture and lose many of their functional and morphological characteristics (Hansen *et al.* 2005;Krause *et al.* 2000). Culture *in vitro* by definition involves removing primary cultures from their physiological niche *in vivo*. Tissue culture provides a vastly altered physiochemical environment resulting in phenotypic and functional changes. LSEC cultures have been shown deteriorate after 1-2 days in culture leading to decreased fenestration and scavenger activity (Hansen *et al,* 2005). In some studies serum (5-20%) has been shown to be toxic to dividing LSEC leading to differentiation from endothelial to stromal like cells (Krause *et al.* 2000). Under normal physiological conditions, cells of the sinusoid are exposed to much lower oxygen tension (5% normoxic) than that of air and standard tissue culture incubators

(20% hyperoxic) (Martinez *et al.* 2008). Culture under more physiological conditions has been shown to improve LSEC survival, endocytic capacity, and production of anti-inflammatory cytokine IL-10 (Martinez *et al.* 2008).

Similarly there are different opinions regarding the most efficient method of isolating LSEC from murine livers; *in situ* perfusion of the whole mouse liver, developed by Smedsrod *et al.* or physical dissociation of liver tissue followed by positive selection using antibody conjugated magnetic beads (Tokairin *et al.* 2002). Several methods using immunomagnetic isolation of LSEC have been published. There has been much speculation over the purity of the endothelium isolated. Initially the endothelial molecule S-Endo 1 antigen (CD146) first discovered on melanoma cells was used but this antibody was not freely available for general use (Tokairin *et al.* 2002). Knolle *et al*. (Knolle *et al.* 2001) and Katz *et al.* (Katz *et al.* 2004) both used negative selection to remove CD45+ KC and CD11b+ DC whereas Onoe *et al.* (Onoe *et al.* 2005) questioned the affectivity of these methods and used CD105 positive selection methods. CD31 has been used to isolate LSEC but it has been observed that CD31 is a better marker for vascular endothelium. This may explain why LSEC isolated using CD31 possessed fewer fenestrations than those isolated by counterflow elutriation. Schrage *et al.* (Schrage *et al.* 2008) have since developed a method for isolating endothelial cells from several murine tissues using SE-1. CD146 is expressed at endothelial cell junctions in a number of different murine tissues, thought to support endothelial cell integrity, the extracellular portion is recognised by the monoclonal antibody ME-9F1. In addition the human molecule is also expressed on T-cells and follicular dendritic cells (Schrage *et al.* 2008).

3.1.3 Brain microvascular endothelial cells

Whilst our lab is predominantly interested in hepatic endothelium and the optimisation of methods for isolating murine LSEC is of major interest, we wanted to compare the phenotype of these cells with those isolated from another primary tissue source. Many groups have reported isolation of cerebral cells including astrocytes and BMEC to study the role of the BBB in vitro. Methods generally involve collecting the small brain capillaries and microvasculature out of which endothelial cells are subsequently isolated (Tontsch *et al.* 1989;Wu *et al.* 2003), and many groups use bovine brain tissue. Most methods involve the removal of the meninges, homogenisation of the tissue, and enzymatic digestion, followed by either gradient centrifugation or antibody selection/depletion (Audus *et al.* 1996;Raub 1992;Rubin *et al.* 1991). BMEC appear to retain many morphological and biochemical properties present *in vivo*, but once isolated, could begin to dedifferentiate in culture due to the absence of external stimuli or direct contact with additional cell types present in the brain environment.

We considered the brain to be an interesting source of endothelium for this study because the tissue is easily accessible, isolation methods have been previously reported and the physiochemical environment of the brain microvasculature is as unique and complex as that of the liver sinusoid. In contrast to the sinusoids brain endothelial cells are exposed to high shear stress (Liu *et al.* 2003) and are in close contact with surrounding astrocytes. Due to the unique microenvironment in which the brain resides and the need to prevent access of pathogens into the brain the recruitment of leukocytes to cerebral tissues, and the molecules involved are tightly regulated. Access is restricted in order to combat inflammation in the CNS and

circulating leukocytes have to overcome the BBB to gain entry (Williams *et al.* 1995). A number of different adhesion molecules, ICAM-1, VCAM-1 and PECAM-1 are involved in the recruitment and transport of leukocytes into the brain parenchyma (Couty *et al.* 2007;Greenwood *et al.* 2002).

3.1.4 Current methodologies to isolate primary endothelial cells

A number of widely accepted methodologies for isolating primary human endothelial cells exist in the literature, in particular for HUVEC and hLSEC. HUVEC have been used successfully for many years, becoming the cells of choice for vascular researchers due to ready availability of tissue and ease of isolation (Jaffe *et al.* 1973). The isolation procedure involves cannulation of the umbilical vein and digestion with the proteolytic enzyme collagenase to release the endothelial cells (Cooke *et al.* 1993). Whilst popular, reproducible and easy to perform for human tissue this methodology is not translatable to rodent systems where cells have been isolated from aortic rings, fat pads, lungs and so on. Furthermore, HUVEC are a macrovascular endothelial population from a large vein, and often research is focused upon the microvasculature, such as cells of the hepatic sinusoid, as this is where disease processes tend to be localised. Isolation methods for cells from microvascular compartments prove more challenging as cannulation is not possible. The majority of methods use physical dissociation of whole tissue followed by enzymatic digestion. Phenotypic analysis may then be restricted to examining adherent cells and identifying those with cobblestone morphology. This is often inadequate as other adherent cells including fibroblasts may be present which tend to outgrow other cell populations in culture. Therefore, in order to minimise non-

endothelial contamination a variety of purification methods can be used. Cell preparations can be separated by size with meshes or filters of varying pore sizes and/or buoyant density via density gradient purification (Percoll, Optiprep). The desired endothelial population can then be positively/negatively selected using antibodies against endothelial markers such as acetylated low-density lipoprotein (AcLDL),CD31 and CD146 using FACS or immunomagnetic beads.

The isolation of human LSEC (hLSEC) is more complicated, the tissue is dissociated and digested using collagenase, non-parenchymal cells (NPC) are separated on the basis of buoyant density on a Percoll gradient. Biliary epithelial cells (BEC) a major constituent of the NPC fraction are removed by positive magnetic bead selection using HEA-125 followed by positive endothelial cell selection with CD31. HSEC are cultured in human basal endothelial cell medium in the presence of human serum and several growth factors (HGF and VEGF) to maintain the *in vivo* phenotype *in vitro* (Lalor *et al.* 2002b;Lalor *et al.* 1999). Human cells require the presence of human serum in culture, whereas the use of autologous serum in murine LSEC (mLSEC) cultures is controversial, as serum has been shown to be toxic (Krause *et al.* 2000). It is important to provide an artificial matrix to for the cells to adhere to, including gelatin, collagen, fibronectin and vitronectin.

Author	Species	Isolation Method	Cells	Medium	Matrix	Expression Profile
Karrar *et al.* 2006	Human Normal Liver	hLSEC method	hLSEC	MCDB1 10% Human Serum	Gelatin	CD54, AcLDL, CD105, L-Sign
Daneker *et al.* 1998	Human Resected Liver	Dispase Percoll	hLSEC	EC Specific Medium 20% Human Serum	Not Detailed	CD31, CD34, CD54, vWF
Martinez *et al.* 2008	Rat	Perfusion	rLSEC	DM10 Tissue SS 5%/20% O_2	Rat Tail Collagen 1	IL-10, IL-6 ICAM-1
DeLeve *et al.* 2006	Rat	Perfusion αCD31 selection	rLSEC	Not Detailed	Fixed 2% Glut	Lack of sieve plates by SEM
Katz *et al.* 2004	Mouse	Perfusion, Collagenase, Percoll, metrizamide	mLSEC	N/A	N/A FACS and Ag Uptake	CD31, CD32, vWF, CD11c
Wu *et al.* 2003	Mouse C57BL/6	Collagenase Dispase, Percoll, αCD31 MACS.	mBMEC	MCDB 131, 10% FCS 30µg/ml ECGS	Rat Tail Collagen 1	vWF, CD31. VCAM-1,ICAM-1 only on stimulated.
Marelli-Berg *et al.* 2000	Mouse CBA C57BL/6 Balb/c	Collagenase αCD31/CD105 /IB4 MACS	Lung Heart	DMEM HEPES GPS 150µl ECGS 20% FCS	2% Gelatin Type B	CD31, CD105, CD106, CD54, CD102, IB4
Cha *et al.* 2005	Mouse Balb/c	Skin flaps, Collagenase, Percoll	Dermal EC	MDCB 131 10% FCS 30µg/ml ECGS	3% Collagen Type 4	CD31, Tie-2, VEGFR2, Ac-LDL
Knolle *et al.* 1999	Mouse Balb/c	Collagenase perfusion 0.05%, 30%Nycodenz, αCD146 MACS.	mLSEC	DMEM 10% FCS 1% Glutamine	Collagen Type 1	Immunological functions

Table 3. 1: Summary of sample of methods for isolating primary endothelial cell populations. Evidence for the variety of methods available for isolation from various organs and markers used to identify endothelial cell populations.

When reviewing the literature regarding endothelial cell isolation methods, there are several stages in common, outlined in Figure 3.1 and Table 3.1. Each isolation

method is broadly split into three stages; dissociation of the tissue, separation of component cell populations and selection of the endothelial cell type of interest.

A single celled suspension of the tissue of interest is obtained using a combination of proteolytic enzymes and physical dissociation. Cells are then separated on the basis of size and relative buoyancy using density centrifugation to remove debris and unwanted cell populations. Cells at the desired gradient interface are then further positively or negatively selected using an antibody bead step and are plated out onto tissue culture plastic coated with basement membrane proteins to aid cell adherence. Similar methods were used based on this framework to optimise the isolation of primary murine endothelial cells. In the sections that follow I will describe the development of each method in our laboratory, discuss any problems encountered, explain how problems were resolved and describe the final outcomes of investigations.

3.2 Results

3.2.1 Isolation of mLSEC via in situ perfusion of murine liver

The gold standard method for LSEC isolation was reported by Smedsrod *et al.* in 1985 (Smedsrod *et al.* 1985). High numbers of LSEC from rat livers were obtained by perfusing the liver via the portal vein. Perfusion involves swift killing of the animal and cannulation of the portal vein through which enzyme containing buffers are perfused utilising the resident vasculature to digest the tissue from within. I visited the Smedsrod laboratory in order to learn this procedure, which is outlined in more detail in Fig. 3.1 This procedure was successfully performed 6 times in Tromso. Primary mLSEC obtained by this procedure (~5-8 $x10^5$/liver) were seeded (10^4/well) onto collagen coated glass coverslips in 24-well plates in basal RPMI. mLSEC were fixed in methanol for 5 mins one-day post-isolation and transported back to the UK in sterile PBS. Figure 3.2 shows the results of preliminary immunochemical analysis of these cells confirming that the mLSEC had appropriate endothelial morphology, were of high purity and were positive for Endoglin and LYVE-1.

Figure 3. 1: Detail of perfusion method for isolating mLSEC.

Simplified methodology of *in situ* perfusion of murine livers in laboratory of B.Smedsrod, Norway. (A) Outline of protocol, (B) Image of perfusion apparatus.

Figure 3. 2: Immunohistochemical staining of mLSEC.

Initial phenotypic analysis of mLSEC obtained as a result of perfusion isolation method carried out in Norway. mLSEC were cultured on glass coverslips, fixed in methanol and stored in PBS. Samples were stained for the presence of a number of adhesion molecules and endothelial markers using DAB method. Images captured at x10 magnification on Axioskop using Axiovision software.

The next step was to recreate the perfusion technique in Birmingham. The perfusion apparatus available resembled that of the Smedsrod group consisting of a water bath, a pump to regulate flow rate, fine gauge tubing and a Venflon to allow portal vein cannulation. The perfusion procedure was performed under a dissection microscope with sufficient light to visualise the portal vein (Fig. 3.2).

Perfusion was carried out as outlined in Figure 3.2 with C57BL/6 mice, however several isolations yielded predominantly cell debris with few obvious cell populations, as shown by representative images in Figure 3.3. Several modifications were made to the procedure including different water sources, cell culture grade buffer reagents, collagenase, assistance in perfusing, anaesthatising animals prior to perfusion, using older mice and so on. However these modifications were unsuccessful in our hands.

Figure 3. 3: Representative images of results of initial perfusion experiments.

Images captured x10 magnification of Axiovision Light Microscope.

3.2.1.1 Isolation of mLSEC using immunomagnetic bead selection with Miltenyi αLSEC microbeads.

Several different immunomagnetic methods devised from commercially available kits and in house reagents were used in order to isolate primary murine endothelial cell populations from both liver and brain. In the initial stages of this project a specific kit manufactured by Miltenyi was used in combination with Collagenase 2 digestion and an Optiprep gradient (Figure 3.4-3.6). Although cells with the appearance of LSEC were isolated in the initial tests of this kit, the procedure was not reliable in latter experiments. We suspected that the α-mLSEC MAb conjugated to the MACS beads might have become detached upon storage. To test for this possibility a sample of α-mLSEC beads were incubated on murine liver sections and then stained with an appropriate FITC conjugated secondary antibody. In addition we acquired a sample of α-mLSEC FITC conjugated MAb from the supplier, which we also tested on liver sections. Figure 6 shows that whilst we saw little or no staining on the samples treated with beads (Fig 3.6-A/B) we observed distinct vascular staining (large vessels and small arteries in the portal areas, arrows on Fig. 3.6 C/D) with the FITC-conjugated antibody. Interestingly however there was very little sinusoidal staining evident.

Figure 3. 4: Schematic isolation of mLSEC using Miltenyi LSEC microbeads.

Outline of initial method used for isolating mLSEC. Resulting cell populations obtained post-MACS separation were plated out into various culture vessels including collagen coated chamberslides, T25's and T75's in DMEM containing 10% FCS, mEGF, HGF and VEGF cultured in a 37°C 5% CO_2 incubator to encourage cell attachment and proliferation.

Figure 3. 5: Light micrograph of cellular matter obtained from LSEC immunomagnetic bead selection.

Schematic diagram of αLSEC MACS isolation method and resultant cell populations. Images are captured at x10 magnification on Axiovision Light Microscope.

Figure 3. 6: Image of cryosectioned murine liver stained by immunofluoresence methods.

Samples were stained using Rat IgG at 5µg/ml (A) and α murine LSEC MACS beads (B) to test the adherence of beads. The α mouse LSEC-FITC was also tested diluted 1/50 (C) and 1/100 (D) of manufacturers stock. Positive stain indicated by arrows. Image captured at x10 and x20 original magnification respectively on Axiovert microscope using Axiovision software.

3.2.1.2 Use of cytometry in conjunction with LSEC-FITC to optimise isolation procedure

Next the αLSEC-FITC MAb was used to determine whether endothelial cells were present at the beginning of the isolation procedure and/or lost during latter stages of the isolation protocol. A 200µl aliquot of cells was removed at various stages (indicated by red numbers) throughout the isolation protocol as outlined in Figure 3.7 and labelled with LSEC-FITC. Figures 3.7-3.9 show representative cytometry scattergrams and histograms from cells immediately after digestion prior to any cell selection. Figure 3.8 indicates that there are a large number of cells present at this stage in the isolation protocol. The hepatocytes form a distinct large population with a few outliers (cell doublets) and some very small cell debris is evident. Figure 9 shows that we saw little non-specific labelling with an isotype matched control antibody (3.9-A). In contrast a distinct peak of FITC fluorescence is apparent and these cells have a location on the scattergram appropriate for endothelium (green cells on scatterplot, 3.9-B)

Figure 3. 7: Schematic diagram summarising the location of LSEC throughout the isolation procedure.

Each stage at which a sample was removed for FACS analysis is labelled with a number in red.

Figure 3. 8: Flowcytograms depicting cells contained within post collagenase digest sample.

The dot plot on the left separates cells by forward scatter and side scatter according to size and granularity respectively we can postulate where the mLSEC lie on the basis of these parameters and fluorescence levels. (A) mLSEC, (B) Hepatocytes. The histogram on the right depicts FITC fluorescence; the red peak is the IgG control and the green peak shift represents α mouse-LSEC-FITC at 1/30 dilution of manufacturers stock, which labels the cells of interest. The percentage quoted represents the number of positively stained cells.

Figure 3. 9: Flowcytograms depicting cells contained within post collagenase digest sample stained with (A) Rat IgG and (B) α mouse LSEC-FITC at 1/30 dilution of manufacturers stock.

The dot plots on the left separates cells by forward scatter and side scatter according to size and granularity respectively limited to 8000 events for clarity. Events in black are red blood cells and debris. Events in green are FITC positive mLSEC in area outlined in Fig 3.10. (A). The histograms on the right depict FITC fluorescence and percentage FITC positive cells.

Table 3.2 shows that as the isolation protocol progresses the number of positively labelled cells changes. After removal of hepatocytes the proportion of LSEC-FITC positive cells increased as expected. However the number of cells decreased dramatically with every subsequent stage in the protocol.

Sample	Isolation Stage	Percentage of positive cells (%).
1	Post Collagenase digest and fine mesh.	5.43
2	Post slow spin 1 sup^{n}	62.69
3	Post slow spin 1 pellet	11.08
4	Post slow spin 2 sup^{n}	15.82
5	Post slow spin pellet	3.31
6	Pelleted NPC's	3.45
7	Post Optiprep gradient centrifugation	2.82
8	MACS Column Waste	0.28

Table 3. 2: Representative Data of FACS experiment determining at which stage of isolation endothelial cells were being lost.

3.2.1.3 Isolation of mLSEC using Easy Sep MACS beads

Next I attempted a method more analogous to that we use for isolating human LSEC. This technique (outlined in Fig. 3.10-A) again involved labelling the mLSECs with the α mLSEC-FITC conjugated MAb after collagenase digestion of tissue. Magnetic beads conjugated to an α-FITC secondary MAb were then used to pull out the labelled cells. However this technique did not select any cells (Fig 3.10-B).

Figure 3. 10: Schematic showing the principle behind the Easy-Sep method.

Light micrograph of cellular debris post Easy-Sep selection cultured in collagen coated T25 flasks with 5ml DMEM + 10% FCS, mEGF, HGF and VEGF. Image captured at x10 magnification on Axiovision microsope

3.2.1.4 Isolation of mLSEC with Miltenyi αCD146 MACS kit.

In the course of my investigation, Schrage *et al.* reported using αCD146 immunomagnetic beads in combination with perfusion to isolate high numbers of pure mLSEC. A CD146 immunomagnetic bead kit was available from Miltenyi as an alternative to αLSEC beads. Therefore I tested this reagent using an adapted protocol similar to that used for the αLSEC reagent (Fig. 3.11). This method was successful and yielded large numbers of mLSEC. For example, in the initial isolation, 50cm2 of confluent cells (2 x10^7) with appropriate LSEC morphology were isolated (Fig. 3.12). Phenotypic analysis of cells isolated using this methodology confirmed that the cell populations were positive for CD31, LYVE-1 and Endoglin (Fig. 3.13).

Figure 3. 11: Diagram of mLSEC isolation using MACS αCD146 kit.

Outline of current version of liver sinusoidal endothelial cell isolation method for approximately 6 livers. The number of livers used in each isolation varied but quantities of reagents were changed in accordance with the amount of tissue.

Figure 3. 12: Light micrograph images of LSEC cell populations resulting liver endothelial cell isolation protocol.

Images captured at x10 and x20 magnification on Axiovision Light Microscope.

Figure 3. 13: Light micrograph and confocal images of primary mLSEC.

mLSEC were seeded into chamberslides or onto glass coverslips and fixed in methanol. Samples were stained for a range of molecules using DAB immunohistochemical and immunofluroescence methods. Images captured at x20 magnification for LM pictures of chamberslides and x63 for fluorescent confocal images.

3.2.1.5 Optimal protocol for LSEC isolation

In summary, several different methods for isolating mLSEC from whole murine livers were attempted (Table 3.3). All of these methodologies have been used by other groups and are reported to be successful. However in our hands, with the equipment available to us, we found some protocols resulted in poor cell yields or did not reproducibly produce high quality cell isolates. We found the best method utilised a combination of Collagenase 4 to digest the tissue, a Percoll gradient to remove parenchymal cells and selection with αCD146 immunomagnetic beads to generate homogeneous mLSEC populations.

Dissociation	Enzyme	Gradient	Selection	Cell Yield
In situ perfusion	Liberase	Percoll 23/50%	KC Adherence	0
Mince/Meshes	Collagenase 2 (0.25%)	Optiprep 60%	α-mLSEC	0
Stomacher/Meshes	Collagenase 4 (0.05mg/ml)	Optiprep 100%	N/A	6 Livers 1 semi confluent T25 0.5×10^6
Mince/Meshes	Collagenase 4 (2mg/ml)	Percoll 23/50%	α-CD146	6 Livers 2 confluent T25's 2×10^6

Table 3. 3: Typical results of the various mLSEC isolation methods used.

Details of method development and modifications leading to final method used to isolate mLSEC from whole murine livers.

3.2.2 Isolation and culture of primary murine brain microvascular endothelial cells (BMEC).

The literature details several methods for isolating BMEC from bovine brain (Raub *et al.* 1992;Rubin *et al.* 1991) involving removal of the meninges, homogenisation of the tissue, enzymatic digestion, and either gradient centrifugation or antibody selection or depletion. I used these methods as described by digesting murine brains with Collagenase 4 and selection of endothelial cells with an αCD31-Biotin antibody and streptavidin conjugated dynabeads (Fig. 3.14). The isolation procedure did generate viable cells in considerable number but the purity of the end results was poor. Figure 3.15 shows that a number of different cell populations were observed in the resulting cell isolates. Endothelial like cells were present initially but diminished as the number of epithelial and fibroblastic cells increased. Small populations of neuronal cells were also observed but these did not appear to proliferate in contrast to epithelial and fibroblastic cells. Despite several attempts to improve the purity of the preparations I was unable to generate a homogenous brain endothelial culture.

Figure 3. 14: Schematic of mBMEC isolation method

Outline of current version of brain microvascular endothelial cell isolation method. The number of brains used in each isolation varied but quantities of reagents were adjusted in accordance with the amount of tissue used.

Figure 3. 15:Light micrograph images of varying cell populations resulting from brain microvascular endothelial cell isolation protocol.

Images captured at x10 magnification

3.3 Discussion

The aim was to isolate primary murine endothelial cell populations from different organs for further *in vitro* experiments to highlight any phenotypic and functional differences. Several different methods for isolating endothelial cell populations are available in the literature (See Table 3.1). Generic methods include, tissue dissociation, cell separation and further selection or depletion to obtain the desired population. Murine liver sinusoidal endothelial cells (mLSEC) were of particular interest due to the unusual phenotype and immunological functions. In addition brain microvascular endothelial cells (mBMEC) were examined as an additional EC population due to the privileged site they inhabit. Murine *in vitro* systems allow the investigator to manipulate parameters more difficult to examine in the whole animal (shear stresses, cytokine stimulation). In addition murine models of inflammatory diseases are available and results can be considered in parallel to human systems.

A number of methods were carried out including both immunomagnetic and perfusion techniques to isolate mLSEC and mBMEC. Isolation of mLSEC proved difficult until the advent of a new commercially available kit (Miltenyi, UK) directed against CD146 a molecule present on endothelial cells in a number of murine organs (Schrage *et al.* 2008). The mBMEC isolation protocol yielded a number of different cell populations including contaminating adherent cells that proved problematic. Each isolation method attempted was further developed from that published to obtain high yields of pure endothelial cells.

3.3.1 Use of perfusion to isolate rodent sinusoidal endothelium

Perfusion of the liver has been used to isolate several different populations from animal livers in particular mice, rats (DeLeve *et al.* 2006;Smedsrod *et al.* 1984) and pigs. In addition to isolating mLSEC Smedsrod *et al.* pioneers of the technique, isolated hepatocytes and cells of the reticuloendothelial system (rLSEC and KC) from rat livers (Smedsrod *et al.* 1985). Elvevold *et al.* (Hansen *et al,* 2005) perfused porcine livers to isolate pLSEC. Perfusing the organ allows a more delicate and comprehensive tissue dissociation by digesting the tissue *in situ*. A variety of proteolytic enzymes can be used including Collagenase and Liberase, a more stable mix of proteases used to avoid enzymatic batch variability found with Collagenase.

Although *in situ* perfusion via the portal vein is a reliable digestion method in many laboratories it is a highly skilled procedure, which requires specialist equipment. When I performed the procedure under expert guidance in Norway it was successful and reproducible. However, many problems were encountered when I attempted to recreate the methodology in Birmingham. Of particular importance is the fact that the perfusion apparatus used here was modified due to cost considerations and availability of more the complicated elements of apparatus. The absence of a heat exchanger to maintain the temperature of the perfusion solutions and buffers probably resulted in inadequate temperature control and it is likely that upon perfusion the reagents were a little cool (24-28°C). The reagents were pre-warmed in a water bath but I resisted maintaining this too hot for fear of adversely affecting enzyme activity. In addition, the procedure needs to be completed as rapidly as possible after death of the animal. In published methods animals are rapidly killed with high concentrations of CO2, but this method is not licensed in the UK. Here the

Home Office permits sacrifice of animals by decreasing O_2 and increasing CO_2 over a number of minutes. Thus our best rapid alternative was cervical dislocation, which was carried out some distance from the perfusion apparatus. Thus by the time animals were ready for cannulation I noted that some blood clotting had occurred which impeded the perfusion of buffer into the livers. This could have been avoided by the injection of heparin into the animals prior to Schedule 1 but this could not be completed without a license, which I do not hold. These issues in combination with some problems arising from different sources of reagents and plasticware meant that I was unable to reproducibly isolate high numbers of pure cells using this methodology and thus moved on to methods based upon immunomagnetic selection.

3.3.1.1 Use of magnetic selection to isolate rodent sinusoidal endothelium

Several methods using immunomagnetic isolation of LSEC have been published, but controversy exists over the purity of the endothelium isolated. Initially the endothelial molecule S-Endo 1 antigen (CD146/mCAM) first discovered on melanoma cells was used but this antibody was not freely available for general use (Tokairin *et al.* 2002). Knolle *et al.* (Knolle *et al.* 2001) and Katz *et al.* (Katz *et al.* 2004) both used negative selection to remove $CD45^+$ KC and $CD11b^+$ DC from endothelium isolated by counterflow elutriation. However Onoe *et al.* (Onoe *et al.* 2005) questioned the efficacy of these methods suggesting CD105–based selection methods were superior. Our laboratory uses CD31 to isolate human LSEC due to its widespread expression on all endothelium particularly in diseased livers. However LSEC isolated using CD31 have been suggested to possess fewer fenestrations than those isolated by counterflow elutriation (DeLeve *et al*. 2006).

Our problems using the initial αmLSEC kit may have several sources, and was not helped by the fact that the identity of the antigen recognised by the antibody in the αmLSEC MACS kit used in 3.7 was not made available by the manufacturer. Additionally we suspected that the antibody could have become detached from the beads rendering them ineffective. Our immunofluorescent staining (Fig. 3.6) indicated that the immunomagnetic beads were binding non-specifically to liver tissue. In addition I believe that LSEC were lost during certain elements of the isolation procedure. Thus an alternative method of immunomagnetic separation was trialled utilising an αLSEC-FITC antibody. However, neither method yielded any cells. I also attempted to remove the specific cell selection step using soley digestion with Collagenase 4 (data not shown) specifically designed for the release of liver cells produced cells resembling mLSEC. However, due to the absence of specific selection, a number of other non-parenchymal cells present in the same density gradient band were obtained in addition to mLSEC. The non-adherent cells were washed off Day 1 post-isolation, but adherent cells such as Kupffer and Stellate cells were present in some cultures, which would affect subsequent phenotypic analysis.

Schrage *et al.* (Schrage *et al.* 2008) have since developed an antibody (ME-9F1) against CD146 can be used to isolate endothelial cells from several murine tissues. CD146 is expressed at endothelial cell junctions in a number of murine tissues and it is thought to support endothelial cell integrity. The extracellular portion of CD146 is recognised by the monoclonal antibody ME-9F1. In addition the human molecule is also expressed on T-cells and follicular DC, however the murine counterpart was only found at low levels on a subset of $NK1.1^{+}$ cells. My experience using this antibody suggested that the αCD146 beads yielded the highest number of pure mLSEC compared to the other available methods

attempted. Immunohistochemical phenotypic analysis of the isolated cells indicated that they expressed CD31, ICAM-2, CD34, VAP-1, LYVE-1, and Endoglin as found in published literature (Table 3.1). Further phenotypic analysis of these cells follows in later chapters.

It is crucial to be able to phenotype and identify primary isolated cell populations. Endothelial cell characteristics include, expression of CD31, CD34, vWF, uptake of ac-LDL, binding of lectins, appearance of 'cobblestone' morphology and the propensity to form tubes in matrigel (Aird 2007a). Although present on populations of EC these features are not universal and vary temporally, spatially *in vitro*, *in vivo* and between cultures, accounting for marked EC heterogeneity. As previously mentioned LSEC are highly endocytic expressing a number of scavenger receptors including stabilin-2 and LYVE-1 that can be used to identify LSEC (Hansen *et al.* 2005). At present no single marker or characteristic is sufficient to confirm liver sinusoidal endothelial cell cultures.

In order to correctly identify endothelial cell populations and to use them in model experimental systems *in vitro* the challenge is to maintain the *in vivo* phenotype *in vitro*. As mentioned previously the best methods for culture of LSEC are controversial. hLSEC are cultured in the presence of serum and a number of growth factors, can be subcultured and maintain their original phenotype up to passage 6**.** Conversely it has been reported that mLSEC do not proliferate in culture, that serum might be toxic to them and that maintainance of original phenotype can be prolonged by culturing cells at lower oxygen tension (5%) (Elvevold *et al.* 2008). The mLSEC obtained with the αCD146 isolation method were cultured in basal RPMI (+PSG) in

the absence of serum in gelatin coated culture vessels. Cells were used in experiments the day after isolation and deteriorated from Day 2 post-isolation onwards. mLSEC did not proliferate even in the presence of hGF and VEGF (10ng/ml) and could not be subcultured. mLSEC died when subjected to passage with Trypsin and Versene (EDTA).

mLSEC are used by a number of different research groups to examine antigen presentation (Knolle *et al.* 1997), endocytic capacity (Matsumoto *et al.* 2000) and their role in inflammation. LSEC are thought to play a role in innate immunity in the liver presenting foreign antigens via FC-γR and pattern recognition receptors (PRR) (Elvevold *et al.* 2008). Blood flowing through the liver contains many benign soluble food antigens to which the immune system is tolerant. LSEC are thought to be important in this process however, there is much debate over their specific role in hepatic tolerance. Early studies by Knolle *et al*. (Knolle *et al.* 2000) showed that LSEC in addition to normal scavenger receptors expressed MHC I/II, CD80/86 and CD40 involved in antigen presentation and induced the differentiation of naïve T-Cells to a Th_0 rather than Th_1 driven by other APC's. However, Katz *et al.* (Katz *et al.* 2004) found that LSEC had a high capacity for taking up antigens and in the absence of costimulation were insufficient to activate naïve T-cells but did not express markers of APC's. Onoe *et al*. (Onoe *et al.* 2005) then discovered LSEC isolated by CD105 positive selection methods expressed MHC II and CD86. When examining data published by these groups it must be considered that methods used to isolate and culture LSEC varied between each group and factors such as selection method, serum concentration, contaminating cell populations and cultivation techniques have affects on phenotype and functional responses (Elvevold *et al.* 2008). As of yet no decisive conclusion can me made on the role of LSEC in liver immunology. The

mLSEC obtained in these studies were not examined for expression of immunological markers involved in antigen presentation. This research is more focussed on the role that mLSEC play in inflammation and subsequent leukocyte recruitment. However this supports the idea that mLSEC are an elusive and complex cell type.

3.3.2 Isolation of Brain microvascular EC

In addition to developing an effective method of isolating mLSEC, an alternative source of homogenous primary microvascular endothelial cells was investigated. Unlike the low shear environment of the liver sinusoids, brain microvascular endothelial cells are exposed to high levels of shear and are an integral part of the BBB (Lui *et al.* 2003).

Much research on brain microvascular cells have used bovine sources to model the blood brain barrier, cells are isolated and can be co-cultured with astrocytes or in astrocyte conditioned media (Dehouck 1990;Rubin *et al.* 1991). Little work has been done using murine sources. Early research used young animals, which were of limited value (DeBault *et al.* 1979;Tontsch *et al.*1989). Wu *et al*. (Wu *et al.* 2003) have since developed a simple method for isolating mBMEC separating cells using Dextran and Percoll and positively selecting EC with αCD31 immunomagnetic beads. Their cells were cultured in MCDB media with 10% FCS and 30µg/ml endothelial cell growth supplement (ECGS). The resulting mBMEC cultures possessed cobblestone morphology, formed tubes and tight junctions in matrigel, expressed vWF and demonstrated uptake of acLDL. TNF-α stimulated mBMEC expressed ICAM-1 and

VCAM-1. The importance of ICAM-1/VCAM-2 and other adhesion molecules have been demonstrated on cytokine stimulated primary mouse, rat and human BMEC and in inflammatory conditions *in vivo* such as the Experimental Autoimmune Encephalitis (EAE) model. In particular ICAM-1 (CD54) and PECAM-1 (CD31) are thought to be involved in downstream signalling events post adhesion, via G-protein coupled receptors and thus to perpetuate further recruitment. For example by inducing cytoskeletal changes and creating 'transmigratory cups' to permit access of subsequent cells (Greenwood *et al.* 2002) (Adamson *et al.* 2002;Couty *et al.* 2007). In such studies, many research groups use the commercially available brain endothelial cell line b.End.5 isolated from hemangiomas (vascular tumours) generated by a retroviral construct encoding polyoma middle-sized T-Ag (Rohnelt *et al.* 1997).

The method I used to isolate primary brain endothelium (outlined in Fig. 3.14) relied on similar methods to that used by Wu *et al.* α-CD31 biotin was used in conjuction with streptavidin conjugated dynabeads to positively select endothelial cells from homogenised tissue. Despite blocking non-specific binding with avidin a number of different cell populations were obtained (Fig. 3.15). In initial days post-isolation a number of endothelial like cells were apparent in culture however as cultures progressed the fibroblast cells outgrew EC a common feature when isolating primary cells. I am confident that the protocol could have been further optimised to minimise contaminating cell populations or to further purify the endothelium, but due to time constraints I instead focussed on isolating mLSEC and opted to use the cell line b.End.5 for comparison.

3.3.3 Primary cells vs. Immortalised Cell Lines.

In vitro systems using primary cells are of most value as they enable the researcher to obtain the most representative impression of the *in vivo* situation. Although the most desirable system to use they pose many experimental difficulties. They are notoriously difficult to isolate and protocols vary widely throughout the literature. Once isolated and removed from the *in vivo* physiochemical environment, EC begin to dedifferentiate into stromal like cells due to the absence of external stimuli (Elvevold *et al.* 2008). Primary hLSEC and mLSEC lose phenotypic markers over time such as L-Sign, and the characteristic fenestrations disappear. Thus cells are generally used up to passage 6 or 1-2 days post culture respectively. There is much controversy over culture conditions with differing opinions on maintained culture, serum levels, growth supplements (hGF, VEGF, ECGS, Tissue SS), oxygen tension and so on (Elvevold *et al.* 2008).

Due to the difficulty of isolating homogeneous primary EC populations immortalised cell lines have been developed to allow further research and understanding of endothelial cell function. Cell lines originate from a primary cell population and are often conditionally immortalised with viral mechanisms to prevent senescence. Immortalised cells can be continually subcultured to high passages maintaining a constant stable phenotype. These characteristics make such cells ideal for studying the effects of inflammation on the phenotype and function of endothelial cells from different organs. Thus we decided to use several cell lines as comparators in our pilot experiments in order to determine the key experiments to take forward when stable primary murine endothelial cell populations were obtained.

A number of immortalised endothelial cell lines were used in this study including mUCEC-1 (Lidington *et al.* 2002), s.END (Bussolino *et al.* 1991) and b.End.5 (Rohnelt *et al.* 1997) originating from heart, skin and brain respectively. Two viral methods of immortalisation were used to generate these lines. H-2K^{B}-tsA58 transgenic mice express a thermolabile strain (tsA58) of the simian virus (SV40) large T-Antigen linked to an inducible major histocompatibility complex H-2K promoter. T-Ag expression is only apparent when cells are cultured at the lower temperature of 33°C and promoter activity can be up regulated by the addition of IFN-γ. A cardiac endothelial cell population (mUCEC-1) immortalised in this manner has been shown to rapidly expand in culture, respond to growth factors and cytokines (TNF-α, IL-1β and LPS) and express appropriate adhesion molecules involved in leukocyte recruitment including CD31, Endoglin, ICAM-1/2, and VCAM-1 (Lidington et al. 2002). Endothelial cells from the 'immortomouse' have been isolated from lung, colon, kidney, heart, brain, pancreas, uterus, ovaries, bladder and prostate (Langley *et al.* 2003). A number of endothelial cell characteristics were examined including; formation of tubes in matrigel, uptake of acLDL, cell morphology and doubling time. Unfortunately no data regarding mLSEC from these animals have been described. However, data has been published using an immortalised liver endothelial cell line from the H-2K^{B}-tsA58 transgenic mouse for use in radial-flow bioreactors to generate artificial liver (Matsuura *et al.* 2003).

In addition cells have been isolated from hemangiomas (vascular tumours) generated by a retroviral construct encoding polyoma middle-sized T-Ag from skin (s.END), heart, brain (b.End.5), kidneys and whole embryos (Bussolino *et al.* 1992). Brain endothelioma cells have been used to model the blood brain barrier, examine the

adhesion and transmigration of T-Cells (Klotz *et al.* 2007;Rohnelt *et al.* 1997) across microvascular endothelium and the role of VCAM-1, ICAM-1 and ICAM-2 (Etienne *et al.* 1998;Etienne-Manneville *et al.* 2000). Skin endothelioma cell lines have been used to investigate signalling pathways (PKC) (Bussolino *et al.* 1992) and cytokine production (Il-6, KC, IL-1α, MCP-1, GM-CSF) (Bussolino *et al.* 1991). Thus we believe that the cell lines we have chosen should represent good models for studying inflammation in different organs. However although cell lines are an invaluable experimental tool, it must be considered that the biology of these cells

could be altered by the presence of the viral constructs.

4. PHENOTYPIC CHARACTERISATION OF ORGAN SPECIFIC ENDOTHELIAL CELLS.

4.1 Introduction

The endothelium could be considered as an organ, which is distributed throughout the body, since endothelial cells form the lining of all blood vessels from arteries to capillaries in the microcirculation. A highly heterogeneous organ both structurally and functionally EC play a role in many physiological processes including vascular permeability, haemostasis, vasomotor tone, blood cell trafficking, proliferation and both innate and adaptive immunity. Not all EC perform all these functions, for example cells of the microcirculation are involved in leukocyte trafficking whereas arterial EC participate in regulating vascular tone. No universal endothelial cell phenotype has been discovered and many endothelial characteristics vary throughout the vasculature. Due to the privileged position of EC, they are involved in or affected by almost every type of disease making them an obvious therapeutic target.

Endothelial cells are highly plastic, moderating their phenotype in response to the local extracellular environment. EC constantly sample the surrounding physiochemical environment from the luminal, abluminal and junctional surfaces. These environmental factors can be biochemical (cytokines, growth factors, hormones, oxygenation etc) or biomechanical including haemodynamic forces such as shear stress and pulsatile flow as a result of the cardiac cycle. These cues activate signalling pathways leading to posttranscriptional modifications and alterations in patterns of gene expression resulting in phenotypic changes. Environmental factors vary temporally and spatially resulting in a constant flux of phenotype (Garlanda, 1997). For instance arterial EC will be more affected by haemodynamic forces compared to microvascular EC that are more affected by

biochemical signals due to close proximity to the underlying tissues. Shear stress varies throughout the vascular tree, from low shear in the microcirculation to high shear pulsatile flow in arteries (Nash, 2004). Flow varies in straight vessels where laminar flow is present, in comparison to arterial bifurcations where EC areas are exposed to disturbed flow (Eddys), which renders them more vulnerable to atherosclerotic plaque formation (Cybulsky, 1991). Patterns of blood flow can be affected by disease, age and exercise. Biochemical fluctuations can be altered post-prandially, and in response to infection, diurnal rhythms and age (Aird 2006).

In addition to changes as a result of alterations in the local environment, EC phenotype can be affected by epigenetic modifications. Epigenetic properties are passed from parental to daughter cells through S-phase without the need for the original signal that induced them. These modifications include DNA methylation, acetylation, histone modification and chromatin remodelling, which are highly dynamic and could be affected by age, disease and therapeutic manipulation (Aird 2006;Aird 2008).

Due to the high importance and relevance of these factors it is of no surprise that there is much dedifferentiation and transdifferentiation in *in vitro* EC systems. EC phenotype appears to be a balance of factors with certain genes being affected by either environmental or epigenetic alterations. Chi *et al* examined gene expression patterns of cultured endothelial cells from various areas of the vasculature and found notable differences between microvascular and macrovascular and arterial and venous sites (Chi *et al.* 2003).

4.1.1 Structure and Function of EC

Endothelial structurally heterogeneity was first demonstrated in the 50's and 60's using an electron microscope (EM) (Aird 2007b). EC structure varies throughout the vasculature, although conventionally flat in vessels they are cuboidal in shape in high endothelial venules (Girard *et al.* 1995) and thickness can vary from 0.1µm in capillaries to 1µm in the aorta. There are 2 main types of junctions between EC, tight junctions (zona occludens) and adherens junctions (zona adherens) (Dejana 2004). Tight junctions form barriers between individual cells and help to maintain cell polarity. These physical barriers vary within the vascular tree with large numbers in the macrovasculature compared to smaller, leakier junctions in the microvasculature according to the functions that they perform (Aird 2007b). Arterial EC are exposed to high shear and pulsatile flow, whereas the microvasculature is involved in leukocyte recruitment and movement of solutes in inflammation. The exception is the BBB where a large number of tight junctions maintain the immunologically privileged state of the brain (Aird 2007a).

4.1.2 Markers of endothelial cells

Endothelial cells (EC) are notoriously difficult to define, as no specific marker of EC's exist. In addition any 'endothelial-like' markers such as CD31 or VE-Cadherin, or structural characteristics for example Weibel-Palade bodies or fenestrations, vary between subsets of EC's and can also be present on additional non-endothelial cell types (Aird 2007b). When isolated for culture, EC are removed from their normal physiological environment and all elements and factors contained within that leading

to phenotypic drift (Aird 2008). This makes identification and phenotypic analysis of isolated cell types more challenging. In order to prevent this, researchers recapitulate the *in vitro* microenvironment by adding serum, conditioned media, basement membrane proteins and try to model exposure to haemodynamic forces (Elvevold *et al.* 2008).

4.1.3 Endothelium in disease

As mentioned previously, EC are involved in the pathology of many different diseases. The location of endothelial cells means they are ideally situated to interact with passing leukocytes in the circulation. It was found in the 80's that if EC are incubated with pro-inflammatory mediators (cytokines and bacterial products) they become activated resulting in pro-adhesive, antigen presenting and procoagulant properties (Bevilacqua *et al.* 1987;Pober *et al.* 1987).

An area of particular research interest regarding endothelial cells is atherosclerosis. This disease is topical due to the increasing prevalence of morbid obesity in the population and the growing number of deaths from heart attacks in which atherosclerotic plaques are a major contributing factor. Atherosclerotic lesions form at sites of disturbed blood flow such as arterial bifurcations, where altered flow patterns are thought to impact on EC expression profiles leading to a phenotype with an increased propensity to respond to systemic changes (high cholesterol/glucose) in a pro-inflammatory fashion. Saphenous veins have been shown to possess arterial like properties when grafted into the coronary circulation including a tendency to become atherosclerotic (Aird 2006).

Under normal situations, the recruitment of neutrophils is an essential mechanism for combating invading pathogens. If however, this process is modified or malfunctions in someway, as is the case in some autoimmune diseases, it can lead to undesirable consequences. If recruitment is ineffective it can increase the host's susceptibility to infection leading to recurrent or persistent infections, which are never resolved effectively. If clearance of tissue resident apoptosing neutrophils is deregulated it can lead to chronic inflammation and organ damage (Morgan *et al.* 2005).

4.1.4 Use of cell lines to study in vitro endothelial cell systems

In vitro systems using primary cells are of most value as they enable the researcher to obtain the most representative impression of the *in vivo* situation in a particular organ. Although the most desirable system to use they pose many experimental difficulties. They are notoriously difficult to isolate and protocols vary widely throughout the literature. Once isolated and removed from the *in vivo* physiochemical environment, EC begin to dedifferentiate into stromal like cells due to the absence of external stimuli (Elvevold *et al.* 2008).

Due to the difficulty of isolating homogeneous primary EC populations immortalised cell lines have been developed to allow further research and understanding of endothelial cell function. Cell lines originate from a primary cell population and are conditionally immortalised with viral mechanisms to prevent senescence. Immortalised cells can be continually subcultured to high passages maintaining a constant stable phenotype. These characteristics provided a favourable cell type on

which to study the effects of inflammation on the phenotype and function of endothelial cells from different organs. A number of immortalised endothelial cell lines were used in studies including mUCEC-1 (Lidington *et al.* 2002), s.END (Bussolino *et al.* 1991) and b.End.5 (Rohnelt *et al.* 1997) originating from heart, skin and brain respectively.

Research in our lab has focussed on the inflammatory response and the process of leukocyte recruitment. Although cell lines are an invaluable experimental tool, it must be considered when interpreting results that the biology of these cells could be altered by the presence of the viral construct.

4.1.5 Recruitment in Kidney and Lung Tissue

The process of leukocyte recruitment in skin, brain, heart and liver was previously discussed in Sections 1.5.1-4. However, the expression pattern of EC markers and adhesion molecules was examined in sections of murine kidney and lung, however we did not examine expression in primary EC cultures or immortalised cell lines from these tissues, recruitment in these tissues is therefore discussed briefly.

ICAM-1 has been reported to be important for recruitment in both lung and kidney. Human glomerular cells were found to express ICAM-1 constititively and lack VCAM-1 and E-Selectin expression (Savage *et al.* 1997). The glomerulus is one of the few sites where recruitment takes place in capillaries, as observed in a murine model of glomerulonephritis (Kitching *et al.* 2009). In addition blockade of CCR1 has been

shown to block the progression of chronic kidney disease in mice (Anders *et al.* 2006).

In the lung ICAM-1 was shown to be involved in leukocyte recruitment but not fibrosis in a mouse model of bleomycin-induced lung injury (Matsuse *et al.* 1999). Chemokines play a role in recruitment in response to granulomatous diseases, KC and MIP-1α were shown to be involved in neutrophil recruitment of *Paracoccidioides brasiliensis*- infected mice in the acute phase reaction (Souto *et al.* 2003).

4.2 Results

4.2 1 Optimisation of methodology for comparison of endothelial cell marker expression.

In order to analyse the expression of particular markers by primary liver endothelial cells and to compare this to expression in situ in tissue we began using a combination of Immunohistochemical (IHC) and cell-based ELISA techniques. In all cases expression was compared to endothelium in other organs and to cell lines isolated from different tissues. Figures contain representative images from at least 3 repeats of each experiment. In every experiment the appropriate isotype matched controls and negative No Pri controls were done (Fig.4.1).

Initially sections of tissues were stained with haematoxylin and eosin to highlight gross anatomy and structure. In the liver, large portal vessels and smaller sinusoids are seen. In the kidney areas of both the cortex and medulla were captured showing glomeruli, capillaries (cortex), arteries and vessels (medulla). In the lung many

alveolar structures are present in addition to small bronchioles and branches of the pulmonary artery. The normal architecture of the brain is present showing the parenchyma. Sections were also stained for CD31 a pan-endothelial cell marker used as a positive control. CD31 expression was high in all tissues, with distinct staining patterns seen in lung and liver. In both kidney and liver there was more intense staining in the parenchyma and on the microvasculature.

Figure 4. 1: Control stained murine tissues.

Representative light micrographs of isotype matched control and no primary stained cryosectioned murine tissues quenched with 0.5% H_2O_2 in methanol and sodium azide, stained by IHC methods and counterstained with haemotoxylin. Primary antibody used at 25µg/ml, secondary at 1/1000. Image captured at x10 original magnification on Axiovert microscope using Axiovision software.

Similar histological methods were used to stain isolated cells grown in chamberslides. Figure 4.2 shows the typical appearance of cells in culture captured using phase contrast microscopy. mUCEC, sEND and b.END.5 cells all resembled EC with classical cobblestone morphology also seen in primary mLSEC. All grew rapidly and were split 1:3 every other day and were viable over extended periods with little or no apparent phenotypic drift (as judged by morphological stability). Of note, mUCEC-1 cells had a tendency to form small clusters on top of the monolayer when close to confluency and s.END cells initially adopted mixed endothelial/fibroblast morphology with some spindle shaped cells present.

Figure 4. 2: Images of immortalised EC lines and mLSEC.

Phase contrast light micrograph images of cell lines and primary mLSEC in culture. Images captured at x10 magnification on Axioskop.

Figure 4. 3: Control stained immortalised EC lines and mLSEC.

Representative light micrographs of isotype matched control and no primary stained methanol fixed EC stained by IHC methods and counterstained with haemotoxylin. Primary antibody used at 25µg/ml, secondary at 1/1000. Image captured at x10 original magnification on Axiovert microscope using Axiovision software.

We decided to use more quantitative ELISA technology to quantify protein expression on the cultured cells and to analyse changes in expression induced by cytokine treatment. In each experiment isotype-matched control reagents were used to determine background absorbance values resulting from non-specific binding. In subsequent figures data is represented as absorbance values minus background signal. The working concentrations of both primary and secondary antibodies were adapted from stock concentrations (data not shown) and optimised as outlined in Table 2.3. However to confirm the reproducibility of the system and to illustrate whether cytokine treatment altered non-specific binding of the antibody, pooled control data is shown in figures 4.1-4.5.

Due to complications and delays due to development of methodology for isolating mLSEC, ELISA experiments were not performed on these cells. Phenotypic analysis was instead performed by whole genome arrays (data not available for thesis).

Figure 4. 4: Rat IgG control samples for cell-based ELISA.

Data summarising ELISA for Rat IgG carried out on (A) mUCEC-1, (B) s.END and (C) b.End.5 cells stimulated with a variety of cytokine treatments for 4/24 hrs. Data expressed as absorbance normalised to control cytokine group. Error bars represent the +/- SEM n=3. One- way ANOVA, Bonferroni post-tests were carried out on all data.

Figure 4. 5: **Rab IgG control samples for cell-based ELISA.**

Data summarising ELISA for Rab IgG carried out on (A) mUCEC-1, (B) s.END and (C) b.End.5 cells stimulated with a variety of cytokine treatments for 4/24 hrs. Data expressed as absorbance normalised to control cytokine group. Error bars represent the +/- SEM n=3. One- way ANOVA, Bonferroni post-tests and were carried out on all data.

4.2.2 Expression of classical endothelial cell markers is maintained in culture.

Next we used the optimised methodologies described above to analyse the expression of key endothelial proteins on our cells in tissue and in culture.

Figure 4. 6: Expression profile of CD31 by IHC

Summary of CD31 expression in whole murine tissues, EC lines and mLSEC. and modulation of expression in response to cytokines. 5µm sections of murine tissue and methanol fixed EC lines and mLSEC cultured in chamberslides were stained using OHC methods. Images captured on Axioskop using Axiovision software at x10 magnification.

Figure 4. 7: Expression profile of CD31 in response to stimuli demonstrated by ELISA.

Analysis of molecule expression using cell-based ELISA on (A) mUCEC-1, (B) s.END and (C) b.End.5 immortalised cell lines treated with a variety of pro-inflammatory substances for 4/24hrs. Error bars represent the +/- SEM n=3.One-way ANOVA, Bonferroni post-tests were used to assess effect of treatment. Two-way ANOVA was used to assess the effect of time.

CD31 expression was high in all tissues (Fig 4.6), with distinct staining patterns seen in lung and liver. In the liver CD31 was present in portal structures and the sinusoids. In both kidney and liver there was more intense staining in the interstitium and microvasculature. All EC lines constitutively expressed CD31 to different degrees, with little variation after prolonged exposure to cytokines in mUCEC-1 cells. The presence of cytokines did not upregulate levels of CD31 above control in mUCEC-1 cells (Fig 4.7-3A). However, cell lines containing the murine polyoma construct (Fig 4.7-3B/C) expressed considerably higher levels of CD31; there was also a dose-dependent response to Il-1β and TNF-α.

Endoglin was present in the larger cerebral vessels in brain and smaller capillaries and in distinct patterns in the kidney vasculature but absent from the lung and liver (Fig. 4.8). Interestingly, modest levels were detected on primary isolated mLSEC, which were not apparent in whole tissue. Cell lines containing the polyoma virus construct (b.END.5 and sEND) expressed higher levels than SV40 immortalised cells (mUCEC-1). In particular expression in sEND cells was high and increased significantly upon prolonged exposure to pro-inflammatory stimuli with IFN-γ having a pronounced effect (Fig. 4.9).

Figure 4. 8: Expression profile of Endoglin by IHC

Summary of Endoglin expression in whole murine tissues, EC lines and mLSEC. and modulation of expression in response to cytokines. 5µm sections of murine tissue and methanol fixed EC lines and mLSEC cultured in chamberslides were stained using OHC methods. Images captured on Axioskop using Axiovision software at x10 magnification.

Figure 4. 9: Expression profile of Endoglin in response to stimuli demonstrated by ELISA.

Analysis of molecule expression using cell-based ELISA on (A) mUCEC-1, (B) s.END and (C) b.End.5 immortalised cell lines treated with a variety of pro-inflammatory substances for 4/24hrs. Error bars represent the +/- SEM n=3. One-way ANOVA, Bonferroni post-tests were used to assess effect of treatment. Two-way ANOVA was used to assess the effect of time. ***<0.001

JAM-2 was observed at low levels in the brain and more widely distributed in lung and liver (although somewhat non-specifically-Fig. 4.10) and diffusely in the kidney. JAM-2 was expressed in all unstimulated EC lines with the highest levels of expression apparent in sEND and mUCEC-1 cells which both significantly changed over time (Fig. 4.11). JAM-2 expression was high by immunohistochemistry but lower in ELISA. However, larger amounts are present in the control at 24 hours. In sEND and b.END.5 cells increased stimulation lead to a decrease in expression unlike mUCEC-1 where expression was slightly increased in particular in response to LPS and TNF-α+IFN-γ.

Figure 4. 10: Expression profile of JAM-2 by IHC

Summary of JAM-2 expression in whole murine tissues, EC lines and mLSEC. and modulation of expression in response to cytokines. 5µm sections of murine tissue and methanol fixed EC lines and mLSEC cultured in chamberslides were stained using OHC methods. Images captured on Axioskop using Axiovision software at x10 magnification.

Figure 4. 11: Expression profile of JAM-2 in response to stimuli demonstrated by ELISA.

Analysis of molecule expression using cell-based ELISA on (A) mUCEC-1, (B) s.END and (C) b.End.5 immortalised cell lines treated with a variety of pro-inflammatory substances for 4/24hrs. Error bars represent the +/- SEM n=3. One-way ANOVA, Bonferroni post-tests were used to assess effect of treatment. Two-way ANOVA was used to assess the effect of time. *<0.05 and ***<0.001

CD34 expression appeared high in lung and kidney sections (Fig. 4.12). However staining was somewhat non-specifically in kidney. In liver, distinct CD34 staining was present in vascular and sinusoidal areas and present in isolated mLSEC. Expression was constitutive in all cell lines with the highest levels present in b.END.5 despite the absence in whole brain tissue (Fig. 4.13). On the whole levels increased over time with stimulation and these changes were significant in mUCEC-1 and s.END cells.

Figure 4. 12: Expression profile of CD34 by IHC

Summary of CD34 expression in whole murine tissues, EC lines and mLSEC. and modulation of expression in response to cytokines. 5µm sections of murine tissue and methanol fixed EC lines and mLSEC cultured in chamberslides were stained using OHC methods. Images captured on Axioskop using Axiovision software at x10 magnification.

Figure 4. 13: Expression profile of CD34 in response to stimuli demonstrated by ELISA.

Analysis of molecule expression using cell-based ELISA on (A) mUCEC-1, (B) s.END and (C) b.End.5 immortalised cell lines treated with a variety of pro-inflammatory substances for 4/24hrs. Error bars represent the +/- SEM n=3. One-way ANOVA, Bonferroni post-tests were used to assess effect of treatment. Two-way ANOVA was used to assess the effect of time. *<0.05

4.2.3 Induction of adhesion molecules in response to cytokine treatment.

Constitutive E-Selectin expression was insignificant in the majority of samples, although modest staining was present in kidney tissue around the glomeruli (Fig. 4.14). In cultured cell lines high dose TNF-α and LPS produced significantly higher expression of E-Selectin in b.END.5 cells and IL-1β 100U/ml in s.END cells. E-Selectin levels significantly decreased in s.END cells over time (Fig. 4.15).

Figure 4. 14: Expression profile of E-Selectin by IHC

Summary of E-Selectin expression in whole murine tissues, EC lines and mLSEC. and modulation of expression in response to cytokines. 5µm sections of murine tissue and methanol fixed EC lines and mLSEC cultured in chamberslides were stained using OHC methods. Images captured on Axioskop using Axiovision software at x10 magnification.

Figure 4. 15: Expression profile of E-Selectin in response to stimuli demonstrated by ELISA.

Analysis of molecule expression using cell-based ELISA on (A) mUCEC-1, (B) s.END and (C) b.End.5 immortalised cell lines treated with a variety of pro-inflammatory substances for 4/24hrs. Error bars represent the +/- SEM n=3. One-way ANOVA, Bonferroni post-tests were used to assess effect of treatment. Two-way ANOVA was used to assess the effect of time. *<0.05, **<0.01 and ***<0.001

ICAM-2 expression was high in sections of liver, kidney and lung. Interestingly intense staining was present in the liver parenchyma and microvasculature but expression was absent on isolated cells (Fig. 4.16). In the kidney ICAM-2 was present in the interstitium and larger vascular structures. However staining was absent in the brain. ICAM-2 was constitutively expressed in immortalised EC lines with higher levels apparent in s.END and b.END.5 cells. A significant increase in expression was produced in s.END cells upon prolonged cytokine stimulation (Fig. 4.17).

Figure 4. 16: Expression profile of ICAM-2 by IHC

Summary of ICAM-2 expression in whole murine tissues, EC lines and mLSEC. and modulation of expression in response to cytokines. 5µm sections of murine tissue and methanol fixed EC lines and mLSEC cultured in chamberslides were stained using OHC methods. Images captured on Axioskop using Axiovision software at x10 magnification.

Figure 4. 17: Expression profile of ICAM-2 in response to stimuli demonstrated by ELISA.

Analysis of molecule expression using cell-based ELISA on (A) mUCEC-1, (B) s.END and (C) b.End.5 immortalised cell lines treated with a variety of pro-inflammatory substances for 4/24hrs. Error bars represent the +/- SEM n=3. One-way ANOVA, Bonferroni post-tests were used to assess effect of treatment. Two-way ANOVA was used to assess the effect of time. **<0.01

VCAM-1 expression was absent or very low in all tissues tested (Fig. 4.18) and on EC lines from brain and skin by ELISA (Fig. 4.19). mUCEC-1 cells in particular expressed VCAM-1 even in the absence of stimuli. In addition the opposing dose dependent response of mUCEC-1 to increasing concentrations of IL-1β seen in a number of different markers was also apparent *(i.e.* increasing dose induced increases in expression at 4hrs compared to decreased expression at 24hrs) however this was not statistically significant. VCAM-1 was present in b.End.5 cells at low levels by ELISA, which can be seen in IHC and low levels were present diffusely in whole brain tissue. VCAM-1 expression significantly increased over time and particular increases in expression were observed following treatment with high dose TNF-α (500U/ml) and TNF-α and IFN-γ combined.

Figure 4. 18: Expression profile of VCAM-1 by IHC

Summary of VCAM-1 expression in whole murine tissues, EC lines and mLSEC. and modulation of expression in response to cytokines. 5µm sections of murine tissue and methanol fixed EC lines and mLSEC cultured in chamberslides were stained using OHC methods. Images captured on Axioskop using Axiovision software at x10 magnification.

Figure 4. 19: Expression profile of VCAM-1 in response to stimuli demonstrated by ELISA.

Analysis of molecule expression using cell-based ELISA on (A) mUCEC-1, (B) s.END and (C) b.End.5 immortalised cell lines treated with a variety of pro-inflammatory substances for 4/24hrs. Error bars represent the +/- SEM n=3. One-way ANOVA, Bonferroni post-tests were used to assess effect of treatment. Two-way ANOVA was used to assess the effect of time. *<0.05, **<0.01 and ***<0.001

4.2.4 Expression of VAP-1 and LYVE-1 is minimally altered by cytokine treatment.

As mentioned previously no characteristic single marker of mLSEC exists. mLSEC are identified by morphological and functional properties in addition to expression of a number of different markers. Although expression of VAP-1 and LYVE-1 are not exclusively limited to liver sinusoidal endothelium dual positivity in cells cultured from liver is indicative of mLSEC.

VAP-1 was generally absent from the murine tissues tested but there were odd darker structures present in liver, which may have been artefacts of staining (Fig. 4.20). In addition diffuse staining was apparent in kidney. VAP-1 was detected by ELISA at very low levels under certain stimulation conditions in s.END and b.End.5 cells, confirmed by IHC (Fig. 4.21). Globally VAP-1 expression significantly decreased over time. Primary mLSEC appeared to express low levels.

Figure 4. 20: Expression profile of VAP-1 by IHC

Summary of VAP-1 expression in whole murine tissues, EC lines and mLSEC. and modulation of expression in response to cytokines. 5µm sections of murine tissue and methanol fixed EC lines and mLSEC cultured in chamberslides were stained using OHC methods. Images captured on Axioskop using Axiovision software at x10 magnification.

Figure 4. 21: Expression profile of VAP-1 in response to stimuli demonstrated by ELISA.

Analysis of molecule expression using cell-based ELISA on (A) mUCEC-1, (B) s.END and (C) b.End.5 immortalised cell lines treated with a variety of pro-inflammatory substances for 4/24hrs. Error bars represent the +/- SEM n=3. One-way ANOVA, Bonferroni post-tests were used to assess effect of treatment. Two-way ANOVA was used to assess the effect of time. **<0.01

LYVE-1 expression was absent from brain and kidney tissue however positive stain was present in lung and liver (Fig. 4.22) In the liver the staining pattern was as expected in the sinusoids and around some hepatic veins, in addition freshly isolated mLSEC were also positive. In the lung LYVE-1 may be staining lymphatic structures. LYVE-1 was present at low levels in all cell lines (Fig. 4.23). However s.END cells in particular expressed higher levels of LYVE-1 at 4 hours and this significantly decreased over time. IHC images show isolated LYVE-1 positive cells present in the population. This could have resulted from contamination of initial cultures with lymphatic EC as the skin contains large amounts of lymphatic structures.

Figure 4. 22: Expression profile of LYVE-1 by IHC

Summary of LYVE-1 expression in whole murine tissues, EC lines and mLSEC. and modulation of expression in response to cytokines. 5µm sections of murine tissue and methanol fixed EC lines and mLSEC cultured in chamberslides were stained using OHC methods. Images captured on Axioskop using Axiovision software at x10 magnification.

Figure 4. 23: Expression profile of CD31 in response to stimuli demonstrated by ELISA.

Analysis of molecule expression using cell-based ELISA on (A) mUCEC-1, (B) s.END and (C) b.End.5 immortalised cell lines treated with a variety of pro-inflammatory substances for 4/24hrs. Error bars represent the +/- SEM n=3. One-way ANOVA, Bonferroni post-tests were used to assess effect of treatment. Two-way ANOVA was used to assess the effect of time. *<0.05

4.3 Discussion

The initial aim of these experiments were to optimise phenotypic assays using whole tissue and immortalised cell lines to in order to determine the best conditions for analysis of primary endothelial cell populations. However, in addition they provided interesting insights into tissue specific variation in expression of endothelial cell markers, adhesion molecules and responses to pro-inflammatory stimuli.

4.3.1 Contribution of immortalised cell lines to research

Primary cells are notoriously difficult to isolate effectively to generate high numbers of pure cell populations, as covered in Chapter 3. An important experimental tool is available to allow researchers to carry out preliminary experiments and optimise conditions for more insightful experiments using primary cells. Immortalised endothelial cell lines have been developed to allow further research and understanding of EC function. In general viral mechanisms are used to prevent senescence. Care must be taken when utilising cell lines as the immortalisation process can result in phenotypic changes or altered responses to stimuli. The EC lines used were hardy and tolerant to stress. However, in some instances the EC lines were unresponsive to levels of cytokine stimulation, which would have been expected to yield a more pronounced response than elicited.

4.3.2 Expression of endothelial markers and adhesion molecules by IHC and response of EC to pro-inflammatory insult.

We examined several murine sources for the expression of a number of endothelial cell markers and adhesion molecules. Samples of murine liver, brain, lung and kidney were obtained from Balb/c mice and small numbers of primary mLSEC for immunohistochemical analysis. In addition expression of all molecules was assessed on a number of immortalised EC lines from heart (mUCEC-1), skin (s.END) and brain (b.End.5). To further support these qualitative techniques, quantitative cell-based ELISAs were used to assess the response of EC lines to pro-inflammatory insult over varying time periods. Expression of most of the markers was consistent with current published research; however, the majority of available data is from human rather than murine tissues (Feuerhake *et al.*1998;Savage *et al.*1997;Steinhoff *et al.* 1993). In general no positive staining was observed in control samples (No Pri, IMC), with the exception of Rat IgG in liver where some non-specific background stain was apparent. All data is summarised in Table 4.1.

The expression profile of CD31 has previously been examined in murine tissues (Daneker *et al.* 1998;Sheibani *et al.* 1999) and is present at high levels in lung, heart and kidney and at lower levels in brain and liver. We also found that expression was high in lung, kidney and liver and lower levels in brain. In concurrence our ELISA data showed that CD31 was expressed on all cell lines and on mLSEC. Expression was more pronounced in EC immortalised with the polyoma construct. However, there was little variation in expression to prolonged exposure to cytokines. This expression is likely to be functionally important as rodent models have indicated that

leukocyte diapedesis can be abrogated with the use of anti CD31 blocking antibodies (Schenkel *et al.* 2004). The process is however not completely lost in a C57BL/6 CD31 knockout mouse but it is thought that this specific strain in the event of inflammation, possesses the ability to compensate for lack of CD31. Though the specific process is unknown, it is most likely due to the action of other unidentified adhesion molecules (Schenkel *et al.* 2004).

CD31 is widely used as a pan-endothelial cell marker and was indeed abundantly expressed on vascular endothelium and to a lesser extent on the hepatic sinusoids. Expression of this marker on sinusoidal endothelium remains controversial (reviewed in (Do *et al.* 1999;Neubauer *et al.* 2000a)), it has been shown to be expressed in murine mLSEC (Do *et al.* 1999) but the presence of this molecule in hLSEC is unclear. Some reports suggest that it is present in cirrhotic liver but minimally in normal liver (Daneker *et al.* 1998) others report the opposite (Medina *et al.* 2005). Data from our group have shown CD31 to be present in both vascular and sinusoidal endothelium (Lalor *et al.* 2006). CD31 expression has been examined by PCR a qualitative method (Unger *et al.* 2002) however it is not recommended to use either method in isolation. CD31 it has been used as a determining feature of hepatic endothelial cells in rat (Ruhnke *et al.* 2003). The data presented here clearly shows that it is expressed on both sinusoidal and vascular endothelium in mouse.

Endoglin is expressed on the majority of EC with levels increasing in activated vascular endothelial cells at sites of angiogenesis, inflammation and wound healing (Cheifetz *et al.* 1992;ten Dijke *et al.* 2008). As a component of the TGF-β receptor Endoglin has been found on EC, activated macrophages, fibroblasts and smooth

muscle cells (Conley *et al.* 2000). The involvement in vascular development, remodelling and angiogenesis (Duff *et al.* 2003) in addition to elevated levels of expression in cancerous tumours make it attractive as a potential therapeutic target (Carmeliet *et al.* 2000). Distinct expression of Endoglin was present on vascular structures of murine brain and kidney. In brain Endoglin is expressed on all EC and in the adventitia (Matsubara et al. 2000) and has been found in human renal cell carcinomas (Sandlund *et al.* 2006). Endoglin was expressed on distinct single mUCEC-1 cells and also present at high levels in s.END and b.End.5 cells sites of angiogenesis and highly vascularised areas. ELISA data showed a particular increase in s.END cell expression in response to IFN-γ. Distinct staining in mUCEC-1 could be due to contaminating vascular EC but this is unusual as this cell line is immortalised cardiac endothelium and expression should be high. Endoglin is involved in the development of the heart and was found to be expressed in epicardial and myocardial vessels (Valeria *et al.* 2008).

The expression pattern of JAM-2 had not previously been examined in the liver, and our data show that it is expressed in the lung and non-specifically in the liver and was also present at low levels in kidney. JAM-2 expression was present in all cell lines and on mLSEC as confirmed by ELISA but the effects of cytokine exposure on expression varied with cell type. JAM-2 has been reported to be expressed on endothelial and lymphatic cells in high endothelial venules (HEV) in mice (Aurrand-Lions *et al.* 2001). In murine studies JAM-2 has shown to greatly increase the proportion of lymphocytes migrating across endothelioma cells in monolayer culture (Johnson-Leger *et al.* 2002). It has also been shown in a human experimental system using HUVEC cultured on transwell inserts that blocking of JAM reduced the transmigration of peripheral blood leukocytes. The same group obtained results that

suggest this is also true in the murine system (Aurrand-Lions *et al.* 2002a;Aurrand-Lions *et al.* 2002b). The concept that JAM-2 is an important molecule involved in directing the transmigration of leukocytes is also interesting as the levels increased in conjunction with ICAM-2, another critical molecule involved in leukocyte recruitment (Springer 1995). Here we describe for the first time the non-specific expression pattern of JAM-2. JAM-2 was present on both vascular and sinusoidal areas. The particularly high expression of JAM-2 in s.END cells in combination with LYVE-1 expression again supports the idea of contamination of these cells by lymphatic EC.

CD34 is a marker of vascular endothelium. It is absent in most sinusoidal cells of normal human liver (Couvelard *et al.* 1993;Daneker *et al.* 1998;Xu *et al.* 2003) but present in disease states following the process of capillarisation (Cui *et al.* 1996;Frachon *et al.* 2001) and during liver development (Nava *et al.* 2005). CD34 expression was high in all non-hepatic tissues and cell types examined here as previously published (Baumhueter *et al.* 1994), and was present in all EC cell lines and primary mLSEC with particularly high levels in b.END.5 cells

Both E and P-Selectin have been shown to be critical for leukocyte recruitment in intravital studies (Lawrence *et al.* 1991;Zimmerman *et al.*1991;Zimmerman *et al.* 1992), however more recent studies have shown that CD44, CD34 and VAP-1 can compensate in their absence (Ley *et al.* 2007). E-Selectin (CD62E) is expressed rapidly and synthesised *de novo* in activated endothelium in response to inflammatory mediators. During an inflammatory response P-Selectin is immediately trafficked to the cell surface from Weibel-Palade bodies, followed closely by E-Selectin leading to enhanced leukocyte recruitment and decreasing rolling velocity, increasing the chances of firm adhesion to the endothelium. Selectins bind to heavily

glycosylated carbohydrate or mucin ligands including sialyl lewis and P-Selectin glycoprotein ligand (PSGL-1). E-Selectin binds both of these ligands in addition to CD43, CD44 and E-Selectin ligand-1 (Ley *et al.* 2007). E-Selectin was absent from all tissues and expressed at low levels in all cell types by ELISA despite stimulation and the inducible nature of E-Selectin. Small responses were seen in with high TNF-α (500U/ml) and LPS, which supports the idea that immortalised cell lines, are more resistant to insult reducing the responsiveness to cytokines. The lack of expression in the liver tissue highlights the absence of a role for selectins in recruitment to the liver. Due to the small size of sinusoidal vessels, and low shear forces present within them, selectins are not required for tethering and rolling along the vascular wall and this role can be compensated for by additional molecules. However, E-Selectin knockout mice were shown to have a reduced responsiveness to Gal/ET liver injury by inhibiting the activation and transmigration of neutrophils (Lawson *et al.* 2000).

ICAM-2 is constitutively expressed on endothelium and is a crucial player in leukocyte recruitment and adhesion (Lehmann *et al.* 2003). This expression in unstimulated endothelial cells could implicate ICAM-2 in the process of immune surveillance where leukocytes traffic through uninflamed tissues. It has been shown by Reiss *et al* that if ICAM-2 deficient mouse endothelioma cells are used in a transmigration assay the migration of T-cells across the endothelial surface was greatly inhibited compared to the migration across wild type cells treated with anti-ICAM-2 functional blocking antibodies (Reiss *et al.* 1999). ICAM-2 was expressed highly in distinct patterns in kidney and liver and at lower levels in lung and brain. Although expression was only apparent in b.End.5 cells by IHC, ELISA's indicated lower expression in mUCEC-1 and s.END cells despite previously reported expression (Ghigo *et al.* 1995). Dose responses to TNF-α and IL-1β were apparent.

The immortalised b.End.5 cells have been reported to express ICAM-1 which is indicated to play a role in actual tissue, hence the absence of staining in whole tissue (Bussolino *et al.* 1991).

VCAM-1 is involved in the initial step of the leukocyte recruitment cascade 'tethering and rolling' the leukocyte in conjunction with the E and P- selectins. Under flow conditions VCAM-1 supports the capture of leukocytes at lower shear stresses than the selectins but it is thought to capture eosinophils very effectively. Expression of VCAM-1 is required *de novo* and synthesis peaks 24 hours after stimulation (Reinhardt *et al.* 1998), as was apparent in our ELISA data. Expression was low in all tissue sections and cultured cells (with the exception of mUCEC-1) by IHC as expected in the absence of any pro-inflammatory stimuli. The levels of VCAM-1 were particularly high in mUCEC-1 cells by ELISA, up to 3-fold higher than all other molecules examined. This finding is concurrent with published research and the high expression, even in the absence of a cytokine stimulus had ramifications in functional experiments (Lidington *et al.* 2002). In contrast s.END and b.End.5 expression was almost absent by ELISA although levels increased in b.End.5 cells after prolonged exposure.

VAP-1, is constitutively expressed on human lymphatic and hepatic endothelium, rabbit endothelium and transfected rat endothelium (Lalor *et al.* 2006) and has shown to bind flowing lymphocytes, but knockout models indicated that the absence of VAP-1 leads to increased rolling velocity and decreased rate of leukocyte transmigration (Kirton *et al.* 2005). In support of this our data showed that VAP-1 was present at low levels in liver and kidney (Kurkijarvi *et al.* 2001). The presence of VAP-1 in mLSEC populations is also in concurrence with previous reports (Lalor *et al.* 2006). The

positive stain is present on sEND cells by ELISA. The skin contains large amounts of lymphatic tissue and VAP-1 has previously been found in the skin and serum of psoriatic patients suggesting a role in inflammation (Madeja *et al.* 2007). It is interesting that both LYVE-1 and VAP-1 which can be considered as positive identifiers of sinusoidal endothelium are expressed on both the lymphatic and sinusoidal endothelium as both maintain a similar immunological environment where a lot of antigen presentation is taking place.

LYVE-1 was has also been demonstrated to be an important molecule in the lymphatics where expression is high on human, mouse and rat endothelial cells (Banerji *et al.* 1999). It has also been found in distinct cohorts of activated tissue macrophages and on LSEC and endothelial cells of the spleen, sites where HA is taken up and degraded (Carreira *et al.* 2001). We found LYVE-1 was absent from brain but distinct staining patterns were present in the lung and liver. Expression also decreased over time unlike mUCEC-1 and b.End.5 cells where expression was low and stable. The previously unreported expression of LYVE-1 on mUCEC-1 and b.End.5 cells is unusual, this lymphatic marker is thought to be expressed in the liver and lymphatics but not the heart or brain. This may be an artefact of immortalisation.

Taken together, this data produces valuable qualitative and quantitative images of expression patterns. Overall the expression profiles provide some useful phenotypic data, which helped correctly identify primary endothelial cells yielded by isolation protocols or from a mixed population of cells or tissue. s.END cells lacked expression of E-Selectin important for recruitment to skin but generally cell lines immortalised with the polyoma virus construct were on the whole more ‘endothelial-like’ with higher expression of CD31, CD34 and Endoglin. The most notable differences were seen

with mUCEC-1 cells, previous reports showed that these cells expressed CD31 but we found limited amounts compared to the high expression of VCAM-1 even in the absence of external stimuli. These differences most likely as a result of immortalisation must be taken into account when considering the functional properties of immortalised cell populations.

mLSEC express markers found on liver tissue and within the sinusoids, in particular LYVE-1, CD31, Endoglin and to some extent VAP-1. Morphologically mLSEC resembled the human counterparts with a cobblestone appearance giving us confidence in the primary cell populations obtained.

5. FUNCTIONAL ANALYSIS OF LEUKOCYTE RECRUITMENT TO ORGAN SPECIFIC ENDOTHELIAL CELLS IN RESPONSE TO CYTOKINE STIMULATION.

5.1 Introduction

The preceding chapters have confirmed that cells isolated from different murine organs maintain a distinct phenotype in culture. EC from heart, brain, skin and liver were positive for classical EC markers such as CD34 and Endoglin and expression of adhesion molecules involved in recruitment was induced by pro-inflammatory stimuli. Therefore this chapter considers the ability of the different cell isolates to support the adhesion and migration of whole purified lymphocytes and CD4+ and CD8+ subsets. In general the process of inflammatory cell recruitment is the same in most tissue beds, however there are some differences, which I will highlight here.

5.1.1 Leukocyte Recruitment via endothelial cells

The recruitment of leukocytes into tissues is a highly regulated process, under physiological conditions. A general paradigm of leukocyte recruitment exists (Fig. 5.1), involving a defined sequence of events divided into several steps (Adams *et al.* 1994;Buckley *et al.* 2000; Springer 1994). Flowing leukocytes must make contact with the vessel wall. On contact with the endothelium, rapidly-reversible interactions are formed with Selectin receptors (Lawrence *et al.* 1991) in general, leading to tethering and rolling of the leukocyte along the vascular wall (Alon *et al.* 2002;Bahra, *et al.* 1998). Chemokines present on the surface of vascular endothelial cells initiate activation of the leukocyte leading to tight adhesion to the vascular surface via integrins and their receptors (Springer 1995). In the final stages, the leukocyte migrates through the endothelium to the surrounding tissue in response to a chemotactic gradient generated by endothelial or resident inflammatory cells. In this

chapter I wanted to investigate how the molecular regulation of this process differs on endothelium from different tissues.

5.1.1.1 STEP ONE: Capture on the endothelium.

The selectins consist of a family of cell adhesion molecules, which share a common structure, consisting of an N-terminal lectin-binding domain, an epidermal growth factor domain, a transmembrane region and a variant number of consensuses repeats. There are three main types of Selectins, L, P and E, named in accordance with the cell type on which they were first discovered, lymphocytes, platelets and endothelium respectively. L-selectin is constitutively expressed on most leukocytes and the levels of expression alter when the cell becomes activated. For example upon neutrophil activation, L-Selectin is rapidly shed from the neutrophil surface (Eriksson *et al.* 2001). This molecule binds to specific carbohydrate moieties on the vascular endothelium (Bevilacqua *et al.* 1993) and is particularly important in recruiting lymphocytes to the lymphatics. P-selectin is involved in platelet aggregation and essential for the clotting response. This molecule is stored in intracellular granules (α-granules in platelets and Weibel-Palade bodies in EC), as it needs to be rapidly mobilised to the cell surface. P-selectin is also found on activated endothelial cells and is up regulated by TNF and histamine. E-selectin is unique to endothelial cells and expression increases in response to proinflammatory cytokines such as IL-1, TNF-α and LPS (Ley *et al.* 2007;Parkin *et al.* 2001). Various selectin ligands have been discovered and all three bind to the oligosaccharide Sialyl Lewis (sLEx) with low affinity. Among the best characterised is P-selectin glycoprotein ligand 1 or PSGL-1(Adams *et al.* 1994;Springer 1994). Interactions between selectin adhesion molecules and ligands are transient. The interaction permits the leukocyte to scan

the vascular surface for activatory messages. If the adherent cell is not activated by specific factors initiating firm adhesion the cell is released in this reversible reaction (Springer 1994;.Sims *et al.* 2002). This close proximity between adherent leukocyte and luminal endothelial surface is favourable for the presentation of surface bound chemokines to initiate subsequent steps in the cascade (Tanaka *et al.* 1993). Selectin mediated adhesion has been found to be particularly important in post capillary venules of tissues with large vessel diameters and high shear environments such as the skin (Hickey *et al.* 1999). However, in tissues such as the liver where the sinusoids are so narrow and shear so low such interactions are unnecessary (Wong *et al.* 1997). Initially cells were thought to become trapped, but further studies have found VCAM-1 and ICAM-1 to be important. In addition adhesion can occur via integrin dependent or independent mechanisms such as the non-classical pathway involving CLEVER-1, the mannose receptor, CD44 and VAP-1 (Lee *et al.* 2008;Shetty *et al.* 2008).

5.1.1.2 STEP TWO: Leukocyte Activation or 'triggering'

After initial capture and/or rolling the leukocyte must become activated by specific resident factors to initiate strong adherence to the vascular endothelium. This activation is mediated by chemokines, a group of chemoattractive cytokines which bind specifically to different subsets of leukocytes bearing appropriate chemokine receptors (Miller *et al.* 1992). These chemokines are produced by various inflammatory cells and activated endothelium and bind to specific G-protein coupled chemoattractant receptors expressed on the surface of leukocytes. Chemokine and receptor contact initiates intracellular signalling pathways, through G-protein coupled receptors resulting in the mobilisation of high-affinity integrin receptors to the cell

surface (Adams *et al.* 1994;Buckley *et al.* 2000). The specificity of chemokine action can be increased by site-specific or activation-specific expression of proteoglycans on the endothelium, which bind and present chemokines to particular leukocyte sub-populations (Adams *et al.* 1994).

Chemokines can be grouped according to the location of two highly conserved cysteine (C) residues within a number of different amino acids (X) in their structure. Thus there are CXC (α-chemokines) and CC (β-chemokines). CXC chemokines can be further subdivided on the presence of a glutamic acid leucine-arginine (ELR) motif prior to CXC. ELR containing CXC chemokines act on neutrophils (IL-8) whereas those lacking the motif act upon T-Cells (ITAC/MIG). CC chemokines act mostly on lymphocytes, eosinophils and monocytes for example MIP and SDF. There are some exceptions; to date only fractalkine (CXXXC) and lymphotactin (C) are known to exist (Murdoch *et al.* 2000;Negus *et al.* 1996). Chemokines are presented on the surface of endothelial cells by binding heparin sulphate proteoglycans (*i.e.* IL-8 and Gro-α) or the Duffy antigen receptor for chemokines (DARC), also found on erythrocytes (Hadley *et al.* 1997). Proteoglycan binding is thought to increase the efficiency of chemokine presentation and binding to leukocytes (Parkin *et al.* 2001).

Aside from chemokine-dependent signalling, adhesion can also be stimulated by a number of phospholipid-derived mediators such as leukotrienes and prostaglandins metabolites of arachidonic acid (AA) and platelet activating factor (PAF). PAF and AA are released by endothelial cells and cellular phospholipases respectively in response to inflammatory mediators. The cycloxygenase pathway generates prostoglandins from AA, stimulating vasodilation whereas the lipoxygenase pathway

produces a number of leukotrienes, which are potent chemotactic agents. PAF was originally named for its ability to aggregate and cause the degranulation of platelets but is also know to interact with neutrophils leading to activation via PAF receptor (Au *et al.* 2001). Juxtacrine signalling in conjunction with P-Selectin tethering the leukocyte to the EC wall leads to activation of β2 integrins (CD11/18) causing tighter adhesion to the endothelium (Prescott *et al.* 1990). In addition products of Cytochrome P450 (CYP450) enzymes activated distinct $Ca2^{+}$ channels regulating B-Cell plasma membrane potential and adhesion to integrins ICAM-1 and VCAM-1 involved in trafficking (Liu *et al.* 2006).

5.1.1.3 STEP THREE: Firm adhesion

Strong and tight adhesion to the luminal endothelial surface is the next step in the extravasation process and is mediated by integrins binding to immunoglobulin-superfamily endothelial ligands. The expression of heterodimeric integrin glycoproteins varies with cell type. Composed of two non-covalently linked alpha (α) and beta (β) sub-units of which the former is the shorter, integrins can be classified according to their β-subunit. The α and β domains can interact in many different combinations, resulting in a wide variety of integrins, only six of which are involved in leukocyte endothelial interaction. The β-1 and β-2 families are most important, α4β1, also known as very-late activation antigen-4 (VLA-4) is expressed by activated T-Cells and αLβ2 or the lymphocyte function associated antigen-1 (LFA-1) is expressed by both naïve and effector T-Cells (Adams *et al.* 1994). In addition β2 integrins (Mac-1) are involved in adhesion of polymorphonuclear neutrophils (PMN) to endothelium aggregation of which induces production of IL-8 (Walzog *et al.* 1999). The counter receptors for leukocyte integrins Intercellular adhesion molecule-1 (ICAM-1) and

ICAM-2 bind to the β2 integrins whereas vascular adhesion molecule-1 (VCAM-1) binds to the β1 integrins (Adams *et al.* 1994). ICAM-2 is constitutively expressed on vascular endothelium, and supports lymphocyte recruitment to uninflamed tissue (Springer 1994). Conversely ICAM-1 and VCAM-1 are induced in response to pro-inflammatory cytokines recruiting leukocytes to the site of infection and inflammation (Bevilacqua *et al.*1993;Springer 1990a;Springer 1990b).

5.1.1.4 STEP FOUR: Transmigration

Next the leukocyte must extravasate or transmigrate across the endothelial wall and enter the surrounding tissues in a process called diapedesis or transendothelial migration (TEM). For a significant period of time it was thought that leukocytes only traversed through the endothelium into the surrounding tissues through the junctions between juxtaposed endothelial cells (*i.e.* a paracellular route) (Feng *et al.* 1998). However, a growing amount of research has demonstrated that leukocytes may also pass through pores in endothelial cell bodies (the transcellular route) but this remains controversial (Burns *et al.* 2003). This migratory process is controlled by various pro-migratory factors including cytokines and chemoattractants. Several molecules are thought to be involved in paracellular transmigration in particular PECAM-1 (CD31), CD99 and Junctional Adhesion Molecules (JAM's) (Muller *et al.* 2003). CD99 and CD31 are both expressed on most types of leukocytes and bind to the same molecule on adjacent EC in homophilic interactions having a synergistic effect on TEM. JAM-A was originally identified in murine tight junctions (TJ) in endothelial and epithelial cells and found to be important in the migration of Neutrophils and monocytes (Martin-Padura *et al.* 1998). Endothelial JAM-A acts as a ligand for LFA-1 and if blocked reduces lymphocyte TEM. JAM-2 has also been shown to enhance

leukocyte TEM and facilitate platelet binding to PMN via CD11b/CD18 (Mac-1) (Liu *et al.* 2004).

Transcellular migration was first described in the 60's, where it was revealed that a significant number of leukocytes traversed the endothelium without disrupting EC junctions suggesting that they migrated through endothelial cytoplasm. This area of research has been under explored since, due to the inability to effectively visualise such events. Now with the advent of the electron microscope, confocal microscopy and computerised image analysis techniques scientists are able to distinguish neutrophils migrating through a transcellular pore distinct from endothelial junctions (Feng *et al.* 1998;Marchesi *et al.* 1964). EC's are heavily involved in regulating vascular permeability and contain several subcellular membrane structures including fenestrae, caveolae and vesiculo-vascular organelles (VVO's) to accommodate for this. The current hypothesis suggests that several of these structures may fuse to form a pore through which the leukocyte can migrate (Carman *et al.* 2007). For example it has been observed that leukocytes transmigrate at caveolin-1 rich sites and knockdown by siRNA decreases TEM (Wittchen *et al.* 2009). Interestingly in one study transcellular migration of lymphocytes accounted for ~30% of total TEM across microvascular endothelium but <10% across macrovascular HUVEC (Carman *et al.* 2007). This implies that EC heterogeneity will result in differential regulation of TEM.

Migrating leukocytes must negotiate several obstacles to enter the surrounding tissues, in addition to tight and adherens junctions in the endothelium cells must penetrate any underlying basement membrane, interstitium and tissue epithelium (Liu *et al.* 2004). These elements differ from one tissue environment to another depending on the characteristics of that vascular bed. Endothelial adherens junctions

(AJ) contain VE-Cadherin a transmembrane protein, which interacts with the actin cytoskeleton, stabilising the cell (Lampugnani *et al.* 1997). Adhesion of neutrophils and monocytes was found to trigger transient displacement of VE-Cadherin due to uncoupling from actin to allow passage of leukocytes via activation of signalling events. In recent years it has been suggested that the EC themselves play an active role in TEM, with the discovery of the transmigratory cup structure (Liu *et al.* 2004). This cellular dock, which partially captures the leukocyte, is rich in actin in addition to α-actinin, vinculin, VASP, the ERM proteins ezrin and moesin, ICAM-1 and VCAM-1. Barreiro *et al* postulated that leukocyte attachment induced clustering of ICAM-1 and VCAM-1 at the endothelial surface, leading to activation of bound ERM proteins, causing local cytoskeletal remodelling forming protrusions, which encased the transmigrating leukocyte (Barreiro *et al.* 2002). It was thought that cup formation was required for efficient capture of leukocytes under shear flow, but this was disproved. It is now suggested that these structures are not for adhesion strengthening but rather required for TEM. Much more research is required to fully characterise this structure but it is an important consideration in TEM.

5.1.2 Modulation of EC responses by their environment

The generic stages in the extravasation process described above are applicable in most settings. However there is growing evidence that the functional responses of endothelial cells can be modulated by their local physiochemical environment (Nash *et al.* 2004). One aspect considered albeit briefly in the current project is the effect of haemodynamic forces on the ability of EC to recruit leukocytes. These forces affect intra-cellular signalling, secretion, and protein and gene expression (Chien *et al.*

1998;Jalali *et al.* 1998). In addition, underlying stromal cells and matrix substrates can modify EC phenotype and their ability to recruit leukocytes (Aird 2003;Nash *et al.* 2004). Interestingly the specific phenotype of endothelial cells isolated from different tissues may be retained *in vitro* for extended periods (Nash *et al.* 2004). For instance, isolated murine cardiac and lung EC, both supported adhesion of flowing T-cells *in vitro*, but were shown to use different mechanisms. Cardiac EC after stimulation with TNF-α were found to used VCAM-1:VLA-4 and RANTES:CCR5 induced mechanisms, whereas in lung EC, ICAM-1, MIP-2 and MIP-1β were thought to be important (Lim *et al.* 2003).

5.1.2.1 Modulation of EC responses by shear stress

Vascular endothelium is exposed to a number of different haemodynamic forces. These include the frictional shear stress imposed by the bloodstream and hydrostatic pressure acting perpendicular to the vessel wall, which exerts compression and circumferential strain (Matharu *et al.* 2006). The most widely studied of these forces is shear stress (Lelkes *et al.* 1999). Shear stress varies in different organs and throughout the vasculature, with arterial stress in the range of 1 to 4 Pa in comparison to 0.1 to 2 Pa in the microcirculation where leukocyte recruitment takes place. Variation in shear stress is dependent on local pressure gradients, flow rate and the diameter of the vessels (Matharu *et al.* 2006).

Endothelium responds to changes in haemodynamic forces by rapidly releasing a number of vasoactive substances including NO. Over time shear stress can also modify levels of expression of genes, a number of which are involved in leukocyte

recruitment (Matharu *et al.* 2006). The altered expressions of some of these genes are too short lived to have a prolonged effect on leukocyte recruitment. Many studies have examined the change in gene expression over time after exposure to shear. Comparisons are made to static controls, or between responses to laminar vs. oscillatory flow (Brooks *et al.* 2002). Gene array analysis has indicated that the expression of a number of genes alters within a short time of exposure to shear stress, but that the expression levels return to normal or less than the baseline after 24 hours (McCormick *et al.* 2001). For example, the expression of genes encoding both ICAM-1 and monocyte chemoattractant protein-1 (MCP-1) increased upon exposure to shear but levels returned to normal after 24 hours (Sheikh *et al.* 2005) (Sampath 1995). Sheikh *et al* (Sheikh *et al.* 2003;Sheikh, Rahman *et al.* 2005) also demonstrated that when HUVEC were cultured under shear for 24 hours the increased levels of the CXC-chemokines, IL-8 and growth related oncogene (Gro-α) normally induced by TNF-α stimulation were inhibited (Sheikh *et al.* 2005).

Furthermore, Nash and colleagues demonstrated that endothelial cells conditioned under low shear stress of 0.3Pa exhibited decreased levels of leukocyte migration in response to TNF-α stimulation (Sheikh *et al.* 2003). At a higher shear stress of 2.0Pa, conditioning lead to reduction of adhesion itself (Matharu *et al.* 2006). This differential response was due to the effects of shear on the ability of EC to upregulate adhesion molecules and chemokines. The effect of shear on the signalling pathways upstream from pro-inflammatory genes has also been examined. The mitogen activated protein kinases (MAPK) signalling pathways including c-Jun, JNK (N-terminal kinase), p38 and extracellular regulated kinases (ERK 1/2) are known to activate gene transcription factors of the NF-kB/Rel family and activating protein 1 (AP-1) in response to TNF-α (Jalali *et al.* 1998) and Il-1β (Jalali *et al.* 1998;Li *et al.*

1996;Surapisitchat *et al.* 2001). Upon application of shear stress ERK, JNK and p38 activity was shown to increase in a variety of endothelial cells (Jalali *et al.* 1998;Surapisitchat *et al.* 2001). However brief exposure to shear was found to inhibit the activation of JNK in response TNF-α and IL-1-β (Surapisitchat *et al.* 2001) while after exposure for extended periods, all three MAPK were inhibited (Yamawaki *et al.* 2005). Studies have found that long term exposure to shear inhibited TNF-α induced activation of NFkB and the associated up-regulation of adhesion molecules and chemokines in HUVEC (Sheikh *et al.* 2005).

The above supports the theory that initial exposure to shear or changes in shear cause transient responses, while prolonged exposure establishes a new phenotype with, for instance, altered response to pro-inflammatory cytokines. This is important because the ability of EC's to alter their phenotype under varying shear stresses could be important in situations where blood flow is disturbed such as ischemia/reperfusion and altered flow as a result of surgery (Nash *et al.* 2004).

5.2 Results

5.2.1 Optimisation of the flow assay using murine neutrophils

In order to optimise use of our flow assay with murine leukocyte populations we began by performing pilot experiments with neutrophils to confirm their adhesion to recombinant adhesion protein. Murine bone marrow neutrophils were perfused over increasing concentrations of purified murine E-Selectin (0.125-2µg/ml) at 0.05Pa and

adhesion was quantified and categorised into static and rolling cells. As expected the total number of adherent neutrophils increased with E-Selectin concentration, whilst rolling velocities decreased in a dose-dependent manner (Fig. 5.1).

In addition the effect of increasing shear stress on neutrophil adhesion to E-selection (1-2µg/ml) was tested (Fig. 5.2). As shear stress increased we observed a dramatic decrease in the number of neutrophils captured. In general the percentage of rolling neutrophils also decreased with increasing shear stress (Fig. 5.2) although interestingly overall rolling velocities appeared unaffected by shear stress. Thus confident that our assay worked appropriately with murine leukocytes we moved on to studies using endothelial monolayers.

Figure 5. 1 Effect of E-Selectin concentration on the number of adherent neutrophils (A), velocity of rolling neutrophils (B).

Murine bone marrow neutrophils were isolated and perfused over glass microslides coated with purified murine E-Selectin. Video microscopic data was collected from 3 functional flow experiments and analysed offline using Image ProPlus. Error bars represent mean +/- SEM, N=3. Data was subject to one-way ANOVA and Dunnets post-test. *<0.05.

Figure 5. 2: The effect of increasing shear stress and E-Selectin concentration on the number of adherent neutrophils (A), percentage rolling of adhered (B) and rolling velocities (C).

Murine bone marrow neutrophils were isolated and perfused over glass microslides coated with purified murine E-Selectin at increasing concentrations at varying fluid shear stresses. Video microscopic data was collected from 3 functional flow experiments and analysed offline using Image ProPlus. Error bars represent mean +/- SEM, N=1.

Here, bone marrow neutrophils were isolated from adult mice and perfused over a mUCEC-1 monolayer stimulated with different doses of TNF-α. We quantified the number of adherent neutrophils, the percentage of these neutrophils that rolled and their rolling velocities. We saw higher levels of neutrophil adhesion to the endothelial monolayer than were previously observed on immobilised E-selectin. Fig. 5.3 shows that increasing TNF-α concentration up to 500U/ml resulted in a dose-dependent increase in the total number of neutrophils adhering to mUCEC-1, whilst a decrease in adhesion was apparent at the highest dose (1000U/ml, Fig 5.3-A). This same pattern occurred when the percentage of rolling neutrophils was calculated (Fig 5.3-B), whilst neutrophil-rolling velocities decreased with increasing concentration of TNFα (Fig 5.3-C).

Figure 5. 3: Effect of TNF-α concentration on the number of adherent neutrophils (A), the percentage of adherent cells that were rolling (B) and the velocity of rolling neutrophils (C).

Murine bone marrow neutrophils were isolated and perfused over glass microslides containing confluent mUCEC-1 monolayers, which had been stimulated with TNF-α at several doses for 4hrs. Video microscopic data was collected from 3 functional flow experiments and analysed offline using Image ProPlus. Error bars represent mean +/- SEM, N=3 with exception of 5.4-C n=1. Statistics were carried out using one-way ANOVA and Dunnets post-test. * $p<0.05$.

5.2.2 Optimisation of the lymphocyte flow assay using murine endothelial monolayers

Again we began our studies by performing some pilot investigations to optimise the system. Firstly mixed lymphocyte populations from murine spleens were perfused over confluent TNF-α stimulated mUCEC-1 monolayers at increasing shear stresses (0.05-0.2Pa). As shear stress increased, a significant reduction in total adhesion of lymphocytes was observed (Fig. 5.4-A) Whilst performing these experiments we observed that the nature of the mUCEC-1 monolayer morphology observed under phase-contrast microscopy (Fig. 2.6) with occasional phase-bright, rounded cells, made it difficult to differentiate adherent lymphocytes. The same was true of experiments using sEND cells.

Figure 5. 4: Effect of increasing shear stress and cell tracker green on the ability of lymphocytes to adhere to a TNF-α stimulated EC monolayers in microslides.

Murine splenocytes were isolated and perfused over glass microslides containing confluent mUCEC-1 monolayers that had been stimulated with TNF-α (100U/ml) for 4hrs at increasing shear stresses (A). In addition cell tracker green lymphocytes were perfused over mUCEC-1 (B) and s.END (C) cells. Video microscopic data was collected from 4 (Shear) or 1 (CTG) functional flow experiment and analysed offline using Image ProPlus. Error bars represent +/- SEM. One-way ANOVA was performed. *<0.05, **<0.01.

Thus in order to accurately quantify lymphocyte-endothelial cell interactions, we labelled the splenocytes with a fluorescent dye, cell tracker green (CTG). We then used fluorescent microscopy to count the adherent cells in the flow assay. First we examined whether fluorescent labelling of lymphocytes altered their ability to adhere to endothelial monolayers. Fig. 5.4-B/C shows results of experiments where we compared adhesion of labelled and unlabelled lymphocytes to confluent mUCEC-1 and s.END monolayers in the presence or absence of TNF-α pretreatment (100U/ml for 4 hours). It was considerably easier to quantify the adhesion of labelled cells, and we saw no effect of the labelling strategy on adhesion to control or stimulated endothelium. Interestingly we observed far greater adhesion to the mUCEC-1 monolayers and minimal effects of a short prestimulation with TNFα on either endothelial cell. We observed a negligible difference in the adhesive properties of labelled and unlabelled lymphocytes. The number of adherent cells increased modestly upon cytokine stimulation above control treatment as expected. We were therefore able to conclude that CTG labelling had no significant deleterious effect and could be used in subsequent experiments.

Figure 5. 5: Effect of tissue culture vessel on the ability of CTG labelled lymphocytes to adhere to endothelial monolayers mUCEC-1 (A), s.END (B) and b.End.5 (C) stimulated with TNF-α+IFN-γ.

Murine splenocytes were isolated and perfused over rat tail collagen coated glass microslides or IBIDI treat VI chambers containing confluent EC monolayers stimulated with TNF-α+IFN-γ (100U/ml) for 4hrs. Video microscopic data was collected from functional flow experiments and analysed offline using Image ProPlus N=2-4.

Whilst these functional studies were underway an alternative to our traditional glass capillary microslide culture system (Rainger *et al.* 1998) became available. IBIDI VI chambers enable culture of EC in small gas permeable tissue culture treated capillaries with favourable optical resolution. We decided to test this system, as the glass microslide system is complex and time consuming to set up. Certainly we observed that endothelium cultured in the IBIDI chambers assumed an appropriate, healthy morphology and grew more efficiently and reproducibly than similar cells cultured in microslides. We then compared the performance of both systems in the flow assay context. Mixed lymphocytes were perfused over endothelial cell monolayers (mUCEC-1 (A), send (B) and b.END.5(C)) cultured to confluence in either rat-tail collagen-coated glass microslides or 'IBIDI-treat' chambers, which had been stimulated for 4 hours with TNF-α and IFN-γ (100U/ml) (Fig.5.5). In general lymphocyte adhesion to EC cultured in IBIDI chambers was lower than that observed using microslides. However for both systems we noted an appropriate response to cytokine stimulation (*i.e.* increased total adhesion) and the magnitude of adhesion on one-endothelium vs another was maintained (*i.e.* mUCEC-1>b.END.5>sEND).

Figure 5. 6: Effect of TNF-α and pertussis toxin (PTX) treated lymphocytes on the number of lymphocytes adhering to mUCEC-1 monolayer (A) and the number of shape-changed lymphocytes (B).

Murine splenocytes were isolated and treated with PTX at 20ng/ml for 15 mins and perfused over glass microslides containing confluent mUCEC-1 monolayers that had been stimulated with TNF-α (100U/ml) for 24hrs. Video microscopic data was collected from 3 functional flow experiments and analysed offline using Image ProPlus. Error bars represent mean +/- SEM, N=3. Statistics were carried out using two-way ANOVA and Bonferroni post-test, ** $p<0.01$.

As a final confirmation of the reliability of our murine flow assay systems we examined the contribution of chemokines to the recruitment and adherence process by incubating lymphocytes with pertussis toxin to block G_i-protein linked signalling. Lymphocyte total adhesion, and shape changed cells (static) across both unstimulated and stimulated (TNF-αU/ml, 24hrs) mUCEC-1 monolayers were compared in the presence and absence of pertussis toxin treatment. Levels of adhesion were increased by TNFα-stimulation of the endothelium due to prolonged exposure (24hrs) and this increased both the number of static and activated cells (Fig. 5.6-A/B). Interestingly, PT treatment reduced total adhesion to both stimulated and unstimulated endothelium, although the effect was more pronounced on stimulated endothelium. Similarly numbers of both shape-changed and statically adherent cells were reduced by PT treatment. Both PTX and TNF-α had effects on adhesion but were not dependent on each other.

5.2.3 Comparison of the ability of endothelium from different organs to support leukocyte adhesion under different conditions.

5.2.3.1 A: The effects of cytokine treatment on lymphocyte adhesion to murine endothelium under flow.

We began by assessing how each of our different immortalised endothelial cell lines responded to cytokine treatment in terms of ability to recruit lymphocytes. Here the endothelial cell monolayers were treated with a number of pro-inflammatory stimuli for 4 (Fig.5.7) or 24 (Fig. 5.8) hours prior to performing flow-based adhesion assays.

Figure 5. 7: Effect of pro-inflammatory stimuli on the number of adherent lymphocytes for 4 hours.

CTG labelled murine splenocytes were isolated and perfused over glass microslides or IBIDI VI chambers containing confluent mUCEC-1 (A), s.END (B) and b.END.5 (C) monolayers that had been stimulated for 4 hours. Video microscopic data was collected from 3 functional flow experiments and analysed offline. Error bars represent mean +/- SEM n=3. Statistics were carried out using a one-way ANOVA and Dunnets post-test. *<0.05, **<0.01, ***<0.001.

Figure 5. 8: Effect of pro-inflammatory stimuli on the number of adherent lymphocytes for 24 hours.

CTG labelled murine splenocytes were isolated and perfused over glass microslides or IBIDI VI chambers containing confluent mUCEC-1 (A), s.END (B) and b.END.5 (C) monolayers that had been stimulated for 24 hours. Video microscopic data was collected from 3 functional flow experiments and analysed offline. Error bars represent mean +/- SEM n=3. Statistics were carried out using a one-way ANOVA and Dunnets post-test. *<0.05.

Short-term exposure (4hrs) to pro-inflammatory stimuli induced variable responses in all cell types. mUCEC-1 and b.End.5 exhibited variable responses dependent upon which cytokine stimulation protocol was used. Adhesion of lymphocytes to mUCEC-1 significantly increased above control in stimulated samples. This cell line also exhibited the highest level of basal adhesion in the absence of stimulation. In addition adhesion to b.END.5 was significantly elevated after stimulation and TNF-α and IFN-γ induced a significant reduction in adhesion. Basal levels of adhesion to b.End.5 were about tenfold less than seen on mUCEC-1. sEND cells supported similar levels of basal adhesion as seen on b.END.5 but showed more consistent elevations in adhesion in response to stimulation with IL-1β and TNF-α and IFN-γ combined leading to significant increases in adhesion above control (Fig. 5.7).

Prolonged exposure produced a reduction in total adhesion in all cell lines with similar responses to quoted treatments at 4 hours. In addition basal levels of adhesion were low with the exception of mUCEC-1 cells where treatments significantly increased levels of adhesion above control. b.END.5 cells however exhibited similar behaviour with a reduction in adhesion across the board but unlike at 4 hours all treatments induced levels of adhesion above baseline controls (Fig. 5.8).

5.2.3.2 B: The ability of murine endothelial cell lines to recruit leukocyte subsets from flow

In addition to analysing recruitment of mixed populations of lymphocytes, subsets of lymphocytes were isolated using MoFlo cell sorting to obtain pure CD4+ and CD8+ cells. Initially pilot studies were done to assess the efficiency of cell sorting. We sorted individual subsets of cells from whole spleens to up to 99% purity as indicated in Fig. 5.9.

Figure 5. 9: Isolation of CD4+/CD8+ single positive cells from whole murine spleen using the MoFlo Cell Sorter.

Murine splenocytes were labelled with αCD8-FITC and αCD4-PE and separated on the expression of these flurochromes into single positive populations from the whole sort (A) using Beckman Coulter MoFlo XDP to over 90% purity. Appropriate compensation was carried out using single colour controls and samples were checked for purity post-sort (B/C).

All three endothelial cell lines were stimulated with the pro-inflammatory treatments used in previous flow based experiments for 4hrs as these parameters had shown the most promising results. As before, highest levels of adhesion were observed on mUCEC.

Figure 5. 10: Effect of pro-inflammatory stimuli on the adherence of lymphocyte subsets.

CTG labelled murine splenocytes were isolated and perfused over IBIDI VI chambers containing confluent EC monolayers that had been stimulated with TNF-α 100U/ml (A), IFN-γ 100U/ml (B), LPS 1µg/ml (C) and TNF-α+IFN-γ 100U/ml (D) for 4 hours. Video microscopic data was collected from 3 functional flow experiments and analysed offline. Error bars represent mean +/- SEM n=3. Statistics were carried out using a two-way ANOVA and Bonferroni post-test to control. CD4+ and CD8+ cells were treated separately for statistics. Statistics shown indicate the impact of cell line but this does not depend on treatment *<0.05, **<0.01 and ***<0.001.

EC stimulated with the panel of treatments recruited CD4+ and CD8+ cells to differing extents. The effect of cell line was significant in all treatments with the exception of CD8+ LPS treatment. With mUCEC-1 vs s.END having a significant effect on CD4+ recruitment in response to LPS ($p<0.05$) and mUCEC-1 vs s.END effecting CD4+/CD8+ ($p<0.001$). Treatment impacted significantly on adhesion of both cell types when treated with IFN-γ and CD4+ with LPS ($p<0.05$). CD4+ recruitment was unaffected by TNF-α however recruitment of CD8+ cells was lower. Pronounced responses were observed in response to LPS (Fig. 5.10-C) in mUCEC-1 and b.End.5 cells, particularly in the recruitment of CD4+ cells with ~50% increase in adhesion. Stimulation increased adhesion above control in all treatments and groups tested.

Levels of recruitment in mUCEC-1 cells were much higher than other cell types as seen in response to TNF-α. This response was not seen with IFN-γ alone but was seen when two cytokines were combined suggesting TNF-α was accounting for the response seen here (Fig. 5.10-D). Small cytokine dependent responses were seen in s.END (LPS) and b.End.5 (IFN-γ) cells with most effect seen in the recruitment of CD4+ cells to s.END cells.

5.2.3.3 C: The effects of cytokine treatment on lymphocyte adhesion to primary murine hepatic endothelium under flow

Immortalised EC lines were used to optimise protocols for use with primary EC populations. A primary murine liver sinusoidal endothelial cell population was obtained using αCD146 magnetic bead isolation from whole Balb/c livers to sufficient

purity (~98%). mLSEC were seeded into ‘IBIDI-treat’ chambers and assessed in functional assays.

Figure 5. 11: Effect of pro-inflammatory stimuli on the number of lymphocytes adhering to mLSEC.

CTG labelled murine splenocytes were isolated and perfused over IBIDI VI chambers containing mLSEC that had been stimulated for 4 (A) or 24 (B) hours. Video microscopic data was collected from 2 functional flow experiments and analysed offline. Error bars represent mean +/- SEM n=4. Statistics were carried out using a one-way ANOVA and Dunnets post-test.

Interestingly, recruitment of lymphocytes to mLSEC was low and comparable to the endothelioma cell lines (Fig. 5.11). Levels of adhesion were far less than we have observed on human sinusoidal endothelium (Shetty *et al.* 2008). After 4 hours, the majority of treatments induced levels of adhesion above control with LPS and TNF-α+IFN-γ having the most effect in accordance with our observations using cell lines. IL-1β had no effect on adhesion after 4 hours stimulation (Fig. 5.11-A). Prolonged exposure to stimuli had no additional stimulatory effect on adhesion and if anything slightly reduced recruitment compared to untreated mLSEC.(Fig. 5.11-B) although none of these treatments were significant. This also supports the trend observed using immortalised cells.

5.2.3.4 D: The ability of primary murine hepatic endothelium to recruit leukocyte subsets from flow and under static conditions

Preliminary experiments were carried out on primary mLSEC to assess total lymphocyte versus subset recruitment using LPS and TNF-α+IFN-γ, which induced the most adhesion in earlier studies.

Figure 5. 12: Effect of LPS and TNF-α+IFN-γ on the adherence of total lymphocytes and subsets.

CTG labelled murine splenocytes, CD4+ and CD8+ cells were isolated and perfused over IBIDI VI chambers containing mLSEC that had been stimulated with LPS 1µg/ml or TNF-α+IFN-γ 100U/ml for 4 hours. Video microscopic data was collected from 2 functional flow experiments and analysed offline. Error bars represent mean +/- SEM n=3. Statistics were carried out using a two-way ANOVA and Bonferroni post-test against control. Cell Lines showed significant difference ***<0.001.

The recruitment of whole unfractionated lymphocytes was unaffected by cytokine treatment, however cell type had a significant effect on adhesion. CD4 cells bound in increased numbers relative to unfractionated cells and binding was modestly elevated by cytokine and LPS stimulation. Levels of CD8+ cell recruitment were similar to the unfractionated population but here there was a marked increase in adhesion following TNF-α+IFN-γ treatment (Fig. 5.12).

In order to compare adhesion to all cell types in parallel and to make best use of the minimal yield of cells available after sorting, an alternative method for functional assessment of adhesion to endothelium was used. Instead of examining endothelial-lymphocyte interactions under flow, labelled lymphocytes were added to stimulated EC monolayers in tissue culture plates. Static adhesion assays were carried out on all cell lines and primary mLSEC stimulated with LPS (1µg/ml) or TNF-α+IFN-γ (100U/ml) treatments, using the same lymphocytes. These treatments were selected due to their effect on recruitment in previous experiments (Fig. 5.13).

Figure 5. 13: Effect of LPS and TNF-α+IFN-γ on the lymphocyte recruitment in static assays.

CTG labelled murine splenocytes were isolated and incubated with EC in 24-well culture plates stimulated with LPS 1µg/ml or TNF-α+IFN-γ 100U/ml for 24 hours. The number of adherent cells was counted in an average of 10 fields. Error bars represent mean +/- SEM n=5. Statistics were carried out using a two-way ANOVA and Bonferroni post-test to control. *<0.05, **<0.01 and ***<0.001.

The relative levels and pattern of adhesion to all cell types was generally similar to that observed in flow based assays although adhesion to non-mUCEC endothelium was slightly higher in the static system. Both cell type and treatment had significant effects on adhesion but was not dependent on each other. As before the high levels of adhesion to mUCEC were minimally altered by cytokine stimulation. However adhesion to the other endothelial cell types was elevated in response to both TNF-α+IFN-γ and LPS stimulation to a degree more pronounced than that observed in the flow assays particularly in b.End.5 cells were increases in adhesion were significant.

5.2.4 Modulation of the ability of endothelium to recruit leukocytes by shear conditioning

Our next aim was to condition all our endothelial populations by exposure to continuous shear stress to determine the effects on recruitment capacity. We were unable to perform these studies in the time available but did manage some proof of concept pilot studies.

Figure 5. 14: The effect of shear conditioning on the total number of adherent neutrophils (A), the percentage of adherent neutrophils that adhered (B) and the velocities of rolling neutrophils (C).

Murine bone marrow neutrophils were isolated and perfused over glass microslides containing cultured mUCEC-1. Endothelial cell monolayers were stimulated with either 5x10-9 g/ml of IL-1β or 1000U/ml TNF-α for 4 hours prior to perfusion of neutrophils. Error bars represent the standard deviation between bolus and wash samples in Fig 5.15-C.

Here mUCEC-1 grown in microslides were preconditioned in shear stresses of 2.0Pa and stimulated with TNF-α (1000U/ml) or IL-1β (5x10-9 g/ml). We then performed standard flow assays using freshly isolated bone marrow neutrophils. Fig. 5.14 shows that cells exposed to culture under static or continuous flow conditions responded appropriately to cytokine stimulation which resulted in elevated total neutrophil adhesion, rolling adhesion and in general in an increase in transmigration. The number of adherent neutrophils was higher in the Il-1β-stimulated groups than the TNF-α-treated groups. Interestingly we observed an increase in total adhesion to IL-1β-stimulated EC under continuous flow compared to static conditions, which was not the case for TNF-α stimulation. However the percentage of cells that rolled was higher after continuous exposure to flow for both cytokine treatments. However it appeared that exposure to continuous flow had little effect on the number of transmigrating cells after cytokine treatments, but did reduce the proportion of cells, which transmigrated across 'unstimulated' endothelium. In addition the high dose of TNF-α could have impacted upon the integrity of the endothelium.

Figure 5. 15: The effect of increasing concentrations of TNF-α on the number of adherent lymphocytes.

A mixed lymphocyte population from murine spleens were perfused over glass microslides containing cultured mUCEC-1 cells. Endothelial cell monolayers were stimulated with increasing doses of TNF-α for 24 hours prior to perfusion of lymphocytes. Error bars represent +/- SEM. One-way ANOVA was performed with Dunnets post-test but no data was significant.

Additional experiments examined the effect of increasing doses of TNF-α on the adhesion of mixed lymphocytes (Fig.5.15). Levels of adhesion increased above control up to 500U/ml after which adhesion was adversely affected, with levels dropping to below control values at 10,000U/ml.

5. Discussion

The aim of functional studies was to determine if there were differences in the ability of tissue specific endothelial cell populations to recruit various leukocyte subsets under static and flow conditions. We isolated a high yield of mixed lymphocyte populations and CD4+ and CD8+ subsets from murine spleens in addition to murine bone marrow neutrophils to relatively high purity. Experiments using purified proteins showed that neutrophils could adhere to E-Selectin under physiologically relevant shear stresses and that some cells rolled on the protein substrate. These experiments lead to further studies to examine the behaviour of leukocytes in endothelial cell systems using immortalised cell lines and primary mLSEC. The specific murine flow system we developed has not been previously used. Neutrophils have previously been isolated from murine bone marrow (Zollner *et al.* 1997) but their functional responses under flow have yet to be reported. There is little literature available on the behaviour of murine endothelial cells under flow. Lim *et al* (Lim, *et al.* 2003) have cultured primary aortic and lung endothelial cells and examined their ability to recruit T-cells. This group has also isolated peripheral blood neutrophils from MMP-9 KO mice and examined their behaviour under flow (Allport *et al.* 2002). Previously published studies similar to those carried out in this project involve

examining leukocyte adherence under static conditions (Barkalow *et al.* 1996) or using different flow methods such as parallel plate flow chambers. A number of experiments have been carried out *in vivo* using intravital microscopy (Mayadas *et al.* 1993), as the parameters being tested have not yet been manipulated *in vitro*.

5.1 Optimisation of leukocyte isolation.

There are a number of different sources from which neutrophils and lymphocytes can be isolated; bone marrow, secondary lymphoid tissues, peripheral blood and whole blood. The total blood volume of a mouse is ~2ml, of which between 05-1ml can be removed. The yield of neutrophils from peripheral blood is low as circulating numbers are low. Therefore the bone marrow is a more ideal source of neutrophils as it contains a large neutrophil pool (Pallister 1998). It must be considered however that not all of the neutrophils here will have reached maturity. The bone marrow isolates used for functional flow experiments were ~70-75% pure as assessed by examining the cellular morphology. Ideally sample purity should be examined using a more quantitative method such as flow cytometry utilising a neutrophil specific mAb, such as murine GR-1. It has also been demonstrated by other groups that neutrophil purity in excess of 90% can be achieved by the inclusion of a B-Cell depletion step using a magnetically activated cell sorting kit. Nevertheless visual observation of our flow assay experiments allowed us to selectively score neutrophil adhesion in our experiments on the occasions where purity was less than ideal.

A mixed lymphocyte population can be isolated from whole murine spleens, which is rich in T and B-Cells. Spleens are disaggregated and contaminating red blood cells

lysed and removed. The remaining lymphocytes can be used whole or sorted to isolate high purity CD4+ and CD8+ cells. Subsets can also be obtained using magnetic bead isolation methods but MoFlo cell sorting was found to be more appropriate for functional experiments. Our MoFlo data confirmed that the populations used were over 90 % pure after being 42.92% (CD4+) and 19.82% (CD8+) of the whole spleen prior to sorting. Therefore we are confident that cells used in flow assays were selective for the population in question.

5.2 Neutrophil adherence to purified E-Selectin

In order to characterise the behaviour of murine bone marrow neutrophils under flow conditions we carried out initial experiments using purified E-selectin coated microslides. We examined the effect of both increasing shear and E-selectin concentration on the number of neutrophils adhering to the microslide surface, the percentage of adherent neutrophils rolling and rolling velocities. Bone marrow neutrophils did adhere to the E-selectin coated surface and were found to spontaneously activate, even in the absence of a chemotactic stimulus. As the

shear rate increased all three parameters decreased. Increasing the concentration of E-selectin in the initial shear experiments did not seem to have any effect. A broader range of E-selectin concentration was tested, to find the optimal concentration to use for further flow experiments. It was found that, as the concentration increased there was a dose dependent increase in the number of adherent neutrophils and decrease in rolling velocity. This observed trend could be explained as an increase in the number of receptor-ligand interactions between the neutrophil and E-selectin with increasing protein concentration, resulting in increased avidity to the microslide

surface and decreased rolling velocity. These experiments have not previously been carried out using murine neutrophils though in similar human experiments, neutrophils did adhere to purified E-selectin (Lawrence *et al.* 1994; Reinhardt *et al.* 1998). Whole blood was perfused over E-selectin coated coverslips at different concentrations and shear stresses, it was found that at the highest shear (4Pa) that neutrophils were the only leukocytes that adhered and all leukocyte adhesion was inhibited with an anti-E-selectin blocking antibody (Lawrence *et al.*1994; Reinhardt *et al.* 1998). Lawrence *et al* (Lawrence *et al.* 1994) showed that L-selectin was also required for neutrophils to adhere to an E-selectin surface under flow conditions and could be a ligand here. This could be confirmed using blocking antibodies to further dissect exact mechanisms involved. Our conclusions from these studies were that our murine cell-based assay was working appropriately, we were able to isolate resting populations of murine neutrophils and that the cells responded as expected in the flow assay. Thus we moved on to experiments using endothelial monolayers.

5.3 Effect of TNF-α on neutrophil recruitment

Functional studies to examine the effect of TNF-α on neutrophil recruitment in the mUCEC-1 system showed that TNF-α elicited a dose dependent increase in the number of leukocytes adhering to the mUCEC-1. In addition the rolling velocities of adherent neutrophils decreased as TNFα concentration increased, and in general adhesion was higher than we noted in the purified E-selectin experiments. This fits with an increased density of multiple ligands being expressed on cytokine-stimulated endothelium. We noted greater variability in neutrophil adhesion, rolling velocity and migration in the endothelial system. This may relate to the fact that the bone marrow

does not contain a homogenous population of neutrophils. As a site of neutrophil haemopoesis, the neutrophils, which we isolate, could be at any stage of development and may not all express the appropriate adhesion molecules at sufficient level to adhere, roll and transmigrate through endothelial cells (Adams *et al.* 2005;Pallister 1998). Additionally it is likely that the endothelial surface, even of a cell line, does not uniformly express receptors between experiments which may add to potential variability. However these pilot studies with neutrophils satisfied us that our murine endothelial adhesion systems worked well enough to move onto comparisons between endothelial cell types in the context of lymphocyte adhesion.

5.4 Characterisation of murine lymphocyte adhesion to immortalised cell lines under flow.

Here we examined the effects of a number of different pro-inflammatory cytokines and endotoxins on the ability of mUCEC-1, s.END, b.End.5 and mLSEC to recruit lymphocytes. In order to visualise the adherent cells lymphocytes were fluorescently labelled with cell tracker green. Previous studies examined the toxicity of first generation fluorescent labels such as cell tracker orange and bisbenzamide and found that they effected the ability of human neutrophils to adhere and migrate to HUVEC (Smith *et al.* 2006) or P-Selectin (Abbitt *et al.* 2000). More recently developed dyes such as cell tracker green and CFSE are designed specifically for functional assays and have been optimised to have minimal detrimental effects on loaded cells. In agreement, our pilot experiments determined that CTG had no effect on the recruitment of murine lymphocytes to mUCEC-1 and s.END cytokine stimulated monolayers.

The majority of functional studies were carried out by culturing EC in glass capillary microslides, a technique pioneered in Birmingham (Buttrum *et al.* 1993). Towards the end of my studies an alternative method became commercially available. IBIDI VI chambers enable culture of EC in gas permeable chambers negating the need for complex flow-culture apparatus used previously. Endothelial cells populations cultured in IBIDI VI chambers appeared morphologically representative of healthy EC populations. Pilot experiments indicated that EC cultured in chambers recruited smaller numbers of lymphocytes and exhibited less of a response to stimuli compared to microslides in all cell lines in particular mUCEC-1. However, EC cultured in chambers exhibited normal adhesive properties and response to stimuli in a more stable state, providing reliable representative data. This altered expression profile could be due to the larger depth of IBIDI VI chambers compared to microslides (HxWxD: 17x3.8x0.4 compared to 50x3x0.3 mm). In addition smaller volumes of cytokine are used in IBIDI VI chambers and this could be impacting upon adhesion.

Functional studies to examine the effects of pro-inflammatory stimuli on leukocyte recruitment in immortalised EC systems revealed differences in EC derived from different tissues. In mUCEC-1 cells TNF-α, LPS and IL-1β elicited the highest levels of adhesion after a short 4-hour exposure. Prolonged exposure for 24 hours resulted in decreased adhesion in particular to IFN-γ alone and in combination with TNF-α. This reduction could be due to deleterious effects of over exposure on the integrity of the EC monolayer. Certainly we noted that endothelial cells in these samples were stressed and granular in appearance, but this was surprising since cell lines often require higher doses of cytokines to yield a similar response to that seen in primary cell isolates (Proudfoot *et al.* 2001)**.** It is possible that prolonged exposure to IFN-γ

may be effecting the growth of mUCEC-1 as the producers of this cell line published that IFN-γ in conjunction with incubation at 33°C was required to switch cells into growth phase by activating an H2-K promoter linked to the SV40 large Tag. Thus whilst proliferating in response to high doses of IFN-γ, it is plausible that the cells did not produce all the relevant surface markers present in normal culture conditions (Lidington *et al.* 2002).

In comparison, although global levels of adhesion were lower, s.END cells were more responsive to stimulation after 4 hours. Treatment with LPS, TNF-α+IFN-γ and IL-1β had most effect with up to 50% increase above control. A similar response was observed at 24 hours with a reduction in adhesion. s.END cells are an immortalised murine skin endothelioma cell line isolated from mice infected with a polyoma midde T oncogene and have been previously shown to retain functional properties of normal endothelial cells; uptake of acLDL, expression of CD31, VCAM-1, and E/P-Selectin, production of chemokines and response to TNF-α and IL-1β (Bussolino *et al.*1991). Physiologically, leukocyte recruitment in the skin involves ICAM-1 and LFA-1 interactions in particular (Iwata *et al.*1996), which fits with our observations following TNF-α and IFN-γ-treatment here.

The b.End.5 cells are immortalised using the same method as s.END cells. Both endothelioma cell lines exhibited similar levels of basal adhesion, but with the exception of LPS, 4 hours cytokine treatment had little effect on adhesion to these cells. However, modest increases in adhesion were noted after most stimuli following 24-hours stimulation. Interestingly b.End.5 cells have previously been used to study the barrier role of the BBB and the role of VCAM-1, ICAM-1 and ICAM-2 in adhesion

within the brain. In comparative studies with primary mBMEC, b.End.5 expressed similar levels of IL-6, PCA and PAF in response to IL-1, LPS and TNF-α stimulation for 4hrs (Bussolino *et al.* 1991). In addition other groups stimulated b.End.5 with 5nM TNF-α for 16 hours to examine CXCR-2 mediated adhesion (Frommhold *et al.* 2008). The function of ICAM-1/VCAM-1 interactions has been demonstrated on cytokine stimulated mouse, rat and human BMEC and in models of EAE (Lee *et al.* 1999) however data is limited on b.End.5 cells. Our data suggests that ICAM-2, CD31 and CD34 were expressed on b.End.5 cells but VCAM-1 was absent from whole tissue and b.End.5 by immunohistochemistry. Low levels were present in b.End.5 cells via ELISA in particular in the presence of high doses of TNF-α and TNF-α+IFN-γ. Due to the number of adhesion molecules expressed b.End.5 were able to recruit leukocytes from the circulation but the induction adhesion molecules produced in response to stimuli was limited.

We also looked at the effect of PT treatment on lymphocyte adhesion and recruitment. Pertussis toxin blocks G_i-protein linked signalling and therefore inhibits signals generated when leukocyte borne chemokine receptors interact with their ligand, inhibiting leukocyte adhesion and transmigration. Treatment with PT adversely affected adherence to both TNF-α stimulated and unstimulated monolayers of mUCEC-1 and s.END cells suggesting a role for chemokines in both settings. In both cell lines a number of different chemokines were constitutively expressed in all conditions, however it must be considered that the possible toxicity of pertussis toxin could be contributing to this effect.

5.5 Characterisation of murine lymphocyte adhesion to primary EC under flow.

Immortalised EC lines were used to set up functional assays and we obtained data highlighting the phenotypic and functional differences between tissue specific EC in terms of cell surface marker expression, response to cytokines and ability to recruit lymphocytes. However the main aim of this project was to isolate and characterise primary liver endothelial cell populations. Pure populations of mLSEC were isolated from whole Balb/c livers and used at P0, one-day post isolation. Liver sinusoidal endothelial cells were exposed to a panel of pro-inflammatory stimuli for 4 or 24 hours and their ability to recruit lymphocytes were assessed. After 4 hours the majority of treatments increased adhesion, with the exception of IL-1β. An additive effect of TNF-α+IFN-γ was apparent inducing the highest levels of adhesion along with LPS. After 24 hours stimulation, adhesion remained above control levels, but was generally not as elevated as after 4 hours treatment. This was in contrast to our cell lines where prolonged cytokine exposure produced a global decrease in adhesion.

Much previous published research has examined the functional capabilities of cultured human LSEC and their ability to recruit subsets of immune cells (*et al.* 2009;Curbishley *et al.* 2005). Similarly murine intravital studies have addressed leukocyte recruitment to the liver sinusoids *in vivo*, such as the role of selectins in endotoxaemic mice (Klintman *et al.* 2002). However, whilst mLSEC have been isolated by a number of different groups to study, endocytosis and immunological function (Knolle *et al.* 2001;Smedsrod *et al.* 2004) the ability of mLSEC to recruit leukocytes from the circulation in flow-based models has not been studied. Thus we

investigated the ability of mLSEC to recruit different lymphocyte populations following cytokine treatment.

5.6 Isolation and recruitment of lymphocyte subsets

Single positive CD4+ and CD8+ lymphocytes were isolated from murine spleens. Global levels of adhesion in response to treatment were similar or lower than that seen in other assays. All EC were cultured in IBIDI VI chambers, which were shown to recruit smaller numbers of lymphocytes unlike microslides used in other assays where adhesion was higher in particular with mUCEC-1 cells. Studies on subset recruitment to each of the different tissues examined, heart, brain, skin and liver focus on leukocytes recruited or present during injury, inflammation and disease.

In the brain, recruitment in murine model of MS, EAE is a Th1 mediated disease (Luster *et al.* 2005). Ghirnikar *et al* (Ghirnikar *et al.* 1998) found that injury to the CNS as a result of stab injury of the cortex initiated the innate immune response leading to recruitment of macrophages (12-24 post injury) followed by T-Cells (up to 8 days) and TNF-α, IL-1β and CCL2 were thought to be involved. Yilmaz *et al* (Yilmaz *et al.*) found that both CD4+/CD8+ cells in addition to platelets were recruited to the cerebral microvasculature in response to I/R injury and suggested a role for regulatory T-Cells in mediating inflammation. Subset recruitment to b.End.5 resulted in responses to LPS and TNF-α+IFN-γ indicating that b.End.5 had the ability to recruit both CD4+ and CD8+ cells.

Liver resident lymphocytes are skewed towards CD8+ cells (Golden-Mason *et al.* 2004) and a number of activated CD8+ T-Cells are recruited and eliminated as part of the immune response (Petri *et al.* 2008). In inflammation however, the type and distribution of infiltrating inflammatory cells due to expression of combinations of chemokines and adhesion molecules determines the type of disease. A large proportion of liver resident lymphocytes are CD45RA+ (effector T-Cells) and are thought to be involved in local immune surveillance (Lalor *et al.* 2002b). Experiments using primary mLSEC were limited due to cell availability. However recruitment and adhesion of CD4+ cells was marked in comparison to CD8+ cells and mixed populations from the same tissue. Stimulation resulted in small responses with CD4+ responsive to LPS in comparison with CD8+ where TNF-α+IFN-γ caused most adhesion. The combination of TNF-α+IFN-γ elicited the highest levels of recruitment, in keeping with human studies, which have shown that this regime induces the interferon inducible chemokines that bind CXCR3 in inflamed hHSEC (Curbishley, *et al.* 2005). Knolle *et al* have done much work on the role of CD8+ cells in murine livers, for example demonstrating that the antigen specific CD8+ T-Cells are retained as a result of antigen cross presentation (von Andrian *et al.* 2008).

Several models of inflammatory skin diseases are available including psoriasis, scleroderma and atopic dermatitis. Zhou *et al* showed that CD4+ cells are recruited and important in scleroderma (Zhou *et al.* 2006). In support of this s.END cells, which exhibited the most typical ‘endothelial-like’ profile of receptor expression recruited low levels of both CD4+ and CD8+ cells with a preponderance to recruit CD4+ T-Cells from flow.

I have previously covered mechanisms of recruitment involved in inflammation in the heart. Whilst cardiac EC recruited the highest number of leukocytes from flow they may not possess the most physiological receptor expression as s.END were found to be more 'endothelial-like', in addition expression of VCAM-1 was unusually high. Nevertheless recruitment of subsets was apparent and responded well to cytokine treatment. We found that TNF-α and TNF-α+IFN-γ induced the largest responses in mUCEC-1 cells, IFN-α alone had less of an effect suggesting response was largely due to TNF-α. In a model of rat cardiac allograft rejection the infiltration of leukocytes was assessed histologically implicating T-Helper cells and macrophages in progression of graft rejection (Forbes *et al.* 1983).

5.7 Static adhesion

Ideally parallel experiments using different EC types with the same isolates of leukocytes would have been performed to directly compare the adhesive capacities of all our endothelial cells under flow. This proved to be too logistically difficult given the availability of LSEC and thus we chose to perform static adhesion assays to maximise the use of both endothelial and leukocyte isolates. A select few stimulatory treatments were chosen, which had induced responses in previous experiments under flow conditions. Global levels of adhesion were much higher than that seen in flow experiments as lymphocytes are incubated with the EC monolayers for 2 hours in the absence of any flow conditions permitting more efficient interactions between cell types. We were pleased to note that the tissue specific differences observed previously were confirmed in these static assays. Levels of adhesion were highest in mUCEC-1 followed by b.End.5. s.END and then mLSEC. Stimulation with LPS and

TNF-α+IFN-γ both induced increased adhesion in all cell types with TNF-α+IFN-γ having most effect. Adhesion to mLSEC was lower than other cell types concurrent with additional adhesion assays. This could be a result of *in vitro* culture, tolerance to LPS or however mLSEC do respond to TNF-α+IFN-γ an important mechanism in hLSEC (Curbishley *et al.* 2005).

5.8 Continuous Flow

We tested the effect of TNF-α and IL-1β used under 'static' conditions to examine what effect they would have on neutrophil recruitment to mUCEC-1 conditioned by continuous flow. TNF-α appeared to have more of an effect than IL-1β on the percentage of adherent neutrophils rolling. Whereas, IL-1β had a more marked effect than TNF-α on the number of adherent neutrophils and the percentage transmigrating. All the cytokine treatments were higher than the control for all parameters tested. Whilst these results are interesting, our limited number of repeats means ideally we repeat this experiment several times more to assess with confidence the significance of the effects TNF-α and IL-1β on neutrophil behaviour.

A static control was also included in each continuous flow experiment. This was used to compare the effects of static versus continuous flow culture as continuous exposure to shear is thought to condition endothelial cells (Sheikh *et al.* 2003). Both the number of adherent neutrophils and the percentage of adherent neutrophils rolling were higher and the rolling velocities were lower in treatment groups exposed to continuous flow. There was no real difference in the percentage of neutrophils transmigrating through the monolayer, but as we have mentioned previously the

proportion of neutrophils transmigrating was much lower than expected. The Birmingham group led by Professor Nash has been the driving force in studying is the combined effect of shear and cytokines on neutrophil recruitment (Sheikh *et al.* 2003;Sheikh *et al.* 2005). Previous results show that HUVEC conditioned by 0.3Pa of shear 4, 8 and 24 hrs after which HUVEC were stimulated with TNF-α at 100U/ml for the last 4 hours of the experiment resulted in the progressive reduction in the proportion of adherent neutrophils that transmigrated through the EC (Sheikh *et al.* 2003). We found that exposure to shear, in contrast increased levels of adhesion in response to TNF-α and IL-1β. However these experiments have not previously been carried out on mUCEC-1 cells. Altered responses could be an artefact of immortalisation, tissue specificity or vascular location.

The natural physiochemical environment of EC is exposure to continuous flow at varied shear stresses depending on the tissue and branch of the vasculature in which they are resident. Matharu *et al* (Matharu *et al.* 2006) reported that the higher the shear stress to which EC are exposed the less likely they are to respond to pro-inflammatory cytokines (Matharu *et al.* 2006;Sheikh *et al.* 2003;Sheikh *et al.* 2005). We found that exposure to shear induced higher levels of neutrophil adhesion and transmigration in mUCEC-1 cells. mUCEC-1 originated from whole murine hearts where the aorta and major pulmonary veins had been removed, even though cells are from cardiac capillaries the heart is exposed to high levels of shear supporting the theory of shear exposure relating to cytokine responsiveness (Lidington *et al.* 2002). The inability of HUVEC exposed to flow to capture flowing neutrophils was thought to be attributed to inhibition of TNF-α induced up regulation of E-Selectin mRNA (Sheikh *et al.* 2003)**.** Impaired neutrophil transmigration was thought to be due to the altered expression of chemokines GRO-α and IL-8 required for successful

transmigration through the EC's (Sheikh *et al.* 2003;Sheikh *et al.* 2005). We found that mUCEC-1 induced neutrophil transmigration despite the absence of IL-8 (KC), suggesting that alternate chemokines which may be unaffected by shear conditioning may be involved here. The cells do however express low levels of E-Selectin. Thus molecules other than E-selectin may contribute to capture after conditioning or it is possible that mUCEC do not regulate selectin expression in response to shear in the same way as HUVEC.

It is thought that EC are conditioned by the physiochemical environment they are exposed to resulting in an altered and stable phenotype (Sheikh *et al.* 2003;Sheikh *et al.* 2005). The EC phenotype produced by the conditioning effects of shear is still somewhat controversial. Other groups have examined the effect of shear in HUVEC and murine lymph nodes (LN). Neutrophil adhesion to HUVEC was shown to increase in shear conditioned samples, compared to static controls and this was attributed to an upregulation of ICAM-1 (Tzima *et al.* 2002). In murine LN, culture under flow for 24-hrs was shown to downregulated VCAM-1 and abrogate neutrophil adhesion (Ando *et al.* 1994). This suggests that responses to shear vary with endothelial origin (e.g. macro *vs.* microvascular or lymphatic), whether the cells are additionally stimulated and what with (*i.e.* which cytokine is used) and depend on which target molecule you are studying. For example E and P-Selectin supported neutrophil adherence when HUVEC were stimulated with TNF-α but in IL-1β stimulated samples additional receptors were involved. This may explain why our responses using mUCEC-1 differ from HUVEC as the expression profile of adhesion molecules varies from EC derived from different locations in the vasculature. In particular VCAM-1 expression is particularly high. No phenotypic data is available on shear-conditioned mUCEC-1 in contrast with that seen in HUVEC discussed above.

Immortalized EC are exposed to limited shear stress in flow chambers to examine leukocyte recruitment, as outlined in this thesis and much research from this group. However, EC populations can be sheared to model systems, for example human brain EC (HCMEC/D3) have been used to model the BBB and were exposed to pulsatile flow between 1-200 dyn/cm but leukocyte recruitment was not assessed (Cucullo *et al.* 2007). Due to the low shear environment in which mLSEC normally occupy in the liver sinusoid one would expect that they would be less responsive to cytokine and that exposure to shear would downregulate responses, as seen in HUVEC. However, we saw upregulation of adhesion in response to stimuli in conditioned mUCEC-1. In addition epigenetic changes induced by the environment could alter the responsiveness and the functional ability of mLSEC.

Such differences in responses to shear have been attributed to downstream signalling or gene transcription pathways activated after cytokines ligate their cognate receptors (Matharu *et al.* 2006). A number of shear conditioned genes exist, gene expression profiles of HUVEC exposed to laminar shear stresses (10dyn/cm^2) compared to static cultures showed that there were 107 differentially expressed shear-responsive genes (2-fold) after 24-hour exposure, including transcription factors, cell cycle regulators and antioxidants a relatively small proportion of the endothelial transcriptome (Wasserman *et al.* 2002).

EC from heart, brain, skin and liver are all exposed to varying shear stresses due to their physiological location. EC in the heart and brain are exposed to high levels of shear stress (2.0Pa) compared to low shear seen in post-capillary venules and liver sinusoids (0.05Pa). It would be interesting to see whether the phenotype and function of EC can be altered if the physiochemical and shear environment was altered

(possible epigenetic modifications), *i.e.* can a sinusoidal EC behave like cardiac EC if exposed to high shear stress? Does this exposure to shear modulate the unique immunological functions of mLSEC? Cultured EC are removed from the physiological environment and external stimuli including shear forces that may affect their phenotype and function. In addition there is evidence to suggest that EC can detect differences in forces to which they are exposed. Andersson *et al* (Andersson *et al.* 2005) showed that HUVEC expressed different sets of genes in response to shear stress and intraluminal pressure. Haemodynamics and shear stress can play a role in disease pathology; one of particular relevance is atherosclerosis. EC exposed to laminar shear stress or turbulent flow showed differential expression of atheroprotective genes that were antioxidant, anticoagulant and antiadhesive important for disease prevention (Topper *et al.* 1996). In liver injury or disease where fibrosis and consequent cirrhosis develop an increase in portal pressure and sinusoidal blood flow is seen, leading to EC capillarisation. Shear could be detected by EC leading to changes in gene expression or phenotype, conditioning the endothelium leading to transient epigenetic modifications or causing the disease to persist.

6. DNA MICROARRAY ANALYSIS OF ENDOTHELIAL POPULATIONS.

6.1 Introduction

The advent of genomic technologies, our ability to map the genomes of several organisms and the availability of data from DNA sequencing projects has impacted highly upon scientific research. Arrays can be used to detect pathogens, perform expression profiling, and genotype organisms to name a few applications. Previous studies tended to apply a 'reductive' approach by examining how genes, protein structure and function or regulons impact on the behaviour of organisms. However, the new 'genomic' trend has permitted examination of whole organism biology, to facilitate understanding how multiple elements interact to produce responses (Twyman 2004).

These experimental tools have provided new insights into areas such as proteomics, metabolomics and gene regulation. The most important of which in this context is the array, a powerful high-throughput, parallel assay used to study interactions between biological molecules (Hobman *et al.* 2007). These assays can use RNA, DNA, proteins or carbohydrates deposited in an ordered arrangement onto a planar solid surface. Each coordinate on the substrate represents a single gene, protein or molecule. Two types of DNA microarray formats exist; microarrays constructed and printed 'in house' (Schena *et al.* 1995) or manufactured arrays offered by companies such as Affymetrix, Agilent, and Nimblegen. In addition to the method of production microarrays also differ in the form of the nucleic acid printed onto the surface including, PCR products, cDNA and expressed sequence tags (EST's). The microarray data outlined in my study was obtained using Agilent Oligo arrays, composed of oligonucleotides up to 60 bases long printed onto glass slides which

include intergenic regions and open reading frames, allowing greater flexibility (Hobman *et al.* 2007).

6.1.2 How do arrays work?

DNA array technology relies on detecting interactions between molecules immobilised on the array surface with molecules present in a complex solution added to the substratum. This is possible due to the ability of nucleic acids to bind complementary sequences under favourable temperatures and salt concentrations (Stoughton 2005). The nucleic acid immobilised to the solid surface (probe) hybridizes with nucleic acids labelled with a radioactive isotype, chemical or dye (target) (Phimister 1999). These interactions can then be quantified.

Arrays can be used to assess the differences between the transcriptional profiles of two samples, for example, stressed versus control cells (Type 1 experiment) (DeRisi *et al.* 1997). In addition, competitive hybridisation can be used to allow direct comparisons within a single array. Here cDNA from both sources is labelled with a different dye and added to the same array. cDNA from each sample competes for binding to the DNA probes, and the reliability of the data can be assessed as control and test samples have the opportunity to interact with the test probes under similar conditions. Type 2 experiments compare a number of parameters by using an invariant control such as genomic DNA (Yang *et al.* 2002).

As mentioned previously, there are several different types of microarrays. The first microarray probes consisted of PCR products with primers designed to hybridise

towards the 3’ to 5’ end of genes of interest. The majority of arrays now utilise oligonucleotides designed from entire genomes or specific groups of genes, which are only as good as the reference gene from which they are designed. Oligonucleotide arrays are less problematic than unreliable PCR products. However, arrays need to be redesigned as new genes emerge to prevent false-positive results. Multiple spots of each gene/probe are printed on each array to increase the reliability and statistical power of the data generated.

6.1.3 Microarray analysis procedure

The specified microarray required is printed or purchased from a manufacturer. The slide is uniformly treated with the nucleic acid of choice, which is crosslinked to the solid surface using UV light or by baking at 80°C. Total RNA is extracted from samples using phenol-chloroform or Qiagen columns and must be of sufficient purity, stability and concentration. RNA quality can be assessed by examining ribosomal RNA (18S/28S) degradation by RNAses using a Bioanalyser (Agilent Technologies). The Bioanalyser uses a RNA electrophoresis chip to measure RNA integrity.

The resulting RNA is then converted to cDNA and directly or indirectly labelled using fluorescent dyes. Direct labelling involves inserting a dye labelled nucleotide directly into the cDNA with reverse transcriptase. For indirect labelling, reverse transcriptase inserts amino-allyl UTP instead of dTTP into the cDNA. This cDNA is then reacted with alkaline NHS esters of CyDyes. The complex solution of target nucleic acids is then added to the array. Slides are subjected to a number of different solutions to reduce autofluorescence, reduce non-specific hybridisation and maximise

interactions between the probe and target. Slides are then washed to remove unbound target, dried and scanned to capture images of where cDNA has hybridised with the test probes. Acquiring high quality images of microarrays is important as this impacts upon any further analysis. Each spot on the array represents one gene and thus the image analysis software must be able to determine between the background signal and the millions of individual spots thus requiring high-resolution power. In addition to detection, the image acquisition must be highly sensitive as different genes are expressed at varying levels. Microarrays can be measured using scanners with narrowband illumination or imagers, which use wideband illumination detected by photomultiplier tubes or charge-coupled devices respectively (Ahmed *et al.* 2004). Several problems with image acquisition exist, particularly when using fluorescently conjugated nucleotides, and these include photobleaching and bleed through (overlap of fluorophore spectrum).

6.1.4 Data Acquisition

Images captured by scanning an array indicate the amount of labelled cDNA bound to each gene probe, and thus give a representation of the level of transcription of that gene. In the case of a Type 1 experiment *i.e* treatment versus control; outliers are removed to identify differentially transcribed genes (DeRisi *et al.* 1997). Data for each gene is used to generate an average, geometric mean and standard deviation. Genes within a quoted log ratio away from the mean are considered outliers (Loos *et al.* 2001). These genes are then further selected on the basis of a fixed fold-change (in this study a fold change of 2) however important genes might be below this threshold so stringency can be altered by manipulating this parameter (Yang *et al.*

2002). Data is then subjected to statistical analysis by t-test, significance analysis of microarrays (SAM) or ANOVA to generate reliable gene lists (Zheng, *et al.* 2007). These gene lists can be used to generate graphical representations of expression in order to highlight differences between populations or treatment groups.

6.1.5 Applications of DNA microarrays in research.

Genome wide analysis can provide useful insights into whole systems biology or in conjunction with more detailed gene lists direct research in a specific area, such as inflammation. Mouse models have been widely used to examine many diseases afflicting humans, and murine microarrays have been used to research multiple sclerosis (C.Lu *et al.* 2008), scleroderma (Zhou *et al.* 2006), psoriasis (Wolfram *et al.* 2009) and atherosclerosis (Yuan *et al.* 2009). In addition microarray analysis of endothelial cell populations has provided useful insights into the non-inflammatory effects of shear (Chen *et al.* 2001) effects of VEGF on angiogenesis (Weston *et al.* 2002) and responses to bacterial products (Zhao *et al.* 2001). The use of such experimental tools may identify useful therapeutic targets and provide information on molecular pathways important for disease pathology allowing research to progress at a faster rate than was previously possible. The aim of our DNA analysis was to highlight tissue specific variation of endothelial cell populations, in addition to confirming expression of endothelial specific genes and particularly those involved in inflammation and leukocyte recruitment.

6.2 Results

RNA samples were extracted from mUCEC-1 and s.END cells stimulated with pro-inflammatory treatments (IFN-γ, TNF-α, LPS and combination of TNF-α+IFN-γ) for 24 hours with an aim to see variation in areas of gene expression associated to endothelial cell function, inflammation and recruitment in response to pro-inflammatory treatments. Samples were assessed for RNA purity and integrity using an Agilent Bioanalyser, cDNA was generated and hybridised to Agilent murine oligo arrays. Differentially expressed genes were analysed using GeneSpring GX 7.3.1. Software and Heatmaps were generated from genes 50% present or marginal (significant probes above baseline gene expression determined from several spots of each probe on the array). More specific gene lists reflecting proteins of interest to the current investigation were generated for each treatment group and cell line. IngenuityTM Pathway Analysis 3.0 (IngenuityTM Systems, CA, USA) was utilised to assemble information on functional networks and pathways of interacting proteins.

Figure 6. 1: Sample of Bioanalyzer data. Representative images of RNA sample purity obtained from Bioanalyzer.

A representative sample of bioanlayzer data from mUCEC-1 and s.END cell samples sent for microarray. The peaks (A) and gel bands (B) represent ribosomal RNA subunits at 18S and 28S the most conserved gene in eukaryotes. The Agilent Bioanalyzer quantifies the amount of RNA and assesses purity and integrity. The RIN Number (C) or RNA Integrity Number ranges from 1-10 with 10 being RNA of the highest quality.

We began by assessing the integrity of RNA samples to be used for microarray analysis using the Agilent Bioanalyzer. The images presented in Fig. 6.1 show a representative section of RNA samples. The Bioanalyzer generates spectra of ribosomal RNA subunits at 18S and 28S (Fig 6.1-A). In addition a pseudo-gel image indicates whether any RNA degradation is apparent in the sample (Fig 6.1-B). These two measures and the RNA Integrity Number (RIN) allow the researcher to be confident in the quality of the RNA (Fig. 6.1-C). All samples run on Agilent Mouse Oligo Arrays were of sufficient quality (Fig. 6.1).

Several heatmaps of microarray data were then generated. Heatmaps are graphical representations of gene expression under a number of different conditions where data in a 2-D map are represented as colours. The values displayed are normalised signal values as log ratios (Log Ratio of 0= Genes with a ratio of 1-Genes unchanged). The key indicates gene intensity and ‘trust’ i.e the degree of reproducibility between spots (probes) for each gene in the array.

Figure 6.2: Heatmap of all genes present or marginal (50%) in mUCEC-1 and s.END cells in all treatments examined.

Each line represents one gene and each column represents the average of 3 spots for each probe. EC were cultured and treated with pro-inflammatory substances for 24 hours prior to RNA isolation with Qiagen RNAeasy columns. Samples were assessed for purity and integrity using Agilent Bioanalyzer and run on Agilent mouse oligo arrays. Extracted data was analysed using GeneSpring GX 7.3.1 software.

Figure 6.3: Heatmap of gene variation. Graph representing genes present in mUCEC-1 and s.END cells.

EC were cultured and treated with pr-inflammatory substances for 24 hours prior to RNA isolation with Qiagen RNAeasy columns. Samples were assessed for purity and integrity using Agilent Bioanalyzer and run on Agilent mouse oligo arrays. Extracted data was analysed using GeneSpring GX 7.3.1 software.

Figure 6.4: Baseline gene expression. Image represents genes expressed in mUCEC-1 and s.END cells treated with control media.

Each column represents one spot of the same gene probe, I,e all replicates of samples n=3. EC were cultured and treated with control TCM prior to RNA isolation with Qiagen RNAeasy columns. Samples were assessed for purity and integrity using Agilent Bioanalyzer and run on Agilent mouse oligo arrays. Extracted data was analysed using GeneSpring GX 7.3.1 software.

The heatmaps in Fig. 6.2/3 show the variation in gene expression in mUCEC-1 and s.END cells when stimulated with a variety of pro-inflammatory stimuli for 24 hours. Each line represents a single gene that was present or marginal (arbitrary levels (flags) of expression generated by the analysis software) in all samples. Fig. 6.2 shows that there were global differences in total gene expression in different cell lines and that whilst expression of individual genes was altered following different treatment strategies the two cell lines maintained their individuality (*i.e.* global gene expression patterns were still maintained). This is demonstrated in a different format in Fig. 6.3 where global gene expression is again represented but individual gene expression changes in response to treatment are indicated by single lines. Here it is clear that again each cell has a distinctive gene expression profile and that the s.END cells have a greater variability in degrees of expression (the chart is spread more than the samples from the mUCEC cell line). However when the data is expressed in this format it is clear that there are some groups of genes, which show large fold-changes in expression in response to cytokine treatment. The data represented by these heatmaps is based upon expression values generated from the average of 3 spots for each probe/gene. The degree of 'trust' or confidence in the data is based on the reproducibility between these spots and is represented by the degree of grey shading on the gene data in Fig. 6.2 and 6.4. This is confirmed in Fig. 6.4 which shows genes expressed in control untreated samples; each of the three columns represents one spot of each probe indicating that variation between spots was minimal in representative control samples from each cell line.

6.2.1 Analysis of expression of key genes of interest using microarrays.

Whilst the heatmap figures for total gene expression data are useful to show global patterns of gene expression between cell types or in response to treatment they are not particularly informative in the context of identifying changes in specific genes. Thus in order to examine gene expression in more detail and to compare the phenotype of cell lines in respect of the data obtained in previous chapters, comprehensive gene lists were generated for specific sets of molecules in the context of endothelial phenotypic markers, inflammation and leukocyte recruitment. As before the specific gene data is shown in colour and positive fold change is indicated by blue, where gene expression is higher than for those genes in yellow (with a fold-change less than 1 compared to normalised expression level of the 44K genes on the array chip set by software). The darker the gene colour (*ie* the greyness of the bar) the less reliable the expression profile is (Trust). As was noted for global gene expression, our key genes differed vastly in expression between mUCEC-1 and s.END cells (Fig. 6.5 – 6.11).

Figure 6.5: Expression of endothelial cell markers.

Heatmap of adhesion molecule gene expression in mUCEC-1 and s.END cell lines treated with pro-inflammatory stimuli for 24 hours. EC were cultured and treated with pr-inflammatory substances for 24 hours prior to RNA isolation with Qiagen RNAeasy columns. Samples were assessed for purity and integrity using Agilent Bioanalyzer and run on Agilent mouse oligo arrays. Extracted data was analysed using GeneSpring GX 7.3.1 software.

The expression patterns of a number of endothelial cell markers were investigated on EC and once again opposing gene expression patterns were apparent between cell lines (Fig 6.5). Interestingly vWF considered a general marker of endothelial cells was absent from both EC from heart and skin. In s.END cells VEGF-B/C and Claudin-3 were highly expressed, whereas mUCEC-1 cells expressed GP38 and VEGF-A. Little variation in expression patterns was seen in response to stimuli.

Figure 6.6: Expression of adhesion molecules.

Heatmap of adhesion molecule gene expression in mUCEC-1 and s.END cell lines treated with pro-inflammatory stimuli for 24 hours. EC were cultured and treated with pr-inflammatory substances for 24 hours prior to RNA isolation with Qiagen RNAeasy columns. Samples were assessed for purity and integrity using Agilent Bioanalyzer and run on Agilent mouse oligo arrays. Extracted data was analysed using GeneSpring GX 7.3.1 software.

Analysis of adhesion molecule expression under basal or cytokine-stimulated conditions (Fig. 6.6) shows that if genes were considered to be present and expressed when coloured blue (i.e. fold gene expression was equivalent to, or above that of the majority of genes expressed in the array used to set the normalisation-percentile shift algorithm set at 75%) the sEND cell line had a more characteristic 'endothelial' pattern of expression with P-Selectin, E-selectin, CD31, ICAM-2, CD34 and endoglin all significantly expressed. In contrast unstimulated mUCEC cells had a more restricted basal expression of P-Selectin, JAM-1, JAM-2 and VCAM-1. For most of these genes in either cell line, expression was minimally altered by cytokine treatment (gene fold- expression colour remain similar across the rows). However there were notable exceptions. ICAM-1 was upregulated by IFNγ and in combination with TNFα in both cell types. In addition this treatment regime induced expression of CD44 in s.END cells. Whereas it appeared that P-Selectin may be downregulated by these cytokines, there also appeared to be a downregulation of P-Selectin in the presence of IFNγ. Interestingly however levels of P-selectin increased in response to LPS stimulation. Neither cell expressed JAM-1, PSGL-1, VAP-1 or LYVE-1.

Figure 6.7: Expression of CCL Chemokines.

Heatmap of adhesion molecule gene expression in mUCEC-1 and s.END cell lines treated with pro-inflammatory stimuli for 24 hours. EC were cultured and treated with pro-inflammatory substances for 24 hours prior to RNA isolation with Qiagen RNAeasy columns. Samples were assessed for purity and integrity using Agilent Bioanalyzer and run on Agilent mouse oligo arrays. Extracted data was analysed using GeneSpring GX 7.3.1 software.

Chemokines and their cognate receptors are integral to leukocyte recruitment. We examined the expression of all groups of chemokine ligands and receptors (Fig.6.7/8). mUCEC-1 and s.END cells express a small number of CC ligands. mUCEC-1 particularly expressed TECK, TARC and MCP-2. Stimulation with IFN-γ , TNF-α+IFN-γ and LPS in mUCEC-1 cells increased expression of these chemokines in addition to MCP-3. RANTES expression was induced by TNF-α, LPS and TNF-α+IFN-γ but absent in IFN-γ treated samples. In contrast s.END cells expressed a more restricted profile including MIP-1β and MCP-1. Interestingly, MCP-3 increased when exposed to LPS and a similar pattern was seen in mUCEC-1 cells.

Figure 6.8: Expression of CXCL Chemokines.

Heatmap of adhesion molecule gene expression in mUCEC-1 and s.END cell lines treated with pro-inflammatory stimuli for 24 hours. EC were cultured and treated with pro-inflammatory substances for 24 hours prior to RNA isolation with Qiagen RNAeasy columns. Samples were assessed for purity and integrity using Agilent Bioanalyzer and run on Agilent mouse oligo arrays. Extracted data was analysed using GeneSpring GX 7.3.1 software.

CXC Ligand expression was globally higher in mUCEC-1 cells including SDF-1, MIP-2γ, CXCL16 and IP-10. In addition MIG was induced in response to IFN-γ and TNF-α+IFN-γ in both cell types. IP-10 was increased in all treatments above control. The addition of LPS induced expression of CXCL5 and KC in both cell types. The expression of chemokine receptors was minimal on endothelial cells as these molecules are generally expressed on leukocytes mediating interactions between leukocytes and the endothelium. Small amounts of CXCR3 are apparent on s.END cells, expression of which has previously been indentified in populations of human microvascular endothelial cells (Romagnani *et al.* 2001) and CCR9/10 in mUCEC-1 cells. CXCR4 has been shown to be expressed on HUVEC and play a role in transendothelial migration (Murdoch *et al.* 2000).

Figure 6.9: Expression of chemokine receptors.

Heatmap of adhesion molecule gene expression in mUCEC-1 and s.END cell lines treated with pro-inflammatory stimuli for 24 hours. EC were cultured and treated with pr-inflammatory substances for 24 hours prior to RNA isolation with Qiagen RNAeasy columns. Samples were assessed for purity and integrity using Agilent Bioanalyzer and run on Agilent mouse oligo arrays. Extracted data was analysed using GeneSpring GX 7.3.1 software.

Figure 6.10: Expression of interleukins and Receptors.

Heatmap of adhesion molecule gene expression in mUCEC-1 and s.END cell lines treated with pro-inflammatory stimuli for 24 hours. EC were cultured and treated with pr-inflammatory substances for 24 hours prior to RNA isolation with Qiagen RNAeasy columns. Samples were assessed for purity and integrity using Agilent Bioanalyzer and run on Agilent mouse oligo arrays. Extracted data was analysed using GeneSpring GX 7.3.1 software.

Interleukins are a group of cytokines initially discovered on leukocytes as a method of communication between different leukocyte populations. Produced by and acting upon leukocytes they induce activation and are involved in development of T, B and haematopoetic cells. Both cell types expressed a limited number of interleukins and receptors and expression levels varied. The majority of markers were absent shown by grey (low trust) s.END cells were found to express IL-6 and lower levels of IL-13 and little change was observed with treatment. mUCEC-1 cells expressed TNFR6 and expression was higher in all treatments above control. CSFM expression was induced in response to IFN-γ and in combination with TNF-α (Fig. 6.10).

6.2.2 Ingenuity Analysis: Pathways

Ingenuity Pathway Analysis can be used to analyse how gene expression and protein interactions identified by microarray analysis interrelate to each other and impact upon each other's function to contribute to changes in cell phenotype or function. We identified differentially expressed genes from our microarray analysis (66 probes in s.END cells and 330 probes in mUCEC-1 cells classified as significantly differentially expressed after treatment via statistical analysis) and used pathway analysis to identify the main biological processes in which these genes are involved. Two sets of pathway analysis were obtained from the microarray data, core and canonical pathways. Core analysis allows rapid assessment of the signalling and metabolic pathways most significantly different between the cell populations. Whereas canonical analysis examines pathways related to each other reduced to the simplest form. Histograms represent the highest rated maps/pathways, which have a significance level that pass the threshold and p-value set. Canonical ratio value is determined by the number of molecules in a given pathway that meet cut off criteria over the total number of molecules that make up that pathway. Ingenuity analysis was limited to samples stimulated with IFN-γ or TNF-α+IFN-γ as these stimuli induced the largest responses and greatest numbers of differentially expressed genes.

Figure 6.12: Canonical pathways in s.END Cells.

Comparison of pathways in which 66 significant probes present in s.END cells treated with IFN or TNF+IFN for 24 hours are present. P-Values set at <0.05. Data analysed using Ingenuity^{TM} Pathway Analysis 3.0

Figure 6.13: Core pathway analysis in s.END Cells.

Ingenuity analysis of core pathways associated with 66 significant probes present in s.END cells treated with TNF+IFN for 24 hours. P-Values set at <0.05. Ratio, is the number of genes from experimental list compared to total number of genes in that pathway. Data analysed using Ingenuity™ Pathway Analysis 3.0 .

Figure 6.14: Canonical pathways in mUCEC-1 Cells.

Comparison of pathways in which 330 significant probes present in mUCEC-1 cells treated with IFN or TNF+IFN for 24 hours are present. P-Values set at <0.05. Data analysed using Ingenuity™ Pathway Analysis 3.0

Figure 6.15: Core pathway analysis in mUCEC-1 Cells.

Ingenuity analysis of core pathways associated with 330 significant probes present in mUCEC-1 cells treated with TNF+IFN for 24 hours. P-Values set at <0.05. Ratio, is the number of genes from experimental list compared to total number of genes in that pathway. Data analysed using Ingenuity™ Pathway Analysis 3.0

Both canonical and core analysis indicated that a majority of the significantly differently expressed genes in s.END cells were associated with immune and endothelial cell functions such as, antigen presentation, endocytosis and recognition of pattern recognition receptors (PRR's) (Fig. 6.12 and 6.13) and that responses to IFNγ were very similar to those elicited in response to the combination of TNFα plus IFNγ. The response of mUCEC-1 was similar (although a greater number of genes was involved), however reassuringly the interferon-signalling pathway was also significantly altered in response to treatment of these cells. The ratio value is the number of molecules in a given pathway that meet cut criteria over the total number of molecules that make up that pathway.

6.2.3 Validation of gene expression using qPCR

In order to confirm expression of differentially expressed genes and to check the validity of our microarray data a number of random genes were additionally analysed using quantitative real-time SYBR® Green PCR (qPCR). Comparisons were made between the fold changes seen in arrays and by qPCR. Fig. 6.16-6.17 show that the validation in both cell lines was successful and the qPCR data supported conclusions drawn from the microarray data. We examined whether the trends in fold changes were similar between microarray and qPCR as they are normalised in different ways so absolute values will differ. The rationale behind this is that Genespring filters data based on $p<0.05$ so 5% of the gene list could be false positives. A multiple testing correction is then applied to reduce this but false positives could still exist so qPCR is used to validate true positives. Negative fold changes are not considered significant as they are less than the fold change defined by arrays (2) and wouldn't have been

considered significant. Of note, one of the genes chosen for the validation, Perp, was absent from s.END cells in both arrays and qPCR hence no values are present for fold expression changes.

Figure 6.16: qPCR Validation in mUCEC-1 cells.

The expression of selected genes was examined using SYBR® Green qPCR. Fold change increase/decrease from control treated samples were compared to data obtained from Gene Arrays.

Figure 6.17: qPCR Validation in s.END cells.

The expression of selected genes was examined using SYBR® Green qPCR. Fold change increase/decrease from control treated samples were compared to data obtained from Gene Arrays.

6.3 Discussion

Microarray analysis, database mining and transcriptional profiling have been used to expand insights into endothelial gene expression and endothelial cell biology (Ho *et al.* 2003). Novel endothelial cell specific genes have been discovered using arrays. Pai *et al* showed that freshly isolated EC from lung and kidney expressed 350 genes at higher levels than surrounding parenchymal cells and that 200 were potentially novel (Pai *et al.* 2005). Tissue specific differences were also apparent with genes encoding ephrin signalling highly expressed in lung. In addition, Ho *et al* examined gene expression in EC from four vascular sources (including lung, heart, and umbilical vein) and five non-endothelial cell types (including astrocytes, keratinocytes and mammary epithelial cells). They found 64 pan-endothelial markers differentially expressed with a minimum of three fold differences such as VE-Cadherin and Endothelial Cell Specific Molecule-1 (ESM-1) (Ho *et al.* 2003). Interestingly matrix *gla* protein, a gene encoding bone development was discovered in murine aortic endothelial cells where it may regulate calcification a causative factor of vascular disease (Yuan *et al.* 2009).

6.3.1 Gene Expression Patterns in mUCEC-1 Cells

The gene expression patterns of mUCEC-1 cells in response to stimuli have not previously been reported, and thus the gene array data obtained in this investigation provides novel insights into responses of cardiac endothelial cells to inflammatory insult, and in particular to molecules associated with inflammation. Expression of EC markers and adhesion molecules had been previously studied in additional chapters. Reassuringly our microarray data was concurrent with phenotypic data obtained with

other techniques (IHC, cell based ELISA). For example, mUCEC-1 cells expressed high levels of VCAM-1, JAM-2 and Endoglin by all detection methods. Interestingly chemokine and chemokine receptor expression was minimal with TARC (CCR4) and Monocyte chemoattractant protein-2 (MCP-2) present on the mUCEC-1 cells in all treatments and control.

We also demonstrated that these cardiac endothelial cells express scavenger receptors including VLDLR and CD36. Our functional observations that TNFα induced adhesion of leukocytes to mUCEC were supported by demonstration of receptors such as TNFR-6 thus conferring the ability to respond to this cytokine.

Ingenuity analysis on mUCEC-1 cells stimulated with combinations of TNF-α and IFN-γ showed as expected that significantly different probes were often involved in immune functions such as antigen presentation and interferon signalling. Given the nature of the immortalisation of these cells and their propensity to proliferate in the presence of IFN-γ it is perhaps not surprising that gene expression is sensitive to the presence of this cytokine.

6.3.2 Gene Expression Patterns in s.END Cells

Although several murine models of skin diseases exist including dermatitis, psoriasis and scleroderma, and sEND cells have been used as model skin endothelial cells in vitro, the gene expression profile of s.End cells in response to pro-inflammatory stimuli has not previously been published. The data in this chapter, in conjunction

with previously obtained phenotypic data, confirms that s.END cells express CD31 and ICAM-2. E-Selectin is also expressed although fold change data from the gene arrays in response to treatment suggest higher changes at the gene level compared to protein level. The array data suggested that chemokine expression was more pronounced in skin EC compared to cardiac EC, and included Monocyte Chemoattractant Protein-1 (MCP-1) and Macrophage Inflammatory Protein 1-β (MIP-1β). Studies in the CD18 hypomorphic (CD18hypo) PL/J mouse model of psoriasis showed that MCP-1 expression was enhanced in the lesions of affected CD18hypo mice (Wang *et al.* 2006). Additionally injection of recombinant murine MCP-1 in conjunction with TNF-α induced psoriasiform skin inflammation around the injection sites with recruitment and activation of macrophages. Our array data also shows induction of MCP-1 expression by our skin cells suggesting it may contribute to the lymphocyte recruitment we noted *in vitro* as well as promoting inflammation *in vivo*.

Genome wide analysis enabled Zhou *et al* to identify early markers of scleroderma using a murine sclerodermatous graft-versus-host disease model. Scleroderma affects the dermal arterioles leading to degradation of EC and subsequent fibrosis accompanied by an infiltration of CD4+ T-Cells (also required in the development of psoriasis). Samples of skin were taken from diseased and control mice 3-5 weeks after administration of bone marrow and spleen cells from B10.D2 and syngeneic Balb/c mice respectively. Consistent differences were found for chemokines (including CCL2,5,17, MIG, IP-10 and ITAC) in conjuction with growth factors (PDGF-C, FGF-1, VEGFα) and adhesion molecules (E,P,L-Selectin and VCAM-1) consistent with inflammatory diseases in particular fibrosing autoimmune conditions (Zhou *et al.* 2006). Interestingly, we found that s.END cells (originating from dermal haemangiomas) expressed low levels of CXCR3, receptor for ligands MIG, ITAC and

IP-10 involved in fibrosis. E-Selectin and P-Selectin (in some treatment) were also expressed in addition to a number of EC markers including VEGF B and C. Pathway analysis produced similar results to mUCEC-1 with significant probes involved in endocytosis and recognition of PRR's. Thus it appears that the skin cell line used in vitro exhibits phenotypic similarity with cells in vivo and responds similarly to inflammatory insult. Thus in contrast to the mUCEC cells, this line represents a realistic model in which to study organ-specific recruitment of leukocytes *in vitro*.

6.3.3 Further investigations of EC phenotype with microarray technologies

In previous chapters in addition to EC from heart, skin and liver, the phenotype and function of brain microvascular endothelial cells (b.End.5) was examined. Our investigations of available literature suggest that comprehensive expression profiling of these cells has been carried out, and that such array analysis would generate interesting, novel data. Much research with primary brain microvascular endothelial cells has investigated the role of the blood brain barrier (BBB). Lu *et al* showed that pertussis toxin (PTX) increases BBB permeability. Mice were treated with PT, which induces experimental autoimmune encephalitis (EAE) and brain microvascular endothelial cells were subsequently isolated and analysed using a cDNA microarray. They found 34 genes that were differentially expressed in response to PT, one third of which were involved in angiogenesis. Further experiments blocking signal transduction pathways were consistent with the concept of PT alteration of BBB due to adverse effects on angiogenesis and tube formation (Lu *et al.* 2008). It would be interesting to see whether our cell line responded similarly to treatment *in vitro*, and also to see whether this cell line exhibits appropriate angiogenic reponses in assays

such as matrigel invasion and scratch wound repair. Such data would indicate whether these cells are indeed a good model of brain endothelium.

Gene array analysis can also be used to identify a specific population of cells or to confirm a successful isolation. Microarrays would have been a useful tool for analysing the primary mLSEC obtained using αCD146 method outlined in Chapter 1. Kobayashi *et al* used DNA microarray analysis to confirm the isolation of aortic endothelial cells and smooth muscle cells from murine aortas (Kobayashi *et al.* 2005). In conjunction with morphological and immunocytochemical analysis EC were found to specifically express CD31 whereas SMC expressed smooth muscle actin. These observations could be extended to include the full panel of phenotypic markers we identified in our staining studies.

To date limited gene array analysis has been performed on mLSEC and we hope to generate more data from our cells in the future. Serial analysis of gene expression (SAGE) has been carried out on RNA isolated from normal and CCl4 damaged mLSEC. Nonaka *et al* discovered 6011 unique transcripts expressed in response to injury. CCl_4 treatment induced upregulation of genes associated with cell growth and differentiation (Cdkn1a, Irf1) and downregulated genes related to protein transportation (Kdr, Ap1b1). In addition they discovered 23 mLSEC specific genes not found in other mouse tissues or cell lines including Stabilin-2 (Nonaka *et al.* 2004), which interestingly we found on immortalised cardiac endothelial cells (mUCEC-1). The limited array data included here (Fig. 6.18-9) showed that human LSEC expressed a number of markers associated with sinusoidal endothelial cells including scavenger receptors, EC markers and growth factors. It would be

interesting to see whether this pattern of expression translated into mice and whether more specific analysis could highlight more interesting differences or similarities between human and murine systems and EC from different vascular beds and tissues.

Macroarrays have also been used to examine the effect of shear stress on the development of cardiac tissue in mES cells. Shear is thought to induce epigenetic modifications of histones activating transcription of VEGF receptor-2 promoter and early induction of cardiovascular markers (Illi *et al.* 2005).

DNA technology as an experimental tool has unlimited potential with increasingly complex formats and resources are available the challenge is mining the large amounts of data generated by such methods and using it as a basis for more in depth studies into mechanisms responsible for physiological responses. In this chapter we have used DNA microarray technology to highlight differences in tissue specific endothelial populations in particular relation to the functional capacity of EC particularly their role in leukocyte recruitment. Array data was used to support previous analysis and to make connections between phenotypic differences and functional responses, perhaps shedding light on the role of particular chemokines or adhesion molecules.

7. DISCUSSION

Endothelial cells are an essential part of the human body and play a vital role in many processes. We examined in particular their role in leukocyte recruitment. The recruitment of leukocytes into tissues as a part of immune surveillance and response to inflammation is an essential process. Alterations in the expression of adhesion molecules and chemokines present on the surface of EC in different tissues enables site specific recruitment of subsets of leukocytes dependent on the unique combination of molecules and receptors present.

A general paradigm of leukocyte recruitment exists, the individual steps of this sequential generic model are widely accepted, but published research and data presented in this thesis have highlighted the specialisation of underlying molecular mechanisms present in different tissues and physiochemical environments. Much previous research has focussed on HUVEC due in part to the ease of access of tissue and simple isolation methodology. However a number of additional endothelial cell sources have been used from both humans and mice. We wanted to know how the tissue origin of endothelium can impact upon and regulate leukocyte recruitment, and in particular how recruitment to the liver microcirculation varies from other sites. Such information can be of use in the investigation of conditions where the host's immune system causes pathology for example in autoimmune or alcohol induced liver injury.

7.1 Isolation of primary murine endothelial cells.

The isolation and successful culture of primary murine endothelial cells, in particular liver sinusoidal endothelial cells, was of particular interest here as mEC can be used

in vitro as a model of human systems. Murine tissue is often more readily available than human samples and murine systems are more amenable to manipulation, be it alterations in shear exposure or inflammatory insult, use of intravital microscopy or genetic alterations in knockout mice or models of human disease. However, primary EC are notoriously difficult to isolate. In addition to the challenge of isolating small number of cells from whole tissues (in particular mLSEC which constitute ~10% of whole liver cell population) it is difficult to maintain the EC in a state that recreates their physiological environment, as a result of which EC tend to dedifferentiate in culture. Steps can be taken to attempt to recapitulate the natural physiochemical environment with the addition of growth factors (HGF, astrocyte conditioned medium), autologous serum and appropriate oxygen tensions (Martinez *et al.* 2008) as well as coculture with proximal cell populations (Alabraba *et al.* 2007). Despite such difficulties, the isolation of a number of human EC populations has been successfully achieved, in particular HUVEC (macrovascular) and hLSEC (microvascular). The majority of methods involve dissociation of the tissue (Knolle *et al.* 1999) on the basis of size or buoyant density using gradient materials and differential centrifugation. In addition selection beads can be used to isolate specific subsets of cells on the basis of expression of certain molecules (CD31, HEA125, CD146).

In contrast to the human situation, fewer studies have utilised cultured primary murine cells, and often rather than isolating primary cells, studies are performed in the whole animal system. Although this has obvious advantages in terms of maintenance of correct endothelial phenotype, the technical complexity of such systems and the potential for contribution of multiple cells and mediators to test responses means that more simplified *ex-vivo* experiments are of value. Thus,

several groups have looked at isolating primary murine EC from brain (Wu *et al.* 2003), lung, heart (Marelli-Berg *et al.* 2000), skin and liver (Katz *et al.* 2004) to examine immunological functions, expression of adhesion molecules, generation of immortalised cell lines (Magid *et al.* 2003) and purely to achieve successful isolation protocols (Marelli-Berg *et al.* 2000).

We attempted to isolate EC from murine brain and liver to assess expression of EC markers and adhesion molecules and how the phenotype of these EC populations affected the functional ability to recruit leukocytes under flow conditions. The most successful isolation methodology in our hands utilised αCD146 magnetic beads to isolate mLSEC. The gold standard method for isolation of mLSEC from whole liver involves *in situ* perfusion of the organ as reported by Smedsrod *et al*. (Smedsrod *et al.* 1985). Perfusing the organ allows a more delicate and comprehensive tissue dissociation but is a complex procedure requiring specialist equipment. Knolle *et al* use this method in combination with CD146 selection to obtain pure populations of mLSEC. However, many problems were encountered when we attempted to recreate this methodology in Birmingham. These issues included availability of the more complicated elements of apparatus, methods available for killing the animal and clotting in the portal vein hindering sufficient perfusion. None of these problems would be impossible to rectify in the longer term, however magnetic bead isolation methods were used in the current studies to permit easy selection of CD146 positive EC with the available resources.

7.1.1 Characterisation of mLSEC.

When isolating primary cell populations it is crucial to be able to identify and phenotype them in order to confirm cell identity and purity. EC characteristics often used for such purposes include expression of CD31, CD34, vWF, uptake of acLDL, binding of lectins and formation of tubes in matrigel (angiogenesis assay). However, at present no single marker or characteristic is sufficient to confirm the identity of murine liver sinusoidal endothelial cells unlike the human counterparts where expression of L-SIGN and DC-SIGN can be used (Shetty *et al.* 2008).

Molecule	IHC
CD31	+++
ICAM-2	-
JAM-2	+
VCAM-1	-
CD34	++
VAP-1	++
Endoglin	++
E-Selectin	-
LYVE-1	++

Table 7. 1: Table summarising expression profile of endothelial markers and adhesion molecules of primary mLSEC cells.

Expression of phenotypic markers was assessed using IHC methods. Expression levels were compared to CD31 positive control in each experiment.

Isolation of mLSEC using αCD146 beads yielded populations with the characteristic 'endothelial-like' cobblestone morphology, which stained positive for CD31, ICAM-2, CD34, VAP-1, LYVE-1 and Endoglin using immunohistochemical techniques (See Table 7.1). However these cells did not proliferate in culture, even in the presence of HGF and VEGF. Interestingly Rainger *et al* (personal communications) have found that primary EC isolated from fat pads and vessels from younger/neonatal animals

tended to proliferate more in culture compared to those isolated from older mice. This reduced propensity of cells from adult mice to proliferate could be due to a finite number of cell divisions relating to animal lifespan. Certainly the activity of telomerase has been shown to impact on angiogenesis in mice by mediating responses to VEGF (Zaccagnini *et al.* 2005) but limited data is available for *in vitro* cultures of murine EC. Several other groups have also examined the phenotype of murine liver endothelium. mLSEC isolated by collagenase perfusion express LYVE-1, Stabilin-2 (Nonaka *et al.* 2007), Endoglin (Onoe *et al.* 2005), ICAM-1, VCAM-1 and CD31 (Do *et al.* 1999). In contrast, limited phenotypic analysis is available for CD146-selected mLSEC, however in the paper describing this method, Schrage *et al* (Schrage *et al.* 2008) found that mLSEC expressed the endothelial markers CD31, CD146, VE-Cadherin and Meca-32 (Hallman *et al.* 1995). None of these markers are sinusoidal specific to the hepatic sinusoid however. Many of the markers examined are expressed in additional locations, for example LYVE-1 in the lymphatics, CD31 on lymphocytes (Lalor *et al.* 2002b) and VE-Cadherin is a component of intercellular junctions found in many cell types. CD146 and Meca-32 are more endothelial specific but not mLSEC specific. Thus to date identification of mLSEC depends upon expression of a number of phenotypic indicators and morphological characterisation (fenestrations, cobblestone morphology). In the future more detailed array analysis (similar to that we currently have in progress) will contribute to this area of research and could identify specific markers or patterns of expression in mLSEC. However, the limited phenotypic analysis obtained in this thesis is concurrent with that found by other research groups.

7.1.2 Functional analysis of mLSEC behaviour in vitro

Currently much of the available data for assessment of the immunological function of mLSEC is focussed on their role in antigen presentation (Knolle *et al.* 2001) and innate immunity (Elvevold *et al.* 2008). In contrast, our functional experiments using mLSEC examined the ability of stimulated cells to recruit mixed lymphocytes from whole spleens and isolated subsets of CD4+/CD8+ cells. We found that after both 4 and 24 hours the majority of treatments increased total levels of adhesion above that of the unstimulated control, with the exception of IL-1β at 4 hrs. The combination of TNF-α+IFN-γ and LPS induced the highest levels of adhesion and these treatments were carried over to 'static' adhesion assays where similar results were observed. Although limited research data is available on the response of mLSEC to these treatments, LPS and TNF-α have previously been reported to play a role in liver injury (Jirillo *et al.* 2002;Lalor *et al.* 2002a). The regulation of inflammation in the liver is complex as the liver is constantly exposed to gut-derived food antigens and has evolved mechanisms to suppress immune responses to harmless antigens whilst maintaining the capacity to respond to infections (Oo *et al.* 2009). Uhrig *et al* (Uhrig *et al.* 2005) showed that mLSEC can be tolerant to LPS and this can subsequently lead to cross-tolerance to IFN-γ stimulation. LPS tolerance resulted in decreased leukocyte adhesion due to down regulated ICAM-1 expression on the endothelial surface. It may be that if LPS primed mLSEC in our system were subsequently challenged they would also demonstrate this tolerance. Nevertheless we did note an increase in adhesion in response to short exposure to LPS alone (albeit a small one) suggesting cells can respond to an initial stimulus.

The combination of TNF-α+IFN-γ induces the expression of CXCR3 ligands, CXCL9, CXCL10 and CXCL11, involved in mediating liver inflammation and infiltration of lymphocytes (Curbishley *et al.* 2005). We confirmed that we saw a modest increase in adhesion of lymphocytes to mLSEC in response to these cytokines, and that the mLSEC supported adhesion of both CD4+ and CD8+ cells. There was a suggestion that proportionally, we saw a greater increase in CD8 cell recruitment in response to stimulation with these cytokines. *In vivo* studies of the proportions of lymphocytes resident in normal and inflamed livers suggest a bias towards CD8 recruitment into the liver. In response to inflammation or liver injury mLSEC express additional adhesion molecules and chemokines such as VCAM-1 and E-Selectin permitting recruitment and retention of effector T-Cell populations. For example CD8+ CD45RO+ cells in livers infected with hepatitis C (Lalor *et al.* 2002b). This selective recruitment relates to differential chemokine receptor expression. In humans CD8+ cells express CXCR3/6 and CCR5 as do CD4+ Th1 cells and in contrast, CD4+ Th2 cells express CCR4 and 8. Specialised subsets of CD4+ T-Cells such as Th17 cells and Treg express CCR4, 6, CXCR3, 6 and CCR4, 5 and 8 respectively. Generally in hepatic inflammation leukocytes recruited into the liver are CXCR3/6, CCR1/5 positive (Kunkel *et al.* 2002;Shields *et al.* 1999) which fits with the expression of ligands for these receptors during human inflammation (Curbishley *et al.* 2005). Our preliminary data also suggests the same trends for inflamed mLSEC *in vitro*.

7.2 Use of immortalised endothelial cell lines

The ideal methods for investigating diverse endothelial functions would focus upon studies of the cells *in vivo* in a physiologically relevant environment. Indeed, with the

advent of techniques such as intravital microscopy, and whole animal imaging facilities researchers are able to examine processes such as leukocyte recruitment in the whole animal. Although these studies are tremendously important it remains difficult to manipulate certain parameters such as shear stress and to hone in on particular molecular interactions between cell types in a whole animal system. Similarly, at least in the UK, studies are limited by the necessity to obtain Home Office licenses to perform any *in vivo* work. As a result *in vitro* systems can be a valuable alternative, ideally with primary cell isolates, since they enable the researcher to obtain the most representative impression of the *in vivo* situation. However, as previously discussed, the challenges isolating primary cell populations from whole tissue are complicated by the difficulty in isolating homogenous populations of cells. However, EC and epithelial cells have been isolated from some tissues, such as the lymphatics (Ager 1987) and gastrointestinal system (Whitehead *et al.* 2009) respectively. Again due to availability of tissue in some institutions, immortalised cell lines have been developed to allow further research and understanding of EC function.

Cell lines originate from a primary cell population and are often conditionally immortalised with viral mechanisms to prevent senescence. However generation of cell lines has uncovered many issues warranting consideration such as altered gene expression compared to the *in vivo* situation and phenotypic drift in culture. These cells can be continually subcultured to high passage generally maintaining a stable phenotype. Several comparisons have been made between primary cells and immortalised cells from the same cell source in order to validate them as a reliable and functionally representative. For example HMEC-1 (Human microvascular endothelial cells) originates from human dermal endothelial cells transfected with

SV40 (Ades *et al.* 1992). HMEC-1 cells were originally shown to form tubules *in vitro*, and exhibit many phenotypic markers characteristic of endothelium. However 12 years after they were originally isolated these cells have now lost this ability (Nisato *et al.* 2004), illustrating the 'phenotypic drift' which can occur with prolonged culture. In addition Lidington *et al* (Lidington *et al.* 1998) compared several EC cell lines to HUVEC and examined expression of CD31, ICAM-1, VCAM-1, E-Selectin, MHC, CD40, CD95 and LFA-3 in response to TNF-α and IFN-γ stimulation and static transmigration assays with PBMC. The most striking differences between HUVEC and cell lines were the induction of VCAM-1 and E-Selectin in response to TNF-α and MHC in response to IFN-γ. Levels of leukocyte transmigration on immortalised cells were also reduced in comparison to HUVEC however this may be due to immortalisation or variation in the vascular beds from which EC were derived. However, experiments by Sahota *et al* (Sahota *et al.* 2004) in models of tissue-engineered skin found no difference in the ability of primary small vessel dermal endothelial cells (HuDMEC) and HMEC-1 to respond to angiogenic factors (VEGF/FGF) and penetrate the dermis. Thus it seems that at least in some model systems, and with careful interpretation, cell lines can be used as good replacement models for primary endothelium. Thus with an appreciation of the limitations of research using cell lines we decided to utilise them as a comparator in our research in order to determine the key experiments to take forward with primary murine EC populations.

A murine immortalised liver sinusoidal endothelial cell line has been reported (M1), and was immortalised with an SV40 construct similar to mUCEC-1 (Saito *et al.* 2007). These cells have been cultured in 3D bioreactors in an attempt to reconstruct liver tissue *in vitro*. However limited subsequent data is available on this cell type, which

suggests it, may not be representative of this specific vascular bed. Certainly In our laboratory historical attempts at immortalisation of hLSEC with SV40 were unsuccessful and resulted in cell senescence (unpublished data).

7.2.1 Characterisation of mUCEC-1 cells.

mUCEC-1, a cardiac EC population, was isolated from the H-2KB-tsA58 immortomouse expressing a thermolabile strain of the simian virus (SV40) large T-Antigen linked to an inducible major histocompatibility complex H2-K promoter. EC from the immortomouse have been isolated from lung, colon, kidney, heart and brain (Langley *et al.* 2003). In addition s.END and b.End.5 cells were isolated from hemangiomas generated by a retroviral construct encoding polyoma middle-sized T-Antigen from skin and brain respectively (Bussolino *et al.* 1991).

mUCEC-1 have previously been shown to express CD31, Endoglin, ICAM-1/2 and VCAM-1 and respond to growth factors and cytokines (TNF-α, IL-1β and LPS).

Molecule	IHC	ELISA (4hrs)	ELISA (24hrs)	Microarray
CD31	+	+	+	++
ICAM-2	+	+	+	+
JAM-2	++	++	++	+++
VCAM-1	+	+++	+++	+++
CD34	+	+	++	+
VAP-1	-	+	+	-
Endoglin	+	+	++	+
E-Selectin	-	+	+	++
LYVE-1	-	+	+	-

Table 7. 2: Table summarising expression profile of endothelial markers and adhesion molecules of mUCEC-1 cells.

Expression of phenotypic markers was assessed using several different methods including, IHC, cell-based ELISA and microarray. Expression levels were compared to CD31 positive control in each experiment.

Our phenotypic studies confirmed expression of all of the molecules mentioned and in addition JAM-2, E-Selectin and CD34 by immunohistochemistry, ELISA and gene array (Table 7.2). Interestingly there was limited response to pro-inflammatory insult. The global heatmap data comparison with sEND cells suggested that the mUCEC genes varied less in response to cytokine stimulation on the whole. Relative expression levels of individual genes were corroborated by each technique used and were concurrent with reported data involving leukocyte recruitment to the heart. Endothelial expression of VCAM-1, CD34 and CD31 has previously been demonstrated in inflamed heart valves. ICAM-1 and VCAM-1 have also been implicated in the infiltration of CD8+ cells into cardiac tissue of patients with severe cardiomyopathy (Soderquist *et al.* 1999). An interesting exception is the lack of E-selectin expression in mUCEC-1 by IHC methods *in vitro*, which has been postulated to be relative to the degree of vascular injury *in vivo* (Bussolino *et al.* 1991;Haverslag *et al.* 2008).

One clear difference in expression between cardiac EC *in situ* and our cell line was the unusually high expression of VCAM-1 even in the absence of stimulation. This clearly impacted on the functional responses of mUCEC-1 to inflammatory insult and to high basal levels of adhesion. Levels of adhesion increased in response to short exposure to TNF-α and Il-1β, which carried through into subset experiments. After prolonged exposure to these cytokines in addition to LPS, which induced a significant increase in leukocyte adhesion. However, there was a tendency to see a reduction in lymphocyte adhesion in response to cytokine after prolonged exposure for 24 hours, as demonstrated by Matharu *et al* in the case of selectins (Matharu 2006). Physiologically these EC are derived from the microvasculature of the heart (with some contamination from the myocardium) the high expression of VCAM-1 could be an adaptation to the high levels of shear stress in the physiochemical environment of the heart. The higher the levels of VCAM-1 present on the endothelium may increase the likelihood of interactions with fast flowing leukocytes in the circulation. mUCEC-1 contain a temperature sensitive interferon inducible promoter as part of the immortalisation process. However, the presence of IFN-γ in cultures could have led to the high constitutive expression of VCAM-1. Investigations by the same group that generated the cell line showed that VCAM-1 was induced in response to TNF-α and IL-1β (Singh *et al.* 2005).

It is likely that the high constitutive expression of VCAM-1 on these cells explains our observation that recruitment of lymphocyte subsets was high in comparison to all other cell types. Recruitment of subsets was high in comparison to all other cell types and recruitment was skewed towards CD4+ cells. We also observed that treatment of lymphocytes with pertussis toxin lead to a reduction in adhesion to both TNF-α stimulated and unstimulated endothelium suggesting a role for chemokines in

adhesion to this cell type. In support of this our whole genome microarrays revealed expression of a variety of chemokines including MCP-2/3, TARC, SDF-1 and IP-10 implicated in the recruitment of monocytes, subsets of T-Cells and activated leukocytes. SDF-1 was expressed in cells stimulated with LPS, TNF-α and IL-1β and CXCL16 in response to TNF-α+IFN-γ treatments where adhesion was increased in functional experiments. Interestingly we also noted expression of TARC by our cardiac EC line, which has previously been associated with macrophages present in atherosclerotic plaques (Ritter *et al.* 2005).

7.2.2 Characterisation of s.END cells.

The skin acts as a barrier from the external environment, combating toxins, pathogens and physical insult. As a result the skin contains a wide range of immunocompetent cells. ICAM-1 is particularly important in recruitment of leukocytes to the skin. It is constitutively expressed on skin EC and is upregulated in response to IL-1, TNF-α and IFN-γ (Iwata *et al.* 1996).

Molecule	IHC	ELISA (4hrs)	ELISA (24hrs)	Microarray
CD31	++	++	+++	+++
ICAM-2	+	+	++	+++
JAM-2	+++	+	+	++
VCAM-1	+	+	+	++
CD34	+++	++	++	++
VAP-1	+	+	-	-
Endoglin	+++	+++	+++	+++
E-Selectin	-	+	-	++
LYVE-1	++	+++	++	+

Table 7. 3: Table summarising expression profile of endothelial markers and adhesion molecules of s.END cells.

Expression of phenotypic markers was assessed using several different methods including, IHC analysis, cell-based ELISA and microarray. Expression levels were compared to CD31 positive control in each experiment.

Our data showed that ICAM-2 was also expressed on s.END, as is common on many endothelial types, and increased upon stimulation. We also demonstrated expression of E-Selectin which has been reported on dermal EC *in vivo* (Fuhlbrigge et al. 1997) and is particularly important for immune surveillance mediated by CLA+, skin-homing T cells (Clark *et al.* 2006). In addition s.END cells expressed CD31, VCAM-1, Endoglin, CD34, VAP-1 and LYVE-1. s.END cells have previously been used to investigate endothelial signalling pathways and cytokine/chemokine production (IL-6, KC, MCP-1 and GM-CSF) (Bussolino *et al.* 1992;Bussolino *et al.* 1991) and shown to express CD31, VCAM-1, E and P-Selectin, in agreement with our observations. However detailed gene expression patterns of for s.END have not previously been published. The results of our DNA microarrays suggested that s.END cells had a more characteristic 'endothelial' expression pattern compared to mUCEC. s.END cells are isolated from the microvasculature of the skin and expressed many of the phenotypic markers and adhesion molecules we were interested in, particularly CD31 and Endoglin. Although levels of E-Selectin protein expression were low as detected by ELISA , message was detected by gene array,

which may be more sensitive. However levels of mRNA are not always totally correlated to protein expression. Interestingly a subset of s.END cells was positive for LYVE-1 which we detected in all our assays. LYVE-1 is a marker of lymphatic endothelium and due to the high density of lymphatics in the skin it is more than likely that the original cell isolate was contaminated with some lymphatic EC, which may be persisting in the immortalised culture.

In functional experiments the levels of adhesion to both endothelioma cell lines were much lower than mUCEC-1 cells, which may in part relate to more appropriate expression of adhesion molecules such as VCAM-1. Adhesion molecules were expressed on s.END cells giving them the ability to recruit leukocytes from flow. However they were shown to be more responsive to cytokine treatment with all treatments increasing adhesion above the control at 4 hours. As with our other cell lines adhesion decreased after prolonged exposure but LPS and the combination of TNF-α and IFN-γ maintained levels of adhesion above control. When subset recruitment was examined both CD4+ and CD8+ cells were recruited in response to stimulation and as with all cell lines more CD4+ cells adhered to EC monolayers. Interestingly expression of chemokines by s.END cells was limited, stimulation with LPS induced expression of KC (murine Il-8) and CXCL5 (ENA-78), a neutrophil chemoattractant with angiogenic potential (Persson *et al.* 2003). *In vivo* CCL27 is known to be involved in leukocyte homing to skin. In models of psoriatic skin inflammation MIP1α, MIP1β and RANTES are thought to be important (de Groot *et al.* 2007) however these chemokines were not expressed in s.END cells. Similarly Giustizieri *et al* (Giustizieri *et al.* 2001) showed that in keratinocytes from patients with atopic dermatitis and psoriasis IP-10 and IL-8 were upregulated in the epidermis

of patients with psoriasis in response to TNF-α and IFN-γ but not in the lesions of patients with dermatitis.

Endothelial cells from haemangiomas have been shown to have an altered phenotypic, morphology and function. Zhang *et al* (Zhang *et al.* 2006) showed that cavernous hemangioma endothelial cells (CHECs) derived from the human liver expressed and released more VEGF-A in addition to other factors compared to primary hLSEC. In addition CHECs exhibited more active angiogenesis capacity and formed abnormal capillary-like structures *in vitro*. This increased angiogenic capacity in EC from haemangiomas could impact on the adhesive properties of both s.END and b.End.5 cells relative to stable or differentiated EC types. Thus s.END cells may be of limited use in modelling skin inflammation *in vitro*.

7.2.3 Characterisation of b.End.5 cells.

Recruitment to the brain microvasculature, like the liver sinusoids differs in comparison to most other vascular beds. Brain EC are exposed to high shear stresses and are in close contact with astrocytes. Leukocytes entering cerebral tissues have to overcome the tightly regulated and restrictive blood brain barrier in order to combat detrimental, unwanted inflammation in the CNS. A number of different adhesion molecules are involved in recruitment including ICAM-1, VCAM-1 and CD31 (Engelhardt *et al.* 1995). The importance of ICAM-1/VCAM-1 has been shown in cytokine stimulated primary mouse, rat and human BMEC. b.End.5 cells have been used to model the BBB and confirm the importance of VCAM-1/ICAM-

1/ICAM-2 in the subsequent adhesion and migration of T-Cells into brain parenchyma (Etienne-Manneville *et al.* 1998;Etienne-Manneville *et al.* 2000).

Molecule	IHC	ELISA (4hrs)	ELISA (24hrs)
CD31	+++	+++	+++
ICAM-2	++	++	++
JAM-2	+	+	+
VCAM-1	-	+	+
CD34	+++	+++	+++
VAP-1	-	+	+
Endoglin	++	+	+
E-Selectin	-	+	+
LYVE-1	++	+	++

Table 7. 4: Table summarising expression profile of endothelial markers and adhesion molecules of b.End.5 cells.

Expression of phenotypic markers was assessed using several different methods including, IHC analysis and cell-based ELISA. Expression levels were compared to CD31 positive control in each experiment.

We found b.End.5 expressed appropriate molecules examined in particular CD31, CD34, Endoglin and ICAM-2 concurrent with the previously reported importance and expression of ICAM and CD31 within the brain microenvironment (Table 7.4).

Functional experiments assessing responses of b.End.5 confirmed that lymphocyte adhesion was higher to these cells than that of s.END cells and that 4 hours cytokine stimulation induced highest levels of adhesion compared to 24 hours with LPS and IL-1β inducing adhesion above control treatment. Both CD4+ and CD8+ cells were recruited and no bias was observed and as with basal adhesion data LPS produced higher levels of adhesion compared to other pro-inflammatory treatments that may be due to the privileged isolation of the CNS from the bloodstream and the ratrity and danger of bacterial infections in this site. This is supported by previous experiments

by Yilmaz *et al* (Yilmaz *et al.*) showing that brain endothelial cells can recruit both CD4+ and CD8+ cells. Several chemokines have been found in the brain *in vivo* in response to injury. Using a rat stab wound model of brain injury Berman *et al* (Berman *et al.* 1996) have shown MCP-1 to be present. In addition Ghirnika *et a*l (Ghirnikar *et al.* 1998) showed RANTES and MIP-1β were present in astrocytes of injured brain tissue. Omari *et al* (Omari *et al.* 2004) stimulated primary cultures of human microvascular EC from patients with CNS inflammation and demonstrated MCP-1 expression. They also suggested that T-Cells expressing CD40L could regulate the production of RANTES thus permitting further recruitment of leukocytes across the BBB. It will be interesting to see if the expression of these chemokines and related molecules is seen in the whole genome microarray data for this cell line. In addition, since the integrity of the BBB is essential for its function analysis of expression and regulation of junctional proteins in stimulated b.End.5 could shed more light on this issue.

7.3 Variation in endothelial gene expression

It is widely accepted that EC play an integral role in a number of different biological processes including vascular specialisation and physiology and that EC phenotype varies throughout the vasculature and in different tissues. However understanding of this diversity is limited. Chi *et al* (Chi *et al.* 2003) sought to investigate this diversity and specialisation by analysing the gene expression of 53 different EC types. These included macro and microvascular EC from the aorta, iliac artery (Arterial), HUVEC, saphenous vein (Venular), skin and intestine (microvasculature) but not liver. They discovered not only characteristic differences in expression in arterial EC and the

microvasculature but also distinct tissue specific variation of gene expression in microvascular EC from varying tissue beds. Importantly these differences persisted in *in vitro* culture. Gene expressions in distinct organs were found to form discrete clusters when displayed in hierarchical maps.

521 arterial specific genes were discovered compared to 2521 microvascular genes involved in diverse roles in EC biology including migration and angiogenesis. For example arterial EC were found to express Hey2 a human homologue of the zebrafish gene ‘gridlock’ which is responsible for inducing expression of additional arterial specific genes. Gene expression could also be linked to functionality at different sites since, for example fibronectin and osteonectin involved in ECM biosynthesis were found in arterial EC, which could be related to the thick vascular walls found in large vessels. Venous EC were found to express genes involved in internal symmetry suggesting a coordinated role for vascular development and the generation of a body plan. Microvascular EC expressed many genes associated with basement membrane generation (Collagen, CD36) possibly due to the close interaction with EC and basement membrane in microvascular structures. In addition genes involved in lipid metabolism (ApoD, ApoL) were expressed implicating EC from small vessels in this process.

This distinct and significant variation in marker expression by different EC types is also supported by our microarray analysis on mUCEC-1 (from a high shear environment) and s.END (from a low shear environment) cell lines, where large global differences in gene expression were found even under pro-inflammatory conditions. We found variation in expression of endothelial markers, chemokines and adhesion molecules, which could impact on the functional properties of the EC.

Future work could examine more extensive gene lists to look at comparisons between the genes examined by Chi *et al*.

It is important to culture isolated cells in an environment that most physiologically resembles the *in vivo* situation, which may be difficult to recapitulate *in vitro*. The microenvironment in which cells are cultured has a distinct effect on endothelial function. For example Wick *et al* (Wick *et al.* 2007) carried out transcriptional comparisons of human dermal lymphatic endothelial cells *ex vivo* and *in vitro*. They examined the expression of 159 genes that were differentially expressed compared to vascular EC. In cultured cells 19 of these genes were retained and 27 newly induced. These new genes were involved in cell turnover and cell metabolism and downregulated genes were components of ECM and those involved in signalling pathways associated with CCL21. Thus it is probable that further changes in gene expression would be apparent in our chosen cell lines should we culture them in conditions more representative of their environment *in vivo*.

In pilot studies we found that exposure to shear, did indeed condition EC leading to decreased functional responses to cytokine treatment. Shear stress is an important component of the physiochemical environment *in vivo* impacting upon EC phenotype and subsequent function and varies throughout the vasculature. A number of different shear conditioned genes have been reported (Wasserman *et al.* 2002) including transcriptions factors and cell cycle regulators. The application of fluid shear stress has been shown to induce changes to the actin cytoskeleton elongating EC in the direction of flow (Osborn *et al.* 2006). Endothelium in the brain is exposed to higher levels of shear stress than that of the microvasculature of the liver and high endothelial venules in the lymphatics. Exposure of these EC to differing shear

stresses could induce transient epigenetic modifications leading to altered function and responses to additional external stimuli. In liver injury EC of the sinusoids are exposed to higher shear stresses as a result of portal hypertension leading to capillarisation. For example in primary biliary cirrhosis, hLSEC have been shown to transform into a continuous vascular EC type, leading to loss of fenestrations, presence of tight junctions and deposition of basement membrane, all of which are important for disease progression (Xu *et al.* 2003). The transient loss of shear stress in the brain has been examined in the context of BBB integrity. As a result of post-ischemic cerebral injury shear stress can be affected. Krizanac-Bengez *et al* (Krizanac-Bengez *et al.* 2003) showed in an *in vitro* model of the BBB with rBMEC and astrocytes that the loss of shear stress alone had no effect on the integrity of the BBB due to a protective cascade of mechanisms involving cytokines and nitric oxide. Further studies to examine the response of primary mLSEC or BMEC to alterations in shear stress are warranted.

7.4 Summary and Future Work

We examined the phenotype and function of a number of different EC populations from organs that varied physiochemically and immunologically. We found that tissue specific variations were apparent including LYVE-1/Endoglin expression in the skin, VCAM-1/JAM-2 in the heart, LYVE-1/VAP-1/Endoglin in the Liver and CD31/CD34 in the brain. In addition these differences impacted on the functional responses of tissue-specific EC to recruit different leukocyte subsets from flow and that there was a differential response to pro-inflammatory stimuli LPS, TNF-α and IL-1β. Importantly, this response to cytokine decreased after prolonged exposure and trends in levels of adhesion in each cell type were apparent throughout different functional experiments

(mUCEC<b.END<s.END<mLSEC). Much of this project focussed on the isolation and culture of primary murine endothelial cell populations. Several groups have strived to culture representative homogenous primary cells; the complexity of this is evidenced by the numerous immortalised cell lines have been generated as a replacement for primary isolates. We isolated a population of murine mLSEC using αCD146 magnetic beads after attempting to optimise several other methods. A number of cell lines were used in this project and were found to express tissue relevant adhesion molecules and markers of endothelial cells. Whole genome DNA microarray analysis was performed on mUCEC-1 and s.END cell lines to assess expression of EC markers, adhesion molecules, chemokines and scavenger receptors.

Future work would utilise microarray analysis to examine differences in the remaining cell populations examined (b.End.5 and mLSEC) to further elucidate possible mechanisms of tissue specific recruitment and to corroborate data already obtained. Samples have been prepared in order to perform these experiments and the data is eagerly anticipated. In the context of this thesis, this data would be interesting to further dissect the mechanisms of recruitment, in particular the role of specific chemokines in recruitment to different tissues and whether this impacts upon subsets of leukocytes recruited to these tissues. In the liver particularly it would be interesting to see if unique mechanisms of recruitment and immune modulation seen in the human liver are conserved in murine systems.

The isolation of the murine counterparts to the hLSEC, routinely isolated in our group, is an important future goal for the laboratory, and thus the data and

methodology contained in this thesis will help to drive this forward. We have access to a number of knockout animals where key genes of interest have been deleted and thus cells from these animals can be compared to wild types for dissection of roles of key receptors *in vitro*. The differential response to cytokine could be investigated by using mLSEC from knockout mice to investigate the role of Toll Like Receptors (TLR) in immune tolerance and LPS sensitivity and dissect contribution of individual receptor bearing cells (*i.e.* EV versus KC). TLR9 has previously been shown to be present in mLSEC and play a role in receptor mediated endocytosis (Martin-Armas *et al.* 2006).

Our group is using *in vivo* recruitment model systems where disease mechanisms may be linked to multiple cell types (EC, KC and stellate cells). The flexibility of supporting such systems with reductionist models using single cell populations in coculture *in vitro* will be very powerful. In murine models of liver disease, haemopoetic stem cells have been shown to migrate to injured liver and influence tissue repair via a VCAM-1 dependent process (Kavanagh *et al.* 2009). Chen *et al* (Chen *et al.* 2009) also showed that murine mesenchymal stem cells trafficked from the bone marrow to injured liver and CCR9, CXCR4 and c-Met were essential in directing this process. Given the therapeutic potential of infused stem cell populations in the context of human disease, and the need to specifically target infused cells to specific hepatic compartments, information on recruitment mechanisms gained through *in vitro* assays with mLSEC and mMSC will be invaluable.

We have shown that the phenotype of cultured EC from different tissues varies, specifically the expression of EC specific markers and adhesion molecules and in addition the pro-inflammatory environment can also modulate this expression. We

optimised and phenotypically verified a method for isolation of murine liver sinusoidal endothelial cells to high purity. In addition to phenotypic analysis we examined how these cells recapitulate the functional capacity of EC to recruit mixed populations of leukocytes and lymphocyte subsets from flow. Finally we looked at whole genome microarrays of EC from heart and skin and found large global differences in gene expression, which supported both ours and others, phenotypic data. There were limitations to this research however, for example due to the difficulty of isolating primary cell populations conditionally immortalised EC lines were used on which there is confounding data on their suitability as a substitute for primary cells. As a consequence although we found phenotypic differences between EC populations from different tissues and vascular beds thus far there doesn't appear to be a mechanism available to definitively link the EC specific phenotypes reported here to their function. In addition microarray analysis on the remaining EC populations is outstanding. Confirmation of the chemokine expression on primary mLSEC in response to stimuli would shed more light on the functional capacity of these cells to recruit specific leukocyte subsets. Nevertheless the data we have generated contributes to an ever-growing volume of research investigating the role of EC specific address codes in subset recruitment and disease pathologies where recruitment is dysregulated.

8. APPENDICES

8.1 Solutions for in situ perfusion of murine liver

Perfusion Buffer Concentrate

103.75g NaCl
6.35g KCl
28.7g HEPES
Dissolved in 300ml UHQ Water
Add 74ml 1M NaOH
Make up to final volume of 500ml with UHQ Water
Aliquot into 40ml volumes
Freeze -20°C

1x Perfusion Buffer is: 40ml PBC + 960ml UHQ Water (Filter)

$CaCl_2$

FW=147 476mM
0.7g in 10ml UHQ Water, filter aliquot in 1ml volumes.
Freeze -20°C

Magnesium Chloride: Stock 500mM, working 5-10mM

FW=95.22 0.5M/500mM
0.476g in 10ml UHQ Water
Filter aliquot in 1ml volumes
Freeze at -20°C

10x PBS

25 Oxoid Tablets in 250mls dH_2O

Liberase Blenzyme 3

Reconstitute 7mg vial of lyophilised enzyme with 1ml milli-Q-water
Place on ice for 30 mins (10 mins still, 20 mins shaking)
Stock 1mg/ml aliquot into 0.143ml (4 Wunsch Units) at -20°C

Collagenase Buffer

49.5ml 1x Perfusion Buffer
0.5ml $CaCl_2$ 476mM
2 tubes Liberase Blenzim-3

Preservation Buffer

250ml 1x Perfusion Buffer
2.5g BSA

DNAse: Stock 3500U/ml Working 200-1000Uml

Preservation Buffer

	V	$MgCl_2$	DNAse
	ml	ml	µl
Cells	50	0.7	14.3
Gradient	10	0.14	2.9

Table 8. 1: Constituents of Preservation Buffer

8.2 Gene lists for DNA Microarray Analysis

Gene	Entrez ID
CLDN4	12740
HGF	15234
VEGFB	22340
VEGFC	22341
TLR 4	21898
CD146	84004
CLDN3	12739
TAPA-1	12520
VWF	22371
CLDN5	12741
EGF	13645
GP38	14726
OCLN	18260
VEGFA	22339
CLDN2	12738
CD62P	20344
JAM-3	83964
CD44	12505
PSGL-1	20345
JAM-1	16456
JAM-2	67374
VCAM1	22329
CD62E	20339
PECAM1	18613
LYVE-1	114332

ICAM2	15896
CD34	12490
Endoglin	13805
ICAM1	15894
AOC3	11754
CXCR5	12145
CCR9	12769
CXCR2	12765
CCR3	12771
CXCR6	80901
MIP-1 αR	12768
CCR2	12772
CCR7	12775
CXCR4	12767
CXCR1	227288
CD195	12774
CCR8	12776
CCR4	12773
CCR9	12769
CCR10	12777
CCR6	12458
MPR46	622798
LDLRAP1	100017
LRP6	16974
VLDLR	22359
CD36	12491
LRP1	16971
IGF-1	16000
LRP2	14725
LDLR	16835
DC-SIGN	170786
STAB2	192188
STAB1	192187
CLEC4G	339390
IL-2	16183
IL-6	16193
IFNγ	15978
IL-13	16163
IL-10	16153
IL1-β	16176
IL-1α	16175
IL-5	16191
IL-4	16189
TNFα	21926
IFNα	15964
GM CSF	12981
TNFR6	14102
CSFM	12977
CCL27	20301
TECK	20300
MCP-2	20307
TARC	20295
MIP-1B	238799

MCP-1	20296
MCP-3	20306
MIP-3 A	20297
EOTAXIN	20292
CCL22	20299
MIP-1 A	20302
CCL24	56221
CCL1	20290
RANTES	20304
CCL28	56838
SDF-1	20315
MIP-2 G	55985
CXCL16	66102
IP-10	15945
IP-9	56066
MIG	17329
CXCL5	20311
BCA-1	55985
PF4	56744
MIP-2	20310

Table 8. 2: PubMed Gene Identities for Microarray analysis

REFERENCES

A.M.Muller, C.Cronen, L.I.Kupferwasser, H.Oelert, & K.M.Muller 2000. Expression of endothelial cell adhesion molecules on heart valves: up-regulation in degeneration as well as acute endocarditis. *The Journal of Pathology*, 191, (1) 54-60

Abbitt, K.B., Rainger, G.E., & Nash, G.B. 2000. Effects of fluorescent dyes on selectin and integrin-mediated stages of adhesion and migration of flowing leukocytes. *J.Immunol.Methods*, 239, (1-2) 109-119

Adams, D.H. & Nash, G.B. 2005. Disturbance of leukocyte circulation and adhesion to the endothelium as factors in circulatory pathology. *British Journal of Anaesthesia* 17-31

Adams, D.H. & Shaw, S. 1994. Leucocyte-endothelial interactions and regulation of leucocyte migration. *Lancet*, 343, (8901) 831-836

Adamson, P.,Wilbourn, B., Etienne-Manneville, S., Calder, V., Beraud, E., Milligan, G., Couraud, P.O., & Greenwood, J. 2002. Lymphocyte trafficking through the blood-brain barrier is dependent on endothelial cell heterotrimeric G-protein signaling. *The FASEB Journal*, 16, (10) 1185-1194

Ades, E.W., Candal, F.J., Swerlick, R.A., George, V.G., Summers, S., Bosse, D.C., & Lawley, T.J. 1992. HMEC-1: Establishment of an immortalised human microvascular endothelial cell line. *J.Invest.Dermatol.*, 99, 683-690

Ager, A. 1987. Isolation and culture of high endothelial cells from rat lymph nodes. *J Cell Sci*, 87, (1) 133-144

Ahmed, A.A., Vias, M., Iyer, N.G., Caldas, C., & Brenton, J.D. 2004. Microarray segmentation methods significantly influence data precision. *Nucleic Acids Research*, 32, (5) e50

Aird, W.C. 2003. Endothelial Cell Heterogeneity. *Crit.Care Med.*, 31, S221-S230

Aird, W.C. 2007a. Phenotypic heterogeneity of the endothelium: II. Representative vascular beds. *Circ.Res.*, 100, (2) 174-190

Aird, W.C. 2006. Mechanisms of Endothelial Cell Heterogeneity in Health and Disease. *Circulation Research*, 98, (2) 159-162

Aird, W.C. 2007b. Phenotypic Heterogeneity of the Endothelium: I. Structure, Function, and Mechanisms. *Circulation Research*, 100, (2) 158-173

Alabraba, E.B., Lai, V., Boon, L., Wigmore, S.J., Adams, D.H., & Afford, S.C. 2007. Coculture of human liver macrophages and cholangiocytes leads to CD40-dependent apoptosis and cytokine secretion. *Hepatology*

Alan R.Schenkel, Tina W.Chew, & William A.Muller. Platelet Endothelial Cell Adhesion Molecule Deficiency or Blockade Significantly Reduces Leukocyte Emigration in a Majority of Mouse Strains. Immunology 173, 6403-6408. 2004.

Allport, J.R., Lim, Y.C., Shipley, J.M., Senior, R.M., Shapiro, S.D., Matsuyoshi, N., Vestweber, D., & Luscinskas, F.W. 2002. Neutrophils from MMP-9- or neutrophil

elastase-deficient mice show no defect in transendothelial migration under flow in vitro. *Journal of Leukocyte Biology*, 71, (5) 821-828

Alon, R. & Feigelson, S. 2002. From rolling to arrest on blood vessels: leukocyte tap dancing on endothelial integrin ligands and chemokines at sub-second contacts. *Semin.Immunol.*, 14, (2) 93-104

Anders, H.J., Ninichuk, V., & Schlondorff, D. 2006. Progression of kidney disease: Blocking leukocyte recruitment with chemokine receptor CCR1 antagonists. *Kidney Int*, 69, (1) 29-32

Anderson, A.O. & Shaw, S. 1993. T cell adhesion to endothelium: The FRC conduit system and other anatomic and molecular features which facilitate the adhesion cascade in lymph node. *Semin.Immunol.*, 5, 271-282

Andersson, M., Karlsson, L., Svensson, P.A., Ulfhammer, E., Ekman, M., Jern+Ñs, M., Carlsson, L.M.S., & Jern, S. 2005. Differential Global Gene Expression Response Patterns of Human Endothelium Exposed to Shear Stress and Intraluminal Pressure. *J Vasc Res*, 42, (5) 441-452

Ando, J., Tsuboi, R., Korenaga, Y., Takada, N., Toyama-Sorimachi, N.M.M., & Kamiya, A. 1994. Shear stress inhibits adhesion of cultured mouse endothelial cells to lymphocytes by downregulating VCAM-1 expression. *American Journal of Physiology and Cell Physiology*, 267, C679-C687

Arstila, T.P., Casrouge, A., Baron, V., Even, J., Kanellopoulos, J., & Kourilsky, P. 1999. A direct estimate of the human alphabeta T cell receptor diversity. *Science*, 286, (5441) 958-961

Aspinall, A.I., Curbishley, S.M., Lalor, P.F., & Adams, D.H. 2009. VAP-1 and fractlakine promote CD16+ monocyte recruitment to the human liver. *Hepatology (in press)*

Au, B.t., Teixeira, M.M., Collins, P.D., & Williams, T.J. 2001. Blockade of PAF receptors controls interleukin-8 production by regulating the activation of neutrophil CD11/CD18. *European Journal of Pharmacology*, 425, (1) 65-

Audus KL ., Borchardt RT, Wang W, & Ng L 1996. Brain microvessel endothelial cell culture systems. *Pharm Biotechnol.*, 8, 239-258

Aurrand-Lions, M., Johnson-Leger, C., & Imhof, B.A. 2002a. The last molecular fortress in leukocyte trans-endothelial migration. *Nat Immunol*, 3, (2) 116-118

Aurrand-Lions, M., Johnson-Leger, C., Lamagna, C., Ozaki, H., Kita, T., & Imhof, B.A. 2002b. Junctional adhesion molecules and interendothelial junctions. *Cells Tissues.Organs*, 172, (3) 152-160

B.Phimister 1999. Going global. *Nat Genet.*, 21, (Suppl) 1

B.Soderquist, K-G.Sundqvist, & T.Vikerfors 1999. Adhesion molecules (E-Selectin, ICAM-1 and VCAM-1) in sera from patients with Staphylococcus aureus bacteraemia with or without endocarditis. *Clin Exp Immunol*, 118, (3) 408-411

Bahra, P., Rainger, G.E., Wautier, J.L., Luu, N.T., & Nash, G.B. 1998. Each step during transendothelial migration of flowing neutrophils is regulated by the stimulatory concentration of tumour necrosis factor alpha. *Cell Adhesion Communications*, 6, 491-501

Banerji, S., Ni, J., Wang, S.X., Clasper, S., Su, J., Tammi, R., Jones, M., & Jackson, D.G. 1999. LYVE-1, a new homologue of the CD44 glycoprotein, is a lymph-specific receptor for hyaluronan. *J.Cell Biol.*, 144, (4) 789-801

Barkalow, F.J., Goodman, M.J., & Mayadas, T.N. 1996. Cultured murine cerebral microvascular endothelial cells contain von Willebrand factor-positive Weibel-Palade bodies and support rapid cytokine-induced neutrophil adhesion. *Microcirculation*, 3, (1) 19-28

Barreiro, O., Yanez-Mo, M., Serrador, J.M., Montoya, M.C., Vicente-Manzanares, M., Tejedor, R., Furthmayr, H., & Sanchez-Madrid, F. 2002. Dynamic interaction of VCAM-1 and ICAM-1 with moesin and ezrin in a novel endothelial docking structure for adherent leukocytes. *J Cell Biol JID - 0375356*, 157, (7) 1233-1245

Baumhueter, S., Dybdal, N., Kyle, C., & Lasky, L.A. 1994. Global vascular expression of murine CD34, a sialomucin-like endothelial ligand for L-selectin. *Blood*, 84, (8) 2554-2565

Bedell, M.A., Jenkins, N.A., & Copeland, N.G. 1997a. Mouse models of human disease. Part I: techniques and resources for genetic analysis in mice. *Genes & Development*, 11, (1) 1-10

Bedell, M.A., Largaespada, D.A., Jenkins, N.A., & Copeland, N.G. 1997b. Mouse models of human disease. Part II: recent progress and future directions. *Genes & Development*, 11, (1) 11-43

Berg, E.L., McEvoy, L.M., Berlin, C., Bargatze, R.F., & Butcher, E.C. 1993. L-selectin-mediated lymphocyte rolling on madcam-1. *Nature*, 366, 695-698

Berlin, C., Berg, E.L., Briskin, M.J., Andrew, D.P., Kilshaw, P.J., Holzmann, B., Weissman, I.L., Hamman, A., & Butcher, E.C. 1993. Alpha 4 beta 7 integrin mediates binding to the mucosal vascular addressin MAdCAM-1. *Cell*, 74, 185-195

Berman, J.W., Guida, M.P., Warren, J., Amat, J., & Brosnan, C.F. 1996. Localization of monocyte chemoattractant peptide-1 expression in the central-nervous-system in experimental autoimmune encephalomyelitis and trauma in the rat. *Journal of Immunology* 156, 3017-3023

Bevilacqua, M.P. & Nelson, R.M. 1993. Selectins. *J.Clin.Invest.*, 91, (2) 379-387

Bevilacqua, M.P., Pober, J.S., Mendrick, D.L., Cotran, R.S., & Gimbrone, M.A. 1987. Identification of an inducible endothelial-leukocyte adhesion molecule. *Proc.Natl.Acad.Sci.USA*, 84, 9238-9242

Bostan, M.D., Constantin, M.C.N.A., Hirt, M., Galatiuc, C., Matei, I., Brasoveanu, L.I., & Lordachescu, D. 2002. Study of chemotactic activity developed by neutrophils from rheumatoid arthritis patients. *Roum Arch Microbiol Immunol.*, 61, (4) 243-258

Braet, F., Vanbesien, J., de Zanger, R., & Wisse, E. 2002. Ageing of the liver sieve and pseudocapillarisation. *Lancet*, 360, (9340) 1171-1172

Brooks, A.R., Lelkes, P.I., & Rubanyi, G.M. 2002. Gene expression profiling of human aortic endothelial cells exposed to disturbed flow and steady laminar flow. *Physiology Genomics*, 9, 27-41

Brown, S.B. & Savill, J. 1999. Phagocytosis triggers macrophage release of Fas ligand and induces apoptosis of bystander leukocytes. *Journal of Immunology*, 162, 480-485

Buckley, C.D. & Simmons, D.L. 2000. Sticky moments with sticky molecules. *Immunol Today*, 21, (12) 601-603

Burns, A.R., Smith, C.W., & Walker, D.C. 2003. Unique Structural Features That Influence Neutrophil Emigration Into the Lung. *Physiological Reviews*, 83, (2) 309-336

Bussolino F, Bosia A, Pescarmona G, Ghigo D, & Guglielmetti A 1992. Protein kinase C activation in murine endothelioma cell lines containing middle T antigen stimulated by platelet-activating factor. *J Lipid Mediat.*, 5, (2) 109-113

Bussolino, F., De Rossi, M., Sica, A., Colotta, F., Wang, J.M., Bocchietto, E., Padura, I.M., Bosia, A., DeJana, E., & Mantovani, A. 1991a. Murine endothelioma cell lines transformed by polyoma middle T oncogene as target for and producers of cytokines. *J Immunol*, 147, (7) 2122-2129

Buttrum, S.M., Hatton, R., & Nash, G.B. 1993. Selectin-mediated rolling of neutrophils on immobilized platelets. *Blood*, 82, (4) 1165-1174

C.Lu, S.Pelech, J.Bond, K.Spach, R.Noubade, E.P.Blankenhorn, & c.Teuscher 2008. Pertussis toxin induces angiogenesis in brain microvascular endothelial cells. *J Neurosci Res*, 86, (12) 2624-2640

Calderwood, J.W., Williams, J.M., Morgan, M.D., Nash, G.B., & Savage, C.O. 2005. ANCA induces beta2 integrin and CXC chemokine-dependent neutrophil-endothelial cell interactions that mimic those of highly cytokine-activated endothelium. *Journal of Leukocyte Biology*, 77, (1) 33-43

Campbell, J.D., Butcher, C.E. 2002. Intestinal attraction: CCL25 functions in effector lymphocyte recruitment to small intestine. *J.Clin.Invest*., 110, 1079-1081.

Carrasco, Y.R., 2004 LFA-1/ICAM-1 interactions lower the threshold of B-Cell activation by facilitating B-Cell adhesion and synapse formation. *Immunity*, 20, 589-599.

Carman, C.V., Sage, P.T., Sciuto, T.E., de la Fuente, M.A., Geha, R.S., Ochs, H.D., Dvorak, H.F., Dvorak, A.M., & Springer, T.A. 2007. Transcellular diapedesis is initiated by invasive podosomes. *Immunity.*, 26, (6) 784-797

Carmeliet, P. & Jain, R.K. 2000. Angiogenesis in cancer and other diseases. *Nature*, 407, 249-257

Caro, C.G., Fitzgerald, J.M., & Schroter, R.C. 1969. Arterial wall shear and distribution of early atheroma in man. *Nature*, 223, (1159) 1161

Carreira, C.M., Nasser, S.M., di Tomaso, E., Padera, T.P., Boucher, Y., Tomarev, S.I., & Jain, R.K. 2001. LYVE-1 is not restricted to the lymph vessels: expression in normal liver blood sinusoids and down-regulation in human liver cancer and cirrhosis. *Cancer Res*, 61, (22) 8079-8084

Cha, S.T., Talavera, D., Demir, E., Nath, A.K., & Sierra-Honigmann, M.R. 2005. A method of isolation and culture of microvascular endothelial cells from mouse skin. *Microvascular Research*, 70, (3) 198-204

Cheifetz, S., Bellon, T., Cales, C., Vera, S., Bernabeu, C., Massague, J., & Letarte, M. 1992. Endoglin is a component of the transforming growth factor-beta receptor system in human endothelial cells. *Journal of Biological Chemistry*, 267, (27) 19027-19030

Chen, B.,Li, Y., Zhao, Y., Chen, K., Li, S., Lao, J., Yuan, S., Shyy, J., & Chien, S. 2001. DNA microarray analysis of gene expression in endothelial cells in response to 24-h shear stress. *Physiological Genomics*, 7, (1) 55-63

Chen, Y., Xiang, L.X., Shao, J.Z., Pan, R.L., Wang, Y.X., Dong, X.J., & Zhang, G.R. 2009. Recruitment of endogenous bone marrow mesenchyman stem cells towards injured liver. *J.Cell.Mol.Med.*

Chi, J.T., Chang, H.Y., Haraldsen, G., Jahnsen, F.L., Troyanskaya, O.G., Chang, D.S., Wang, Z., Rockson, S.G., van de Rijn, M., Botstein, D., & Brown, P.O. 2003a. Endothelial cell diversity revealed by global expression profiling. *Proceedings of the National Academy of Sciences of the United States of America*, 100, (19) 10623-10628

Chien, S., Li, S., & Shyy, J.Y.J. 1998. Effects of mechanical forces on signal transduction and gene expression in endothelial cells. *Hypertension*, 31, 162-169

Clark, R.A., Chong, B., Mirchandani, N., Brinster, N.K., Yamanaka, K., Dowgiert, R.K., & Kupper, T.S. 2006. The vast majority of CLA+ T cells are resident in normal skin. *J.Immunol.*, 176, (7) 4431-4439

Conley, B.A., Smith, J.D., Guerrero-Esteo, M., Bernabeu, C., & Vary, C.P.H. 2000. Endoglin, a TGF-beta receptor-associated protein, is expressed by smooth muscle cells in human atherosclerotic plaques. *Atherosclerosis*, 153, (2) 323-335

Cooke, B.M., Usami, S., Perry, I., & Nash, G.B. 1993. A simplified method for culture of endothelial cells and analysis of adhesion of blood cells under conditions of flow. *Microvasc.Res.*, 45, (1) 33-45

Couty, J.P., Rampon, C., Leveque, M., Laran-Chich, M.P., Bourdoulous, S., Greenwood, J., & Couraud, P.O. 2007. PECAM-1 engagement counteracts ICAM-1-induced signaling in brain vascular endothelial cells. *Journal of Neurochemistry*, 103, (2) 793-801

Couvelard, A., Scoazec, J.Y., & Feldmann, G. 1993. Expression of cell-cell and cell-matrix adhesion proteins by sinusoidal endothelial cells in the normal and cirrhotic human liver. *Am.J.Pathol.*, 143, (3) 738-752

Cucullo, L., Couraud, P.O., Weksler, B., Romero, I.A., Hossain, M., Rapp, E., & Janigro, D. 2007. Immortalized human brain endothelial cells and flow-based vascular modeling: a marriage of convenience for rational neurovascular studies. *J Cereb Blood Flow Metab*, 28, (2) 312-328

Cui, S., Hano, H., Sakata, A., Harada, T., Liu, T., Takai, S., & Ushigome, S. 1996. Enhanced CD34 expression of sinusoid-like vascular endothelial cells in hepatocellular carcinoma. *Pathol.Int.*, 46, (10) 751-756

Cunningham, K.S. & Gotlieb, A.I. 2005. The role of shear stress in the pathogenesis of atherosclerosis. *Laboratory Investigations*, 85, 9-23

Curbishley, S.M., Eksteen, B., Gladue, R.P., Lalor, P., & Adams, D.H. 2005. CXCR3 Activation Promotes Lymphocyte Transendothelial Migration across Human Hepatic Endothelium under Fluid Flow. *Am J Pathol.*, 167, (3) 887-

D.W.Melton 1994. Gene targeting in the mouse. *Bioessays*, 16, 633-638

D.W.Threadgill, A.A.Dlugosz, L.A.Hansen, T.Tennenbaum, U.Lichti, & D.Yee 1995. Targeted disruption of mouse EGF receptor: Effect of genetic background on mutant phenotype. *Science*, 269, (230) 234

D.Zheng, C.Constantindou, J.L Hobman, & S.D.Minchin 2007, "In vitro analysis of gene expression," *In Microarray Technology Through Applications*, F.Falciani, ed., Oxford: Taylor and Francis, pp. 108-123.

Daneker, G.W., Lund, S.A., Caughman, S.W., Swerlick, R.A., Fischer, A.H., Staley, C.A., & Ades, E.W. 1998. Culture and characterization of sinusoidal endothelial cells isolated from human liver. *In Vitro Cell Dev.Biol.Anim*, 34, (5) 370-377

David G.Jackson, Remko Prevo, Steven Clasper, & Suneale Banjeri. LYVE-1, the lymphatic system and tumour lymphangiogenesis. Trends in Immunology 22[6], 317-321. 2001.

de Groot M, Ortonne JP, Lambert JR, Naeyaert JM, Picavet DI, Arreaza MG, Simon JS, Kraan M, Bos JD, de Rie MA, & Teunissen MB 2007. Expression of the chemokine receptor CCR5 in psoriasis and results of a randomized placebo controlled trial with a CCR5 inhibitor. *Arch.Dermatol.Res.*, 299, (7) 305-313

Dean PJ Kavanagh, , L.E.D., , H.A.C., Patricia F Lalor, Jon Frampton, , D.H.A., & Neena Kalia 2009. Haematopoietic stem cell recruitment to injured murine liver sinusoids depends on 41 integrin / VCAM-1 interactions. *Gut*

DeBault LE, Kahn LE, Frommes SP, & Cancilla PA 1979. Cerebral microvessels and derived cells in tissue culture: isolation and preliminary characterization. *In Vitro*, 15, (7) 473-487

Dehouck MP, M.S.D.P.F.J.C.R. 1990. An easier, reproducible, and mass-production method to study the blood-brain barrier in vitro. *J Neurochem.*, 54, (5) 1798-1801

Dejana, E. 2004. Endothelial cell-cell junctions: happy together. *Nat Rev Mol Cell Biol*, 5, (4) 261-270

DeLeve, L.D., Wang, X., Hu, L., McCuskey, M.K., & Mccuskey, R.S. 2004. Rat liver sinusoidal endothelial cell phenotype is maintained by paracrine and autocrine regulation. *Am J Physiol Gastrointest Liver Physiol*

Delisser, H.M., Newman, P.J., & Albelda, S.M. 1993. Platelet endothelial cell adhesion molecule (CD31). *Curr.Top.Microbiol.Immunol.*, 184, 37-45

Delves, P.J. & Roitt, I.M. 2000. The immune system. First of two parts. *N.Engl.J.Med.*, 343, (1) 37-49

DeRisi, J.L., Iyer, V.R., & Brown, P.O. 1997. Exploring the Metabolic and Genetic Control of Gene Expression on a Genomic Scale. *Science*, 278, (5338) 680-686

Do, H., Healey, J.F., Waller, E.K., & Lollar, P. 1999. Expression of factor VIII by murine liver sinusoidal endothelial cells. *J.Biol.Chem.*, 274, (28) 19587-19592

Duff, S.E., Li, C., Garland, J.M., & Kumar, S. 2003. CD105 is important for angiogenesis: evidence and potential applications. *FASEB J*, 17, 984-992

Eghtesad, M., Jackson, H.E. & Cunningham, A.C. 2001. Primary human alveolar epithelial cells can elicit the transmigration of CD14+ monocytes and CD3+ lymphocytes. *Immunology*., 102, 157-164.

E.S.Wittchen 2009. Endothelial signaling in paracellular and transcellular leukocyte migration. *Front Biosci*, 14, 2522-2545

Elvevold, K., Smedsrod, B., & Martinez, I. 2008. The liver sinusoidal endothelial cell: a cell type of controversial and confusing identity. *AJP - Gastrointestinal and Liver Physiology*, 294, (2) G391-G400

Engelhardt, B., Conley, F.K., Kilshaw, P.J., & Butcher, E.C. 1995. Lymphocytes infiltrating the CNS during inflammation display a distinctive phenotype and bind to VCAM-1 but not to MAdCAM-1. *International Immunology*, 7, (3) 481-491

Eriksson, E.E., Xie, X., Werr, J., Thoren, P., & Lindbom, L. 2001. Importance of Primary Capture and L-Selectin-Dependent Secondary Capture in Leukocyte Accumulation in Inflammation and Atherosclerosis in Vivo. *The Journal of Experimental Medicine*, 194, (2) 205-218

Etienne, S., Adamson, P., Greenwood, J., Strosberg, A.D., Cazaubon, S., & Couraud, P.O. 1998. ICAM-1 signaling pathways associated with Rho activation in microvascular brain endothelial cells. *J.Immunol.*, 161, (10) 5755-5761

Etienne-Manneville, S., Manneville, J.B., Adamson, P., Wilbourn, B., Greenwood, J., & Couraud, P.O. 2000. ICAM-1-coupled cytoskeletal rearrangements and transendothelial lymphocyte migration involve intracellular calcium signaling in brain endothelial cell lines. *The Journal of Immunology*, 165, (6) 3375-3383

Fausto N 1991. Growth factors in liver development, regeneration and carcinogenesis. *Prog Growth Factor Res*, 3, (3) 219-234

Feng, D., Nagy, J.A., Pyne, K., Dvorak, H.F., & Dvorak, A.M. 1998. Neutrophils emigrate from venules by a transendothelial cell pathway in response to FMLP. *The Journal of Experimental Medicine*, 187, (6) 903-915

Feuerhake, F., F++chsl, G., Bals, R., & Welsch, U. 1998. Expression of inducible cell adhesion molecules in the normal human lung: immunohistochemical study of their distribution in pulmonary blood vessels. *Histochemistry and Cell Biology*, 110, (4) 387-394

Fisher, G.H., Rosenberg, F.J., Straus, S.E., Dale, J.K., Middelton, L.A., Lin, A.Y., Strober, W., Lenardo, M.J., & Puck, J.M. 1995. Dominant interfering fas gene mutations impair apoptosis in a human autoimmune lymphoproliferative syndrome. *Cell*, 81, (6) 935-946

Fonsatti, E. & Maio, M. 2004. Highlights on endoglin (CD105): from basic findings towards clinical applications in human cancer. *J Transl Med*, 2, 18

Forbes RD, Guttmann RD, Gomersall M, & Hibberd J 1983. Leukocyte subsets in first-set rat cardiac allograft rejection. A serial immunohistologic study using monoclonal antibodies. *Transplantation*, 36, (6) 681-686

Frachon, S., Gouysse, G., Dumortier, J., Couvelard, A., Nejjari, M., Mion, F., Berger, F., Paliard, P., Boillot, O., & Scoazec, J.Y. 2001. Endothelial cell marker expression in dysplastic lesions of the liver: an immunohistochemical study. *J.Hepatol.*, 34, (6) 850-857

Frankel, W.N., Taylor, B.A., Noebels, J.L., & Lutz, C.M. 1994. Genetic Epilepsy Model Derived From Common Inbred Mouse Strains. *Genetics*, 138, (2) 481-489

Frankel, W.N. 1995. Taking stock of complex trait genetics in mice. *Trends in Genetics*, 11, (12) 471-477

Frommhold, D., Ludwig, A., Bixel, M.G., Zarbock, A., Babushkina, I., Weissinger, M., Cauwenberghs, S., Ellies, L.G., Marth, J.D., Beck-Sickinger, A.G., Sixt, M., Lange-Sperandio, B., Zernecke, A., Brandt, E., Weber, C., Vestweber, D., Ley, K., & Sperandio, M. 2008. Sialyltransferase ST3Gal-IV controls CXCR2-mediated firm leukocyte arrest during inflammation. *J.Exp.Med.*, 205, (6) 1435-1446

Fuhlbrigge, R.C., Kieffer, J.D., Armerding, D., & Kupper, T.S. 1997. Cutaneous lymphocyte antigen is a specialized form of PSGL-1 expressed on skin-homing T cells. *Nature*, 389, (6654) 978-981

Garlanda, C., & Dejana, C. 1997. Heterogeneity of Endothelial Cells. *Art. Throm.Vasc.Bio*., 17, 1193-1202.

Garrood, T., Lee, L., & Pitzalis, C. 2006. Molecular mechanisms of cell recruitment to inflammation sites: general and tissue specific pathways. *Rheumatology*, 45, 250-260

G.G.Singer, A.C Carrera, A.Marshak-Rothstein, C.Martinez, & A.K.Abbas 1994. Apoptosis, Fas and systemic autoimmunity: The MRL-lpr/lpr model. *Curr.Opin.Immunol.*, 6, 913-920

Gerlach, J., ., Zeilinger, K., Spatkowski, G., Hentschel, F., Schnoy, N., Kolbeck, S., Schindler, R.K., & Neuhaus, P. 2001. Large-Scale Isolation of Sinusoidal Endothelial Cells from Pig and Human Liver. *Journal of Surgical Research*, 100, (1) 39-45

Ghigo, D., Arese, M., Todde, R., Vecchi, A., Silvagno, F., Costamagna, C., Dong, Q.G., Alessio, M., Heller, R., & Soldi, R. 1995. Middle T antigen-transformed

endothelial cells exhibit an increased activity of nitric oxide synthase. *The Journal of Experimental Medicine*, 181, (1) 9-19

Ghirnikar, R.S., Lee, Y.L., He, T.E., & Eng, L.F. 1998. Chemokine expression in rat stab wound brain injury. *Journal of Neuroscience Research*, 46, (6) 727-733

Girard, J.P. & Springer, T.A. 1995. High endothelial venules (HEVs): specialized endothelium for lymphocyte migration. *Immunol.Today*, 16, (9) 449-457 available from: PM:7546210

Giustizieri, M.L., Mascia, F., Frezzolini, A., De Pita, O., Chinni, L.M., Giannetti, A., Girolomoni, G., & Pastore, S. 2001. Keratinocytes from patients with atopic dermatitis and psoriasis show a distinct chemokine production profile in response to T cell-derived cytokines. *Journal of Allergy and Clinical Immunology*, 107, (5) 871-877

Golden-Mason, L., Douek, D.C., Koup, R.A., Kelly, J., Hegarty, J.E., & O'Farrelly, C. 2004. Adult Human Liver Contains CD8pos T Cells with Naive Phenotype, but Is Not a Site for Conventional {alpha}{beta} T Cell Development. *The Journal of Immunology*, 172, (10) 5980-5985

Goldsmith, H.L. & Spain, S. 1984. Margination of leukocytes in blood flow through small tubes. *Microvascular Research*, 27, (2) 204-222

Grant, A.J., Goddard, S., Ahmed-Choudhury, J., Reynolds, G., Jackson, D.G., Briskin, M., Wu, L., Hubscher, S.G., & Adams, D.H. 2002. Hepatic expression of secondary lymphoid chemokine (CCL21) promotes the development of portal-associated lymphoid tissue in chronic inflammatory liver disease. *Am.J.Pathol.*, 160, (4) 1445-1455

Greenwood, J., Etienne-Manneville, S., Adamson, P., & Couraud, P.O. 2002. Lymphocyte migration into the central nervous system: Implication of ICAM-1 signalling at the blood-brain barrier. *Vascular Pharmacology*, 38, (6) 315-322

Gustav Steinhoff, Matthias Behrend, Bettina Schrader, Adrain M.Duijvestijn, & Kurt Wonigeit. Expression Patterns of Leukocyte Adhesion Ligand Molecules on Human Liver Endothelia. American Journal of Pathology 142, 481-488. 1993.

Hadley, T.J. & Peiper, S.C. 1997. From Malaria to Chemokine Receptor: The Emerging Physiologic Role of the Duffy Blood Group Antigen. *Blood*, 89, (9) 3077-3091 available from: http://bloodjournal.hematologylibrary.org

Hallman, R., Mayer, D.N., Berg, E.L., Broermann, R., & Butcher, E.C. 1995. Novel mouse endothelial cell surface marker is suppressed during differentiation of the blood brain barrier. *Dev.Dyn.*, 202, (4) 325-332

Hansen, B., Longati, P., Elvevold, K., Nedredal, G.I., Schledzewski, K., Olsen, R., Falkowski, M., Kzhyshkowska, J., Carlsson, F., Johansson, S., Smedsrod, B., Goerdt, S., Johansson, S., & McCourt, P. 2005. Stabilin-1 and stabilin-2 are both directed into the early endocytic pathway in hepatic sinusoidal endothelium via interactions with clathrin/AP-2, independent of ligand binding. *Exp.Cell Res.*, 303, (1) 160-173

Hickey, M.J., Granger, D.N., & Kubes, P. 1999. Molecular mechanisms underlying IL-4-induced leukocyte recruitment in vivo: a critical role for the alpha 4 integrin. *The Journal of Immunology*, 163, (6) 3441-3448

Hillis, G.S. & Flapan, A.D. 1998. Cell adhesion molecules in cardiovascular disease: a clinical perspective. *Heart*, 79, (5) 429-431

Ho, M., Yang, E., Matcuk, G., Deng, D., Sampas, N., Tsalenko, A., Tabibiazar, R., Zhang, Y., Chen, M., Talbi, S., Ho, Y.D., Wang, J., Tsao, P.S., Ben Dor, A., Yakhini, Z., Bruhn, L., & Quertermous, T. 2003. Identification of endothelial cell genes by combined database mining and microarray analysis. *Physiological Genomics*, 13, (3) 249-262

Homburg, C.H.E. & Roos, D. 1996. Apoptosis of neutrophils. *Current Opinions in Haematology* 94-99

Illi, B., Scopece, A., Nanni, S., Farsetti, A., Morgante, L., Biglioli, P., Capogrossi, M.C., & Gaetano, C. 2005. Epigenetic Histone Modification and Cardiovascular Lineage Programming in Mouse Embryonic Stem Cells Exposed to Laminar Shear Stress. *Circulation Research*, 96, (5) 501-508

Iwata, T., Kamei, Y., Esaki, S., Takada, T., Torii, S., Yamashita, A., Tomida, S., Tamatani, T., Miyasaka, M., & Yoshikai, Y. 1996. Immunosuppression by anti-ICAM-1 and anti-LFA-1 monoclonal antibodies of free and vascularized skin allograft rejection. *Immunobiology*, 195, (2) 160-171

J.L Hobman, A.jones, & C.Constantindou 2007, "Introduction to microarray technologies.," *In Microarray technology through applications.*, F.Falciani, ed., Oxford: Taylor and Francis, pp. 1-51.

Jaakkola, K., Kaunismaki, K., Tohka, S., Yegutkin, G., Vanttinen, E., Havia, T., Pelliniemi, L.J., Virolainen, M., Jalkanen, S., & Salmi, M. 1999. Human vascular adhesion protein-1 in smooth muscle cells. *American Journal of Pathology*, 155, (6) 1953-1965

Jackson, D.G. 2003. The lymphatics revisited: new perspectives from the hyaluronan receptor LYVE-1. *Trends Cardiovasc.Med.*, 13, (1) 1-7

Jaffe, E.A., Nachman, R.L., Becker, C.G., & Minick, C.R. 1973. Culture of human endothelial cells derived from umbilical veins. identification by morphologic and immunologic criteria. *Journal of Clinical Investigation*, 52, (11) 2745-2756

Jalali, S., Li, M., Sotoudeh, S., Yuan, S., Li, S., Chien, S., & Shyy, J.Y.J. 1998. Shear stress activates p60src-ras-mapk signalling pathways in vascular endothelial cells. *Arterioscler.Thromb.Vasc.Bio.*, 18, 227-234

Jirillo, E., Caccavo, D., Magrone, T., Piccigallo, E., Amati, L., Lembo, A., Kalis, C., & Gumenscheimer, M. 2002. Review: The role of the liver in the response to LPS: experimental and clinical findings. *Journal of Endotoxin Research*, 8, (5) 319-327

John Wong, Brent Johnston, Samuel S.Lee, Daniel C.Bullard, C.Wayne Smith, Arthur L.Beaudet, & Paul Kubes. A minimal role for selectins in the recruitment of leukocytes into the inflamed liver microvasculature. Journal of Clinical Investigation 99[11], 2782-2790. 1997.

Johnson-Leger, C., Aurrand-Lions, M., & Imhof, B.A. 2000. The parting of the endothelium: miracle, or simply a junctional affair? *J Cell Sci*, 113 (Pt 6), 921-933

Johnson-Leger, C. & Imhof, B.A. 2003. Forging the endothelium during inflammation: pushing at a half-open door? *Cell Tissue Res.*, 314, (1) 93-105

Johnson-Leger, C.A., urrand-Lions, M., Beltraminelli, N., Fasel, N., & Imhof, B.A. 2002. Junctional adhesion molecule-2 (JAM-2) promotes lymphocyte transendothelial migration. *Blood*, 100, (7) 2479-2486

Karrar, A., Broome, U., Uzunel, M., Qureshi, A.R., & Sumitran-Holgersson, S. 2007. Human liver sinusoidal endothelial cells induce apoptosis in activated T cells: a role in tolerance induction. *Gut*, 56, (2) 243-252

Katz, S.C., Pillarisetty, V.G., Bleier, J.I., Shah, A.B., & DeMatteo, R.P. 2004. Liver sinusoidal endothelial cells are insufficient to activate T cells. *Journal of Immunology*, 173, 230-235

Kinard, F., Javorski, K., Sergent-Engelen, T., & Goldstein, D. 2001. Smooth muscle cells influence monocytes responses to LDL as well as their adhesion and transmigration in a coculture model of the arterial wall. *J.Vasc.Res*., 38, 479-491.

Kirton, C.M., Laukkanen, M.L., Nieminen, A., Merinen, M., Stolen, C.M., Armour, K., Smith, D.J., Salmi, M., Jalkanen, S., & Clark, M.R. 2005. Function-blocking antibodies to human vascular adhesion protein-1: a potential anti-inflammatory therapy. *Eur.J.Immunol.*, 35, (11) 3119-3130

Kitching, A. R., Kuligowski, M. P., & Hickey, M. J. 2009, "In Vivo Imaging of Leukocyte Recruitment to Glomeruli in Mice Using Intravital Microscopy," pp. 1-9.

Klintman, D., Schramm, R., Menger, M.D., & Thorlacius, H. 2002. Leukocyte recruitment in hepatic injury: selectin-mediated leukocyte rolling is a prerequisite for CD18-dependent firm adhesion. *J Hepatol JID - 8503886*, 36, (1) 53-59

Klotz, L., Diehl, L., Dani, I., Neumann, H., von, O.N., Dolf, A., Endl, E., Klockgether, T., Engelhardt, B., & Knolle, P. 2007. Brain endothelial PPARgamma controls inflammation-induced CD4+ T cell adhesion and transmigration in vitro. *J.Neuroimmunol.*, 190, (1-2) 34-43

Knolle, P.A. & Gerken, G. 2000. Local control of the immune response in the liver. *Immunol.Rev.*, 174, 21-34

Knolle, P.A. & Limmer, A. 2001. Neighborhood politics: the immunoregulatory function of organ-resident liver endothelial cells. *Trends Immunol.*, 22, (8) 432-437

Knolle, P.A., Loser, E., Protzer, U., Duchmann, R., Schmitt, E., zum Buschenfelde, K.H., Rose-John, S., & Gerken, G. 1997. Regulation of endotoxin-induced IL-6 production in liver sinusoidal endothelial cells and Kupffer cells by IL-10. *Clin.Exp.Immunol.*, 107, (3) 555-561

Knolle, P.A., Schmitt, E., Jin, S., Germann, T., Duchmann, R., Hegenbarth, S., Gerken, G., & Lohse, A.W. 1999. Induction of cytokine production in naive CD4(+) T

cells by antigen- presenting murine liver sinusoidal endothelial cells but failure to induce differentiation toward Th1 cells. *Gastroenterology*, 116, (6) 1428-1440

Kobayashi, M., Inoue, K., Warabi, E., Minami, T., & Kodama, T. 2005. A Simple Method of Isolating Mouse Aortic Endothelial Cells. *Journal of Atherosclerosis and Thrombosis*, 12, (3) 138-142

Kohda D, Morton CJ, Parkar AA, Hatanaka H, Inagaki FM, Campbell ID, & Day AJ 1996. Solution structure of the link module: a hyaluronan-binding domain involved in extracellular matrix stability and cell migration. *Cell*, 86, (5) 767-775

Krause, P., Markus, P.M., Schwartz, P., Unthan-Fechner, K., Pestel, S., Fandrey, J., & Probst, I. 2000. Hepatocyte-supported serum-free culture of rat liver sinusoidal endothelial cells. *Journal of Hepatology*, 32, (5) 718-726

Krizanac-Bengez, L., Kapural, M., Parkinson, F., Cucullo, L., Hossain, M., Mayberg, M.R., & Janigro, D. 2003. Effects of transient loss of shear stress on blood-brain barrier endothelium: role of nitric oxide and IL-6. *Brain Research*, 977, (2) 239-246

Kunkel, E.J. & Butcher, E.C. 2002. Chemokines and the tissue-specific migration of lymphocytes. *Immunity.*, 16, (1) 1-4

Kupper, T.S. 1990. Immune and inflammatory processes in cutaneous tissues. Mechanisms and speculations. *The Journal of Clinical Investigation*, 86, (6) 1783-1789

Kurkijarvi, R., Jalkanen, S., Isoniemi, H., & Salmi, M. 2001. Vascular adhesion protein-1 (VAP-1) mediates lymphocyte-endothelial interactions in chronic kidney rejection. *European Journal of Immunology*, 31, (10) 2876-2884

Lalor, P.F. & Adams, D.H. 2002. The Liver : a model of organ-specific lymphocyte recruitment. *Expert Reviews in Molecular Medicine* 1-16

Lalor, P.F. & Adams, D.H. 1999. Adhesion of lymphocytes to hepatic endothelium. *Mol.Pathol.*, 52, (4) 214-219 available from: PM:10694942

Lalor, P.F., Edwards, S., McNab, G., Salmi, M., Jalkanen, S., & Adams, D.H. 2002. Vascular adhesion protein-1 mediates adhesion and transmigration of lymphocytes on human hepatic endothelial cells. *J Immunol*, 169, (2) 983-92

Lalor, P.F., Lai, W.K., Curbishley, S.M., Shetty, S., & Adams, D.H. 2006. Human hepatic sinusoidal endothelial cells can be distinguished by expression of phenotypic markers related to their specialised functions in vivo. *World J.Gastroenterol.*, 12, (34) 5429-5439

Lalor, P.F., Shields, P., Grant, A., & Adams, D.H. 2002c. Recruitment of lymphocytes to the human liver. *Immunol.Cell Biol.*, 80, (1) 52-64

Lampugnani, M.G. & DeJana, E. 1997. Interendothelial junctions: structure, signalling and functional roles. *Curr.Opin.Cell Biol.*, 9, (5) 674-682

Langley, R.R., Ramirez, K.M., Tsan, R.Z., Van Arsdall, M., Nilsson, M.B., & Fidler, I.J. 2003. Tissue-specific Microvascular Endothelial Cell Lines from H-2Kb-tsA58

Mice for Studies of Angiogenesis and Metastasis. *Cancer Research*, 63, (11) 2971-2976

Laurie D.DeLeve, Xiangdong Wang, Margaret K.McCuskey, & Robert S.McCuskey 2006. Rat liver endothelial cells isolated by anti-CD31 imunomagnetic seperation lack fenestrae and sieve plates. *American Journal of Physiology-Gastrointestinal and Liver Phsyiology*, 291, G1187-G1189

Lawrence, M.B., Bainton, D.F., & Springer, T.A. 1994. Neutrophil tethering to and rolling on E-selectin are separable by requirement for L-selectin. *Immunity.*, 1, (2) 137-145

Lawrence, M.B. & Springer, T.A. 1991. Leukocytes roll on a selectin at physiologic flow rates: Distinction from and prerequisite for adhesion through integrins. *Cell*, 65, 859-873

Lawson, J.A., Burns, R.A., Farhood, A., Lyn Bajt, M., Collins, R.G., Smith, C.W., & Jaeschke, H. 2000. Pathophysiologic importance of E- and L-selectin for neutrophil-induced liver injury during endotoxemia in mice. *Hepatology*, 32, (5) 990-998

Lee, S.J. & Benveniste, E.N. 1999. Adhesion molecule expression and regulation on cells of the central nervous system. *Journal of Neuroimmunology*, 98, (2) 77-88

Lee, W.Y. & Kubes, P. 2008. Leukocyte adhesion in the liver: distinct adhesion paradigm from other organs. *J.Hepatol.*, 48, (3) 504-512

Lehmann, J.C.U., Jablonski-Westrich, D., Haubold, U., Gutierrez-Ramos, J.C., Springer, T., & Hamann, A. 2003. Overlapping and Selective Roles of Endothelial Intercellular Adhesion Molecule-1 (ICAM-1) and ICAM-2 in Lymphocyte Trafficking. *The Journal of Immunology*, 171, (5) 2588-2593

Lelkes, P.I. 1999. *Mechanical Forces and the Endothelium* Amsterdam, Harwood Academic Press.

Ley, K., Laudanna, C., Cybulsky, M.I., & Nourshargh, S. 2007. Getting to the site of inflammation: the leukocyte adhesion cascade updated. *Nat.Rev.Immunol.*, 7, (9) 678-689

Li, Y.S., Shyy, J.Y.J., Lee, J., Su, B., Karin, M., & Chien, S. 1996. The Ras-JNK pathwayis involved in shear-induced gene expression. *Molecular and Cellular Biology*, 16, 5947-5954

Libby, P. & Theroux, P. 2005. Pathophysiology of coronary artery disease. *Circulation*, 111, 3481-3488

Lidington, E.A., McCormack, A.M., Yacoub, M.H., & Rose, M.L. 1998. The effects of monocytes on the transendothelial migration of T lymphocytes. *Immunology*, 94, (2) 221-227

Lidington, E.A., Rao, R.M., Marelli-Berg, F.M., Jat, P.S., Haskard, D.O., & Mason, J.C. 2002. Conditional immortalization of growth factor-responsive cardiac endothelial cells from H-2Kb-tsA58 mice. *Am J Physiol Cell Physiol*, 282, (1) C67-C74

Lim, Y.C., Garcia-Cardena, G., Allport, J.R., Zervoglos, M., Connolly, A.J., Gimbrone, M.A., Jr., & Luscinskas, F.W. 2003. Heterogeneity of endothelial cells from different organ sites in T-cell subset recruitment. *Am.J.Pathol.*, 162, (5) 1591-1601

Limmer, A. & Knolle, P.A. Liver sinusoidal endothelial cells: a new type of organ-resident antigen-presenting cell. *Arch.Immunol.Ther.Exp.(Warsz.) 2001.;49.Suppl.1.:S7.-11.*, 49 Suppl 1:S7-11., S7-11

Liu L & Kubes P. 2003. Molecular mechanisms of leukocyte recruitment: organ-specific mechanisms of action. *Thromb Haemost.*, 89, (2) 213-220

Liu, X., Zhu, P., & Freedman, B.D. 2006. Multiple eicosanoid-activated nonselective cation channels regulate B-lymphocyte adhesion to integrin ligands. *AJP - Cell Physiology*, 290, (3) C873-C882

Liu, Y., Shaw, S.K., Ma, S., Yang, L., Luscinskas, F.W., & Parkos, C.A. 2004. Regulation of Leukocyte Transmigration: Cell Surface Interactions and Signaling Events. *The Journal of Immunology*, 172, (1) 7-

Loos, A., Glanemann, C., Willis, L.B., O'Brien, X.M., Lessard, P.A., Gerstmeir, R., Guillouet, S., & Sinskey, A.J. 2001. Development and Validation of Corynebacterium DNA Microarrays. *Applied and Environmental Microbiology*, 67, (5) 2310-2318

Luscinskas, F.W., Ma, S., Nusrat, A., Parkos, C.A., & Shaw, S.K. 2002a. Leukocyte transendothelial migration: a junctional affair. *Semin Immunol*, 14, (2) 105-113

Luscinskas, F.W., Ma, S., Nusrat, A., Parkos, C.A., & Shaw, S.K. 2002b. The role of endothelial cell lateral junctions during leukocyte trafficking. *Immunol Rev JID - 7702118*, 186, 57-67

Luster, A.D., Alon, R., & von Andrian, U.H. 2005. Immune cell migration in inflammation: present and future therapeutic targets. *Nat.Immunol.*, 6, (12) 1182-1190

M.Schena, D.Shalon, R.W.Davis, & P.O.Brown 1995. Quantitative monitoring of gene expression patterns with a complementary DNA microarray. *Science*, 270, (5235) 467-470

Mackay, C.R. 1993. Immunological memory. *Advances In Immunology*, 53, 217-265

Madeja, A., Reich, A., Orda, A., & Szepietowski, C.J. 2007. Vascular adhesion protein-1 (VAP-1) is overexpressed in psoriatic patients. *Journal of teh European Academy of Dermatology and Venereology*, 21, (1) 72-78

Magid R., Martinson D., Hwang J., Jo H., & Galis Z.S. 2003. Optimization of isolation and functional characterization of primary murine aortic endothelial cells. *Endothelium*, 10, (2) 103-109

Mantovani, A., Bussolino, F., & Dejana, E. 1992. Cytokine regulation of endothelial cell function. *FASEB*, 6, 2591-2599

Marchesi VT & Gowans JL. The migration of lymphocytes through the endothelium of venules in lymph nodes. Proc.R.Soc.Lond. 159, 283-290. 1964.
Ref Type: Generic

Marelli-Berg, F.M., Peek, E., Lidington, E.A., Stauss, H.J., & Lechler, R.I. 2000. Isolation of endothelial cells from murine tissue. *Journal of Immunological Methods*, 244, (1-2) 205-215

Martin-Armas, M., Simon-Santamaria, J., Pettersen, I., Moens, U., Smedsrod, B., & Sveinbjornsson, B. 2006. Toll-like receptor 9 (TLR9) is present in murine liver sinusoidal endothelial cells (LSECs) and mediates the effect of CpG-oligonucleotides. *J.Hepatol.*, 44, (5) 939-946

Martin-Padura, I., Lostaglio, S., Schneemann, M., Williams, L., Romano, M., Fruscella, P., Panzeri, C., Stoppacciaro, A., Ruco, L., Villa, A., Simmons, D., & Dejana, E. 1998. Junctional Adhesion Molecule, a Novel Member of the Immunoglobulin Superfamily That Distributes at Intercellular Junctions and Modulates Monocyte Transmigration. *The Journal of Cell Biology*, 142, (1) 117-127

Martinez, I., Nedredal, G., Oie, C., Warren, A., Johansen, O., Le Couteur, D., & Smedsrod, B. 2008. The influence of oxygen tension on the structure and function of isolated liver sinusoidal endothelial cells. *Comparative Hepatology*, 7, (1) 4

Matharu, N.M., Rainger, G.E., Vohra, R., & Nash, G.B. 2006. Effects of disturbed flow on endothelial cell function: Pathogenic implications of modified leukocyte recruitment. *Biorheology*, 43, 31-44

Matsubara, S., Bourdeau, A., terBrugge, K.G., Wallace, C., & Letarte, M. 2000. Analysis of Endoglin Expression in Normal Brain Tissue and in Cerebral Arteriovenous Malformations. *Stroke*, 31, (11) 2653-2660

Matsumoto, K., Sano, H., Nagai, R., Suzuki, H., Kodama, T., Yoshida, M., Ueda, S., Smedsrod, B., & Horiuchi, S. Endocytic uptake of advanced glycation end products by mouse liver sinusoidal endothelial cells is mediated by a scavenger receptor distinct from the macrophage scavenger receptor class A. *Biochem.J.2000.Nov.15.;352.Pt.1.:233.-40.*, 352 Pt 1:233-40., 233-240

Matsumoto, T. & Kawakami, M. 1982. The unit-concept of hepatic parenchyma--a re-examination based on angioarchitectural studies. *Acta Pathol Jpn*, 32 Suppl 2, 285-314

Matsuse, T., Teramoto, S., Katayama, H., Sudo, E., Ekimoto, H., Mitsuhashi, H., Uejima, Y., Fukuchi, Y., & Ouchi, Y. 1999. ICAM-1 mediates lung leukocyte recruitment but not pulmonary fibrosis in a murine model of bleomycin-induced lung injury. *European Respiratory Journal*, 13, (1) 71-77

Matsuura T, Kawada M, Hasumura S, Nagamori S, Obata T, Yamaguchi M, Hataba Y, Tanaka H, Shimizu H, Unemura Y, Nonaka K, Iwaki T, Kojima S, Aizaki H, Mizutani S, & Ikenaga H 2003. High density culture of immortalized liver endothelial cells in the radial-flow bioreactor in the development of an artificial liver. *Int J Artif Organs.*, 21, (4) 229-234

Mayadas, T.N., Johnson, R.C., Rayburn, H., Hynes, R.O., & Wagner, D.D. 1993. Leukocyte rolling and extravasation are severely compromised in P-Selectin deficient mice. *Cell*, 74, (3) 541-554

McCormick, S.M., Eskin, S.G., McIntire, L.V., Teng, C.L., Lu, C.M., Russell, C.G., & Chittur, K.J. 2001. DNA Microarray reveals changes in gene expression of shear stressed human umbilical vein endothelial cells. *PNAS*, 98, 8955-8960

McGettrick, H.M., Lord, J.M., Wang, K., Rainger, G.E., Buckley, C.D., & Nash, G.B. 2006. Chemokine and adhesion dependent survival of neutrophils after transmigration though cytokine stimulated endothelium. *Journal of Leukocyte Biology*

Medina, J., Sanz-Cameno, P., Garcia-Buey, L., Martin-Vilchez, S., Lopez-Cabrera, M., & Moreno-Otero, R. 2005. Evidence of angiogenesis in primary biliary cirrhosis: an immunohistochemical descriptive study. *J.Hepatol.*, 42, (1) 124-131

Michel Aurrand-Lions, Lidia Duncan, Christoph Ballestrem, & Beat A.Imhof 2001. JAM-2, a novel immunoglobulin superfamily molecule, expressed by endothelial and lymphatic cells. *The Journal Of Biological Chemistry*, 276, (4) 2733-2741

Miller, M.D. & Krangel, M.S. 1992. Biology and biochemistry of the chemokines: a family of chemotactic and inflammatory cytokines. *Crit.Rev.Immunol.*, 12, 17-46

Morgan, M.D., Harper, L., Lu, X., Nash, G.B., Williams, J., & Savage, C.O.S. 2005. Can neutrophils be manipulated in vivo? *Journal of Leukocyte Biology*, 44, 597-601

Moser, B., Wolf, M., Walz, A., & Loetscher, P. 2004. Chemokines: multiple levels of leukocyte migration control. *Trends Immunol.*, 25, (2) 75-84

Muller, W.A. 2003. Leukocyte-endothelial-cell interactions in leukocyte transmigration and the inflammatory response. *Trends Immunol.*, 24, (6) 327-334

Murdoch, C. & Finn, A. 2000. Chemokine receptors and their role in inflammation and infectious diseases. *Blood*, 95, (10) 3032-3043

Nash, G.B., Buckley, C.D., & Rainger, E. 2004. The local physiochemical environment conditions the proinflammatory response of endothelial cells and thus modulates leukocyte recruitment. *FEBS Letters*, 569, 13-17

Nava s, Westgren M, Jaksch M, Tibell A, Broome U, Ericzon BG, & Sumitran-Holgersson S 2005. Characterization of cells in the developing human liver. *Differentiation*, 73, (5) 249-260

Negus, P.R.M. & Balkwill, F.R. 1996. Cytokines in tumor-growth, migration and metastasis. *World Journal Of Urology*, 14, 157-165

Neubauer, K., Wilfling, T., Pitzel, A., & Ramadori, G. 2000a. Platelet endothelial cell adhesion molecule-1 gene expression in liver sinusoidal endothelial cells during liver injury and repair. *J.Hepatol.*, 32, 921-932

Neubauer, K., Ritzel, A., Saile, B., & Ramadori, G. 2000b. Decrease of platelet-endothelial cell adhesion molecule 1-gene-expression in inflammatory cells and in endothelial cells in the rat liver following CCl(4)-administration and in vitro after treatment with TNFalpha. *Immunol.Lett.*, 74, (2) 153-164

Newman, P.J., Berndt, M.C., Gorski, J., White, G.C., II, Lyman, S., Paddock, C., & Muller, W.A. 1990. PECAM-1 (CD31) cloning and relation to adhesion molecules of the immunoglobulin gene superfamily. *Science*, 247, 1219-1222

Newton, J.P., Hunter, A.P., Simmons, D.L., Buckley, C.D., & Harvey, D.J. 1999. CD31 (PECAM-1) exists as a dimer and is heavily N-glycosylated [In Process Citation]. *Biochem Biophys Res Commun*, 261, (2) 283-291

Nisato, R.E., Harrison, J.A., Buser, R., Orci, L., Rinsch, C., Montesano, R., Dupraz, P., & Pepper, M.S. 2004. Generation and characterization of telomerase-transfected human lymphatic endothelial cells with an extended life span. *Am.J.Pathol.*, 165, (1) 11-24

Nonaka H, Tanaka M, Suzuki K, & Miyajima A 2007. Development of murine hepatic sinusoidal endothelial cells characterized by the expression of hyaluronan receptors. *Developmental Dynamics*, 236, 2258-2267

Nonaka, H., Sugano, S., & Miyajima, A. 2004. Serial analysis of gene expression in sinusoidal endothelial cells from normal and injured mouse liver. *Biochemical and Biophysical Research Communications*, 324, (1) 15-24

Ohmori S, Shiraki K, Sugimoto K, Sakai T, Fukikawa K, Wagayama H, Takase K, & Nakano T 2003. High expression of CD34-positve sinusoidal endothelial cells is a risk factor for hepatocellular carcinoma in patients with HCV-associated chronic liver diseases. *Human Pathology*, 32, (12) 1363-1370

Omari, K.M., Chui, R., & Dorovini-Zis, K. 2004. Induction of [beta]-chemokine secretion by human brain microvessel endothelial cells via CD40/CD40L interactions. *Journal of Neuroimmunology*, 146, (1-2) 203-208

Onoe, T., Ohdan, H., Tokita, D., Shishida, M., Tanaka, Y., Hara, H., Zhou, W., Ishiyama, K., Mitsuta, H., Ide, K., & Asahara, T. 2005. Liver sinusoidal endothelial cells tolerize T cells across MHC barriers in mice. *J.Immunol.*, 175, (1) 139-146

Oo, Y.H. & Adams, D.H. 2009. The role of chemokines in the recruitment of lymphocytes to the liver. *J.Autoimmun.*

Oppenheimer-Marks, N., Davis, L.S., Bogue, D.T., Ramberg, J., & Lipsky, P.E. 1991. Differential ultilisation of ICAM-1 and VCAM-1 during the adhesion and transendothelial migration of human T lymphocytes. *J.Immunol.*, 147, 2913-2921

Osborn, E.A., Rabodzey, A., Dewey, C.F., Jr., & Hartwig, J.H. 2006. Endothelial actin cytoskeleton remodeling during mechanostimulation with fluid shear stress. *Am J Physiol Cell Physiol*, 290, (2) C444-C452

Pai, J.t. & Ruoslahti, E. 2005. Identification of endothelial genes up-regulated in vivo. *Gene*, 347, (1) 21-33

Pallister, C. 1998, "Blood Cell Formation," *In Blood:Physiology and Pathophysiology*, Butterworth-Heinemann. Oxford, pp. 11-32.

Parkin, J. & Cohen, B. 2001. An overview of the immune system. *Lancet*, 357, (9270) 1777-1789

Patel, K.D., Nollert, M.U., & McEver, R.P. 1995. P-selectin must extend a sufficient length from the plasma membrane to mediate rolling of neutrophils. *J.Cell Biol.*, 131, (6) 1893-1902

Paul H.Reinhardt & Paul Kubes 1998. Differential leukocyte recruitment from whole blood via endothelial adhesion molecules under shear conditions. *Blood*, 92, (12) 4691-4699

Persson, T., Monsef, N., Andersson, P., Bjartell, A., Malm, J., Calafat, J., & Egesten, A. 2003. Expression of the neutrophil-activating CXC chemokine ENA-78/CXCL5 by human eosinophils. *Clin.Exp.Allergy*, 33, (4) 531-537

Petri, B., Phillipson, M., & Kubes, P. 2008. The Physiology of Leukocyte Recruitment: An In Vivo Perspective. *The Journal of Immunology*, 180, (10) 6439-6446

Piali, L., Hammel, P., Uherek, C., Bachmann, F., Gisler, R.H., Dunon, D., & Imhof, B.A. 1995. CD31/PECAM-1 is a ligand for alpha v beta 3 integrin involved in adhesion of leukocytes to endothelium. *J.Cell Biol.*, 130, (2) 451-460

Picker, L.J. 1992. Mechanisms of lymphocyte homing. *Curr.Opin.Immunol.*, 4, 277-286

Pober, J.S., Lapierre, L.A., Stolpen, A.H., Brock, T.A., Springer, T.A., Fiers, W., Bevilacqua, M.P., Mendrick, D.L., & Gimbrone, M.A., Jr. 1987. Activation of cultured human endothelial cells by recombinant lymphotoxin: comparison with tumor necrosis factor and interleukin 1 species. *J.Immunol.*, 138, (10) 3319-3324

Prescott, S.M., McIntyre, T.M., & Zimmerman, G.A. 1990. The role of platelet-activating factor in endothelial cells. *Thromb.Haemost.*, 64, 99-103

Prevo, R., Banerji, S., Ferguson, D.J., Clasper, S., & Jackson, D.G. 2001. Mouse LYVE-1 is an endocytic receptor for hyaluronan in lymphatic endothelium. *J Biol Chem*, 276, (22) 19420-19430

Proudfoot, A.E., Fritchley, S., Borlat, F., Shaw, J.P., Vilbois, F., Zwahlen, C., Trkola, A., Marchant, D., Clapham, P.R., & Wells, T.N. 2001. The BBXB motif of RANTES is the principal site for heparin binding and controls receptor selectivity. *J.Biol.Chem.*, 276, (14) 10620-10626

R.Haverslag, G.Pasterkamp, & I.E.Hoefer 2008. Targeting Adhesion Molecules in Cardiovascular Disorders. *Cardiovascular and Hematological Disorders*, 8, (4) 252-260

R.M Twyman 2004, "From genomics to proteomics," *In Principles of Proteomics*, Oxford: BIOS Scientific Publishers, pp. 1-22.

R.W.Hyman, S.Frank, C.H.Warden, A.Daluiski, R.Heller, & A.J.Lusis 1994. Quantitative trait locus analysis of susceptibility to diet-induced atherosclerosis in recombinant inbred mice. *Biochem.Genet.*, 32, (397) 407

Racanelli, V. & Rehermann, B. 2006. The liver as an immunological organ. *Hepatology.*, 43, (2 Suppl 1) S54-S62

Rainger, G.E., Rowley, A.F., & Nash, G.B. 1998. Adhesion-Dependent Release of Elastase From Human Neutrophils in a Novel, Flow-Based Model: Specificity of Different Chemotactic Agents. *Blood*, 92, (12) 4819-4827

Raub TJ, K.S.S.GA. 1992. Permeability of bovine brain microvessel endothelial cells in vitro: barrier tightening by a factor released from astroglioma cells. *Exp Cell Res.*, 199, (2) 330-340

Reed, R.K. & Laurent, U.B. 1992. Turnover of hyaluronan in the microcirculation. *Am.Rev.Respir.Dis.*, 1460, S37-S39

Reiss, Y. & Engelhardt, B. 1999. T cell interaction with ICAM-1-deficient endothelium in vitro: transendothelial migration of different T cell populations is mediated by endothelial ICAM-1 and ICAM-2. *Int Immunol*, 11, (9) 1527-1539

Reiss, Y., Hoch, G., Deutsch, U., & Engelhardt, B. 1998. T cell interaction with ICAM-1-deficient endothelium in vitro: essential role for ICAM-1 and ICAM-2 in transendothelial migration of T cells. *Eur J Immunol*, 28, (10) 3086-3099

Resenzweig, S.D. & Holland, S.M. 2002. Phagocyte immunodeficiencies and their infections. *Journal of Allergy and Clinical Immunology*, 113, 620-626

Ritter, M., Goggel, R., Chaudhary, N., Wiedenmann, A., Jung, B., Weith, A., & Seither, P. 2005. Elevated expression of TARC (CCL17) and MDC (CCL22) in models of cigarette smoke-induced pulmonary inflammation. *Biochem.Biophys.Res.Commun.*, 334, (1) 254-262

Roberts, W.G. & Palade, G.E. 1995. Increased microvascular permeability and endothelial fenestration induced by vascular endothelial growth factor. *J.Cell Sci.*, 108, (Pt 6) 2369-2379

Rohnelt, R.K., Hoch, G., Reiss, Y., & Engelhardt, B. 1997. Immunosurveillance modelled in vitro: naive and memory T cells spontaneously migrate across unstimulated microvascular endothelium. *International Immunology*, 9, (3) 435-450

Romagnani, P., Annunziato, F., Lasagni, L., Lazzeri, E., Beltrame, C., Francalanci, M., Uguccioni, M., Galli, G., Cosmi, L., Maurenzig, L., Baggiolini, M., Maggi, E., Romagnani, S., & Serio, M. 2001. Cell cycle dependent expression of CXC chemokine receptor 3 by endothelial cells mediates angiostatic activity. *The Journal of Clinical Investigation*, 107, (1) 53-63

Rubin, L.L., Hall, D.E., Porter, S., Barbu, K., Cannon, C., Horner, H.C., Janatpour, M., Liaw, C.W., Manning, K., & Morales, J. 1991. A cell culture model of the blood-brain barrier. *The Journal of Cell Biology*, 115, (6) 1725-1735

Ruhnke M, Ungefroren H, zehle G, Bader M, Kremer B, & Fandrich F 2003. Long term culture and differentiation of rat embryonic stem cell like cells into neuronal, glial, endothelial, and hepatic lineages. *Stem Cells*, 21, 428-436

Rui Li, Pekka Nortamo, Leena Valmu, Martti Tolvanene, Jarkko Huuskonen, Carmela Kantor, & Carl G.Gahmberg. A peptide from ICAM-2 binds to the leukocyte integrin CD11a/CD18 and inhibits endothelial cell adhesion. The Journal Of Biological Chemistry 268[23], 17513-17518. 1993.

Sahota PS, Brown NJ, Burn JL, & MacNeil S 2004. Approaches to improve angiogenesis in tissue-engineered skin. *Wound Rep Reg* (12) -635

Saito M, K.I.T.H.B.F., Matsuura T, Nagatsuma K, Tanaka K, Maehashi H, Shimizu K, Hataba Y, & Kato F 2007. The functional interrelationship between gap junctions and fenestrae in endothelial cells of the liver organoid. *J.Membr.Biol.*, 217, (1-3) 115-121

Salmi, M. & Jalkanen, S. 2001. VAP-1: an adhesin and an enzyme. *Trends Immunol.*, 22, (4) 211-216

Salmi, M., Yegutkin, G.G., Lehvonen, R., Koskinen, K., Salminen, T., & Jalkanen, S. 2001. A cell surface amine oxidase directly controls lymphocyte migration. *Immunity*, 14, (3) 265-276

Sampath, R.K.G.S.C.E.S.M.LV. 1995. Shear stress-mediated changes in the expression of leukocyte adhesion receptors on human umbilical vein endothelial cells in vitro. *Ann.Biomed.Eng.*, 23, (247) 256

Sandlund, J., Hedberg, Y., Grankvist, K., Bergh, A., Uungberg, B., & Rasmuson, T. 2006. Endoglin (CD105) expression in human renal cell carcinoma. *BJU International*, 97, (4) 706-710

Savage C.O.S, Rooks, C.J., Adu, D., Richards, G., & Howie, A.J. 1997. Cell adhesion molecule expression within human glomerular and kidney organ culture. *Journal of Pathology*, 181, 111-115

Schenkel, A.R., Mamdouh, Z., Chen, X., Liebman, R.M., & Muller, W.A. 2002. CD99 plays a major role in the migration of monocytes through endothelial junctions. *Nat.Immunol.*, 3, (2) 143-150

Schrage, A., Loddenkemper, C., Erben, U., Lauer, U., Hausdorf, G., Jungblut, P.R., Johnson, J., Knolle, P.A., Zeitz, M., Hamann, A., & Klugewitz, K. 2008. Murine CD146 is widely expressed on endothelial cells and is recognized by the monoclonal antibody ME-9F1. *Histochem.Cell Biol.*, 129, (4) 441-451

Scoazec, J.Y. & Feldmann, G. 1991. In situ immunophenotyping study of endothelial cells of the human hepatic sinusoid: results and functional implications. *Hepatology*, 14, (5) 789-797

Scoazec, J.Y. & Feldmann, G. 1994. The cell adhesion molecules of hepatic sinusoidal endothelial cells. *J.Hepatol.*, 20, (2) 296-300

Sheibani N, Frazier WA, & Sorenson CM 1999. Tissue specific expression of alternatively spliced murine PECAM-1 isoforms. *Dev Dyn*, 214, (1) 44-54

Sheikh, S., Gale, Z., Rainger, E., & Nash, G.B. 2004. Methods for exposing multiple cultures of endothelial cells to different shear stresses and cytokines, for subsequent analysis of inflammatory function. *Journal of Immunological Methods*, 288, 35-46

Sheikh, S., Rahman, M., Gale, Z., Thin Luu, N., Ston, P.C.W., Matharu, N.M., Rainger, E., & Nash, G.B. 2005. Differing mechanisms of leukoyte recruitment and sensitivity to conditioning by shear stress for endothelial cells treated with tumour necrosis factor-alpha or interleukin-1beta. *British Journal of Pharmacology*, 000, 1-10

Sheikh, S., Rainger, E., Gale, Z., Rahman, M., & Nash, G.B. 2003. Exposure to fluid shear stress modulates the ability of endothelial cells to recruit neutrophils in response to tumour necrosis factor-alpha: a basis for local variations in vascular

sensitivity to inflammation. *Haemostasis, Thrombosis, and Vascular Biology*, 102, (8) 2828-2834

Sherlock, S. & Dooley, J. 1993. *Diseases of the Liver and Biliary System*, Nineth ed. Oxford, United Kingdom, Blackwell Scientific Publications.

Shetty, S., Lalor, P.F., & Adams, D.H. 2008. Lymphocyte recruitment to the liver: Molecular insights into the pathogenesis of liver injury and hepatitis. *Toxicology*

Shields, P.L., Morland, C.M., Salmon, M., Qin, S., Hubscher, S.G., & Adams, D.H. 1999. Chemokine and chemokine receptor interactions provide a mechanism for selective T cell recruitment to specific liver compartments within hepatitis C-infected liver. *J.Immunol.*, 163, (11) 6236-6243

Singh RJ, Mason JC, Lidington EA, Edwards DR, Nuttall RK, Khokha R, Knauper V, Murphy G, and Gavrilovic J, 2005. *Cytokine stimulated vascular cell adhesion molecule-1 (VCAM-1) ectodomain release is regulated by TIMP-3.*,

Smedsrod, B. 2004. Clearance function of scavenger endothelial cells. *Comp Hepatol.*, 3 Suppl 1:S22., S22

Smedsrod, B., De Bleser, P.J., Braet, F., Lovisetti, P., Vanderkerken, K., Wisse, E., & Geerts, A. 1994. Cell biology of liver endothelial and Kupffer cells. *Gut*, 35, (11) 1509-1516

Smedsrod, B. & Pertoft, H. 1985. Preparation of pure hepatocytes and reticuloendothelial cells in high yield from a single rat liver by means of Percoll centrifugation and selective adherence. *Journal of Leukocyte Biology*, 38, (2) 213-230

Smedsrod, B., Pertoft, H., Eggertsen, G., & Sundstrom, C. 1985. Functional and morphological characterization of cultures of Kupffer cells and liver endothelial cells prepared by means of density separation in Percoll, and selective substrate adherence. *Cell Tissue Res*, 241, (3) 639-649

Smedsrod, B., Pertoft, H., Eriksson, S., Fraser, J.R., & Laurent, T.C. 1984. Studies in vitro on the uptake and degradation of sodium hyaluronate in rat liver endothelial cells. *Biochem J*, 223, (3) 617-626

Smith E., Lally F, Stone MA, Shaw JS, Nash GB, Buckley CD, & Ed Rainger 2006. Phototoxicity and fluorotoxicity combine to alter the behavior of neutrophils in fluorescence microscopy based flow adhesion assays. *Microsc.Res.Tech.*, 69, (11) 875-884

Smith, C.W., Rothlein, R., Hughes, B.J., Mariscalco, M.M., Rudloff, H.E., Schmalstieg, F.C., & Anderson, D.C. 1988. Recognition of an endothelial determinant for CD 18-dependent human neutrophil adherence and transendothelial migration. *J.Clin.Invest.*, 82, 1746-1756

Souto, J.T., Aliberti, J.C., Campanelli, A.P., Livonesi, M.C., Maffei, C.M.L., Ferreira, B.R., Travassos, L.R., Martinez, R., Rossi, M.A., & Silva, J.S. 2003. Chemokine Production and Leukocyte Recruitment to the Lungs of Paracoccidioides brasiliensis-Infected Mice Is Modulated by Interferon-{gamma}. *American Journal of Pathology*, 163, (2) 583-590

Springer, T.A. 1990a. Adhesion receptors of the immune system. *Nature*, 346, (6283) 425-434

Springer, T.A. 1990b. Leucocyte adhesion to cells. *Scand.J.Immunol.*, 32, (3) 211-216

Springer, T.A. 1993. Signals on endothelium for lymphocyte recirculation and leukocyte emigration: the area code paradigm. *Harvey Lect.*, 89, 53-103

Springer, T.A. 1994. Traffic signals for lymphocyte recirculation and leukocyte emigration: the multistep paradigm. *Cell*, 76, (2) 301-314

Springer, T.A. 1995. Traffic signals on endothelium for lymphocyte recirculation and leukocyte emigration. *Annu.Rev.Physiol.*, 57:827-72

Steinhoff, G., Behrend, M., Schrader, B., Duijvesttijn, A.M., & Wonigkeit, K. 1993. Expression patterns of leukocyte adhesion ligand molecules on human liver endothelia. Lack of ELAM-1 and CD62 inducibility on sinusoidal endothelia and distinct distribution of VCAM-1, ICAM-1, ICAM-2, and LFA-3. *American Journal of Pathology*, 142, (2) 481-488

Stoolman, L.M. 1993. Adhesion Molecules Involved in Leukocyte Recruitment and Lymphocyte Recirculation. *Chest*, 103, (2 Supplement) 79S-86S

Stoughton, R.B. 2005. Applications of DNA Microarrays in Biology. *Annual Review of Biochemistry*, 74, (1) 53-82

Surapisitchat, J., Hoefen, R.J., Pi, X., Yoshizumi, M., Yan, C., & Berk, BC. 2001. Fluid shear stress inhibits TNF-alpha activation of JNK but not ERK 1/2 or p38 in human umbilical vein endothelial cells: Inhibitory crosstalk among MAPK family members. *PNAS*, 98, 6476-6481

T.P.Knecht & C.K.Glass 1995. The influence of molecular biology on our understanding of lipoprotein metabolism and the pathobiology of atherosclerosis. *Adv.Genet.*, 32, 141-199

Tanaka, Y., Adams, D.H., & Shaw, S. 1993. Proteoglycans on endothelial cells present adhesion-inducing cytokines to leukocytes. *Immunol Today*, 14, (3) 111-5

Tasha N.Sims & Michael L.Dustin. The Immunological Synapse: integrins take the stage. Immunological Reviews 186, 100-117. 2002.

ten, D.P., Goumans, M.J., & Pardali, E. 2008. Endoglin in angiogenesis and vascular diseases. *Angiogenesis.*, 11, (1) 79-89

Tokairin, T., Nishikawa, Y., Doi, Y., Watanabe, H., Yoshioka, T., Su, M., Omori, Y., & Enomoto, K. 2002. A highly specific isolation of rat sinusoidal endothelial cells by the immunomagnetic bead method using SE-1 monoclonal antibody. *Journal of Hepatology*, 36, (6) 725-733

Tontsch, U. & Bauer, H.C. 1989. Isolation, characterization, and long-term cultivation of porcine and murine cerebral capillary endothelial cells. *Microvascular Research*, 37, (2) 148-161

Topper JN., Falb D, Cai J, & Gimbrone MA Jr 1996. Identification of vascular endothelial genes differentially responsive to fluid mechanical stimuli: cyclooxygenase-2, manganese superoxide dismutase, and endothelial cell nitric oxide synthase are selectively up-regulated by steady laminar shear stress. *PNAS*, 93, (19) 10417-10422

Tzima, E., Del Pozo, M.A., Kiosses, W.B., Mohamed, S.A., Li, S., Chien, S., & Shwartz, M.A. 2002. Activation of Rac1 by shear stress in endothelial cells mediates both cytoskeletal reorganisation and effects on gene expression. *EMBO*, 21, 6791-6800

U.Henseleit, K.Steinbrink, M/ Goebbler, J.Roth, D.Vestweber, C.Sorg, & C.Sunderkotter 1999. E-Selectin expression in experimental models of inflammation in mice. *J.Path.*, 180, (3) 317-325

Uhrig, A., Banafsche, R., Kremer, M., Hegenbarth, S., Hamann, A., Neurath, M., Gerken, G., Limmer, A., & Knolle, P.A. 2005. Development and functional consequences of LPS tolerance in sinusoidal endothelial cells of the liver. *J.Leukoc.Biol.*, 77, (5) 626-633

Unger, R.E., Krump-Konvalinkova, V., Peters, K., & Kirkpatrick, C.J. 2002. In vitro expression of the endothelial phenotype: comparative study of primary isolated cells and cell lines, including the novel cell line HPMEC-ST1.6R. *Microvasc.Res.*, 64, (3) 384-397

Valeria, B., Maddalena, G., Enrica, V., Onofrio, T., & Gaetano, B. 2008. Endoglin (CD105) Expression in the Human Heart Throughout Gestation: An Immunohistochemical Study. *Reproductive Sciences*, 15, (10) 1018-1026

von, O.N., Schurich, A., Hegenbarth, S., Stabenow, D., Tolba, R., Weiskirchen, R., Geerts, A., Kolanus, W., Knolle, P., & Diehl, L. 2008. Systemic antigen cross-presented by liver sinusoidal endothelial cells induces liver-specific CD8 T-cell retention and tolerization. *Hepatology*

W.C.Aird 2008. Endothelium in Health and Disease. *Pharmacological Reports*, 60, 139-143

Walzog, B., Weinmann, P., Jeblonski, F., Scharffetter-Kochanek, K., Bommert, K., & Gaehtgens, P. 1999. A role for {beta}2 integrins (CD11/CD18) in the regulation of cytokine gene expression of polymorphonuclear neutrophils during the inflammatory response. *The FASEB Journal*, 13, (13) 1855-1865

Wang, H., Peters, T., Kess, D., Sindrilaru, A., Oreshkova, T., Van Rooijen, N., Stratis, A., Renkl, A.C., Sunderk+Âtter, C., Wlaschek, M., Haase, I., & Scharffetter-Kochanek, K. 2006. Activated macrophages are essential in a murine model for T cell mediated chronic psoriasiform skin inflammation. *The Journal of Clinical Investigation*, 116, (8) 2105-2114

Wasserman, S.M., Mehraban, F., Komuves, L.G., Yang, R.B., Tomlinson, J.E., Zhang, Y., Spriggs, F., & Topper, J.N. 2002. Gene expression profile of human endothelial cells exposed to sustained fluid shear stress. *Physiological Genomics*, 12, (1) 13-23

West, D.B., Goudey-Lefevre, J., York, B., & Truett, G.E. 1994. Dietary obesity linked to genetic loci on chromosomes 9 and 15 in a polygenic mouse model. *The Journal of Clinical Investigation*, 94, (4) 1410-1416

Weston, G.C., Haviv, I., & Rogers, P.A.W. 2002. Microarray analysis of VEGF-responsive genes in myometrial endothelial cells. *Molecular Human Reproduction*, 8, (9) 855-863

Whitehead, R.H. & Robinson, P.S. 2009. Establishment of conditionally immortalized epithelial cell lines from the intestinal tissue of adult normal and transgenic mice. *Am J Physiol Gastrointest Liver Physiol*, 296, (3) G455-G460

Wick, N., Saharinen, P., Saharinen, J., Gurnhofer, E., Steiner, C.W., Raab, I., Stokic, D., Giovanoli, P., Buchsbaum, S., Burchard, A., Thurner, S., Alitalo, K., & Kerjaschki, D. 2007. Transcriptomal comparison of human dermal lymphatic endothelial cells ex vivo and in vitro. *Physiological Genomics*, 28, (2) 179-192

Williams KC & Hickey WF 1995. Traffic of hematogenous cells through the central nervous system. *Curr Top Microbiol Immunol.*, 202, 221-245

Wilson, C., Bellen, H.J., & Gehring, W.J. 2003. Position Effects on Eukaryotic Gene Expression. *Annual Review of Cell Biology*, 6, (1) 679-714 available from: http://dx.doi.org/10.1146/annurev.cb.06.110190.003335

Wolfram, J.A., Diaconu, D., Hatala, D.A., Rastegar, J., Knutsen, D.A., Lowther, A., Askew, D., Gilliam, A.C., McCormick, T.S., & Ward, N.L. 2009. Keratinocyte but Not Endothelial Cell-Specific Overexpression of Tie2 Leads to the Development of Psoriasis. *American Journal of Pathology*, 174, (4) 1443-1458

Worthylake, R.A. & Burridge, K. 2001. Leukocyte transendothelial migration: orchestrating the underlying molecular machinery. *Curr Opin Cell Biol JID - 8913428*, 13, (5) 569-577

Wu, Z., Hofman, F.M., & Zlokovic, B.V. 2003. A simple method for isolation and characterization of mouse brain microvascular endothelial cells. *Journal of Neuroscience Methods*, 130, (1) 53-63

Xiaoyan, S., , Yanjun, Z., , Hongmei, Y., , Jinlin, H., , & Yanlei, H. 2001. The effect of fluid shear stress on ICAM-1 expression of rat brain microvascular endothelial cells. *Technology and Health Care*, 9, (3) 287-293

Xu, B., Broome, U., Uzunel, M., Nava, S., Xupeng, G., Kumagai-Braesch, M., Hultenby, K., Christensson, B., Ericzon, B.G., Holgersson, J., & Sumitran-Holgersson, S. 2003. Capillarisation of hepatic sinusoid by liver endothelial cell reactive autoantibodies in patients with cirrhosis and chronic hepatitis. *Am-J-Pathol.*, 163, (4) 1275-1289

Yamawaki, H., Pan, S., Lee, R.T., & Berk, B.C. 2005. Fluid shear stress inhibits vascular inflammation by decreasing thioredoxin-interacting protein in endothelial cells. *Journal of Clinical Investigation*, 115, 733-738

Yang, Y.H. & Speed, T. 2002. Design issues for cDNA microarray experiments. *Nat Rev Genet*, 3, (8) 579-588

Yilmaz, G. & Granger, D. Leukocyte Recruitment and Ischemic Brain Injury. *NeuroMolecular Medicine*

Yuan, Z., Miyoshi, T., Bao, Y., Sheehan, J.P., Matsumoto, A.H., & Shi, W. 2009. Microarray analysis of gene expression in mouse aorta reveals role of the calcium signaling pathway in control of atherosclerosis susceptibility. *AJP - Heart and Circulatory Physiology*, 296, (5) H1336-H1343

Zaccagnini, G., Gaetano, C., Della Pietra, L., Nanni, S., Grasselli, A., Mangoni, A., Benvenuto, R., Fabrizi, M., Truffa, S., Germani, A., Moretti, F., Pontecorvi, A., Sacchi, A., Bacchetti, S., Capogrossi, M.C., & Farsetti, A. 2005. Telomerase Mediates Vascular Endothelial Growth Factor-dependent Responsiveness in a Rat Model of Hind Limb Ischemia. *J.Biol.Chem.*, 280, (15) 14790-14798

Zarbock, A. & Ley, K. 2009, "New Insights Into Leukocyte Recruitment by Intravital Microscopy," pp. 129-152.

Zhang, W., Ye, L., Wu, L., Xin, Y., Gu, F., Niu, J., Yang, Z., Zhu, G., Grau, G.E., & Lou, J. 2006. Morphologic, Phenotypic and Functional Characteristics of Endothelial Cells Derived from Human Hepatic Cavernous Hemangioma. *J Vasc Res*, 43, (6) 522-532

Zhao, B., Bowden, R.A., Stavchansky, S.A., & Bowman, P.D. 2001. Human endothelial cell response to gram-negative lipopolysaccharide assessed with cDNA microarrays. *AJP - Cell Physiology*, 281, (5) C1587-C1595

Zhou, L., Askew, D., Wu, C., & Gilliam, A.C. 2006. Cutaneous Gene Expression by DNA Microarray in Murine Sclerodermatous Graft-Versus-Host Disease, a Model for Human Scleroderma. *J Invest Dermatol*, 127, (2) 281-292

Zimmerman, G.A., Prescott, S.M., & McIntyre, T.M. 1991. Endothelial cell interactions with granulocytes: tethering and signaling molecules. *Immunol.Today*, draft / in press,

Zimmerman, G.A., Prescott, S.M., & McIntyre, T.M. 1992. Endothelial cell interactions with granulocytes: tethering and signaling molecules. *Immunol.Today*, 13, 93-99

Zirger, J.M., Barcia, C., Liu, C., Puntel, M., Mitchell, N., Campbell, I., Castro, M., & Lowenstein, P.R. 2006. Rapid Upregulation of Interferon-Regulated and Chemokine mRNAs upon Injection of 108 International Units, but Not Lower Doses, of Adenoviral Vectors into the Brain. *J.Virol.*, 80, (11) 5655-5659

Zocchi, M.R., Ferrero, E., Leone, B.E., Rovere, P., Bianchi, E., Toninelli, E., & Pardi, R. 1996. CD31/PECAM-1-driven chemokine-independent transmigration of human T lymphocytes. *Eur J Immunol*, 26, (4) 759-767

Zollner, O., Lenter, M.C., Blanks, J.E., Borges, E., Steegmaier, M., Zerwes, H.G., & Vestweber, D. 1997. L-selectin from human, but not from mouse neutrophils binds directly to E-selectin. *J.Cell Biol.*, 136, (3) 707-716

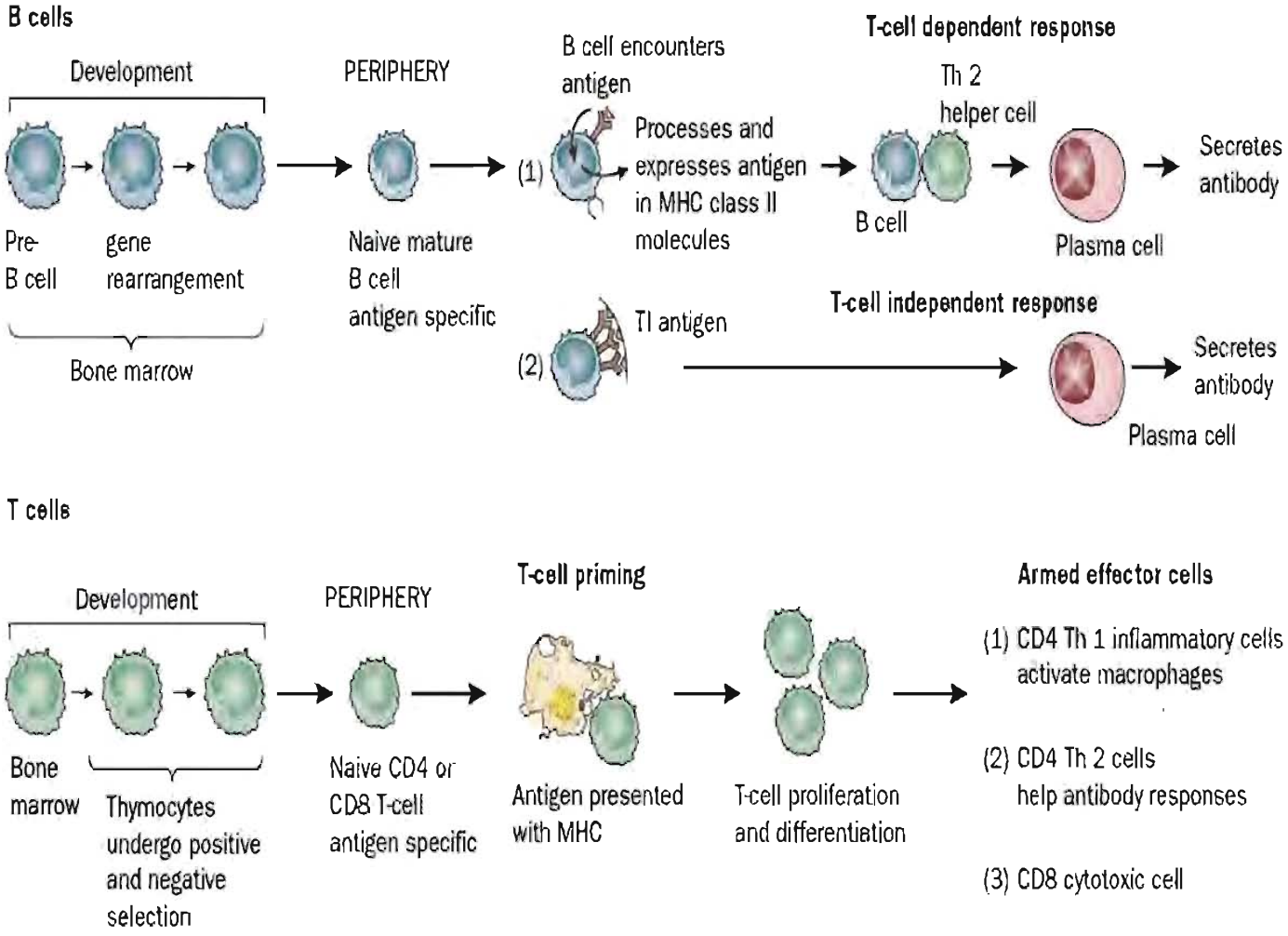
B cells
Development
PERIPHERY
B cell encounters antigen
T-cell dependent response
Th 2 helper cell
Processes and expresses antigen in MHC class II molecules
(1)
Secretes antibody
Pre-B cell
gene rearrangement
Naive mature B cell antigen specific
B cell
Plasma cell
Bone marrow
(2)
TI antigen
T-cell independent response
Secretes antibody
Plasma cell
T cells
Development
PERIPHERY
T-cell priming
Armed effector cells
(1) CD4 Th 1 inflammatory cells activate macrophages
Bone marrow
Thymocytes undergo positive and negative selection
Naive CD4 or CD8 T-cell antigen specific
Antigen presented with MHC
T-cell proliferation and differentiation
(2) CD4 Th 2 cells help antibody responses
(3) CD8 cytotoxic cell

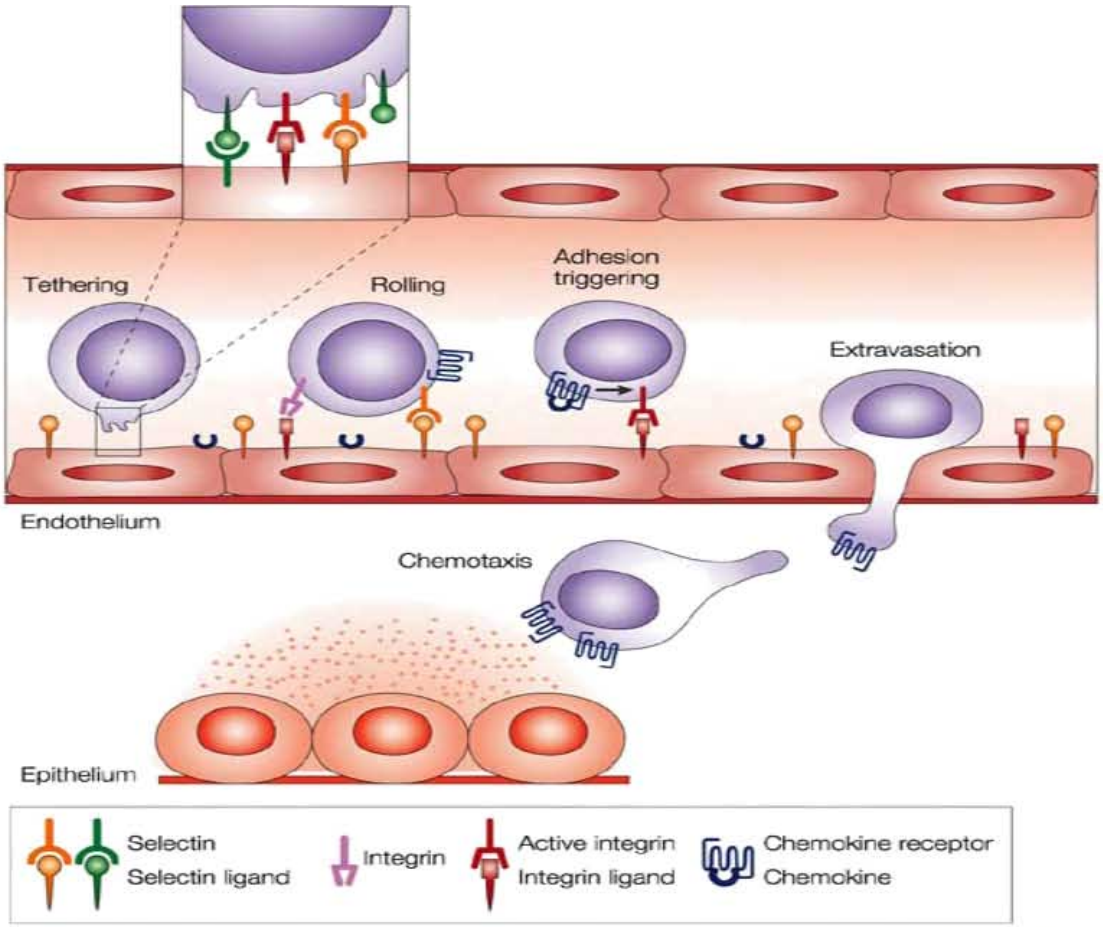

Nature Reviews | Immunology

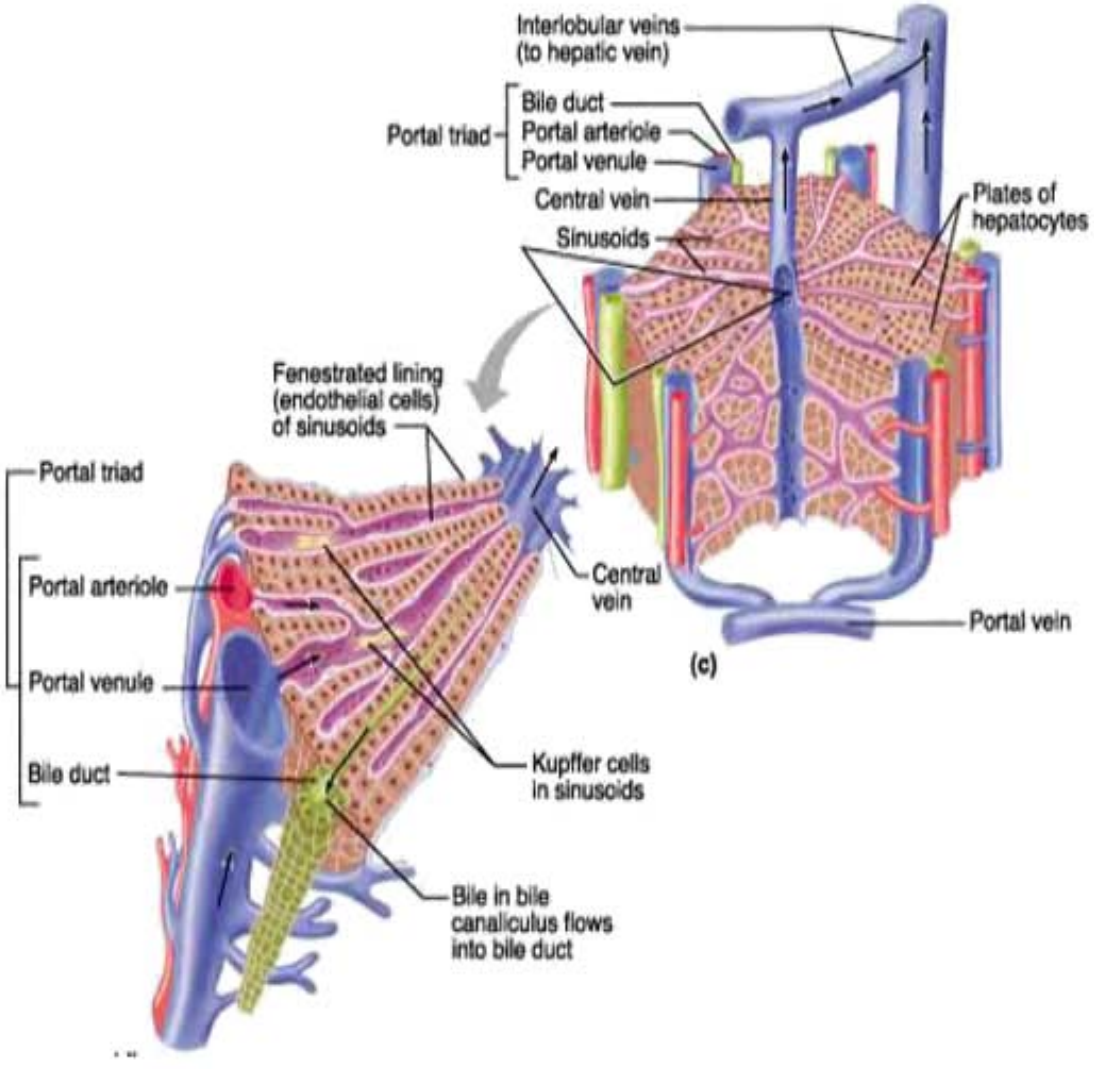
Interlobular veins
(to hepatic vein)
Portal triad
Bile duct
Portal arteriole
Portal venule
Central vein
Sinusoids
Plates of
hepatocytes
Fenestrated lining
(endothelial cells)
of sinusoids
Portal triad
Portal arteriole
Portal venule
Bile duct
Central
vein
Portal vein
(c)
Kupffer cells
in sinusoids
Bile in bile
canaliculus flows
into bile duct

Digestion → Gradient → Selection

- Liberase
- Collagenase 2/4
- Sieve
- Stomacher

- Optiprep (60%)
- Optiprep (Neat)
- Percoll (23/50)

- Miltenyi aLSEC
- CD31-Biotin:Strep Dynabeads
- Miltenyi aCD146

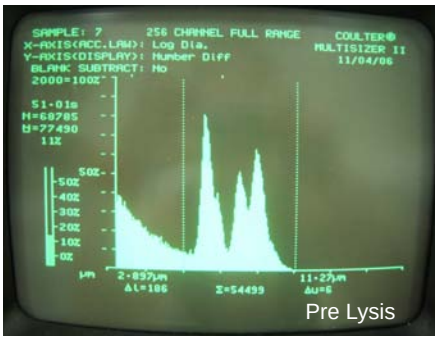

Pre Lysis

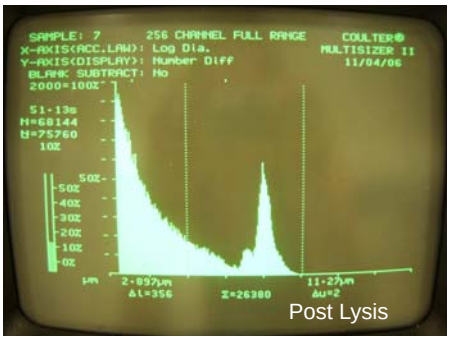

Post Lysis

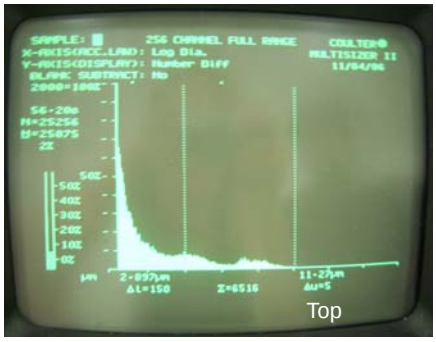

Top

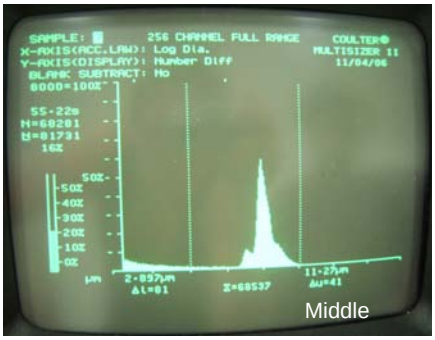

Middle

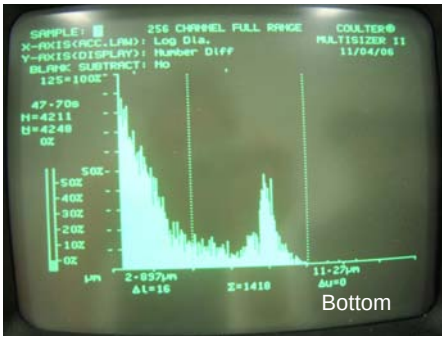

Bottom

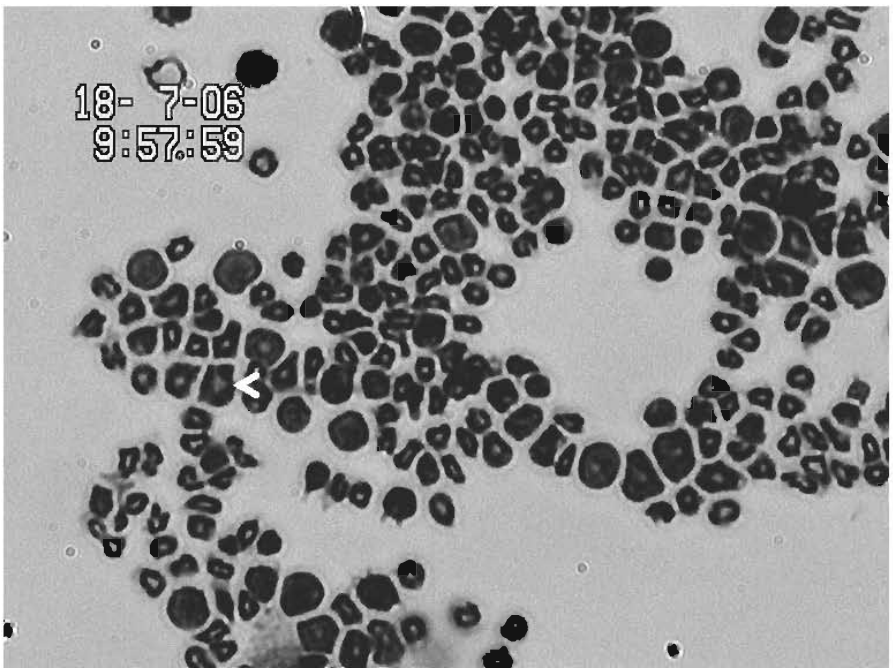
18- 7-06
9:57:59

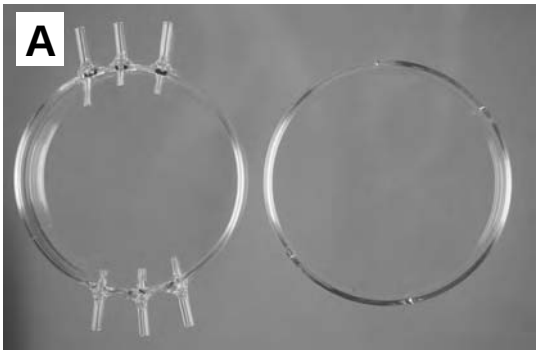

C

CO_2 Incubator @ 37^{0}C

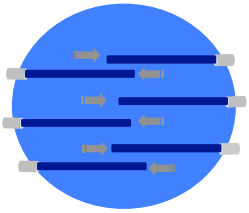

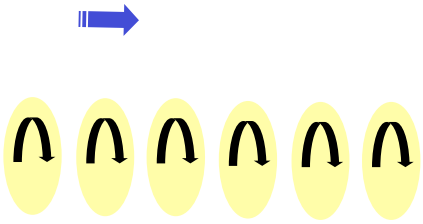

Multi-channel
Pump
(30s each hour)

Waste

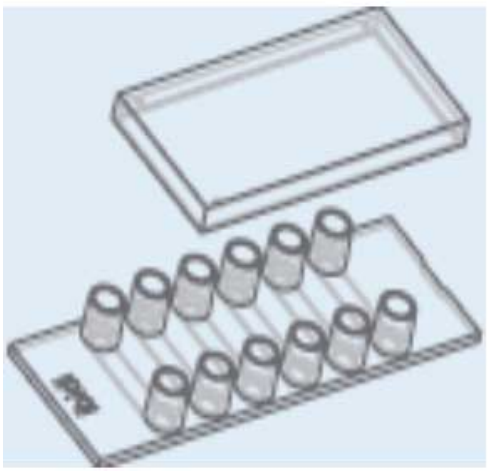

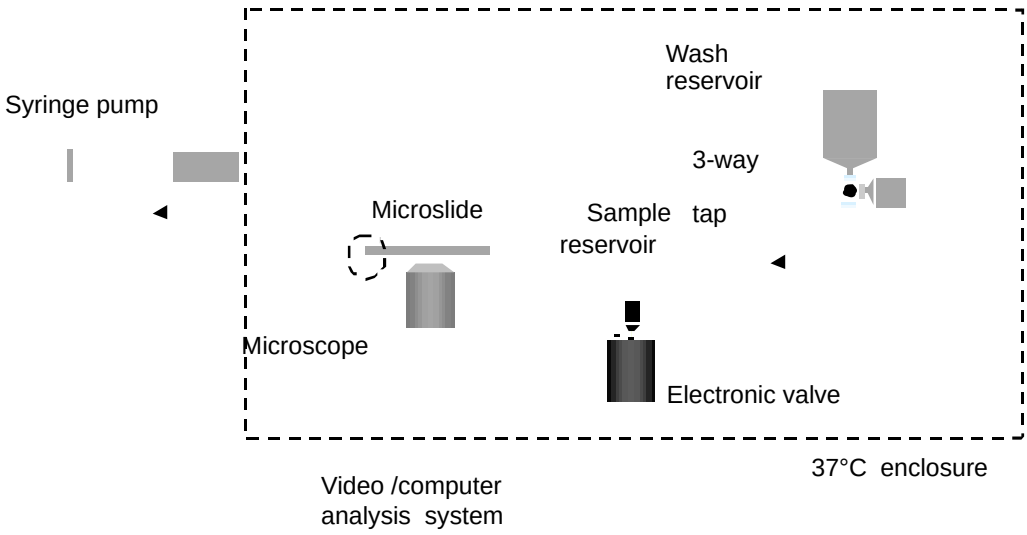
Syringe pump
Wash
reservoir
3-way
tap
Microslide
Sample
reservoir
Microscope
Electronic valve
37°C enclosure
Video /computer
analysis system

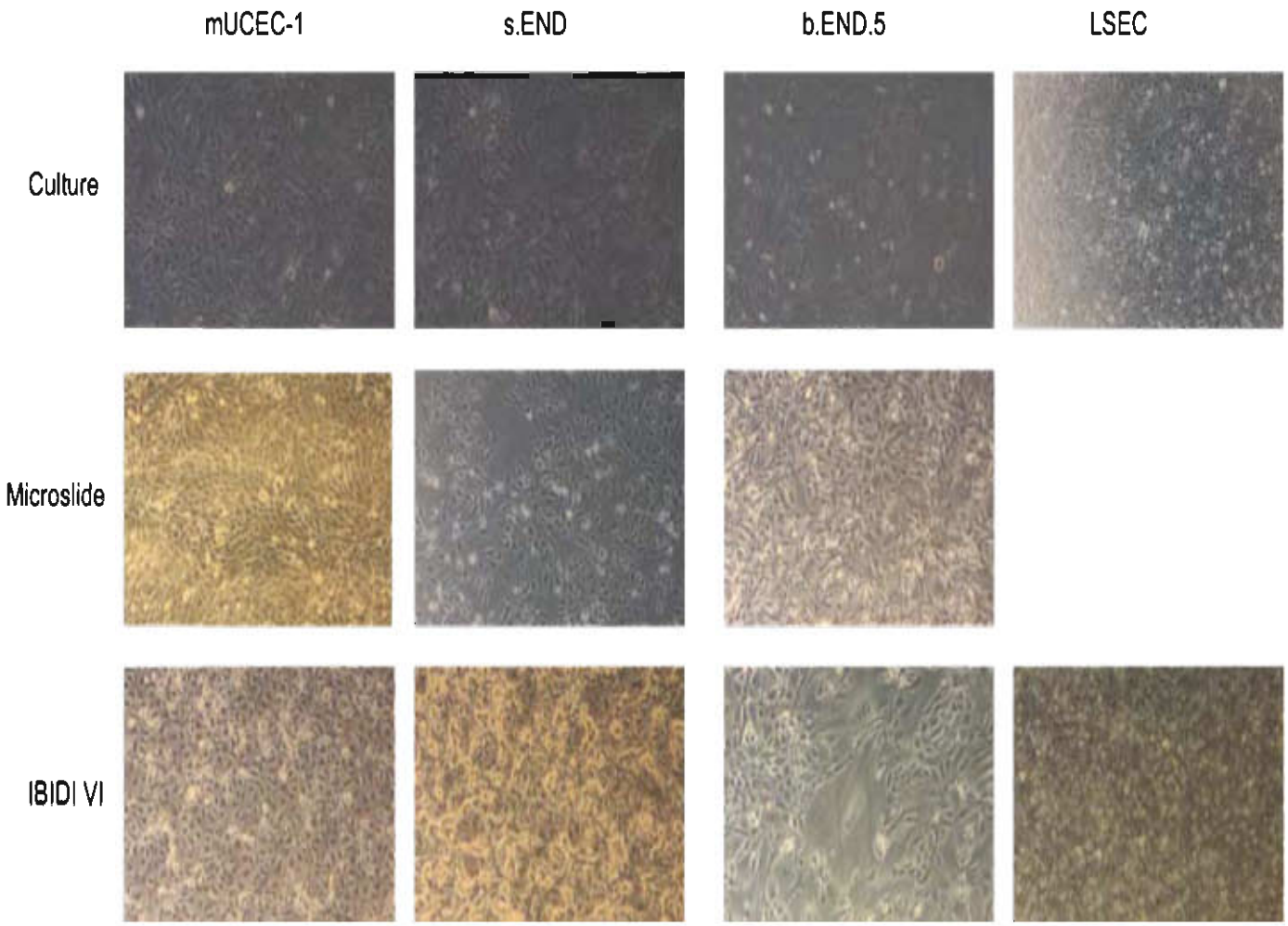
mUCEC-1
s.END
b.END.5
LSEC
Culture
Microslide
IBIDI VI

A

In Animal Facility

Pin mouse onto platform. Cut peritoneum exposing liver and portal vein. Cannulate PV, cut IVC, wash blood out of liver.

Perfuse Liberase to digest, lobes become transparent.

Remove cannula, and gall bladder. Transfer liver to petri- dish in perfusion buffer. Remove glissons capsule and disaggregate cells. Store in perfusion buffer at 4c.

In Laboratory

Pellet hepatocytes. Spin down supernatants and resuspend in 5ml buffer. Layer onto Percoll gradient (23/50 %). Remove cells at interface, wash out Percoll

Remove Kuppfer cells by plastic adherence. Wash cells vigorously several times to remove non-adherent LSEC. Count

Seed into collagen coated culture vessels for 30 mins at 37c. Wash with PBS and allow LSEC to spread.

B

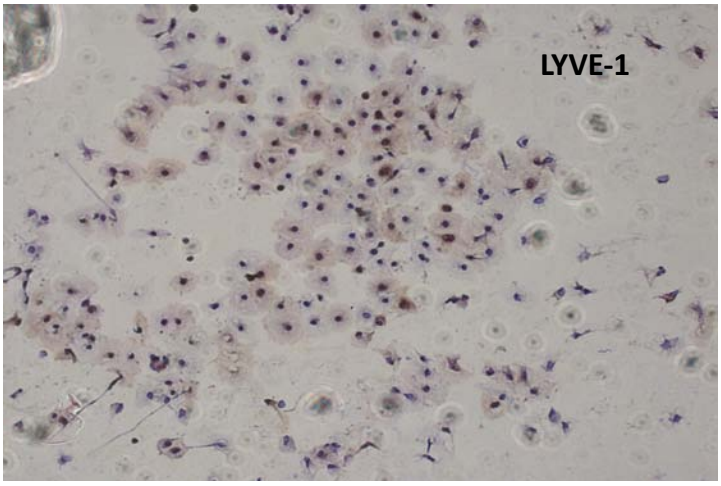
LYVE-1

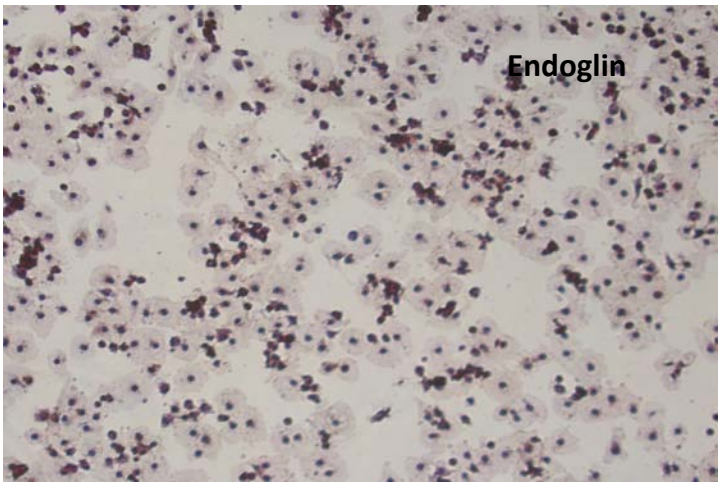
Endoglin

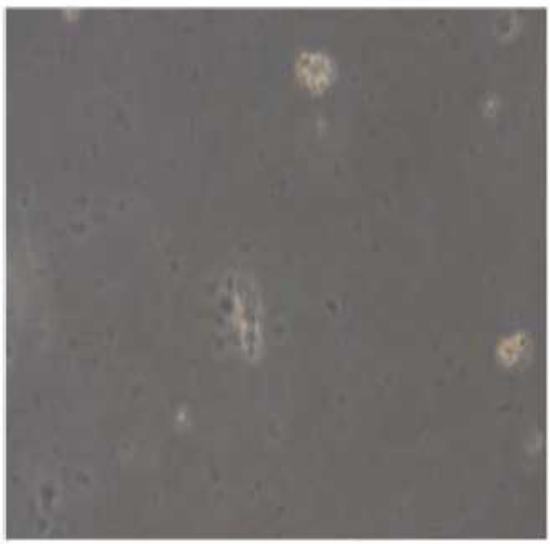

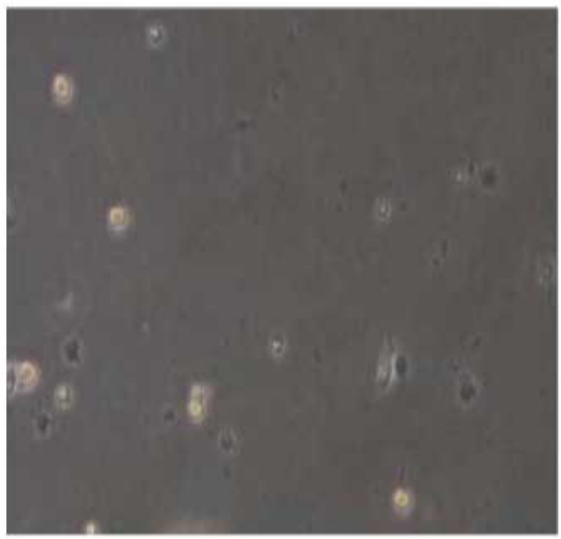

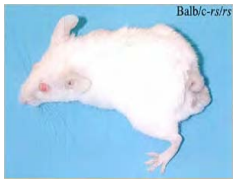

Mince tissue and add 5ml **0.25%** Collagenase 2

Add 30-100mls RPMI+10% FCS to quench enzyme

Sieve through fine mesh (60µm) in an excess of PBS using a syringe bung to help. Make final volume up to **200ml** with PBS

Spin cells at **30g/10 mins x3** Keeping supernatants and discarding hepatocyte pellet

Pellet NPC **300g/10mins.** Resuspend pellet in ~6ml RPMI +10%FCS

Place 1.5ml cell suspension in 15ml tube+ 3ml 60% Optiprep (diluted using 0.85% filtered NaCl), mix well and + 4ml plain DMEM on top, spin at **400G/ 15mins.**

Collect cells at interface (bright red) spin again **400G/5min** to remove Optiprep

Resuspend pellet in small volume of PBS ~100ul and add typically for 2-3 livers **15-20ul** of α-mouse LSEC microbeads. Make up to 1 ml with media and incubate on ice for **15-20** mins agitating every so often

Vary # of columns depending on amount of tissue

Place column of magnet, add 500ul PBS to wash, an appropriate volume of cell suspension ~2-300ul, elute with 500ul PBS. Remove columns from magnet add 1ml PBS and flush out magnetically labelled cells with plunger add some media.

Spin cells **400G/5min** and distribute between tissue culture vessels.

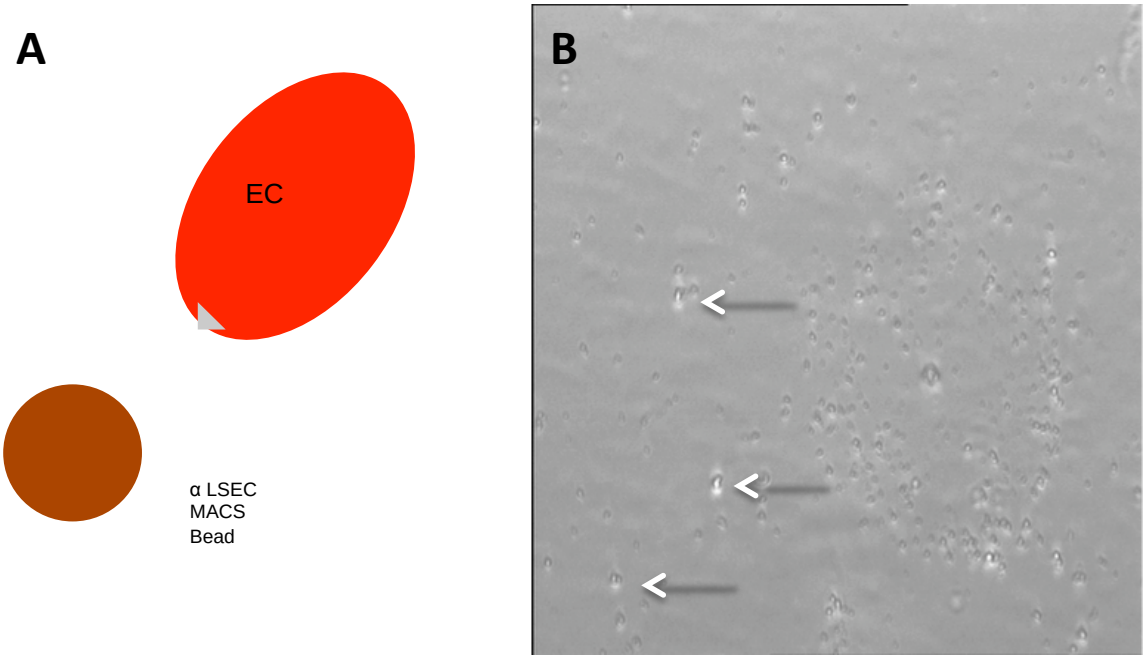
A
EC
α LSEC
MACS
Bead
B

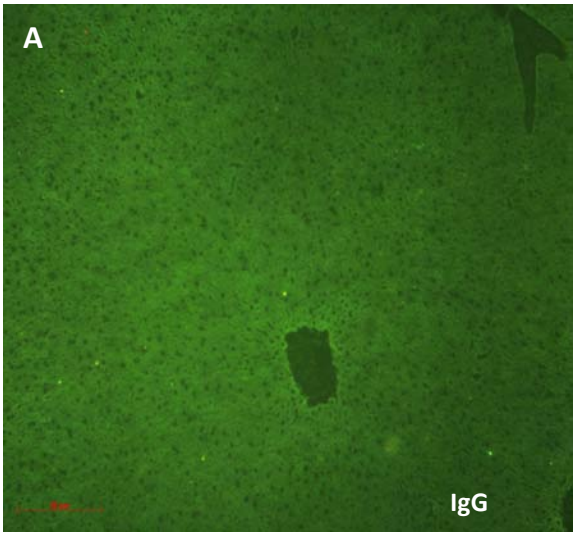
A
IgG

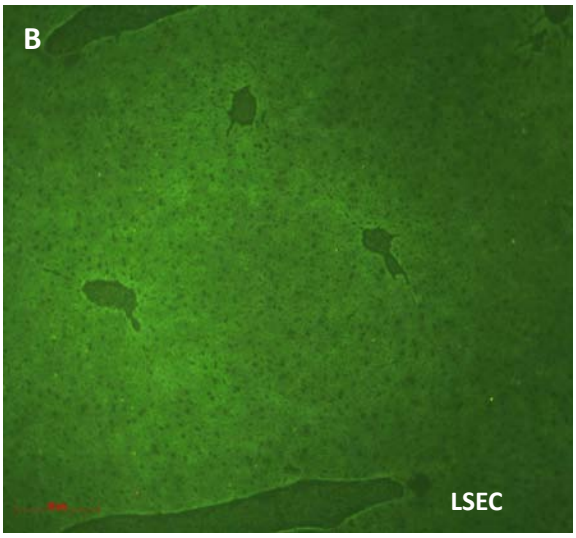
B
LSEC

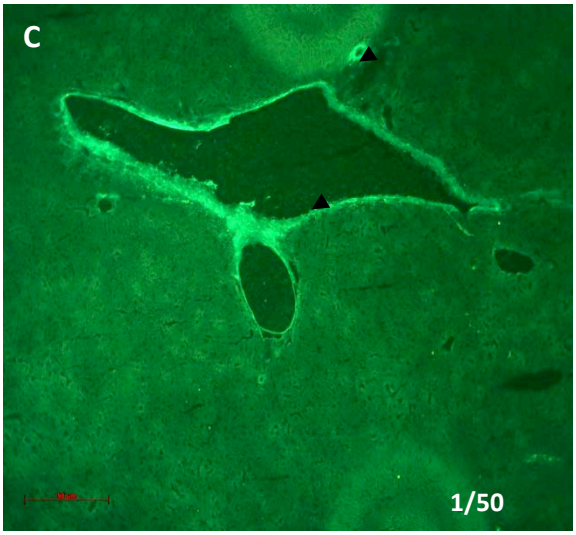
C
1/50

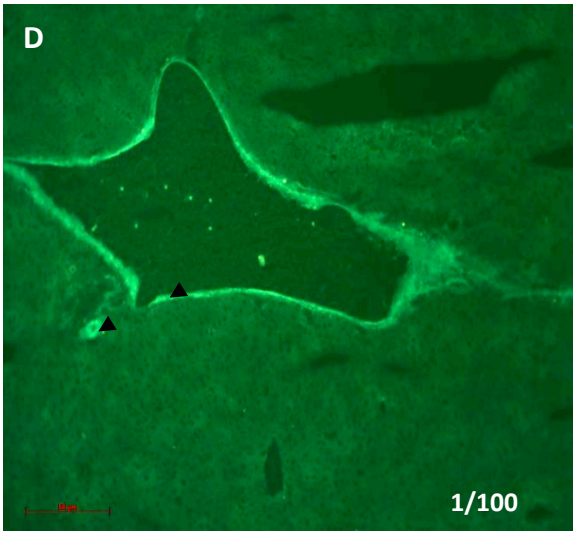
D
1/100

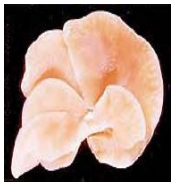

Mince and digest with collagenase **(1)**

▼

Slow spin to remove hepatocytes

▼ ▼

(2) Supernatant (NPC's) | Pellet (Hepatocytes) **(3)**

▼ ▼

Repeat Slow Spin **(4)** **(5)**

▼ ▼

Supernatant (NPC's) **(6)** | Pellet (Hepatocytes) | Discarded

▼

Density Gradient: OptiPrep **(7)**

▼

MACS Column

▼

Labelled Cells | Waste **(8)**

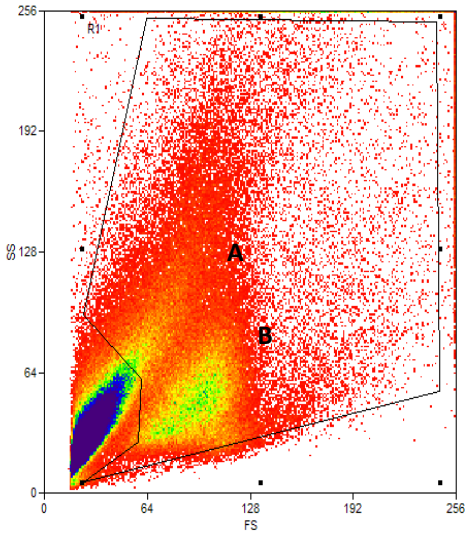
R1
A
B
SS
FS
256
192
128
64
0
0
64
128
192
256

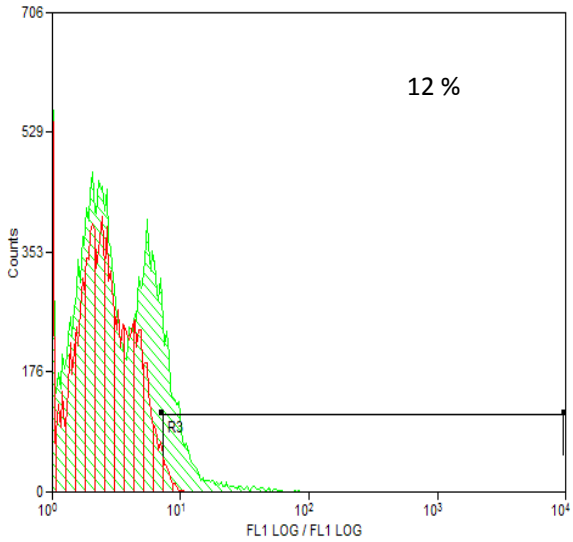
12 %
R3
Counts
FL1 LOG / FL1 LOG
706
529
353
176
0
10^0
10^1
10^2
10^3
10^4

A

0.28%

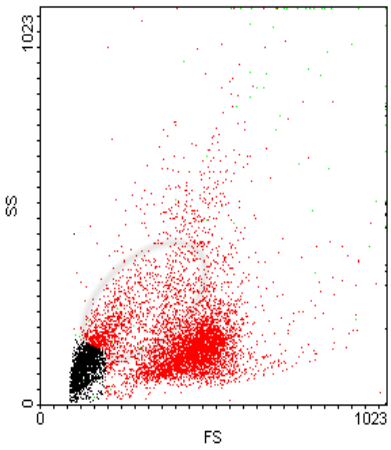
1023
SS
0
0
FS
1023

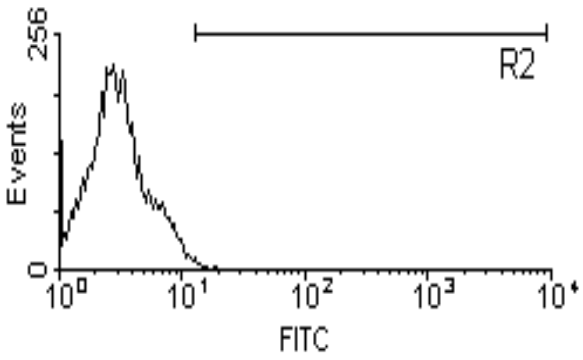
256
Events
0
R2
10^0
10^1
10^2
10^3
10^4
FITC

5.43 %

B

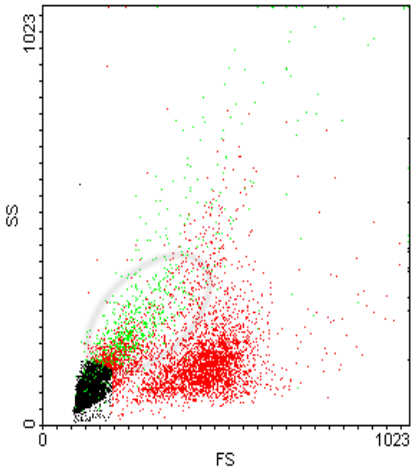
1023
SS
0
0
FS
1023

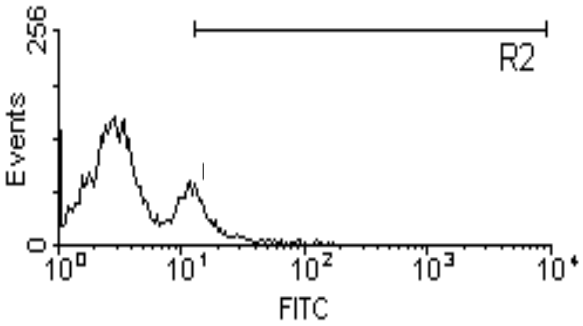
256
Events
0
R2
10^0
10^1
10^2
10^3
10^4
FITC

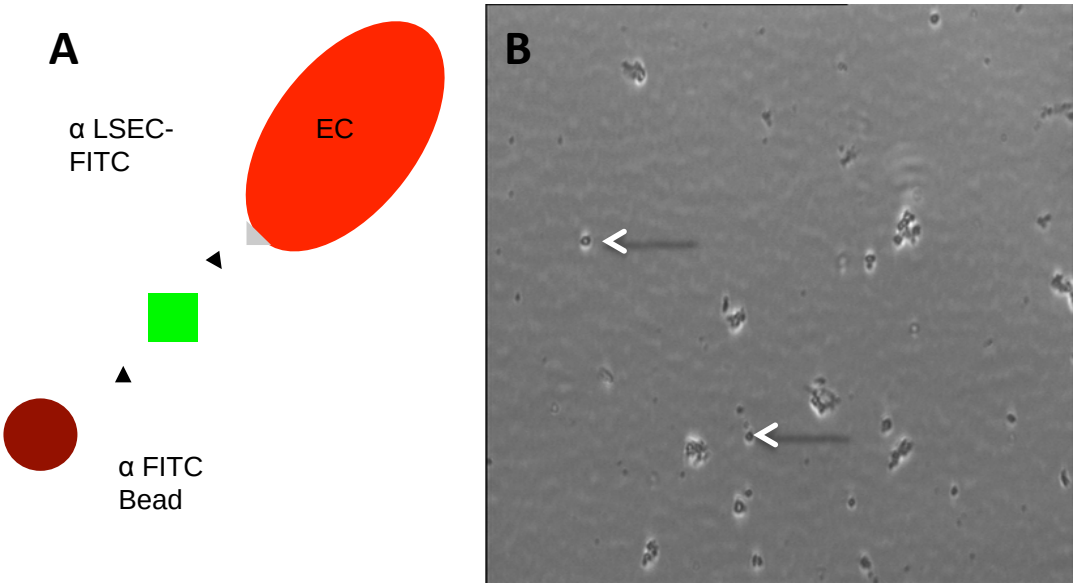
A
α LSEC-
FITC
EC
α FITC
Bead
B

Mince tissue and add 5ml/ liver **0.05mg/ml** Collagenase IV in DMEM 10% FCS

Incubate for 40 mins at 37°C. Mechanically digest tissue suspension using stomacher 250 for 30secs

Sieve through fine mesh (60um) in an excess of PBS using a syringe bung to help. Make final volume up to **200ml** with PBS

Spin cells at **400G/5min** Discard supernatants, resuspend pellets in PBS

Spin several times at **40G/3mins**, keep supernatants and discard hepatocyte pellets. Spin **400G/5min** to pellet cells.

Combine pellets in total volume of 10ml PBS. Add 4ml of pure Optiprep and mix. Split between 2 15ml Falcon tubes and layer on 1ml of PBS. Spin at **400G/20min.**

Collect cells at interface (white), add an excess of PBS and spin again **400G/ 5min** to remove Optiprep Wash again with PBS 800G/5min.

Resuspend pellet in complete endothelial basal medium (10% FCS) and plate out in appropriate collagen coated tissue culture vessels and culture at 37°C.

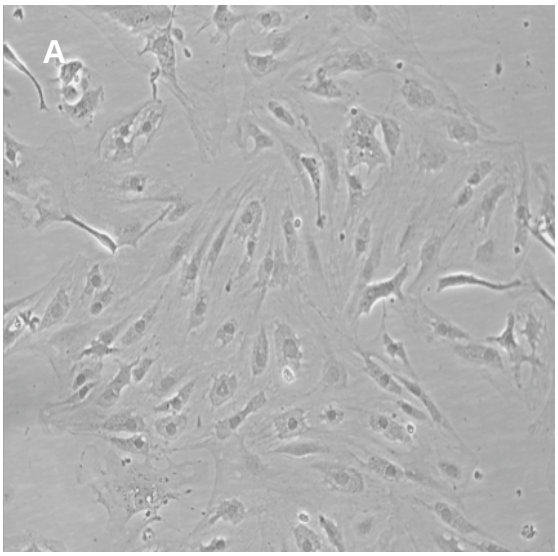
A

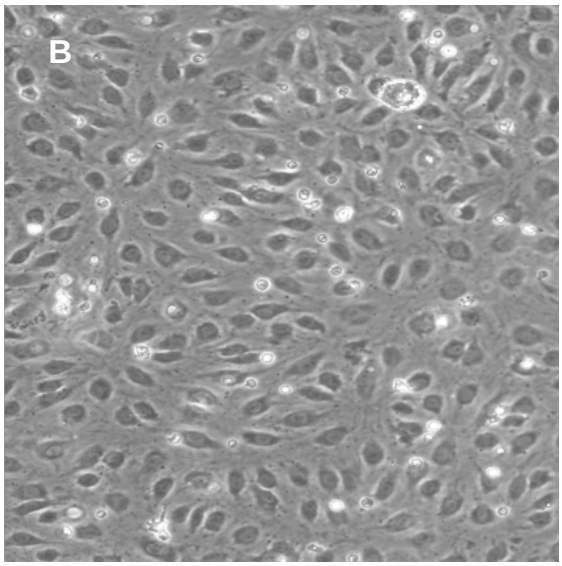
B

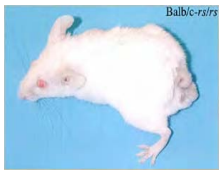

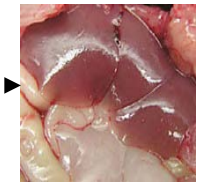

Wash tissue in PBS and inject livers with **2mg/ml** Collagenase IV in DMEM 10% FCS

Add remaining Collagenase and mince tissue with scalpels.

Incubate for 40 mins at 37°C agitating every 5mins.

Sieve through coarse mesh (250µm) followed by fine mesh (63µm) in an excess of PBS using a syringe bung.

Spin cells at **2500rpm/ 7min** Resuspend pellets in ~20ml PBS

Prepare Percoll gradient 2 50ml Falcons. 23%/50%. 20mls of each. Layer 10mls of cell suspension onto gradient. Spin **2500rpm/30mins/4c**.

Remove cells from the gradient interface and wash in an excess of PBS 2500rpm/7min/4°c. Resuspend in an appropriate volume of buffer and add α-CD146 microbeads (90µl buffer to 10µl beads per 10^7 cells). Incubate on ice shaking for ~15mins.

Prepare MACS columns, wash cell suspension with PBS (2500rpm/5min/4°c). Pass through MS columns and collect 'waste' and 'cell' fractions

Spin down both fractions. 2500rpm/7min/4°c. Resuspend pellets in RPMI+PSG and plate out into gelatin coated tissue culture vessels and culture at 37°C.

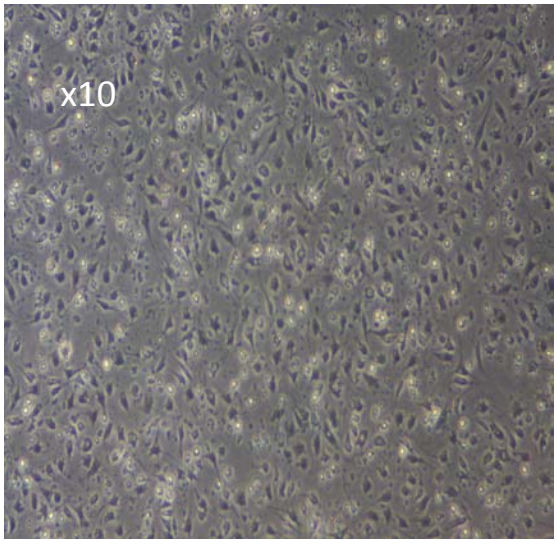
x10

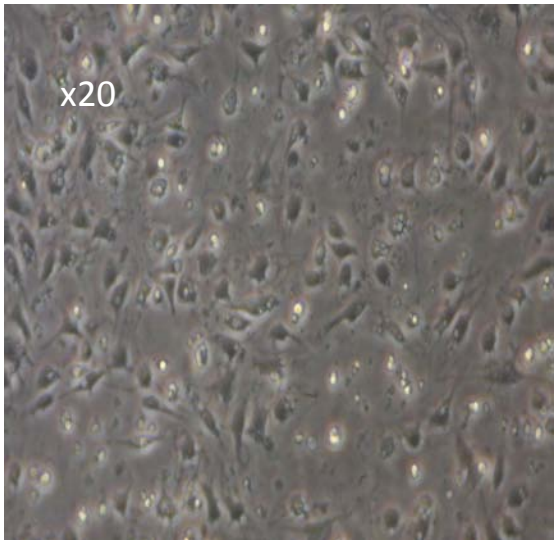
x20

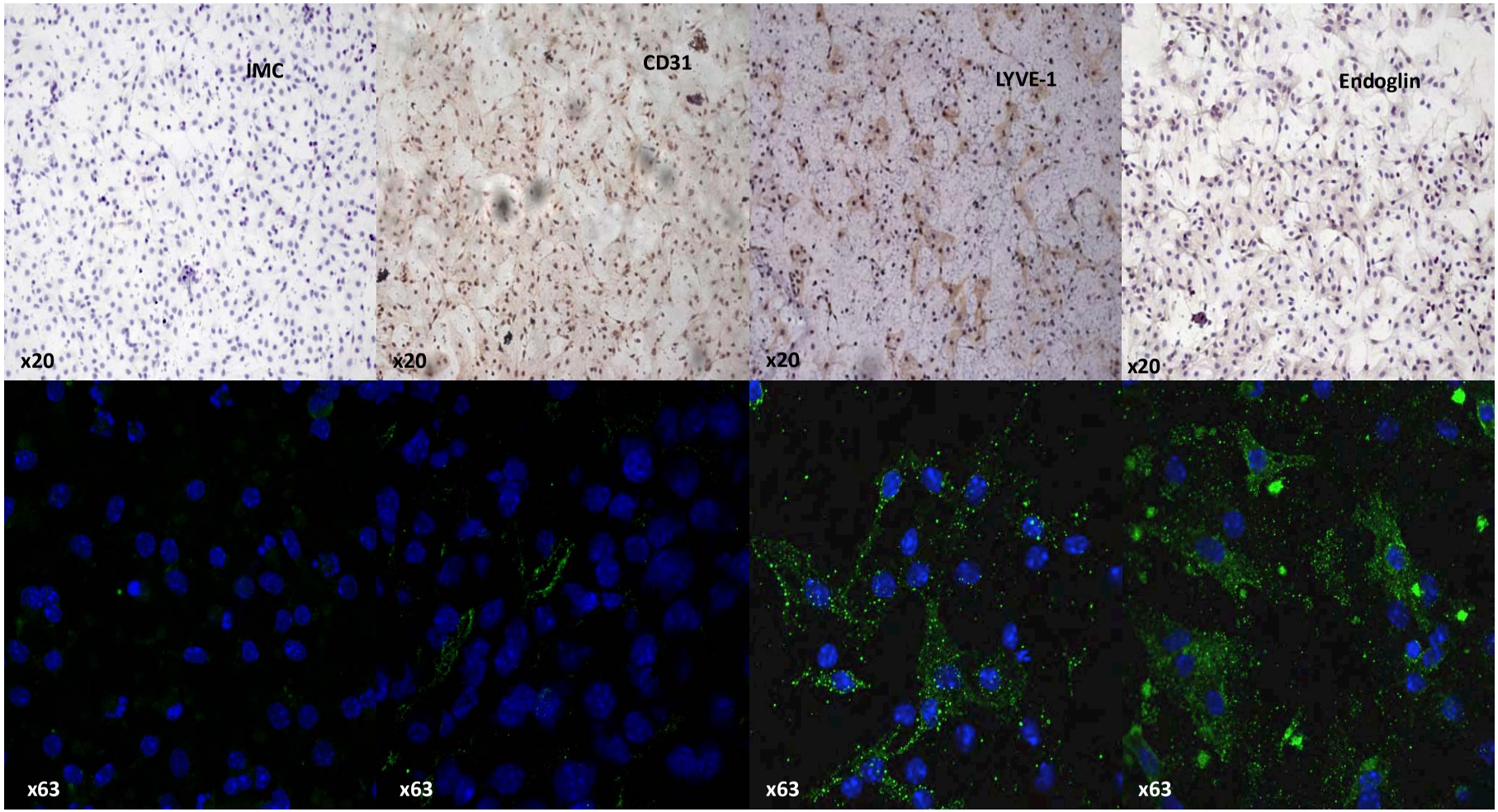
IMC
CD31
LYVE-1
Endoglin
x20
x20
x20
x20
x63
x63
x63
x63

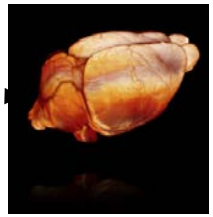

Wash and mince tissue and add 5ml/ brain **0.05mg/ml** Collagenase IV in DMEM 10% FCS

Incubate for 15 mins at 37°C agitating every 5mins. Wash PBS/ FCS

Sieve through Sigma cup followed by fine mesh (60µm) in an excess of PBS using a syringe bung.

Spin cells at **400G/5min** Resuspend in 15ml Sigma TrypLE, incubate at 37°C for 10mins

Wash in PBS/FCS and spin **400G/5min** to pellet cells. Resuspend pellet in PBS/FCS and pass through 4 MACS filters to obtain single cell suspension

Incubate with murine IgG (2.5µg Abcam) for 30mins at 4°C, wash and block with avidin for 30mins, wash and incubate with Biotin (Vectorshield) for 30mins, wash and add CD31-Biotin (3µg Cymbus Biotech) for 30mins. Resuspend pellet and add Rat IgG (5µg Sigma) and strep-Dynabeads (60µl Dynal) for 15mins at 4°C

Using EasySep magnet add half of cell pellet and leave for 5mins, pour of sup^{n}, wash 2x with PBS for 2mins. Remove tube from magnet and wash in PBS to obtain beads+cells.

Spin down cells+beads and waste fractions. **400G/5min**. Resuspend pellets in complete BMEC basal medium and plate out in appropriate gelatin coated tissue culture vessels and culture at 37°C.

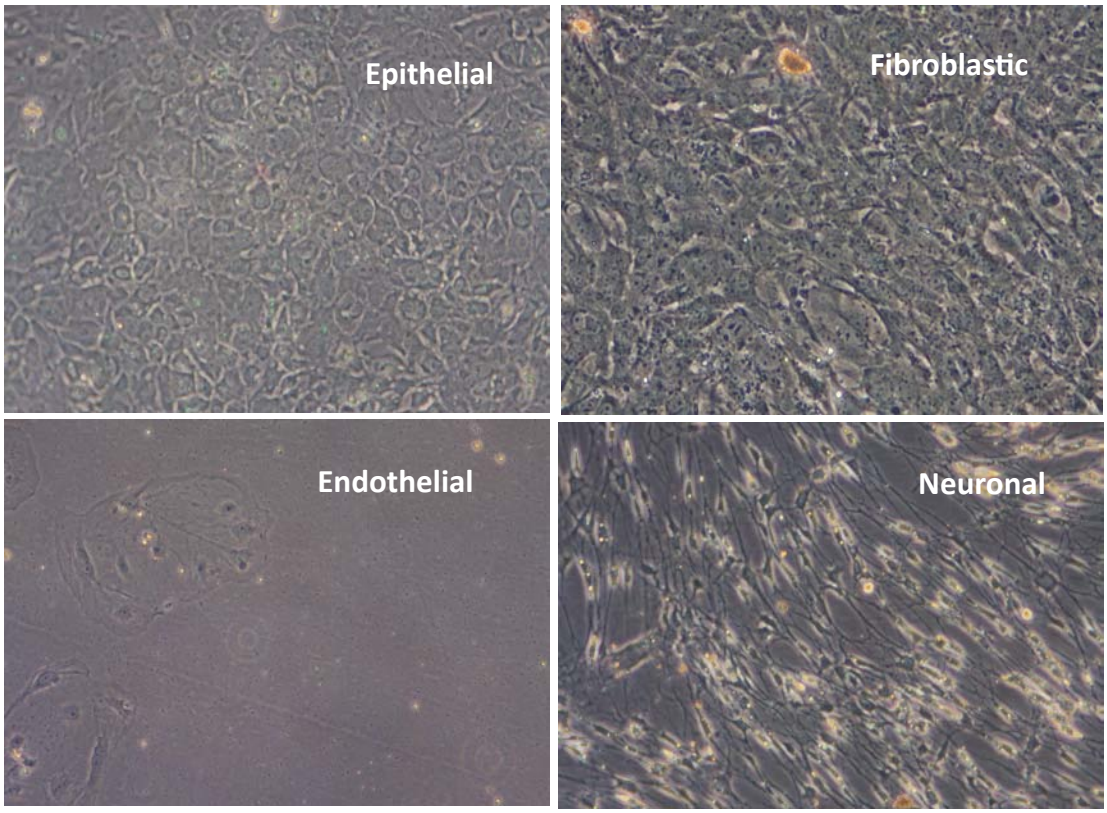
Epithelial
Fibroblastic
Endothelial
Neuronal

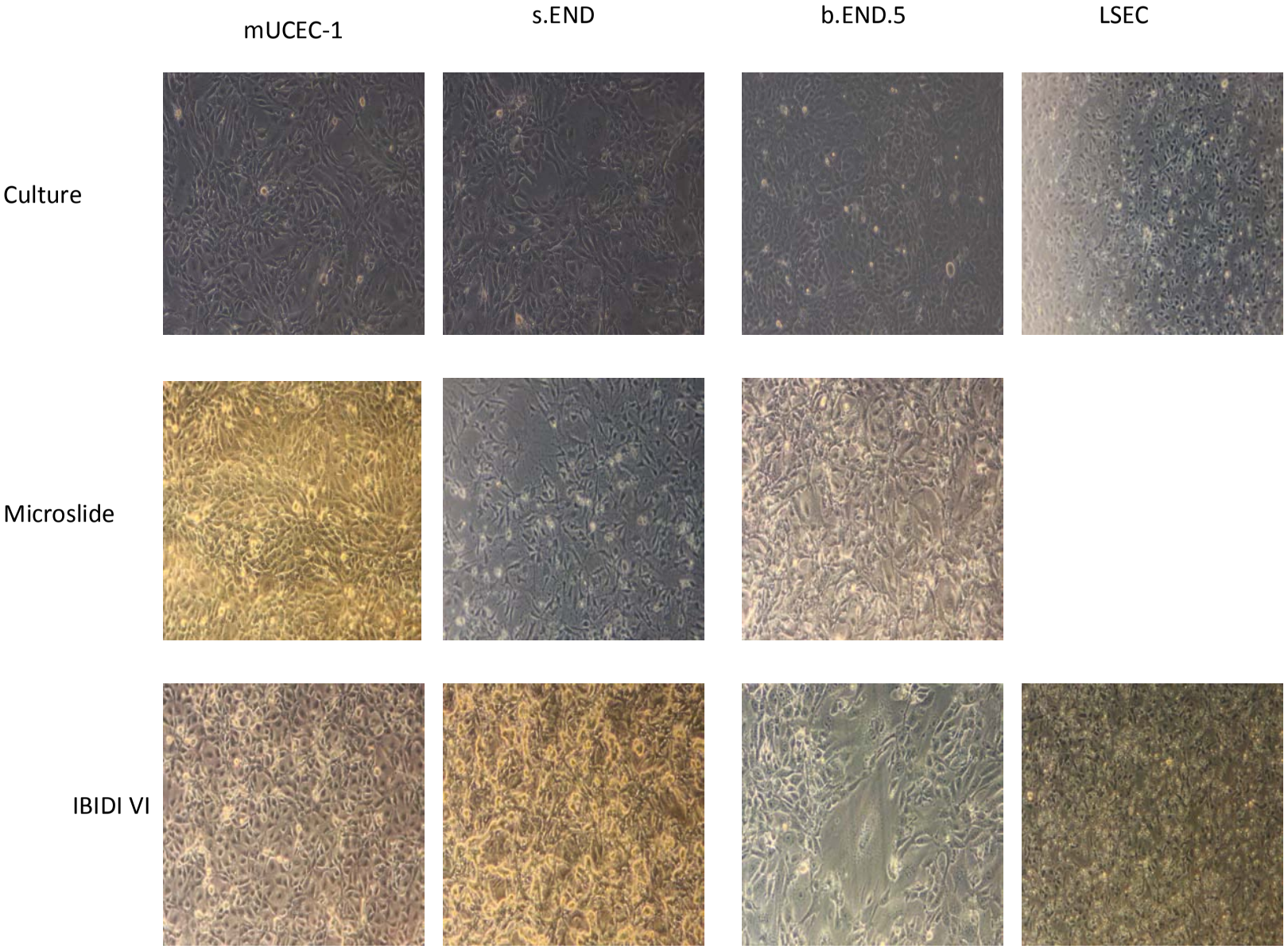
mUCEC-1
s.END
b.END.5
LSEC
Culture
Microslide
IBIDI VI

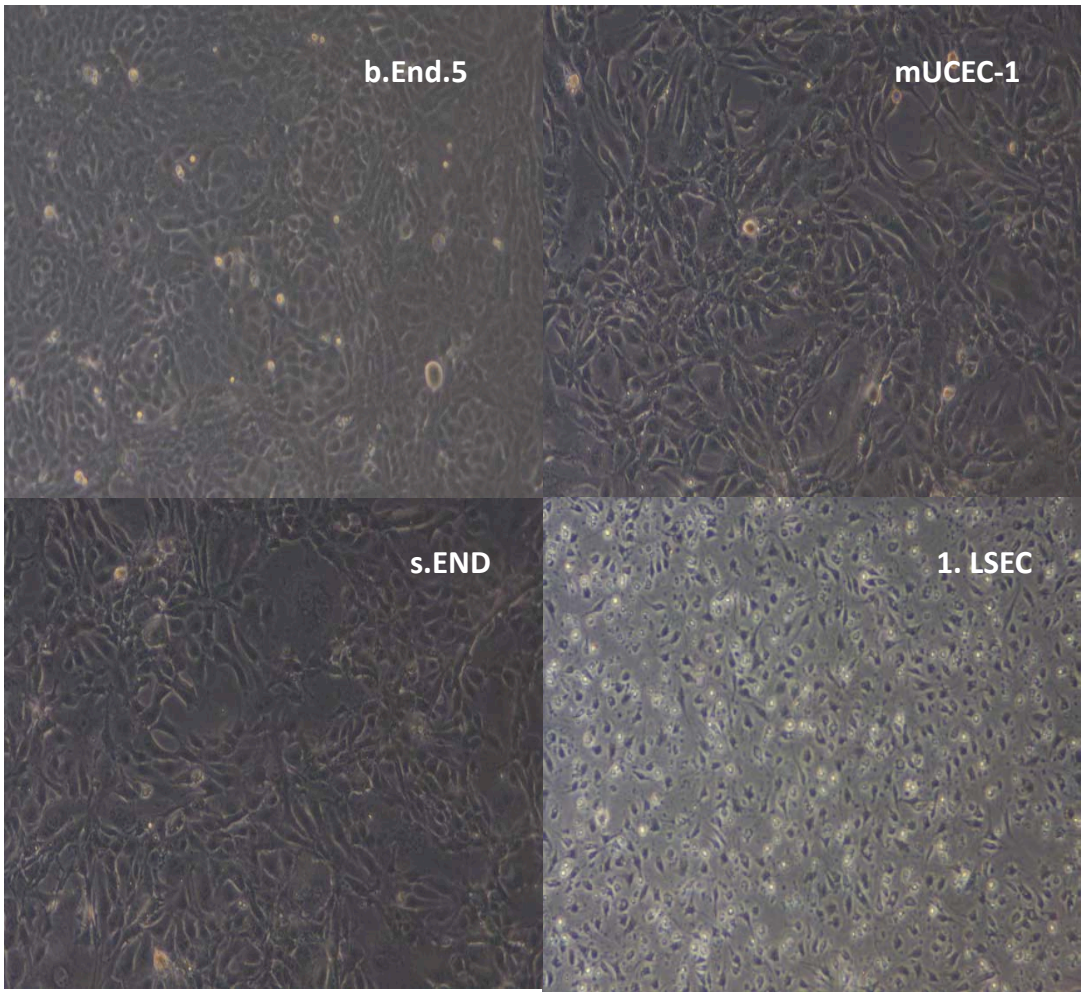
b.End.5
mUCEC-1
s.END
1. LSEC

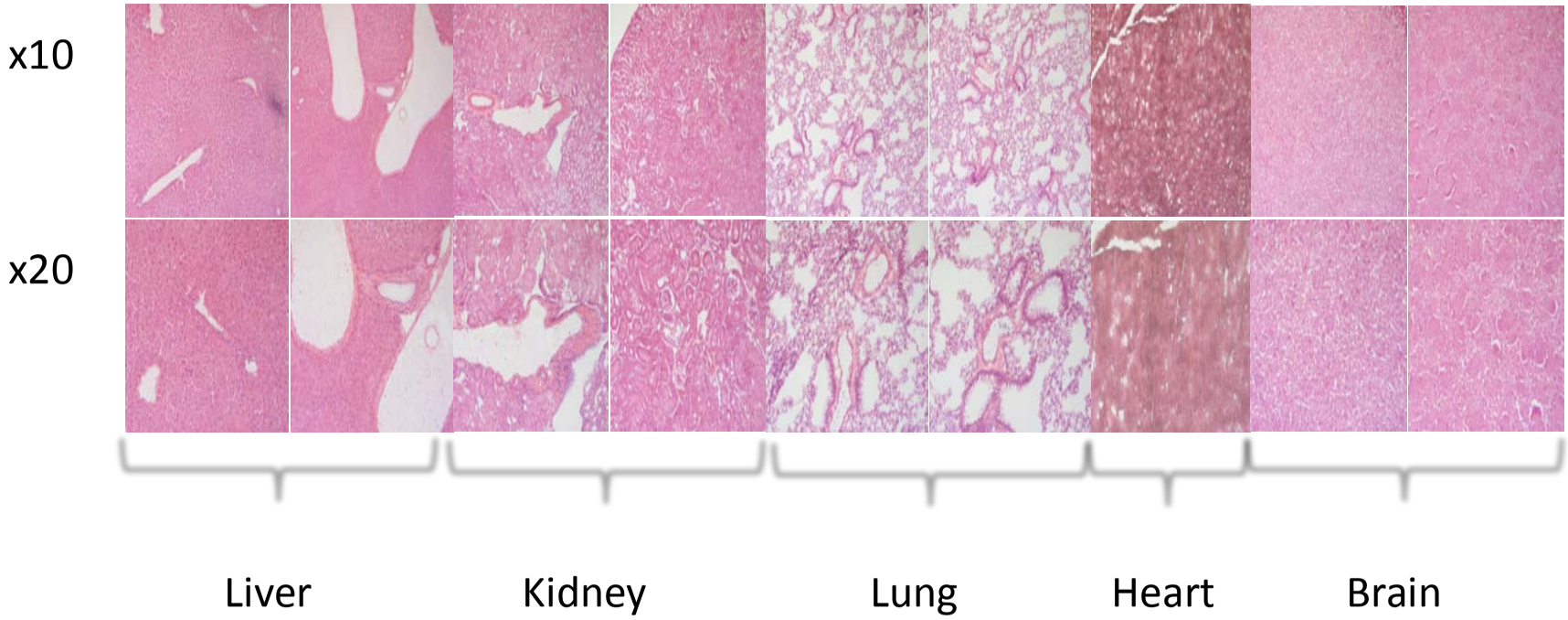
x10
x20
Liver
Kidney
Lung
Heart
Brain

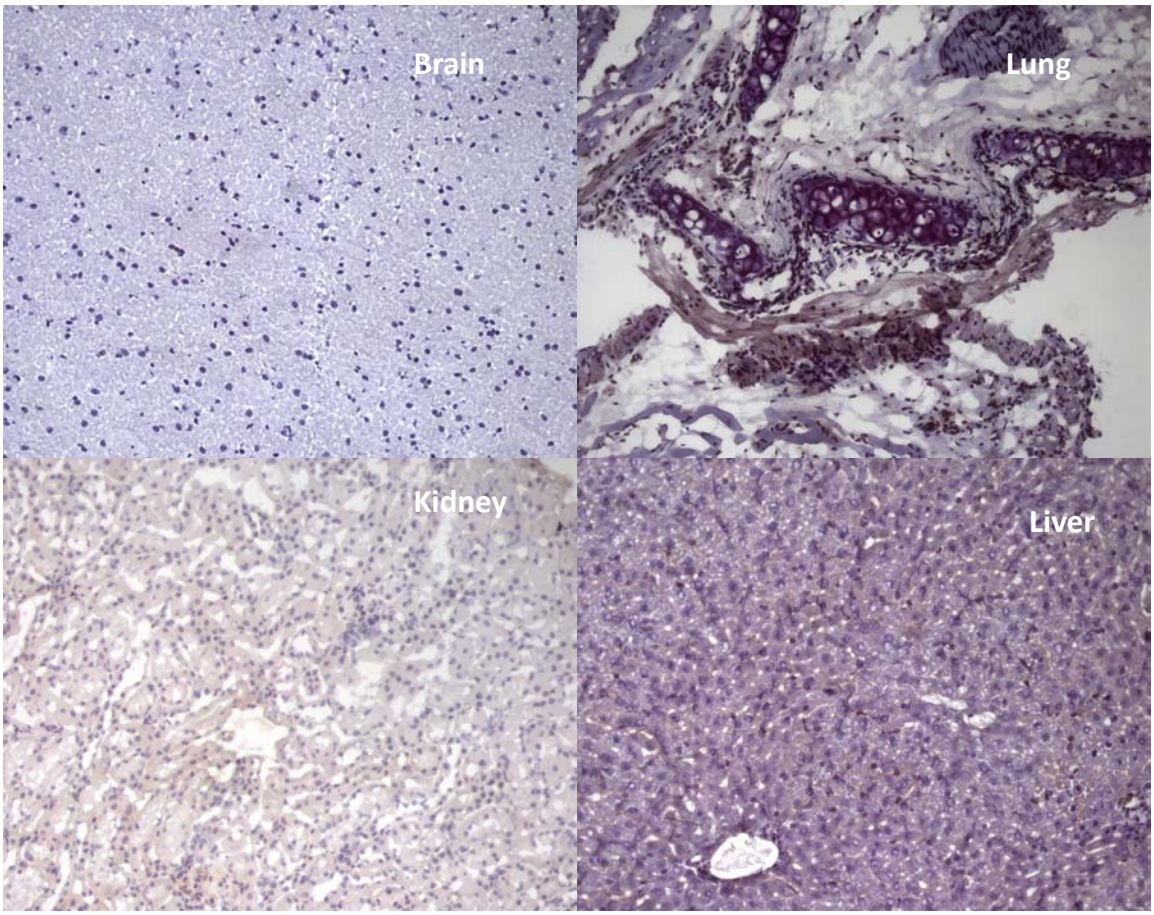
Brain
Lung
Kidney
Liver

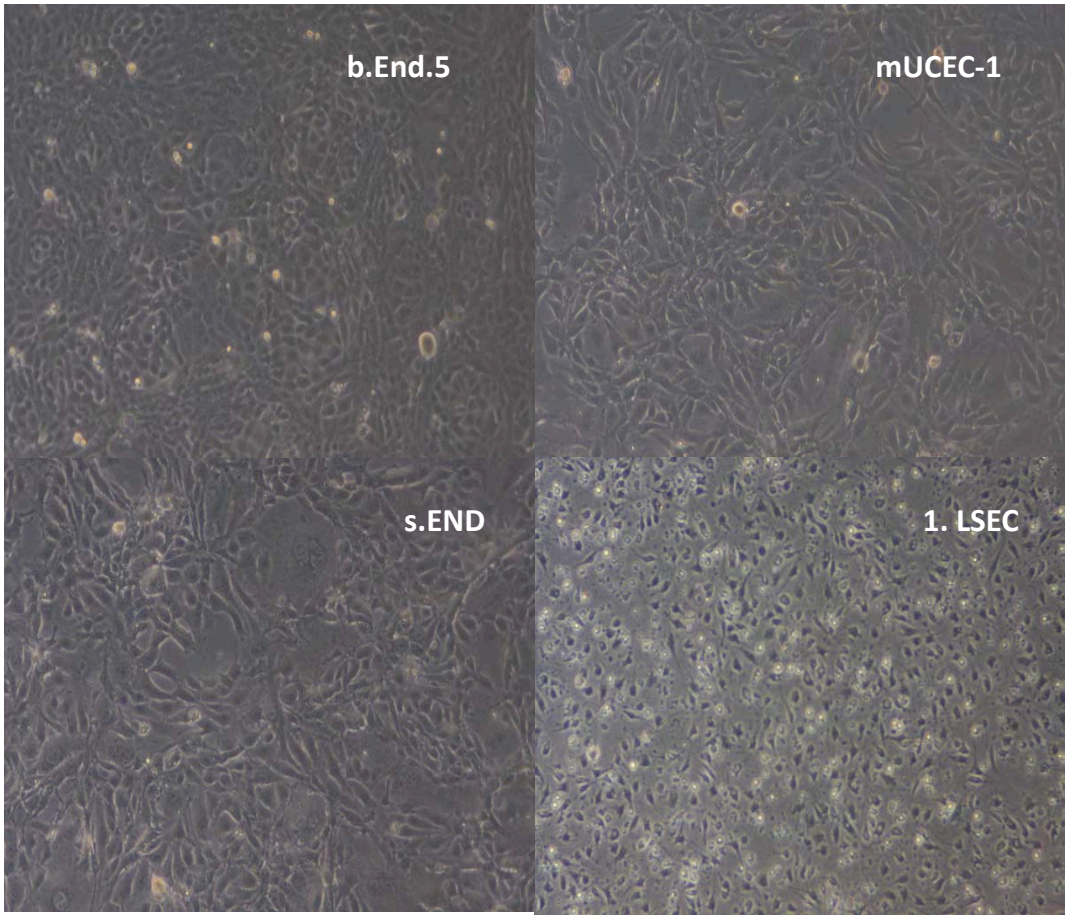
b.End.5
mUCEC-1
s.END
1. LSEC

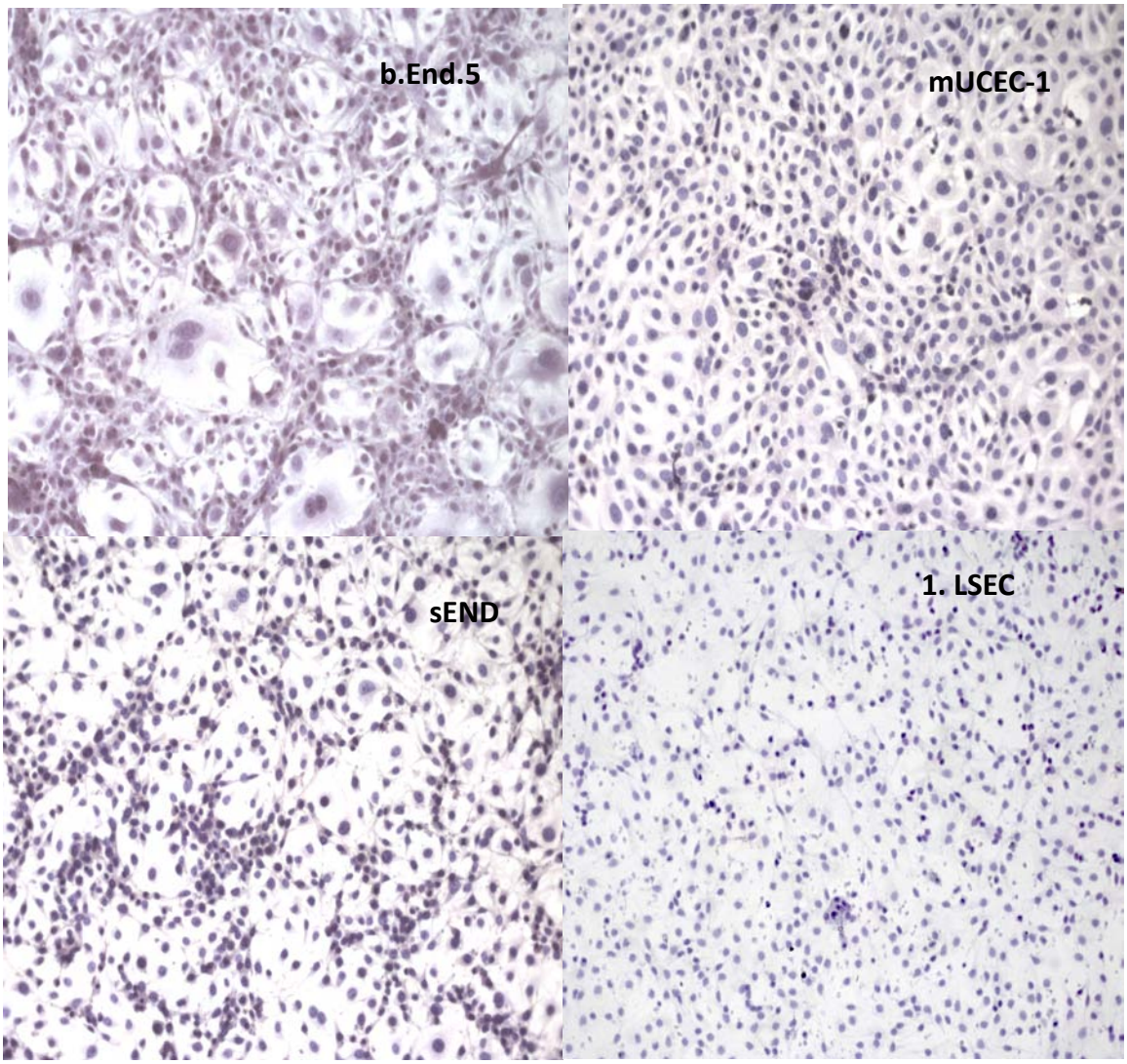
b.End.5
mUCEC-1
sEND
1. LSEC

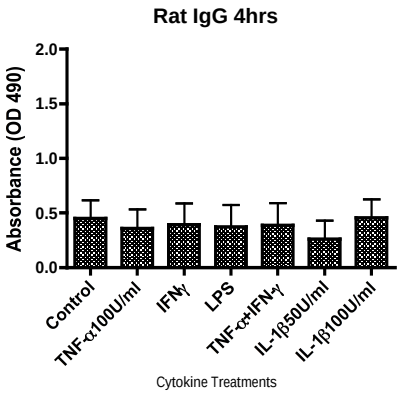
Rat IgG 4hrs
Absorbance (OD 490)
2.0
1.5
1.0
0.5
0.0
Control
TNF-α100U/ml
IFNγ
LPS
TNF-α+IFN-γ
IL-1β50U/ml
IL-1β100U/ml
Cytokine Treatments

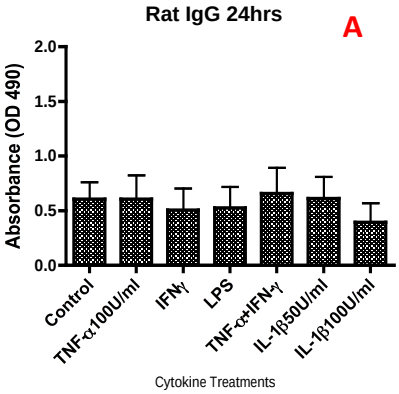
Rat IgG 24hrs
A
Absorbance (OD 490)
2.0
1.5
1.0
0.5
0.0
Control
TNF-α100U/ml
IFNγ
LPS
TNF-α+IFN-γ
IL-1β50U/ml
IL-1β100U/ml
Cytokine Treatments

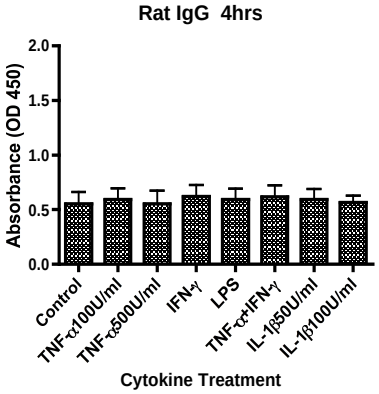
Rat IgG 4hrs
Absorbance (OD 450)
2.0
1.5
1.0
0.5
0.0
Control
TNF-α100U/ml
TNF-α500U/ml
IFN-γ
LPS
TNF-α+IFN-γ
IL-1β50U/ml
IL-1β100U/ml
Cytokine Treatment

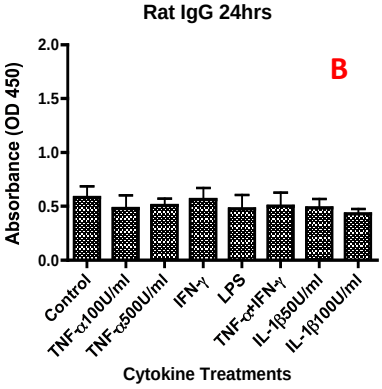
Rat IgG 24hrs
B
Absorbance (OD 450)
2.0
1.5
1.0
0.5
0.0
Control
TNF-α100U/ml
TNF-α500U/ml
IFN-γ
LPS
TNF-α+IFN-γ
IL-1β50U/ml
IL-1β100U/ml
Cytokine Treatments

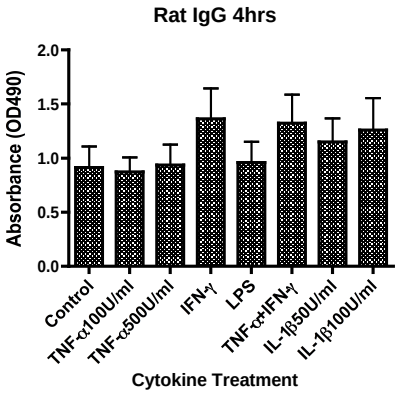
Rat IgG 4hrs
Absorbance (OD490)
2.0
1.5
1.0
0.5
0.0
Control
TNF-α100U/ml
TNF-α500U/ml
IFN-γ
LPS
TNF-α+IFN-γ
IL-1β50U/ml
IL-1β100U/ml
Cytokine Treatment

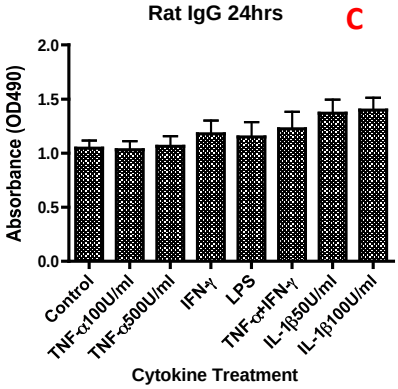
Rat IgG 24hrs
C
Absorbance (OD490)
2.0
1.5
1.0
0.5
0.0
Control
TNF-α100U/ml
TNF-α500U/ml
IFN-γ
LPS
TNF-α+IFN-γ
IL-1β50U/ml
IL-1β100U/ml
Cytokine Treatment

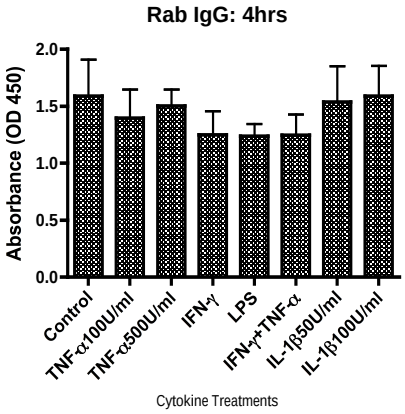
Rab IgG: 4hrs
Absorbance (OD 450)
2.0
1.5
1.0
0.5
0.0
Control
TNF-α100U/ml
TNF-α500U/ml
IFN-γ
LPS
IFN-γ+TNF-α
IL-1β50U/ml
IL-1β100U/ml
Cytokine Treatments

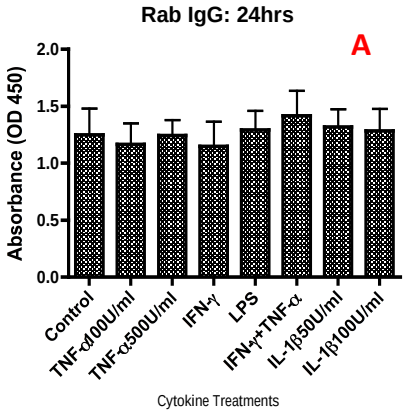
Rab IgG: 24hrs
A
Absorbance (OD 450)
2.0
1.5
1.0
0.5
0.0
Control
TNF-α100U/ml
TNF-α500U/ml
IFN-γ
LPS
IFN-γ+TNF-α
IL-1β50U/ml
IL-1β100U/ml
Cytokine Treatments

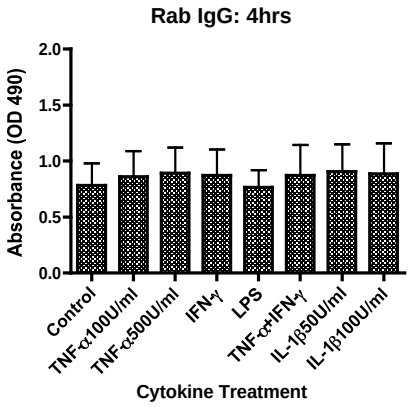
Rab IgG: 4hrs
Absorbance (OD 490)
2.0
1.5
1.0
0.5
0.0
Control
TNF-α100U/ml
TNF-α500U/ml
IFN-γ
LPS
TNF-α+IFN-γ
IL-1β50U/ml
IL-1β100U/ml
Cytokine Treatment

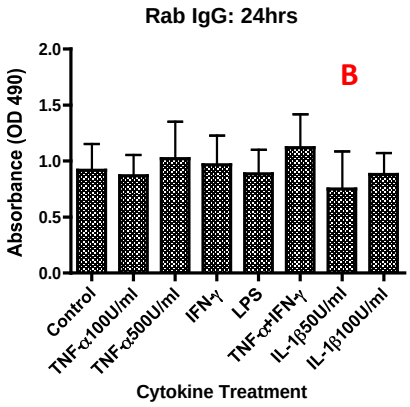
Rab IgG: 24hrs
B
Absorbance (OD 490)
2.0
1.5
1.0
0.5
0.0
Control
TNF-α100U/ml
TNF-α500U/ml
IFN-γ
LPS
TNF-α+IFN-γ
IL-1β50U/ml
IL-1β100U/ml
Cytokine Treatment

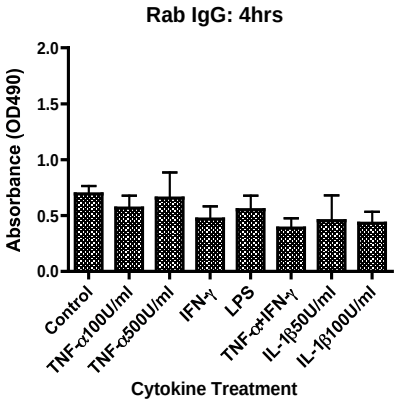
Rab IgG: 4hrs
Absorbance (OD490)
2.0
1.5
1.0
0.5
0.0
Control
TNF-α100U/ml
TNF-α500U/ml
IFN-γ
LPS
TNF-α+IFN-γ
IL-1β50U/ml
IL-1β100U/ml
Cytokine Treatment

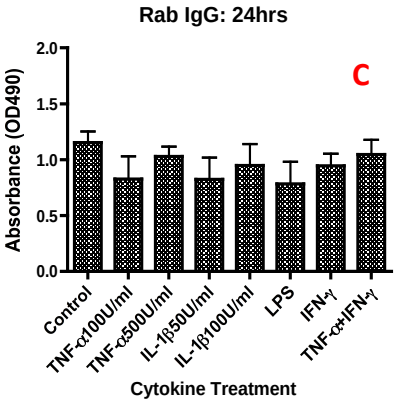
Rab IgG: 24hrs
C
Absorbance (OD490)
2.0
1.5
1.0
0.5
0.0
Control
TNF-α100U/ml
TNF-α500U/ml
IL-1β50U/ml
IL-1β100U/ml
LPS
IFN-γ
TNF-α+IFN-γ
Cytokine Treatment

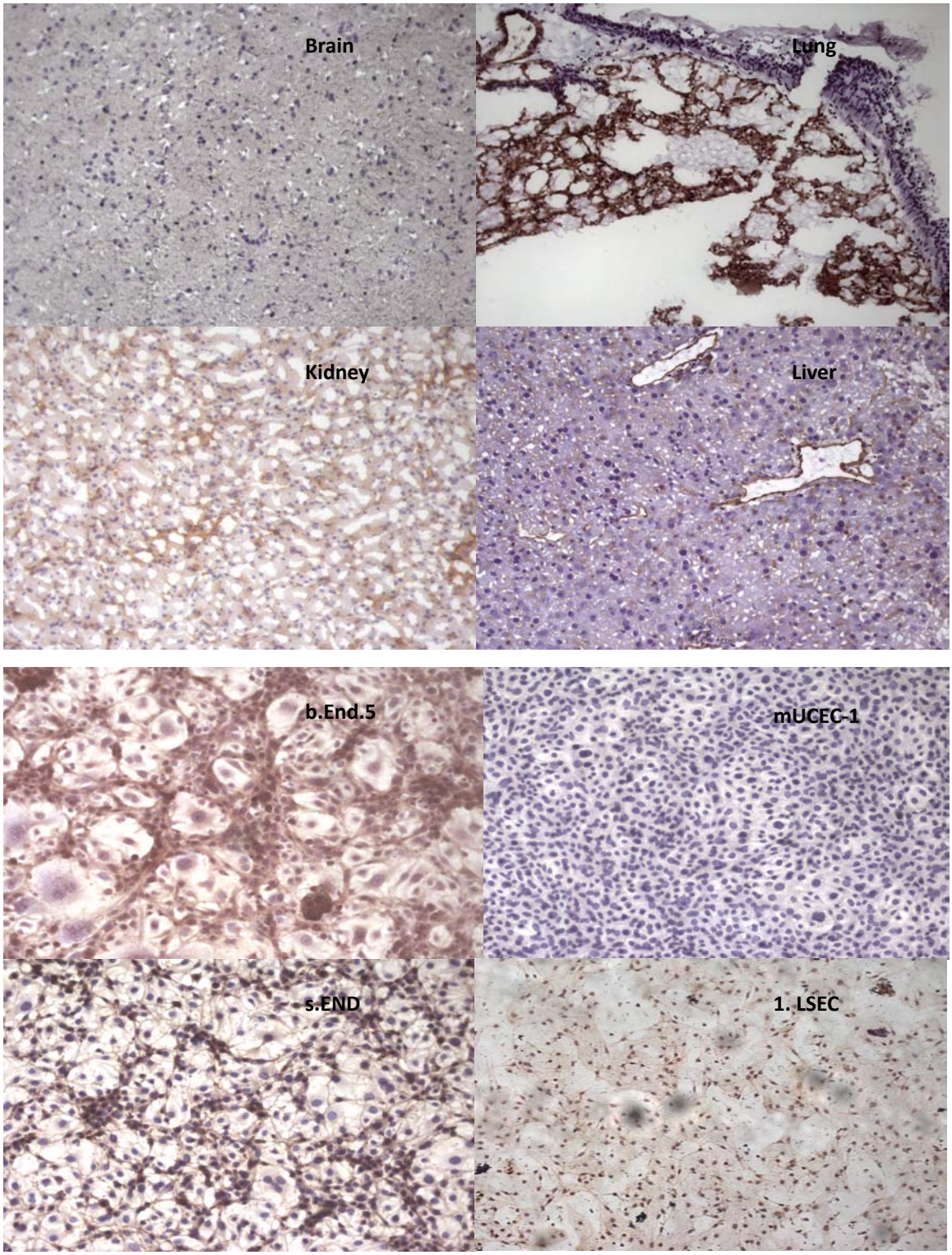
Brain
Lung
Kidney
Liver
b.End.5
mUCEC-1
s.END
1. LSEC

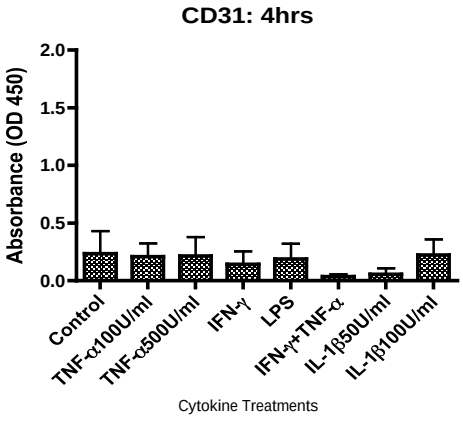
CD31: 4hrs
Absorbance (OD 450)
2.0
1.5
1.0
0.5
0.0
Control
TNF-α100U/ml
TNF-α500U/ml
IFN-γ
LPS
IFN-γ+TNF-α
IL-1β50U/ml
IL-1β100U/ml
Cytokine Treatments

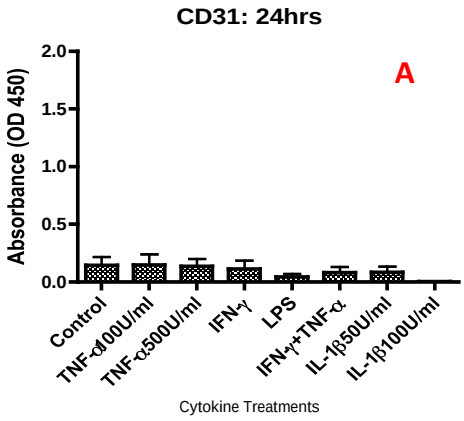
CD31: 24hrs
A
Absorbance (OD 450)
2.0
1.5
1.0
0.5
0.0
Control
TNF-α100U/ml
TNF-α500U/ml
IFN-γ
LPS
IFN-γ+TNF-α
IL-1β50U/ml
IL-1β100U/ml
Cytokine Treatments

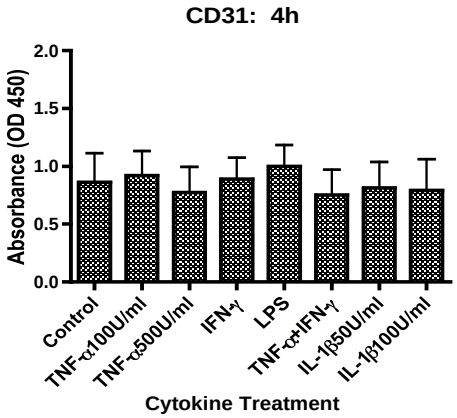
CD31: 4h
Absorbance (OD 450)
2.0
1.5
1.0
0.5
0.0
Control
TNF-α100U/ml
TNF-α500U/ml
IFN-γ
LPS
TNF-α+IFN-γ
IL-1β50U/ml
IL-1β100U/ml
Cytokine Treatment

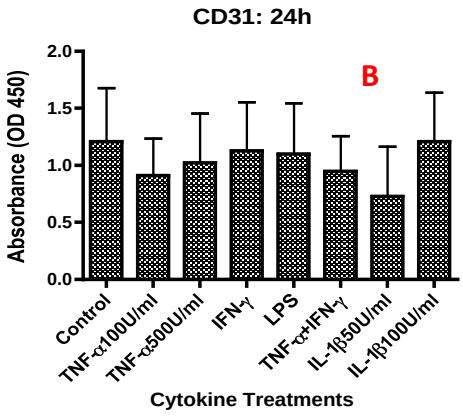
CD31: 24h
B
Absorbance (OD 450)
2.0
1.5
1.0
0.5
0.0
Control
TNF-α100U/ml
TNF-α500U/ml
IFN-γ
LPS
TNF-α+IFN-γ
IL-1β50U/ml
IL-1β100U/ml
Cytokine Treatments

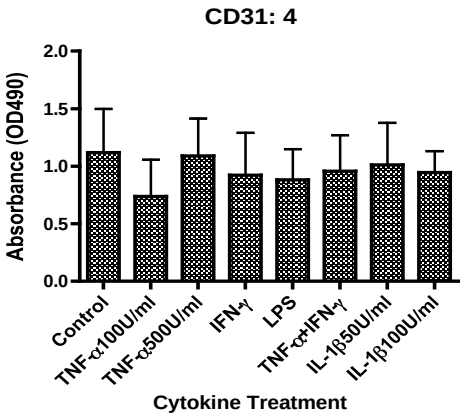
CD31: 4
Absorbance (OD490)
2.0
1.5
1.0
0.5
0.0
Control
TNF-α100U/ml
TNF-α500U/ml
IFN-γ
LPS
TNF-α+IFN-γ
IL-1β50U/ml
IL-1β100U/ml
Cytokine Treatment

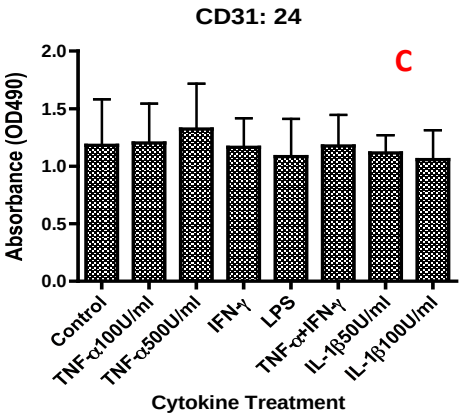
CD31: 24
C
Absorbance (OD490)
2.0
1.5
1.0
0.5
0.0
Control
TNF-α100U/ml
TNF-α500U/ml
IFN-γ
LPS
TNF-α+IFN-γ
IL-1β50U/ml
IL-1β100U/ml
Cytokine Treatment

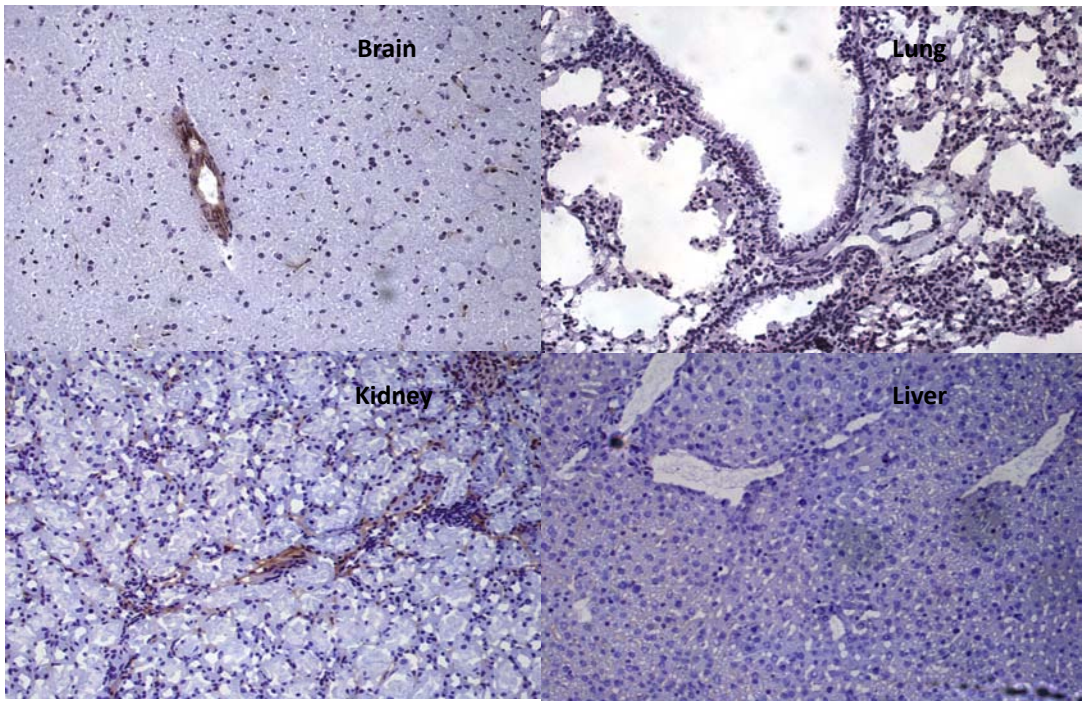
Brain
Lung
Kidney
Liver

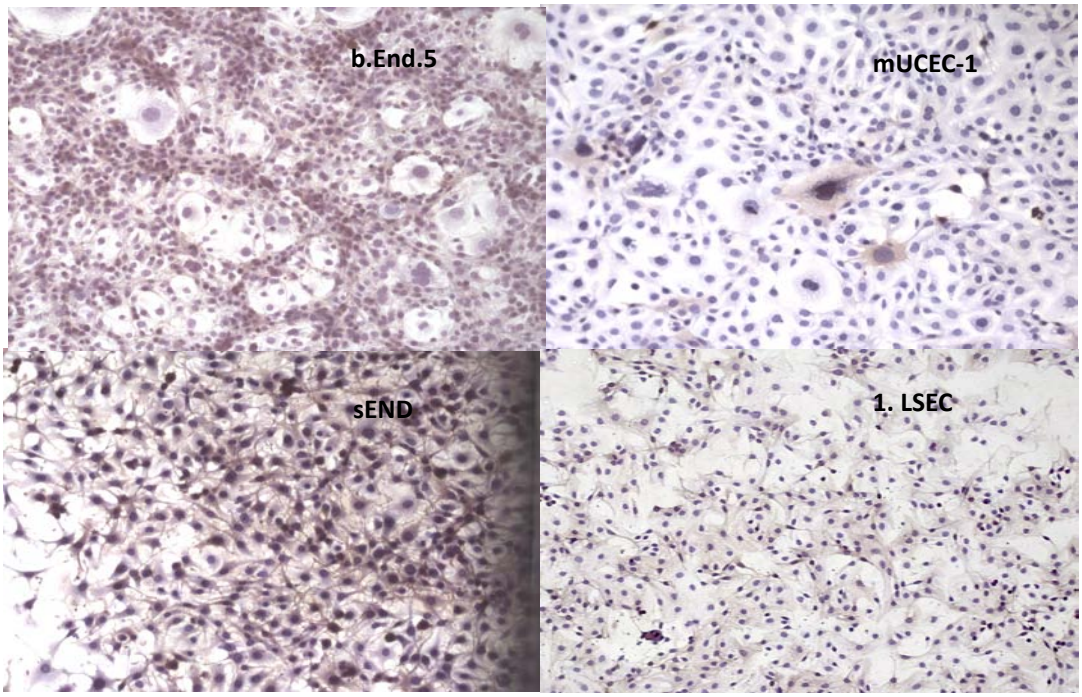
b.End.5
mUCEC-1
sEND
1. LSEC

***

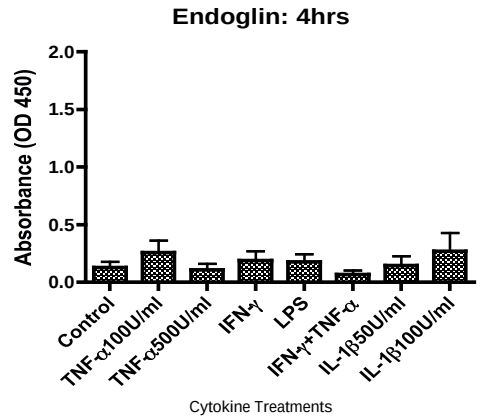
Endoglin: 4hrs
Absorbance (OD 450)
2.0
1.5
1.0
0.5
0.0
Control
TNF-α100U/ml
TNF-α500U/ml
IFN-γ
LPS
IFN-γ+TNF-α
IL-1β50U/ml
IL-1β100U/ml
Cytokine Treatments

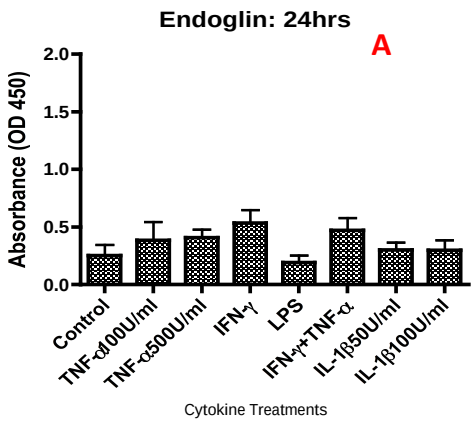
Endoglin: 24hrs
A
Absorbance (OD 450)
2.0
1.5
1.0
0.5
0.0
Control
TNF-α100U/ml
TNF-α500U/ml
IFN-γ
LPS
IFN-γ+TNF-α
IL-1β50U/ml
IL-1β100U/ml
Cytokine Treatments

***

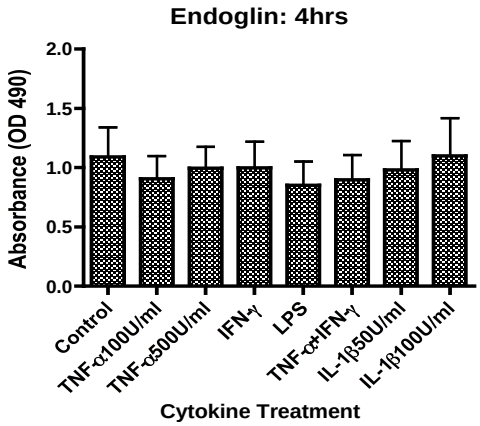
Endoglin: 4hrs
Absorbance (OD 490)
2.0
1.5
1.0
0.5
0.0
Control
TNF-α100U/ml
TNF-α500U/ml
IFN-γ
LPS
TNF-α+IFN-γ
IL-1β50U/ml
IL-1β100U/ml
Cytokine Treatment

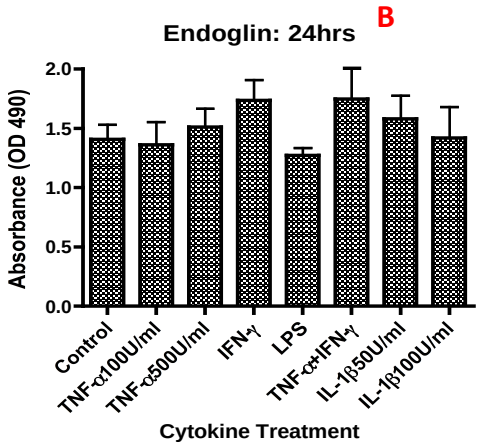
Endoglin: 24hrs
B
Absorbance (OD 490)
2.0
1.5
1.0
0.5
0.0
Control
TNF-α100U/ml
TNF-α500U/ml
IFN-γ
LPS
TNF-α+IFN-γ
IL-1β50U/ml
IL-1β100U/ml
Cytokine Treatment

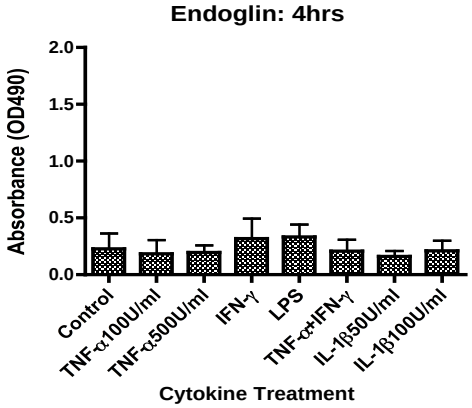
Endoglin: 4hrs
Absorbance (OD490)
2.0
1.5
1.0
0.5
0.0
Control
TNF-α100U/ml
TNF-α500U/ml
IFN-γ
LPS
TNF-α+IFN-γ
IL-1β50U/ml
IL-1β100U/ml
Cytokine Treatment

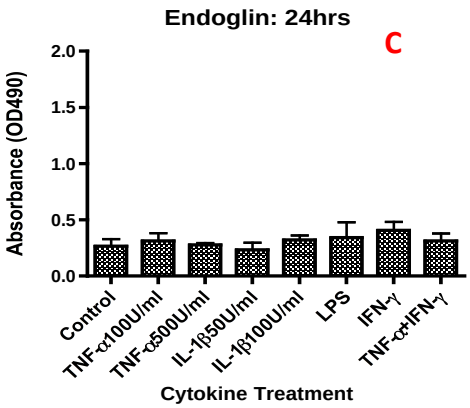
Endoglin: 24hrs
C
Absorbance (OD490)
2.0
1.5
1.0
0.5
0.0
Control
TNF-α100U/ml
TNF-α500U/ml
IL-1β50U/ml
IL-1β100U/ml
LPS
IFN-γ
TNF-α+IFN-γ
Cytokine Treatment

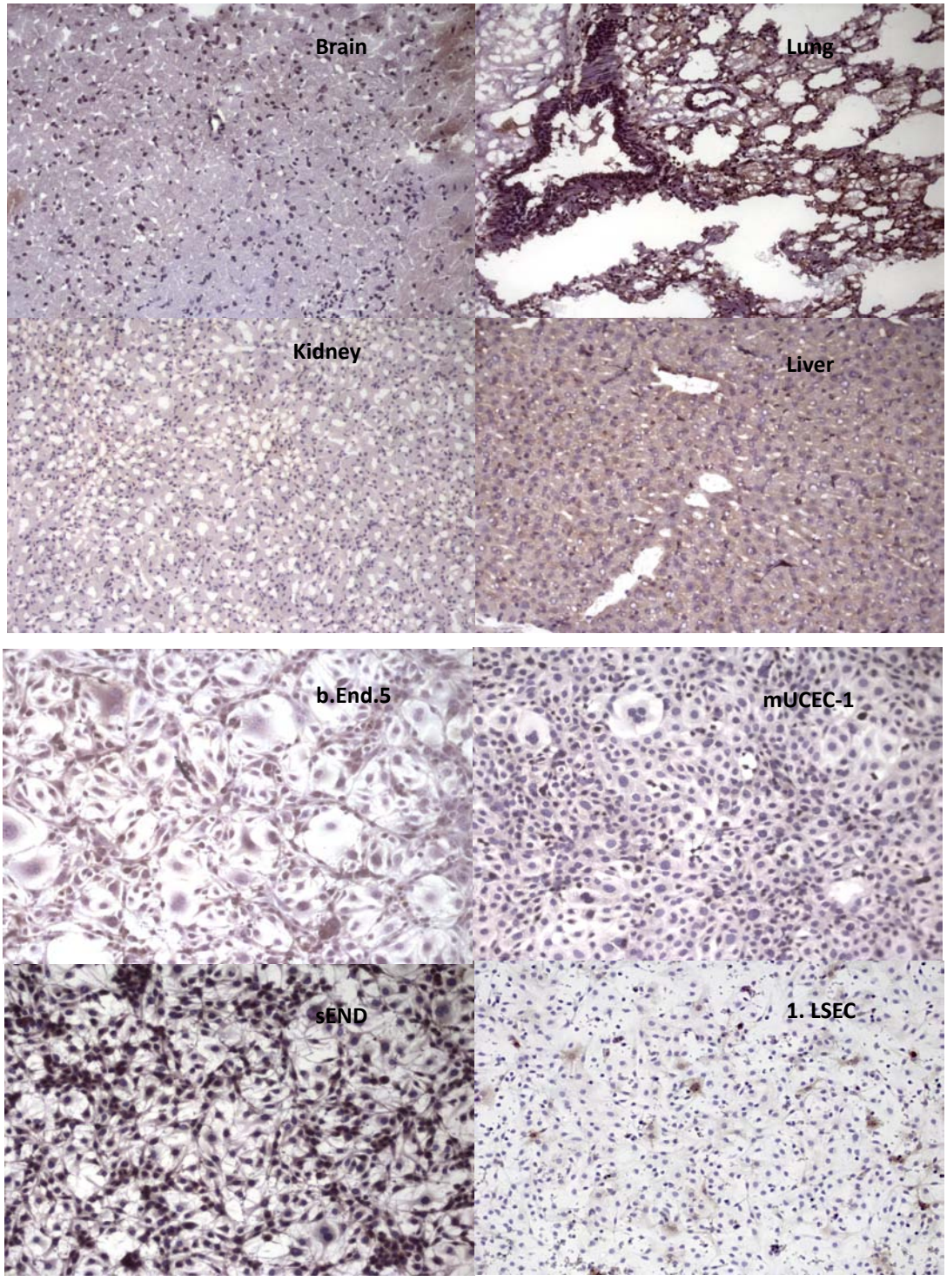
Brain
Lung
Kidney
Liver
b.End.5
mUCEC-1
sEND
1. LSEC

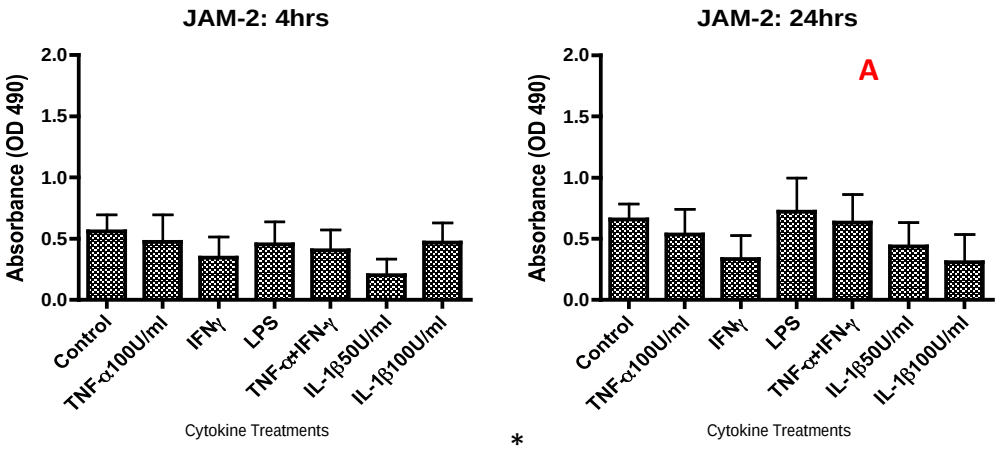
JAM-2: 4hrs
Absorbance (OD 490)
2.0
1.5
1.0
0.5
0.0
Control
TNF-α100U/ml
IFNγ
LPS
TNF-α+IFN-γ
IL-1β50U/ml
IL-1β100U/ml
Cytokine Treatments
JAM-2: 24hrs
A
Absorbance (OD 490)
Cytokine Treatments

*

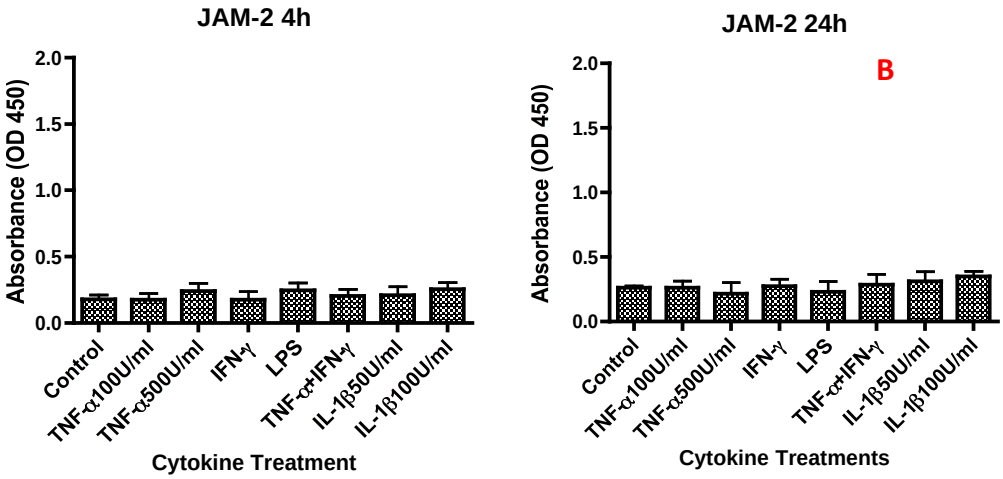
JAM-2 4h
Absorbance (OD 450)
Control
TNF-α100U/ml
TNF-α500U/ml
IFN-γ
LPS
TNF-α+IFN-γ
IL-1β50U/ml
IL-1β100U/ml
Cytokine Treatment
JAM-2 24h
B
Absorbance (OD 450)
Cytokine Treatments

***

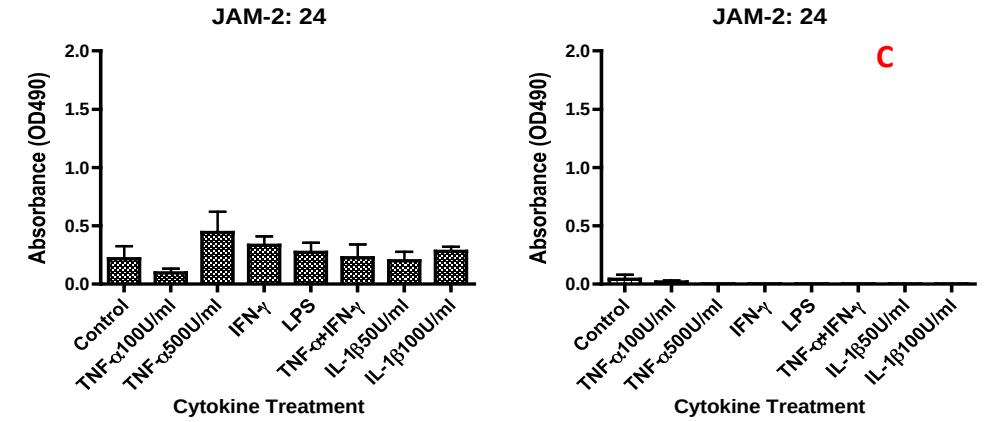
JAM-2: 24
Absorbance (OD490)
Control
TNF-α100U/ml
TNF-α500U/ml
IFN-γ
LPS
TNF-α+IFN-γ
IL-1β50U/ml
IL-1β100U/ml
Cytokine Treatment
JAM-2: 24
C
Absorbance (OD490)
Cytokine Treatment

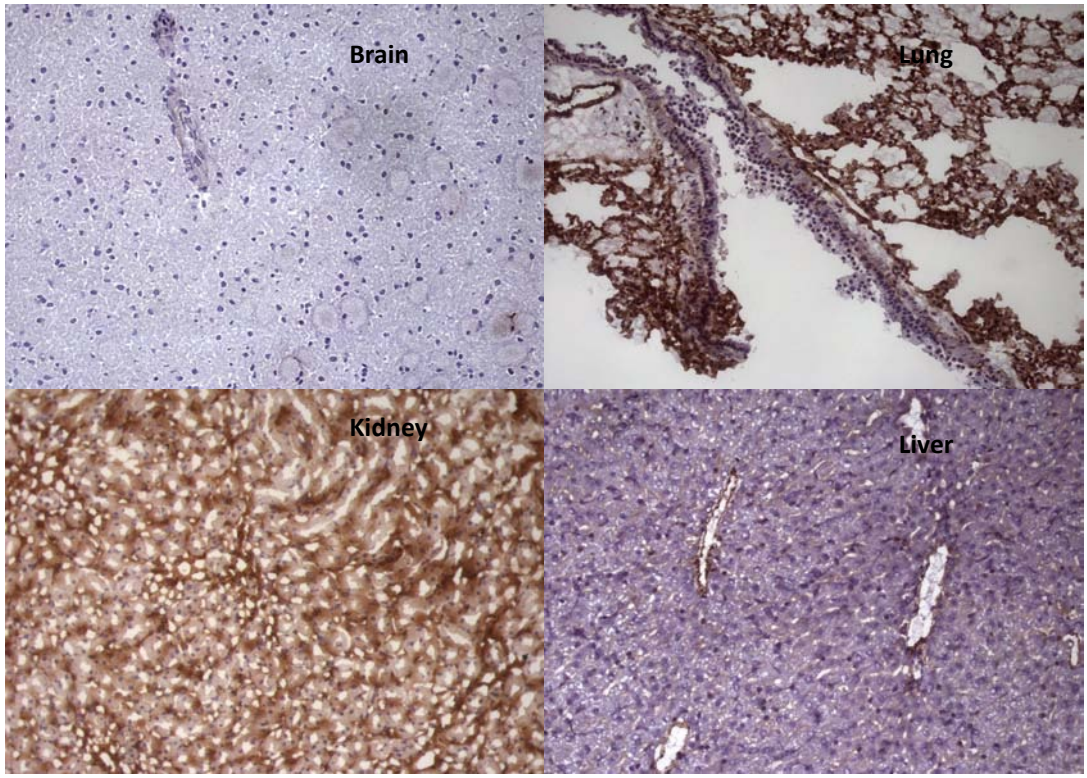
Brain
Lung
Kidney
Liver

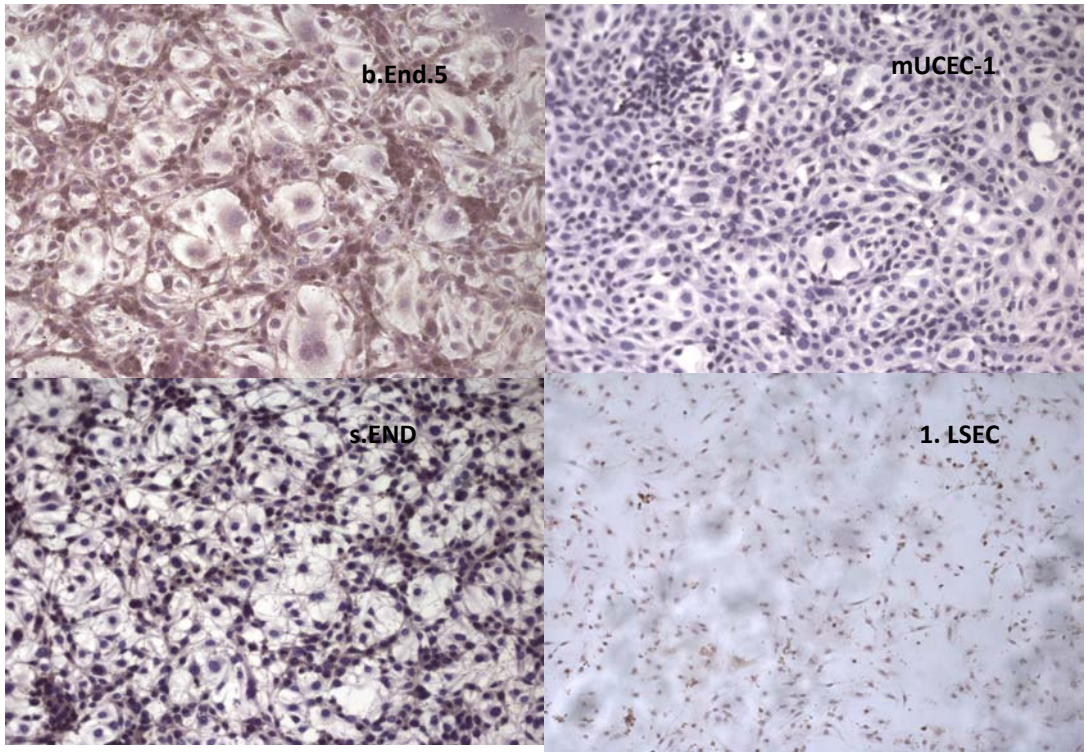
b.End.5
mUCEC-1
s.END
1. LSEC

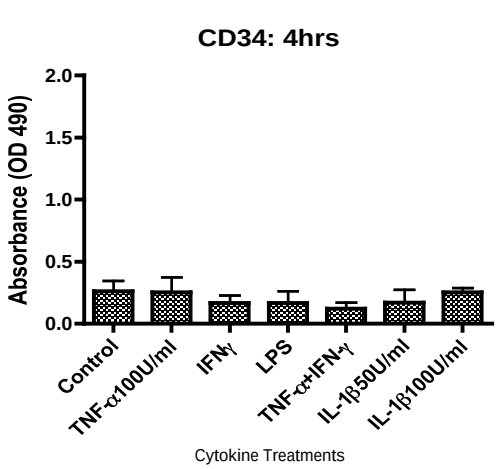
CD34: 4hrs
Absorbance (OD 490)
2.0
1.5
1.0
0.5
0.0
Control
TNF-α100U/ml
IFNγ
LPS
TNF-α+IFN-γ
IL-1β50U/ml
IL-1β100U/ml
Cytokine Treatments

*

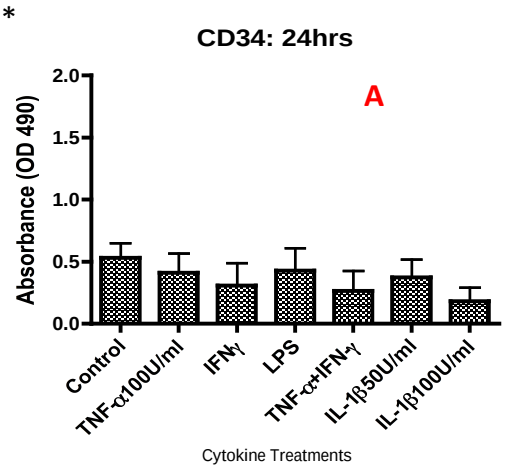
CD34: 24hrs
A
Absorbance (OD 490)
2.0
1.5
1.0
0.5
0.0
Control
TNF-α100U/ml
IFNγ
LPS
TNF-α+IFN-γ
IL-1β50U/ml
IL-1β100U/ml
Cytokine Treatments

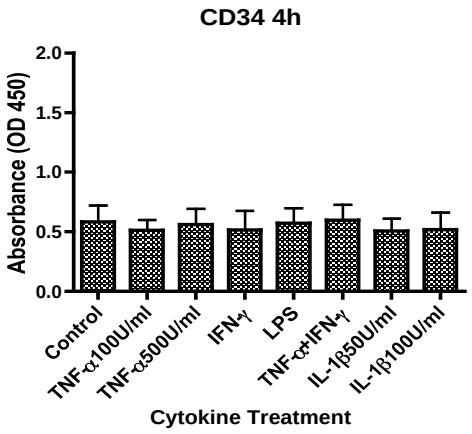
CD34 4h
Absorbance (OD 450)
2.0
1.5
1.0
0.5
0.0
Control
TNF-α100U/ml
TNF-α500U/ml
IFN-γ
LPS
TNF-α+IFN-γ
IL-1β50U/ml
IL-1β100U/ml
Cytokine Treatment

*

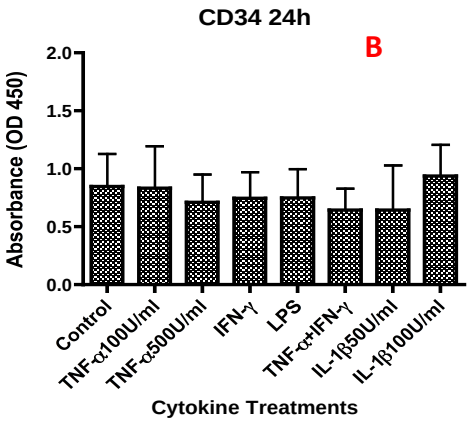
CD34 24h
B
Absorbance (OD 450)
2.0
1.5
1.0
0.5
0.0
Control
TNF-α100U/ml
TNF-α500U/ml
IFN-γ
LPS
TNF-α+IFN-γ
IL-1β50U/ml
IL-1β100U/ml
Cytokine Treatments

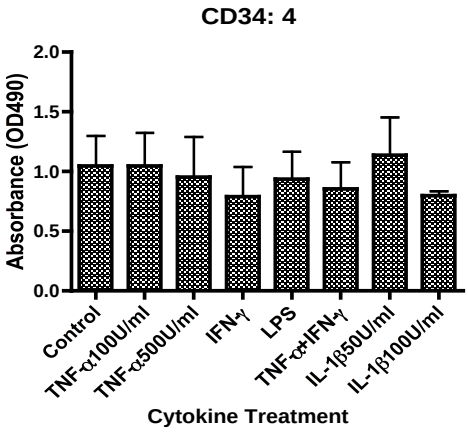
CD34: 4
Absorbance (OD490)
2.0
1.5
1.0
0.5
0.0
Control
TNF-α100U/ml
TNF-α500U/ml
IFN-γ
LPS
TNF-α+IFN-γ
IL-1β50U/ml
IL-1β100U/ml
Cytokine Treatment

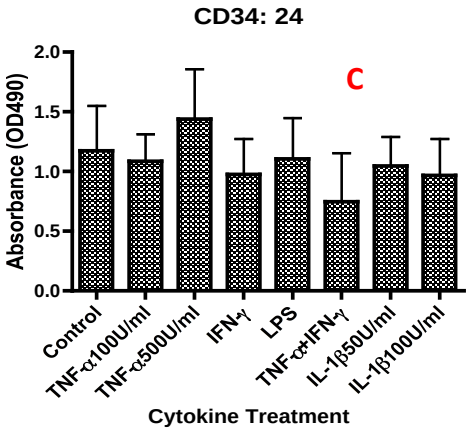
CD34: 24
C
Absorbance (OD490)
2.0
1.5
1.0
0.5
0.0
Control
TNF-α100U/ml
TNF-α500U/ml
IFN-γ
LPS
TNF-α+IFN-γ
IL-1β50U/ml
IL-1β100U/ml
Cytokine Treatment

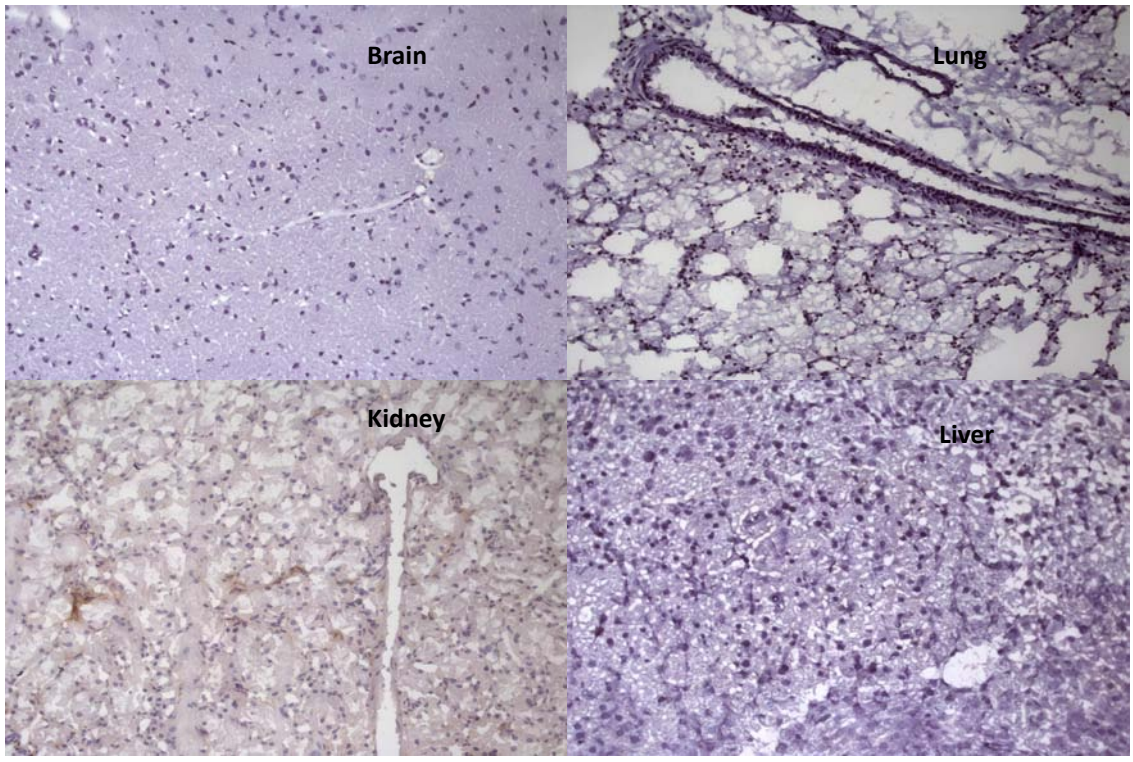
Brain
Lung
Kidney
Liver

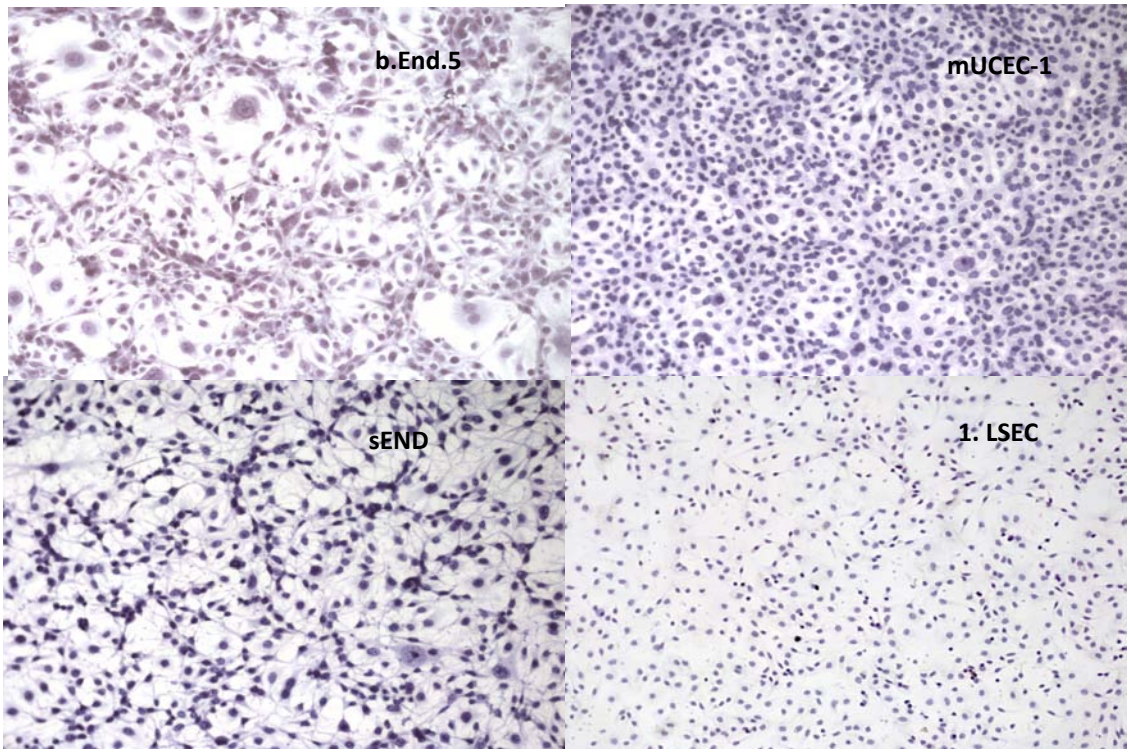
b.End.5
mUCEC-1
sEND
1. LSEC

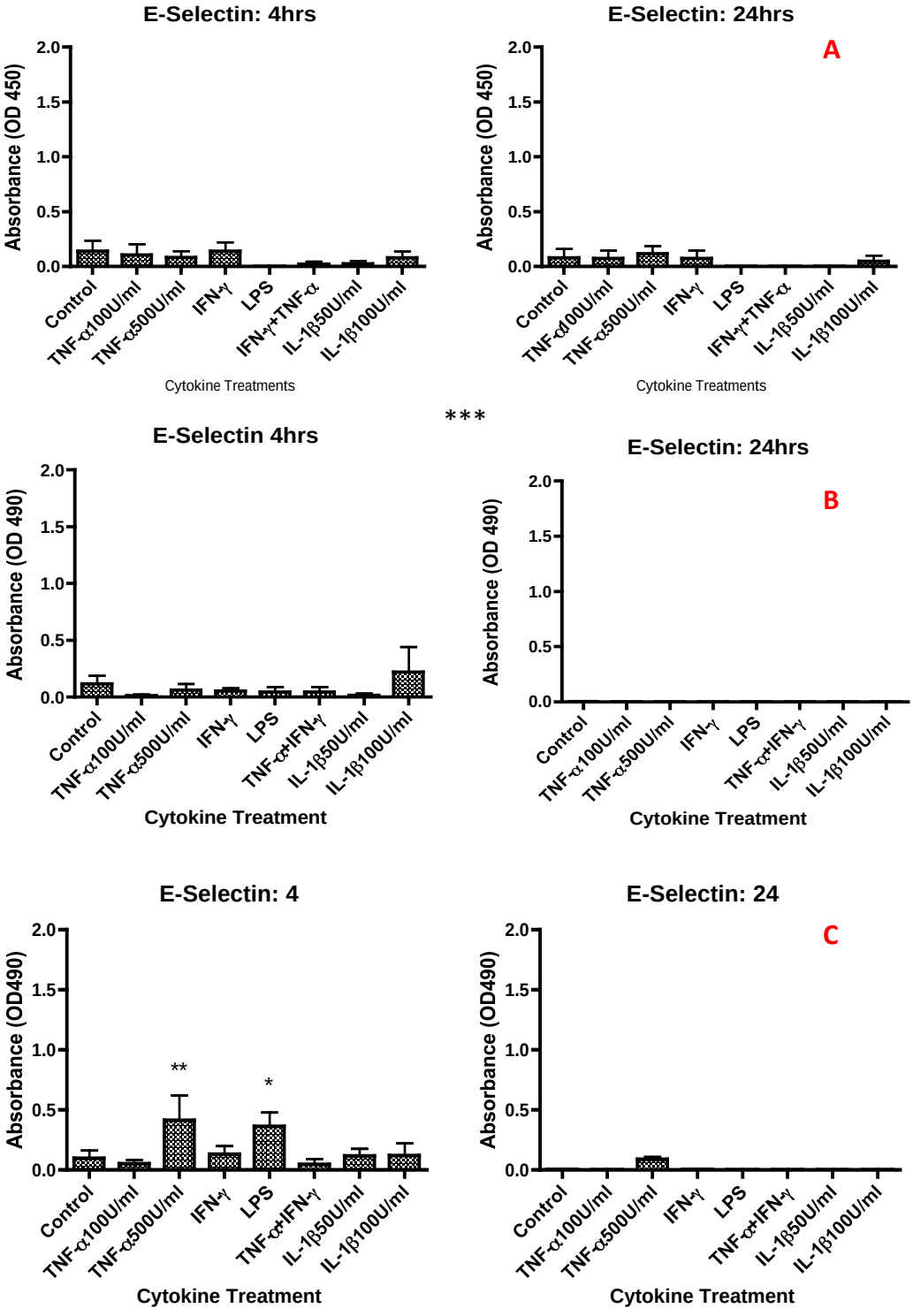
E-Selectin: 4hrs
Absorbance (OD 450)
2.0
1.5
1.0
0.5
0.0
Control
TNF-α100U/ml
TNF-α500U/ml
IFN-γ
LPS
IFN-γ+TNF-α
IL-1β50U/ml
IL-1β100U/ml
Cytokine Treatments
E-Selectin: 24hrs
A
Absorbance (OD 450)
Cytokine Treatments
***
E-Selectin 4hrs
Absorbance (OD 490)
Control
TNF-α100U/ml
TNF-α500U/ml
IFN-γ
LPS
TNF-α+IFN-γ
IL-1β50U/ml
IL-1β100U/ml
Cytokine Treatment
E-Selectin: 24hrs
B
Absorbance (OD 490)
Cytokine Treatment
E-Selectin: 4
Absorbance (OD490)
**
*
Cytokine Treatment
E-Selectin: 24
C
Absorbance (OD490)
Cytokine Treatment

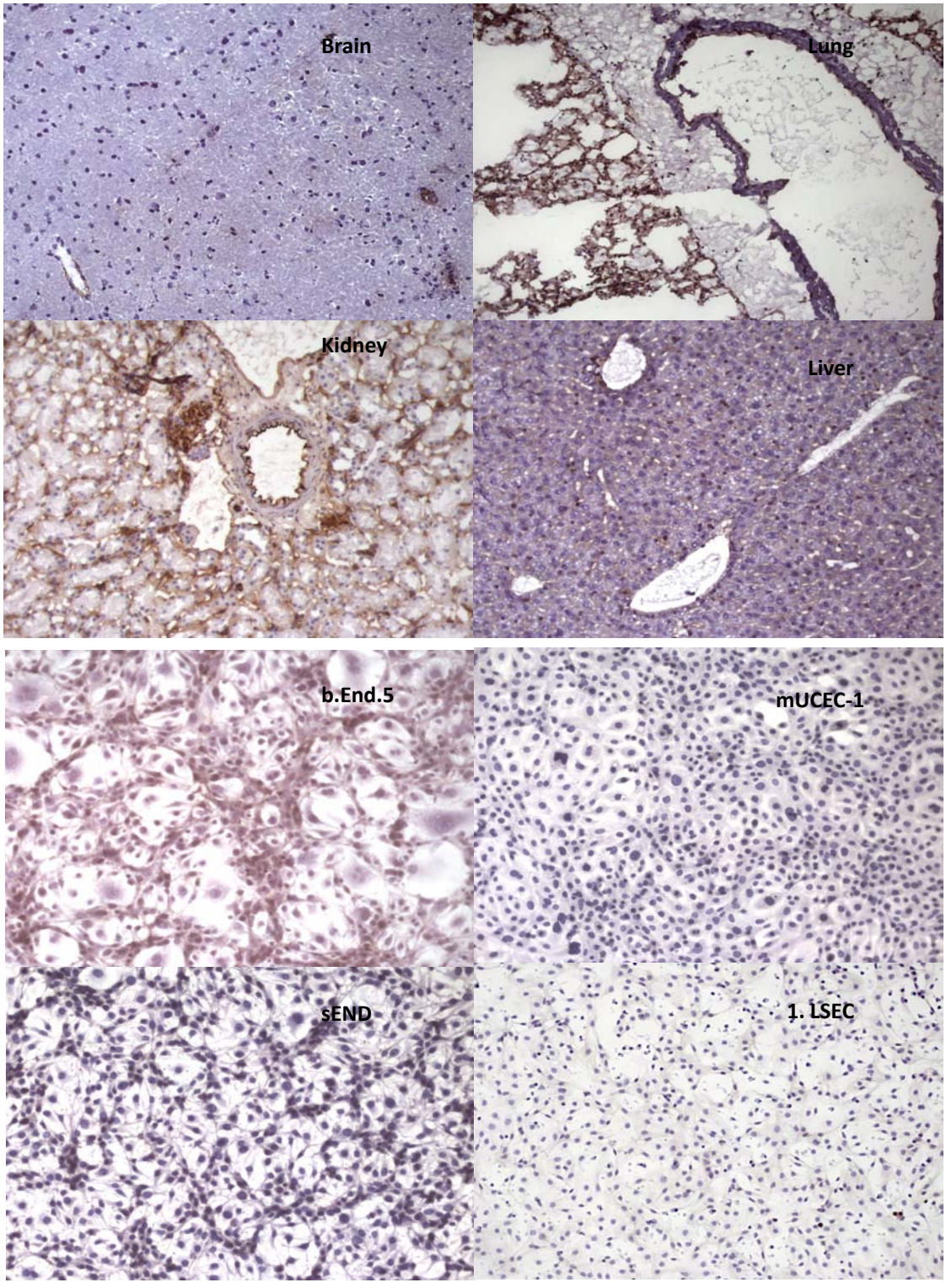
Brain
Lung
Kidney
Liver
b.End.5
mUCEC-1
sEND
1. LSEC

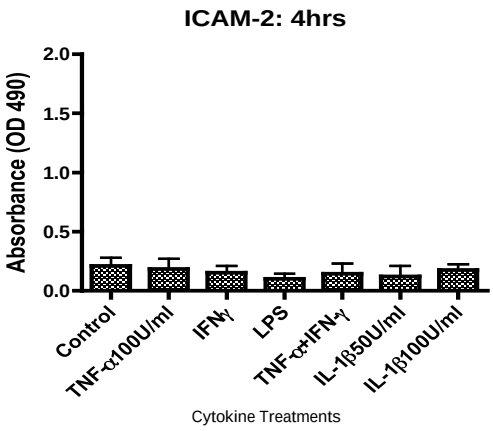
ICAM-2: 4hrs
Absorbance (OD 490)
2.0
1.5
1.0
0.5
0.0
Control
TNF-α100U/ml
IFNγ
LPS
TNF-α+IFN-γ
IL-1β50U/ml
IL-1β100U/ml
Cytokine Treatments

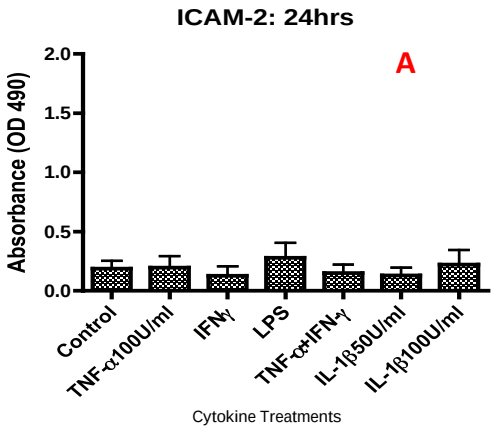
ICAM-2: 24hrs
A
Absorbance (OD 490)
2.0
1.5
1.0
0.5
0.0
Control
TNF-α100U/ml
IFNγ
LPS
TNF-α+IFN-γ
IL-1β50U/ml
IL-1β100U/ml
Cytokine Treatments

**

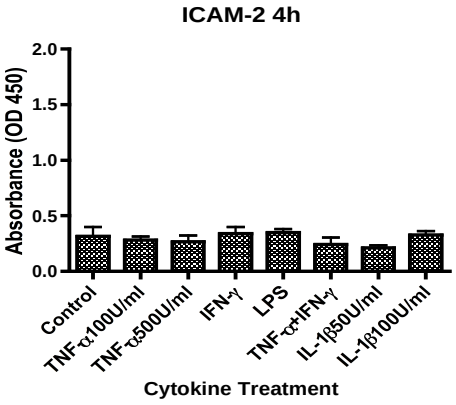
ICAM-2 4h
Absorbance (OD 450)
2.0
1.5
1.0
0.5
0.0
Control
TNF-α100U/ml
TNF-α500U/ml
IFN-γ
LPS
TNF-α+IFN-γ
IL-1β50U/ml
IL-1β100U/ml
Cytokine Treatment

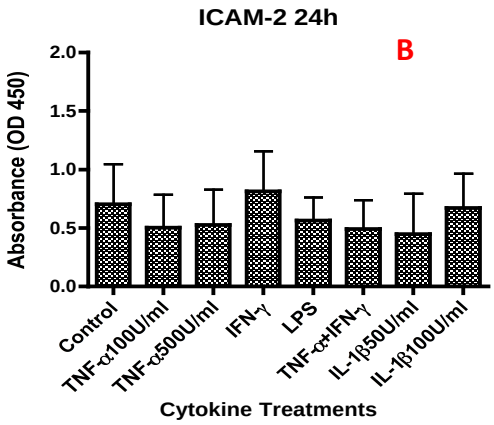
ICAM-2 24h
B
Absorbance (OD 450)
2.0
1.5
1.0
0.5
0.0
Control
TNF-α100U/ml
TNF-α500U/ml
IFN-γ
LPS
TNF-α+IFN-γ
IL-1β50U/ml
IL-1β100U/ml
Cytokine Treatments

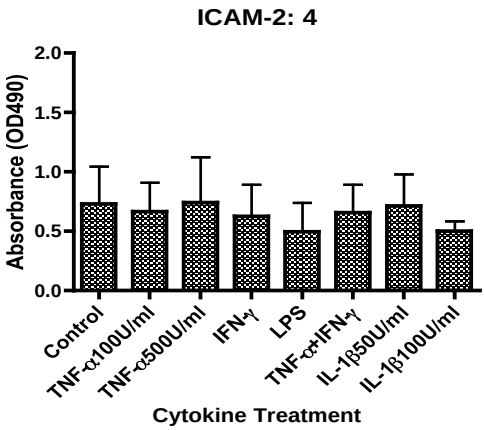
ICAM-2: 4
Absorbance (OD490)
2.0
1.5
1.0
0.5
0.0
Control
TNF-α100U/ml
TNF-α500U/ml
IFN-γ
LPS
TNF-α+IFN-γ
IL-1β50U/ml
IL-1β100U/ml
Cytokine Treatment

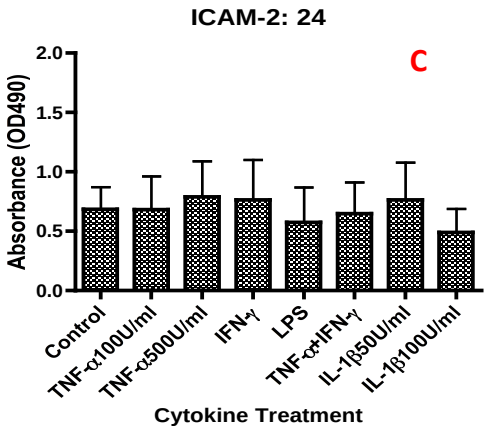
ICAM-2: 24
C
Absorbance (OD490)
2.0
1.5
1.0
0.5
0.0
Control
TNF-α100U/ml
TNF-α500U/ml
IFN-γ
LPS
TNF-α+IFN-γ
IL-1β50U/ml
IL-1β100U/ml
Cytokine Treatment

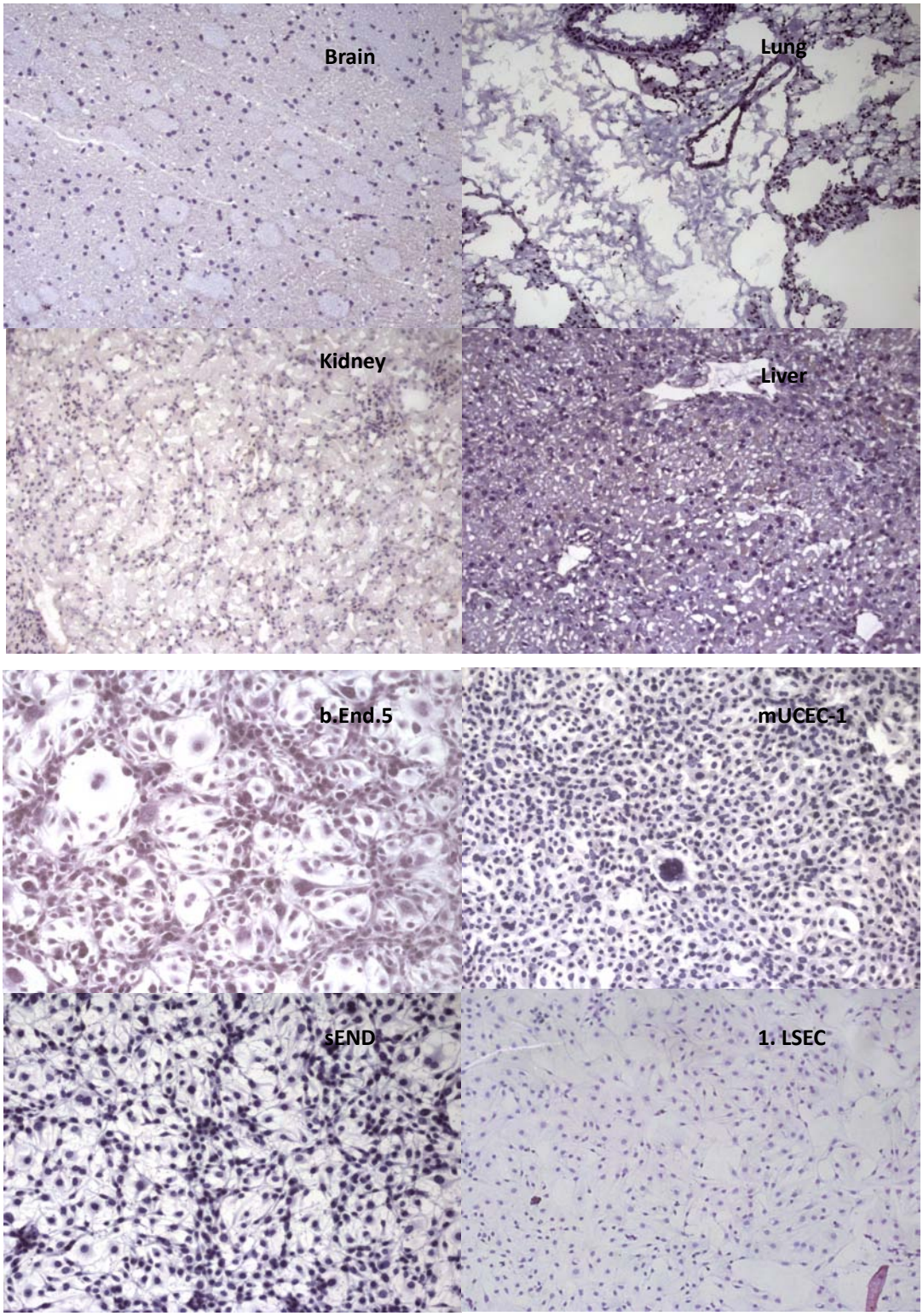
Brain
Lung
Kidney
Liver
b.End.5
mUCEC-1
sEND
1. LSEC

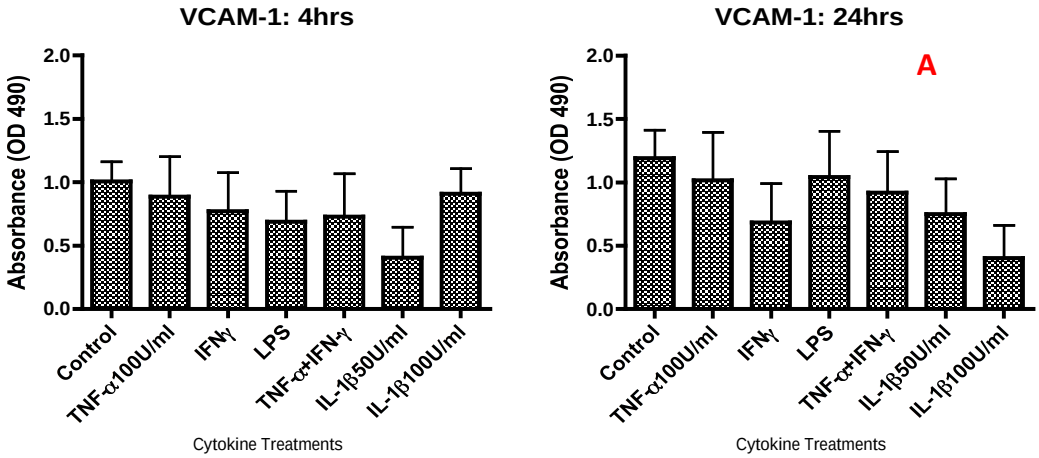
VCAM-1: 4hrs
Absorbance (OD 490)
2.0
1.5
1.0
0.5
0.0
Control
TNF-α100U/ml
IFNγ
LPS
TNF-α+IFN-γ
IL-1β50U/ml
IL-1β100U/ml
Cytokine Treatments

VCAM-1: 24hrs
A
Absorbance (OD 490)
2.0
1.5
1.0
0.5
0.0
Control
TNF-α100U/ml
IFNγ
LPS
TNF-α+IFN-γ
IL-1β50U/ml
IL-1β100U/ml
Cytokine Treatments

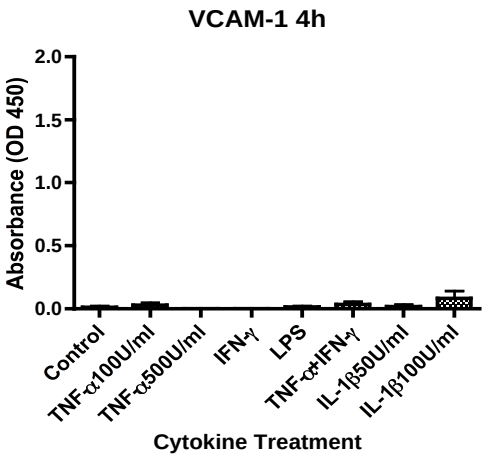
VCAM-1 4h
Absorbance (OD 450)
2.0
1.5
1.0
0.5
0.0
Control
TNF-α100U/ml
TNF-α500U/ml
IFN-γ
LPS
TNF-α+IFN-γ
IL-1β50U/ml
IL-1β100U/ml
Cytokine Treatment

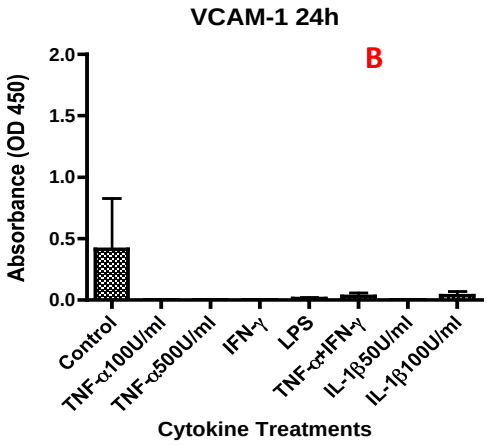
VCAM-1 24h
B
Absorbance (OD 450)
2.0
1.5
1.0
0.5
0.0
Control
TNF-α100U/ml
TNF-α500U/ml
IFN-γ
LPS
TNF-α+IFN-γ
IL-1β50U/ml
IL-1β100U/ml
Cytokine Treatments

**

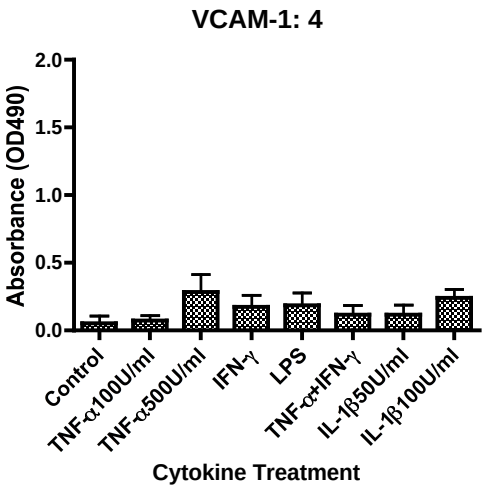
VCAM-1: 4
Absorbance (OD490)
2.0
1.5
1.0
0.5
0.0
Control
TNF-α100U/ml
TNF-α500U/ml
IFN-γ
LPS
TNF-α+IFN-γ
IL-1β50U/ml
IL-1β100U/ml
Cytokine Treatment

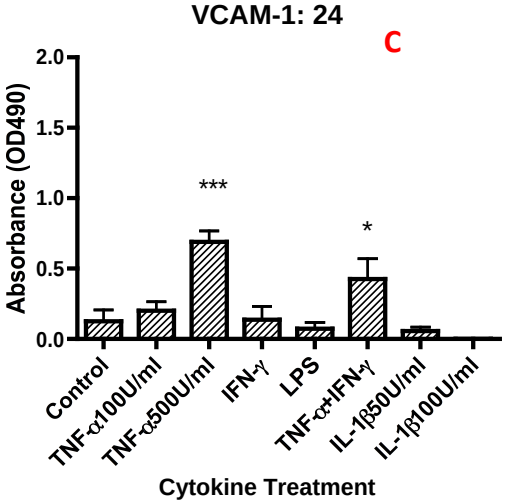
VCAM-1: 24
C
***
*
Absorbance (OD490)
2.0
1.5
1.0
0.5
0.0
Control
TNF-α100U/ml
TNF-α500U/ml
IFN-γ
LPS
TNF-α+IFN-γ
IL-1β50U/ml
IL-1β100U/ml
Cytokine Treatment

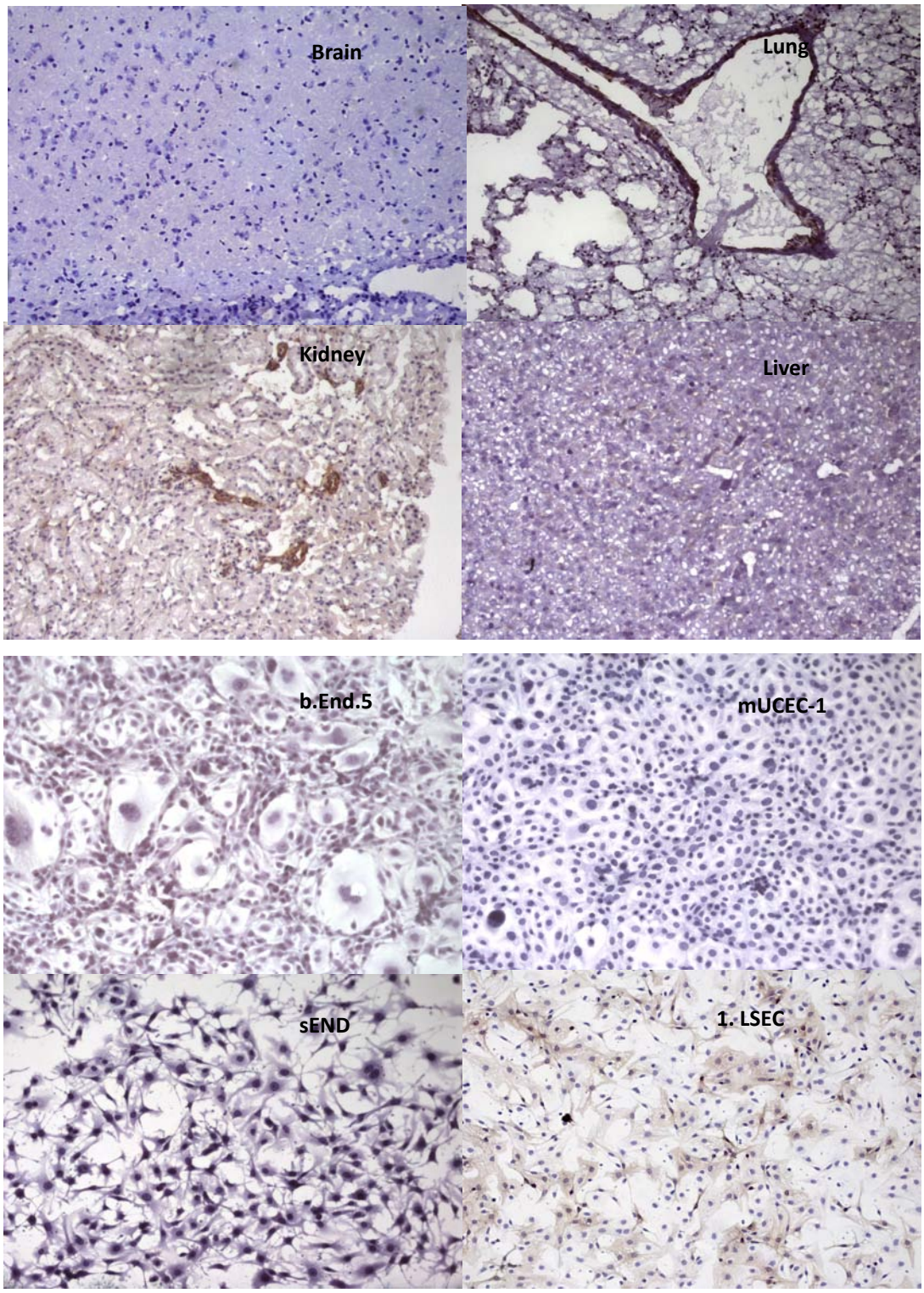
Brain
Lung
Kidney
Liver
b.End.5
mUCEC-1
sEND
1. LSEC

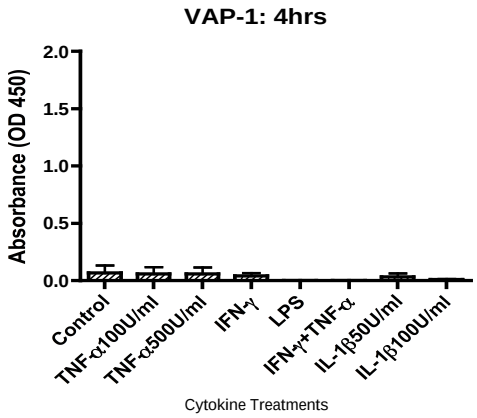
VAP-1: 4hrs
Absorbance (OD 450)
2.0
1.5
1.0
0.5
0.0
Control
TNF-α100U/ml
TNF-α500U/ml
IFN-γ
LPS
IFN-γ+TNF-α
IL-1β50U/ml
IL-1β100U/ml
Cytokine Treatments

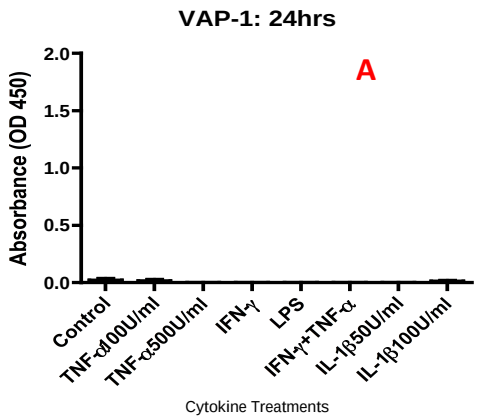
VAP-1: 24hrs
A
Absorbance (OD 450)
2.0
1.5
1.0
0.5
0.0
Control
TNF-α100U/ml
TNF-α500U/ml
IFN-γ
LPS
IFN-γ+TNF-α
IL-1β50U/ml
IL-1β100U/ml
Cytokine Treatments

**

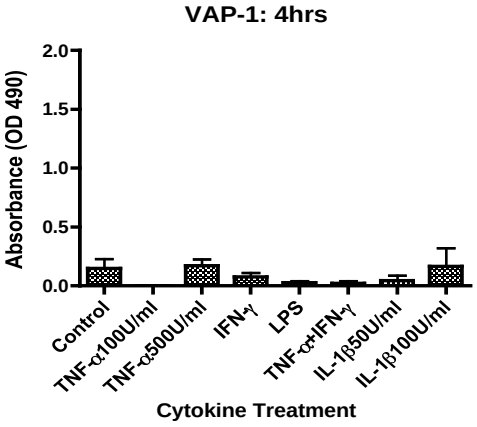
VAP-1: 4hrs
Absorbance (OD 490)
2.0
1.5
1.0
0.5
0.0
Control
TNF-α100U/ml
TNF-α500U/ml
IFN-γ
LPS
TNF-α+IFN-γ
IL-1β50U/ml
IL-1β100U/ml
Cytokine Treatment

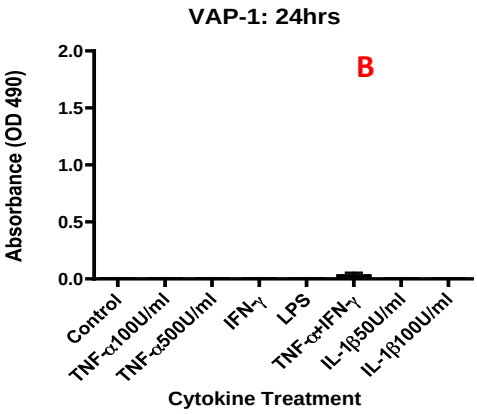
VAP-1: 24hrs
B
Absorbance (OD 490)
2.0
1.5
1.0
0.5
0.0
Control
TNF-α100U/ml
TNF-α500U/ml
IFN-γ
LPS
TNF-α+IFN-γ
IL-1β50U/ml
IL-1β100U/ml
Cytokine Treatment

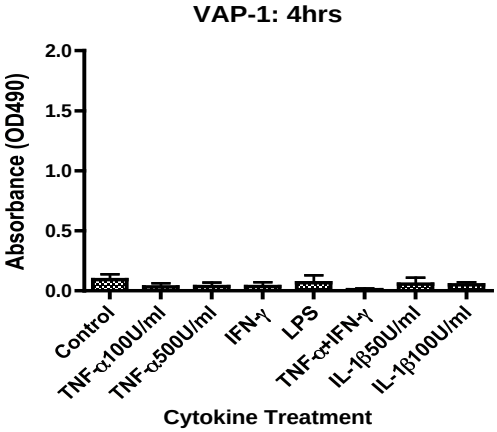
VAP-1: 4hrs
Absorbance (OD490)
2.0
1.5
1.0
0.5
0.0
Control
TNF-α100U/ml
TNF-α500U/ml
IFN-γ
LPS
TNF-α+IFN-γ
IL-1β50U/ml
IL-1β100U/ml
Cytokine Treatment

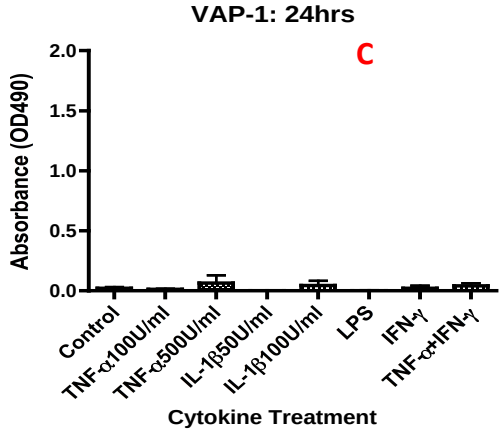
VAP-1: 24hrs
C
Absorbance (OD490)
2.0
1.5
1.0
0.5
0.0
Control
TNF-α100U/ml
TNF-α500U/ml
IL-1β50U/ml
IL-1β100U/ml
LPS
IFN-γ
TNF-α+IFN-γ
Cytokine Treatment

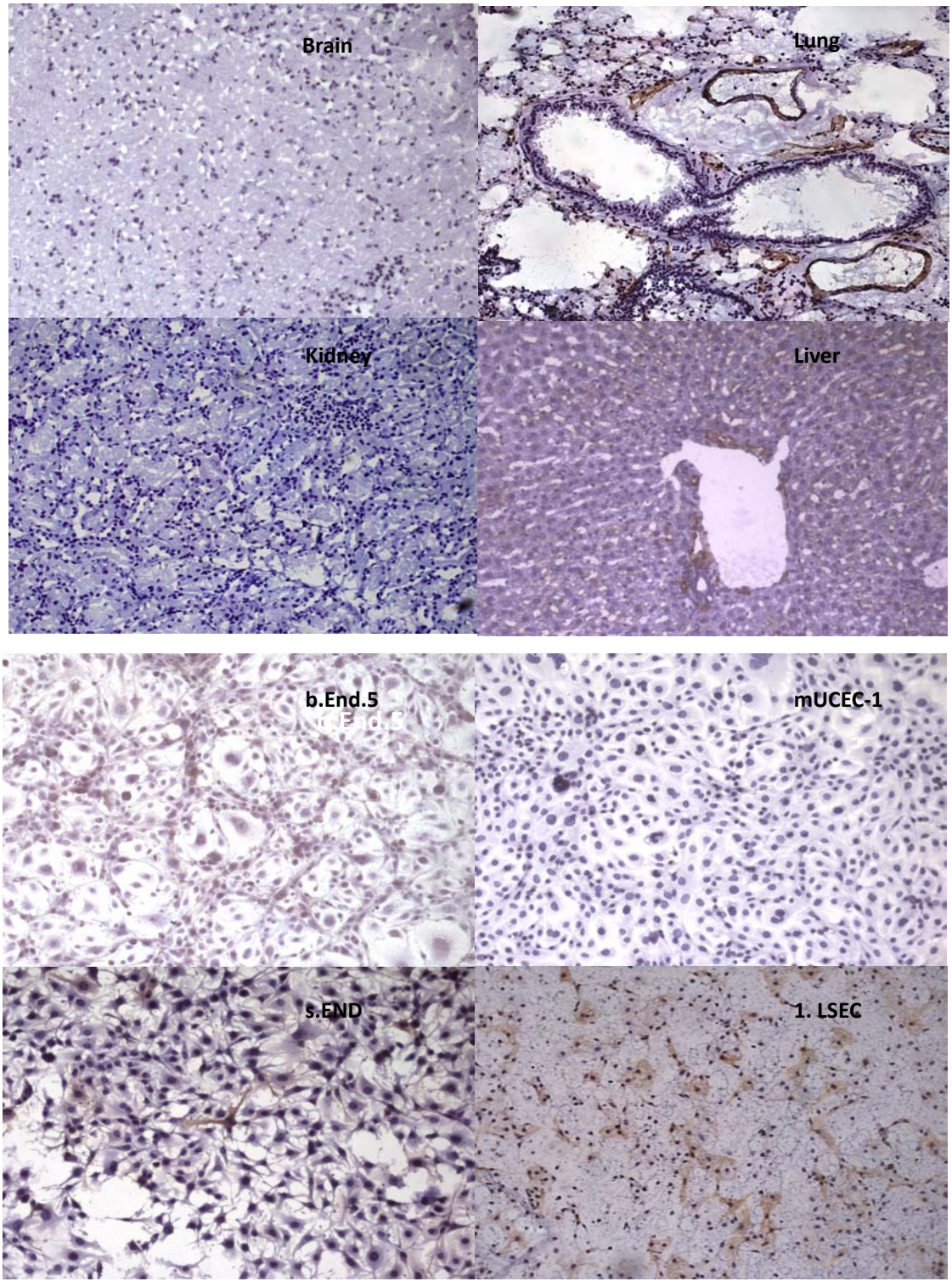
Brain
Lung
Kidney
Liver
b.End.5
mUCEC-1
s.END
1. LSEC

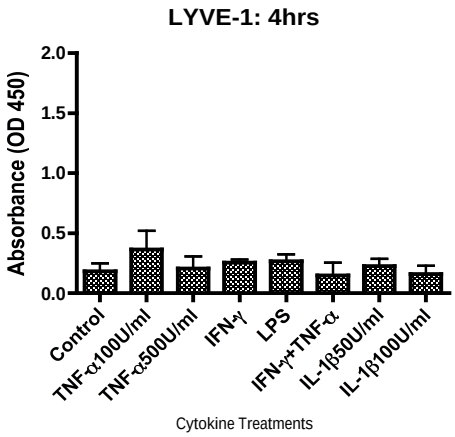
LYVE-1: 4hrs
Absorbance (OD 450)
2.0
1.5
1.0
0.5
0.0
Control
TNF-α100U/ml
TNF-α500U/ml
IFN-γ
LPS
IFN-γ+TNF-α
IL-1β50U/ml
IL-1β100U/ml
Cytokine Treatments

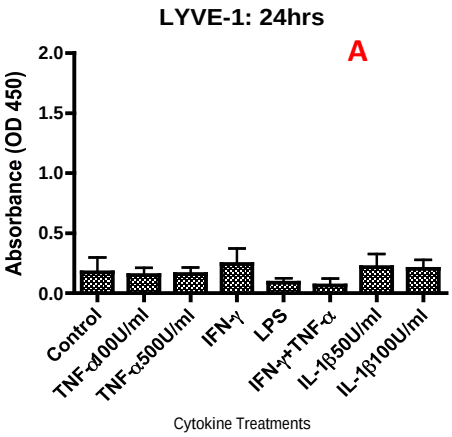
LYVE-1: 24hrs
A
Absorbance (OD 450)
2.0
1.5
1.0
0.5
0.0
Control
TNF-α100U/ml
TNF-α500U/ml
IFN-γ
LPS
IFN-γ+TNF-α
IL-1β50U/ml
IL-1β100U/ml
Cytokine Treatments

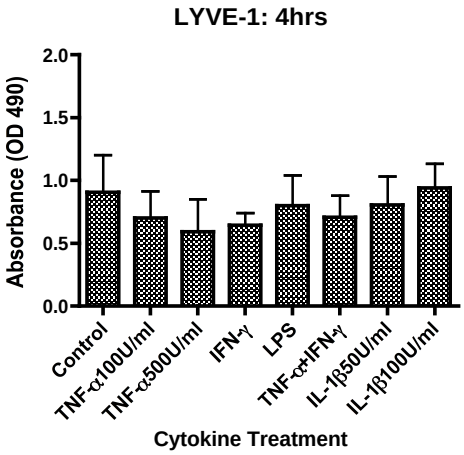
LYVE-1: 4hrs
Absorbance (OD 490)
2.0
1.5
1.0
0.5
0.0
Control
TNF-α100U/ml
TNF-α500U/ml
IFN-γ
LPS
TNF-α+IFN-γ
IL-1β50U/ml
IL-1β100U/ml
Cytokine Treatment

*

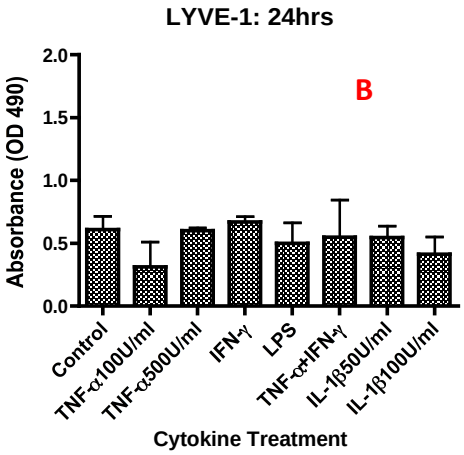
LYVE-1: 24hrs
B
Absorbance (OD 490)
2.0
1.5
1.0
0.5
0.0
Control
TNF-α100U/ml
TNF-α500U/ml
IFN-γ
LPS
TNF-α+IFN-γ
IL-1β50U/ml
IL-1β100U/ml
Cytokine Treatment

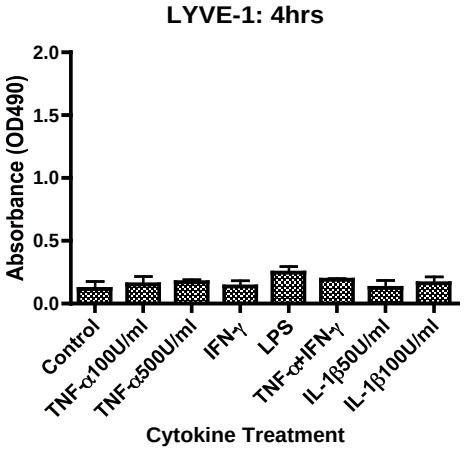
LYVE-1: 4hrs
Absorbance (OD490)
2.0
1.5
1.0
0.5
0.0
Control
TNF-α100U/ml
TNF-α500U/ml
IFN-γ
LPS
TNF-α+IFN-γ
IL-1β50U/ml
IL-1β100U/ml
Cytokine Treatment

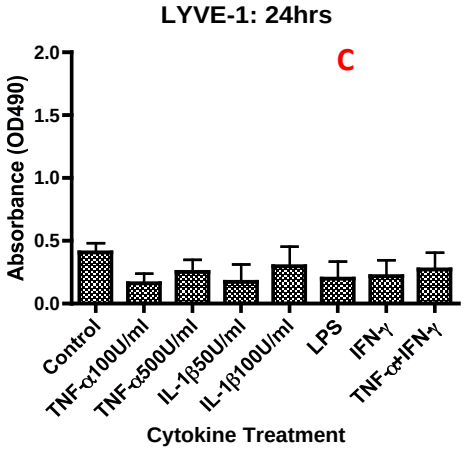
LYVE-1: 24hrs
C
Absorbance (OD490)
2.0
1.5
1.0
0.5
0.0
Control
TNF-α100U/ml
TNF-α500U/ml
IL-1β50U/ml
IL-1β100U/ml
LPS
IFN-γ
TNF-α+IFN-γ
Cytokine Treatment

	mUCEC-1				s.END			
	IHC	ELISA (4)	ELISA (24)	Gene Array	IHC	ELISA (4)	ELISA (24)	Gene Array
CD31	+	+	+	++	++	++	+++	++++
ICAM-2	+	+	+	+	+	+	++	+++
JAM-2	++	++	++	++++	+++	+	+	++
VCAM-1	+	+++	+++	++++	+	+	+	++
CD34	+	+	++	+	+++	++	++	++
VAP-1	-	+	+	-	+	+	-	-
Endoglin	+	+	++	+	+++	+++	+++	++++
E-Selectin	-	+	+	++	-	+	-	++
LYVE-1	-	+	+	-	++	+++	++	+

	B.End.5				mLSEC			
	IHC	ELISA (4)	ELISA (24)	Gene Array	IHC	ELISA (4)	ELISA (24)	Gene Array
CD31	+++	+++	+++		+++			
ICAM-2	++	++	++		-			
JAM-2	+	+	+		+			
VCAM-1	-	+	+		-			
CD34	+++	+++	+++		++			
VAP-1	-	+	+		++			
Endoglin	++	+	+		++			
E-Selectin	-	+	+		-			
LYVE-1	++	+	++		++			

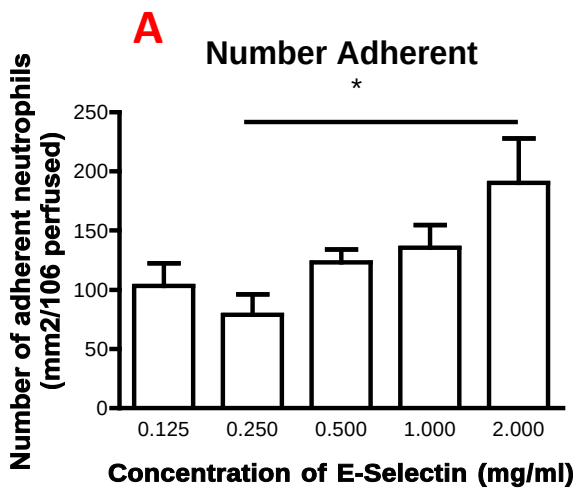
A
Number Adherent
*
Number of adherent neutrophils (mm2/106 perfused)
250
200
150
100
50
0
0.125
0.250
0.500
1.000
2.000
Concentration of E-Selectin (mg/ml)

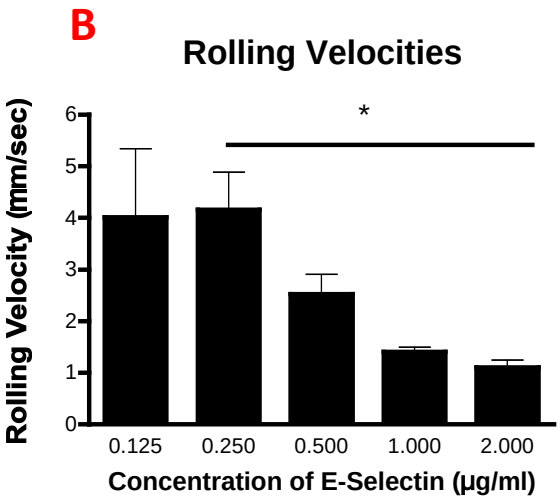
B
Rolling Velocities
*
Rolling Velocity (mm/sec)
6
5
4
3
2
1
0
0.125
0.250
0.500
1.000
2.000
Concentration of E-Selectin (µg/ml)

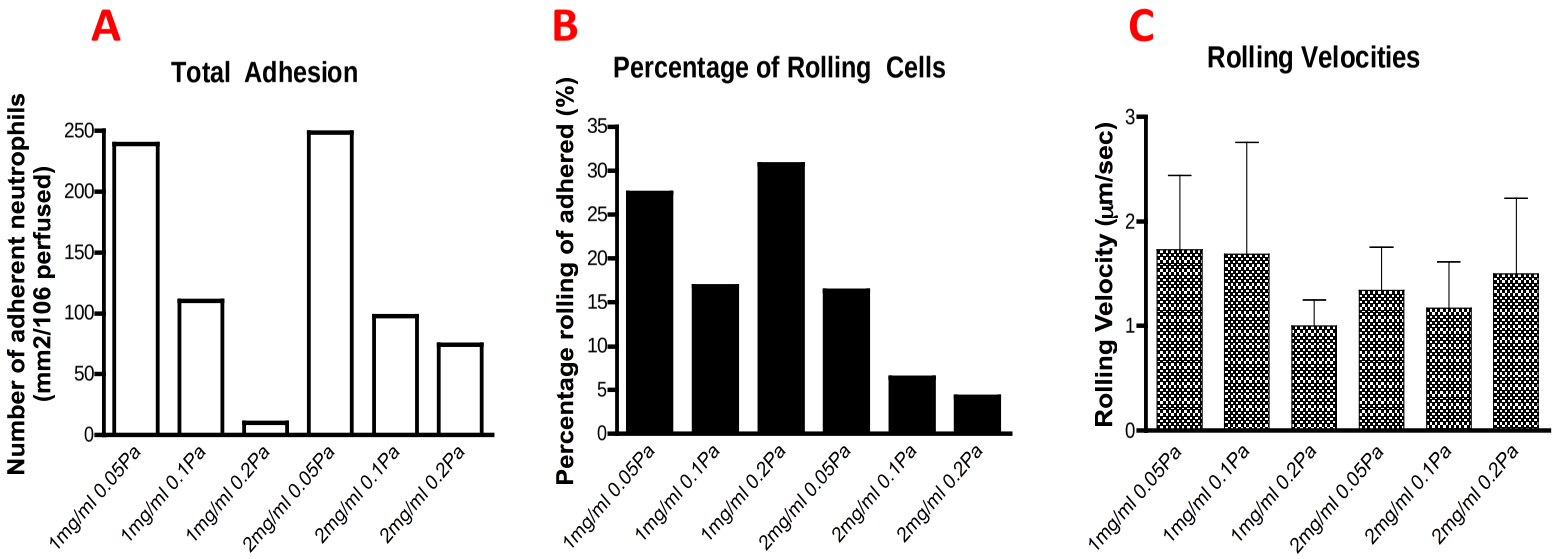
A
Total Adhesion
Number of adherent neutrophils (mm2/106 perfused)
250
200
150
100
50
0
1mg/ml 0.05Pa
1mg/ml 0.1Pa
1mg/ml 0.2Pa
2mg/ml 0.05Pa
2mg/ml 0.1Pa
2mg/ml 0.2Pa
B
Percentage of Rolling Cells
Percentage rolling of adhered (%)
35
30
25
20
15
10
5
0
1mg/ml 0.05Pa
1mg/ml 0.1Pa
1mg/ml 0.2Pa
2mg/ml 0.05Pa
2mg/ml 0.1Pa
2mg/ml 0.2Pa
C
Rolling Velocities
Rolling Velocity (μm/sec)
3
2
1
0
1mg/ml 0.05Pa
1mg/ml 0.1Pa
1mg/ml 0.2Pa
2mg/ml 0.05Pa
2mg/ml 0.1Pa
2mg/ml 0.2Pa

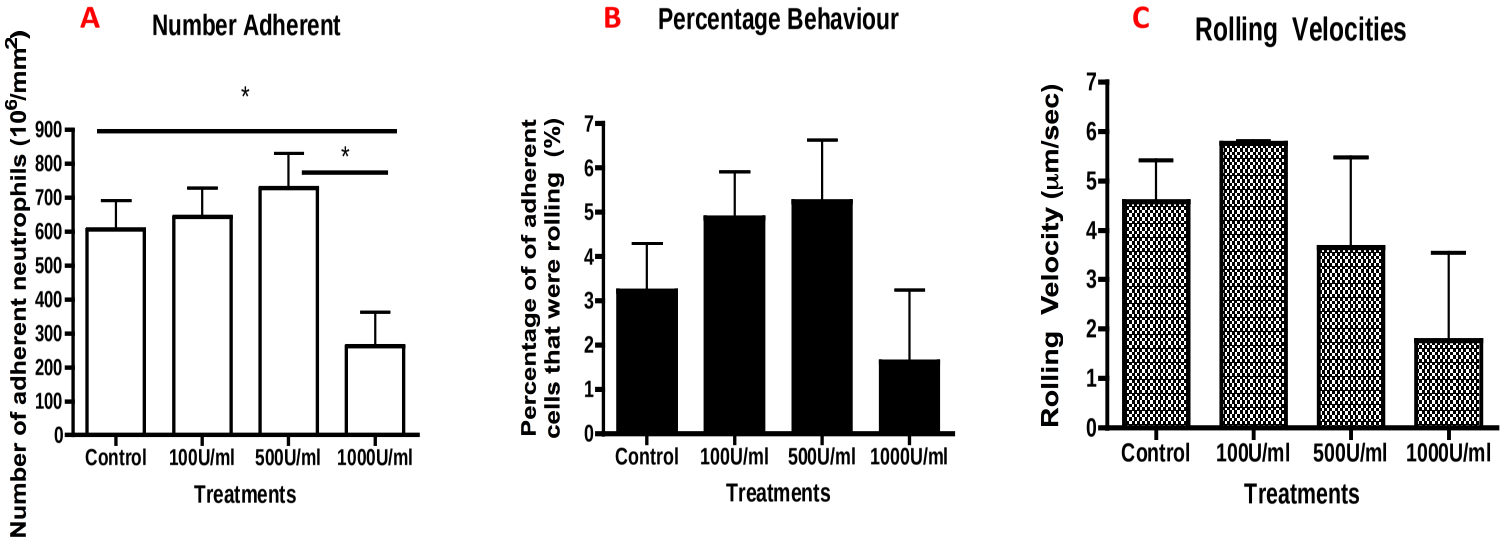
A
Number Adherent
Number of adherent neutrophils (10^6/mm^2)
900
800
700
600
500
400
300
200
100
0
*
*
Control
100U/ml
500U/ml
1000U/ml
Treatments
B
Percentage Behaviour
Percentage of of adherent cells that were rolling (%)
7
6
5
4
3
2
1
0
Control
100U/ml
500U/ml
1000U/ml
Treatments
C
Rolling Velocities
Rolling Velocity (μm/sec)
7
6
5
4
3
2
1
0
Control
100U/ml
500U/ml
1000U/ml
Treatments

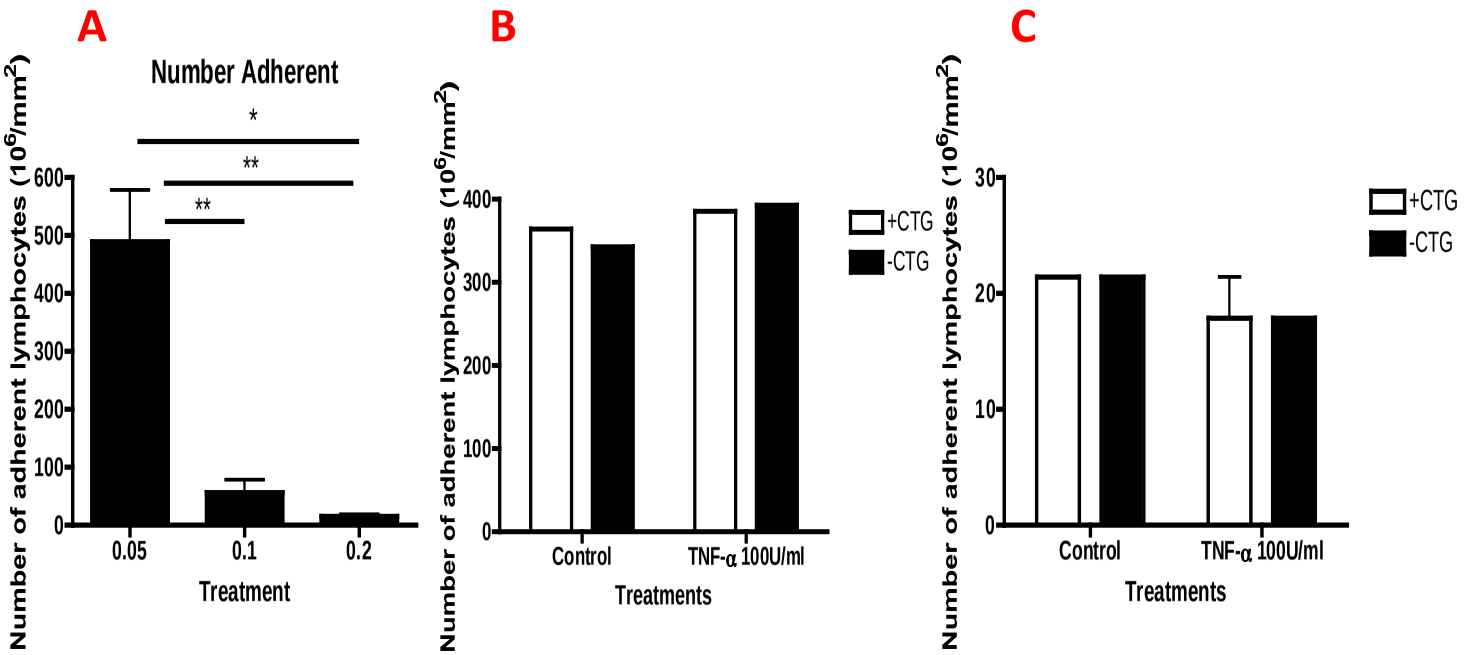
A
Number Adherent
Number of adherent lymphocytes (10^6/mm^2)
600
500
400
300
200
100
0
*
**
**
0.05
0.1
0.2
Treatment
B
Number of adherent lymphocytes (10^6/mm^2)
400
300
200
100
0
Control
TNF-α 100U/ml
Treatments
+CTG
-CTG
C
Number of adherent lymphocytes (10^6/mm^2)
30
20
10
0
Control
TNF-α 100U/ml
Treatments
+CTG
-CTG

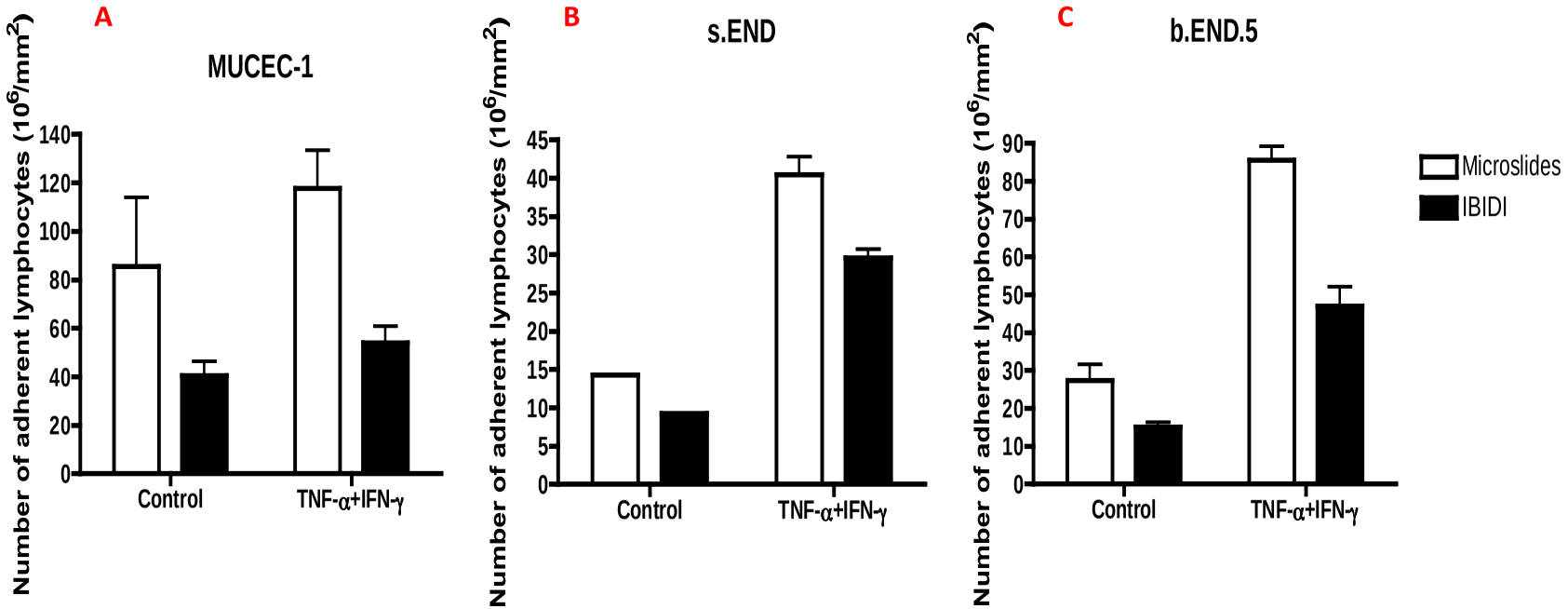
A
MUCEC-1
Number of adherent lymphocytes (10^6/mm^2)
140
120
100
80
60
40
20
0
Control
TNF-α+IFN-γ
B
s.END
Number of adherent lymphocytes (10^6/mm^2)
45
40
35
30
25
20
15
10
5
0
Control
TNF-α+IFN-γ
C
b.END.5
Number of adherent lymphocytes (10^6/mm^2)
90
80
70
60
50
40
30
20
10
0
Control
TNF-α+IFN-γ
Microslides
IBIDI

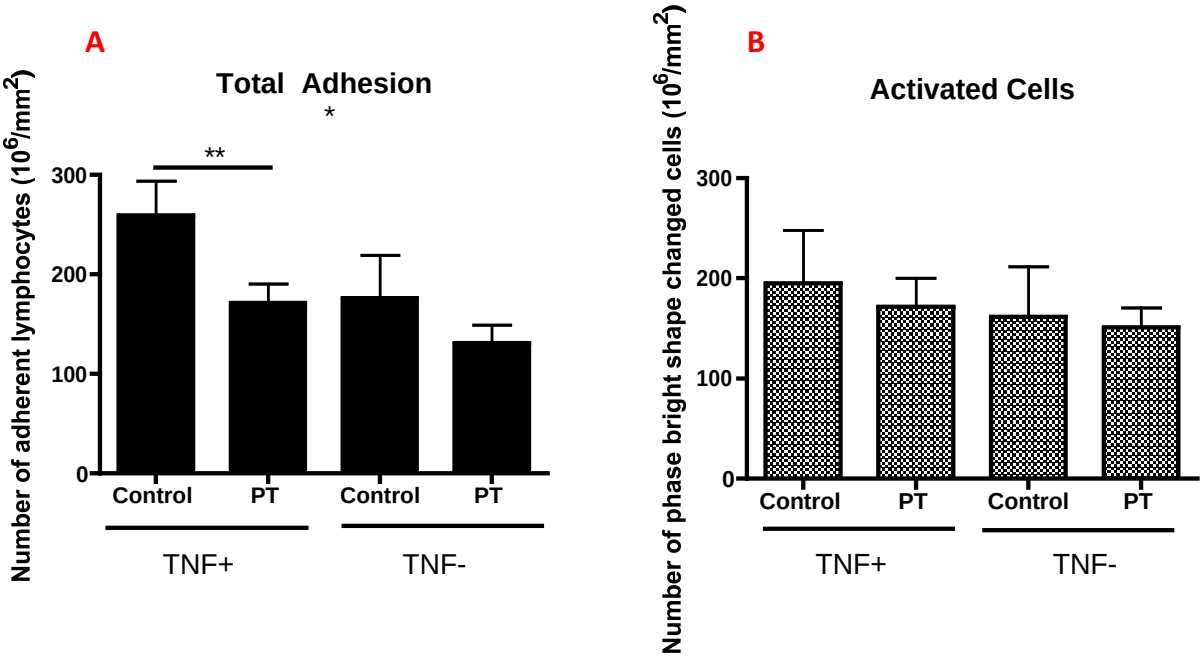
A
Total Adhesion
*
**
Number of adherent lymphocytes (10^6/mm^2)
300
200
100
0
Control
PT
Control
PT
TNF+
TNF-
B
Activated Cells
Number of phase bright shape changed cells (10^6/mm^2)
300
200
100
0
Control
PT
Control
PT
TNF+
TNF-

4 Hours Treatment

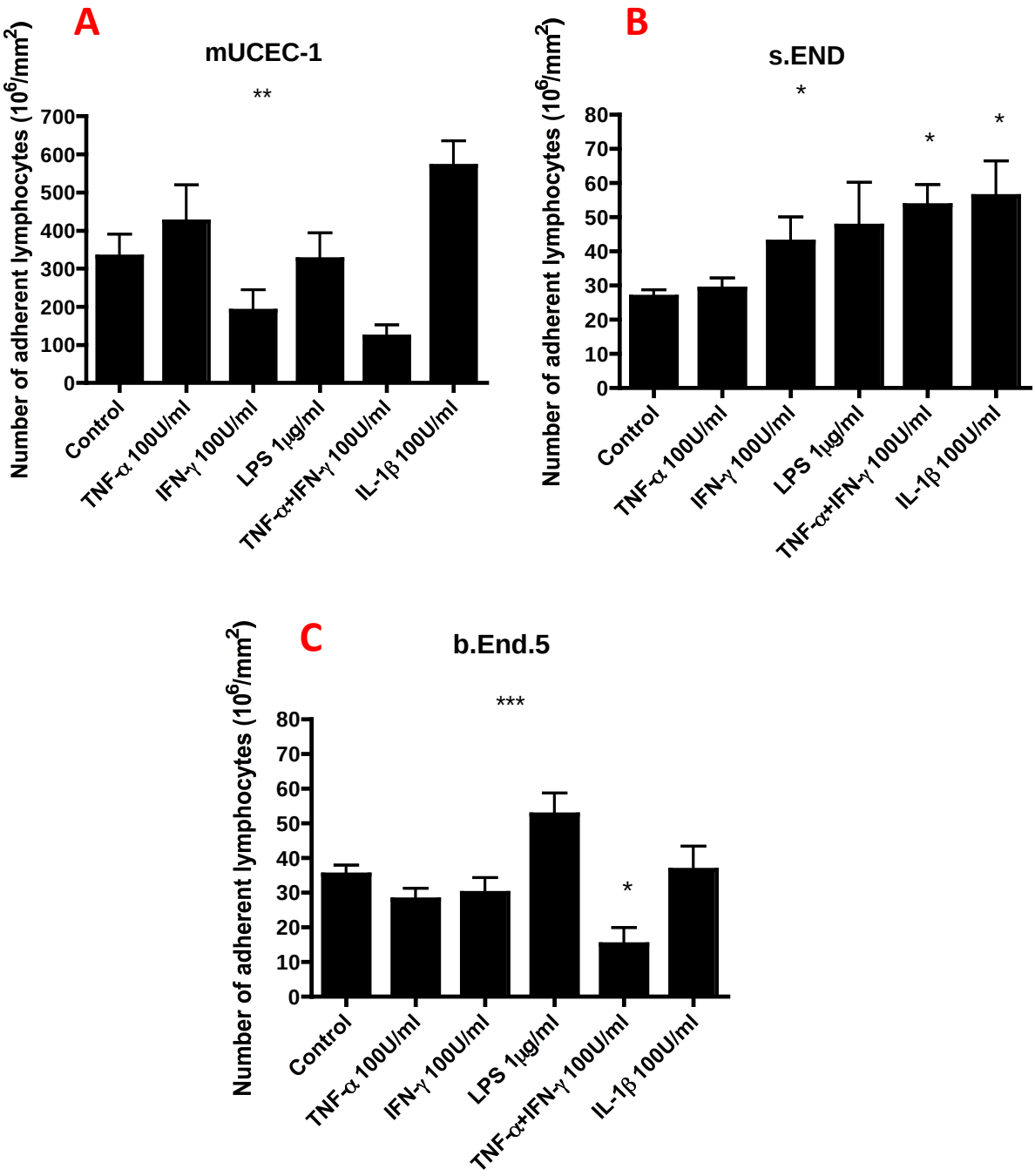

24 Hours Treatment

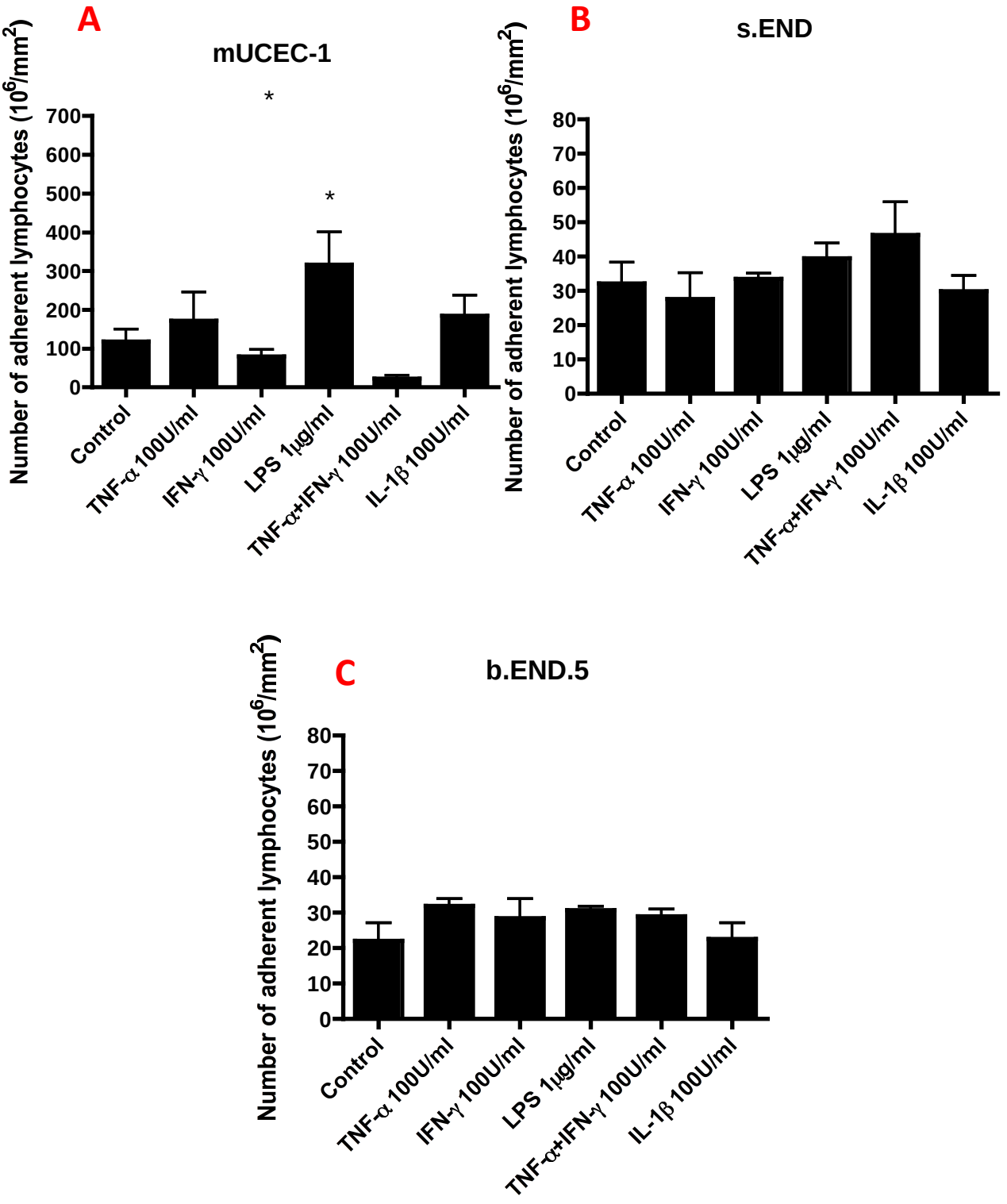

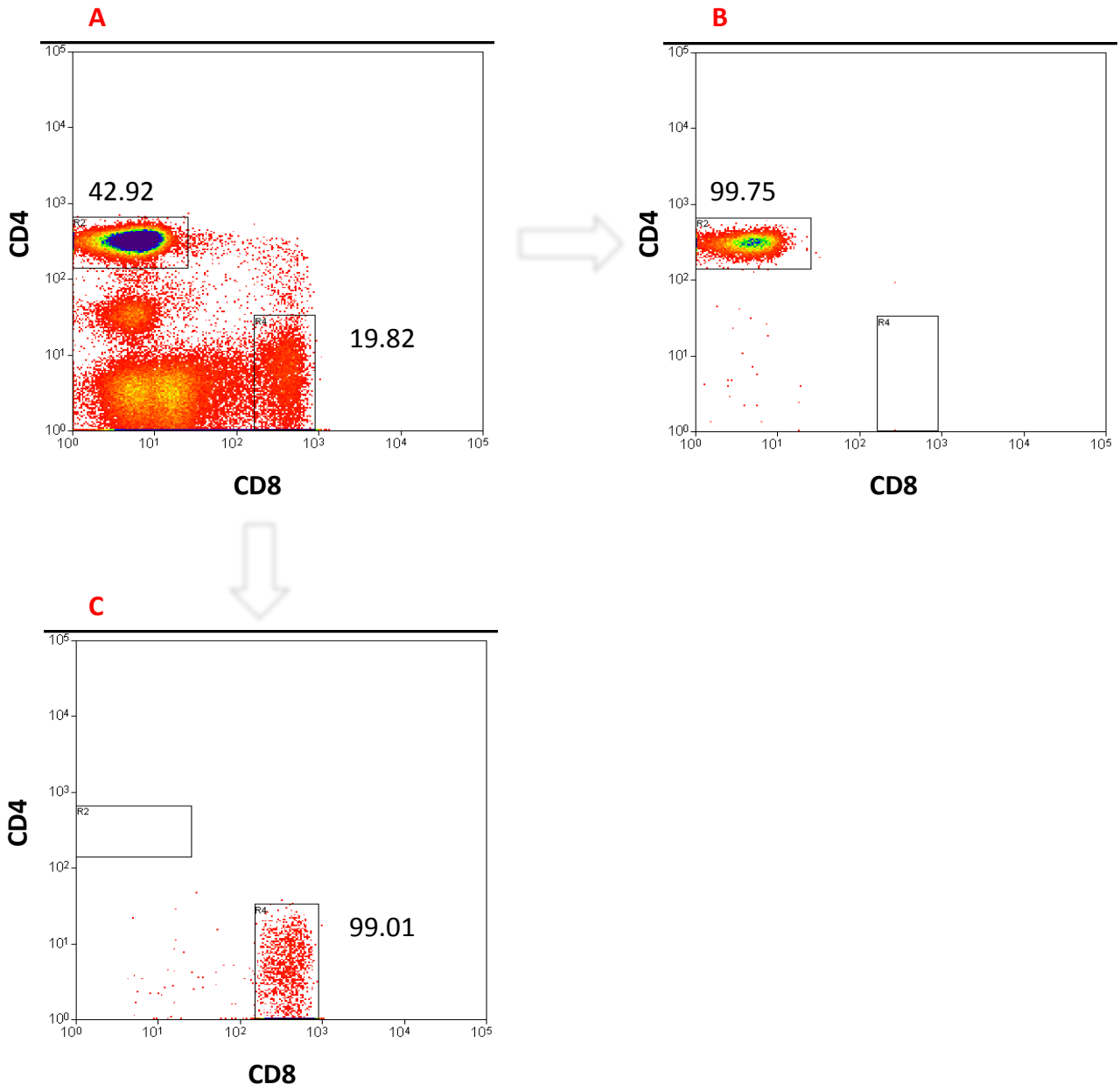
A
B
C
42.92
19.82
99.75
99.01
R2
R4
CD4
CD8

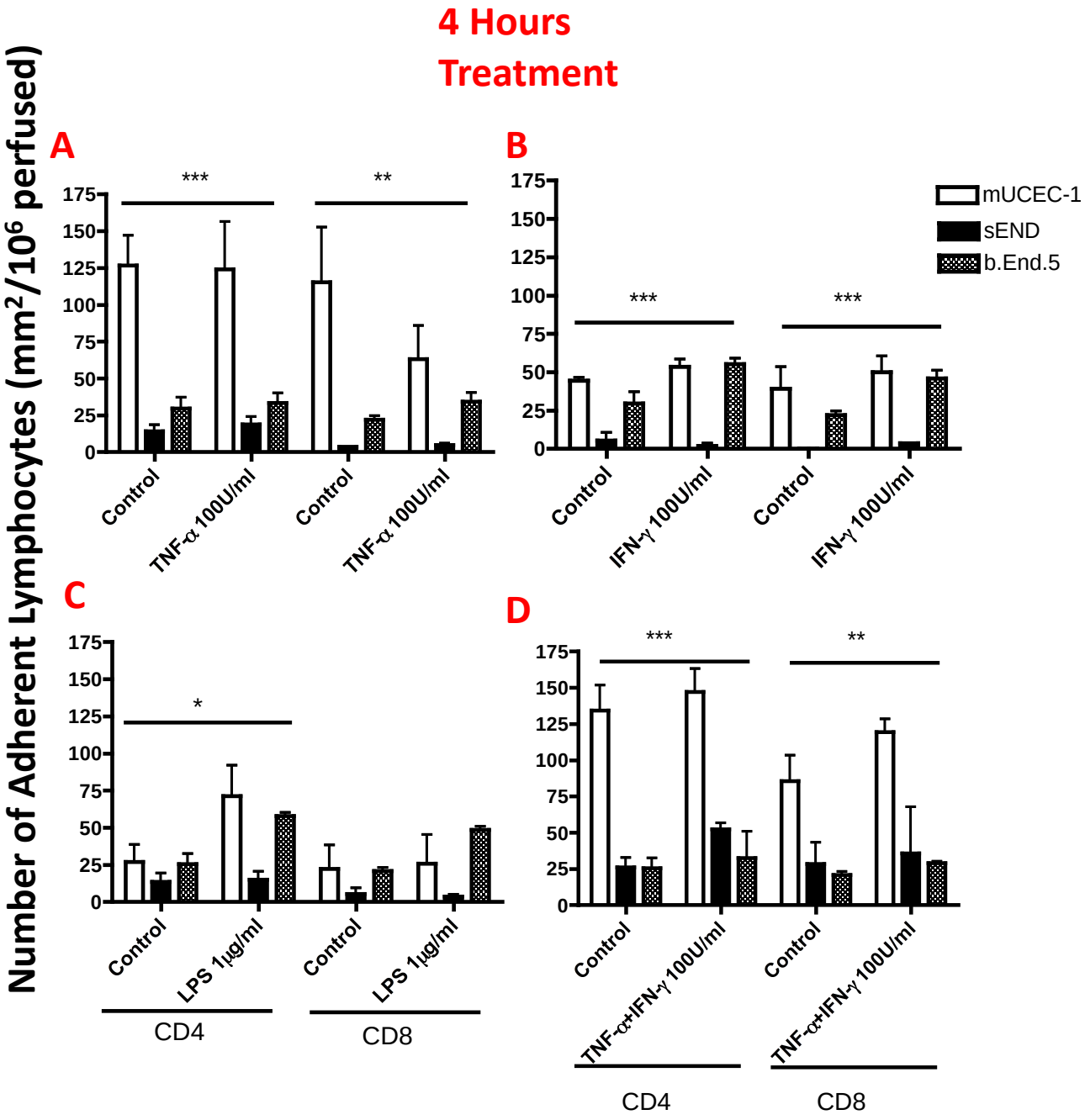
4 Hours
Treatment
A
B
C
D
Number of Adherent Lymphocytes (mm²/10⁶ perfused)
mUCEC-1
sEND
b.End.5
***
**
*
Control
TNF-α 100U/ml
IFN-γ 100U/ml
LPS 1μg/ml
TNF-α+IFN-γ 100U/ml
CD4
CD8

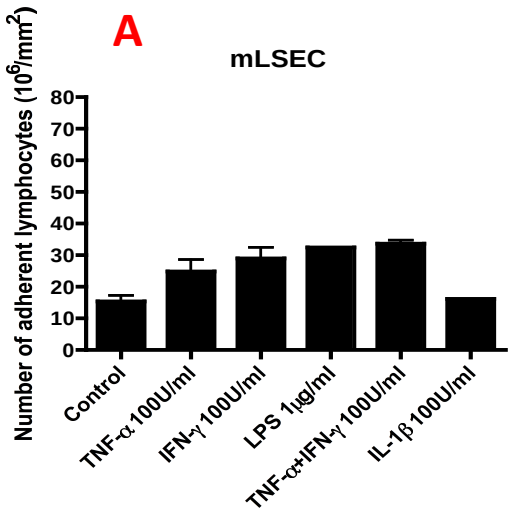
A
mLSEC
Number of adherent lymphocytes (10^6/mm^2)
80
70
60
50
40
30
20
10
0
Control
TNF-α 100U/ml
IFN-γ 100U/ml
LPS 1μg/ml
TNF-α+IFN-γ 100U/ml
IL-1β 100U/ml

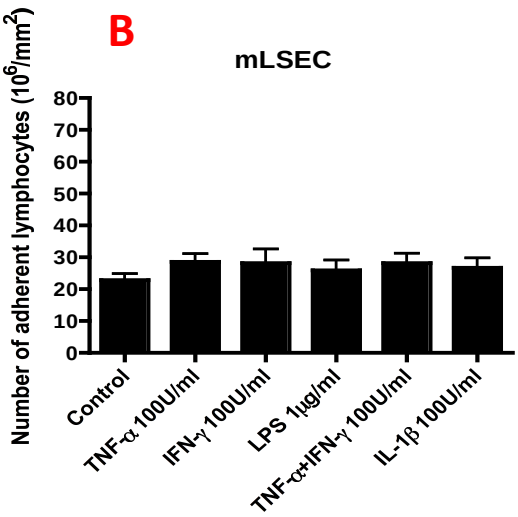
B
mLSEC
Number of adherent lymphocytes (10^6/mm^2)
80
70
60
50
40
30
20
10
0
Control
TNF-α 100U/ml
IFN-γ 100U/ml
LPS 1μg/ml
TNF-α+IFN-γ 100U/ml
IL-1β 100U/ml

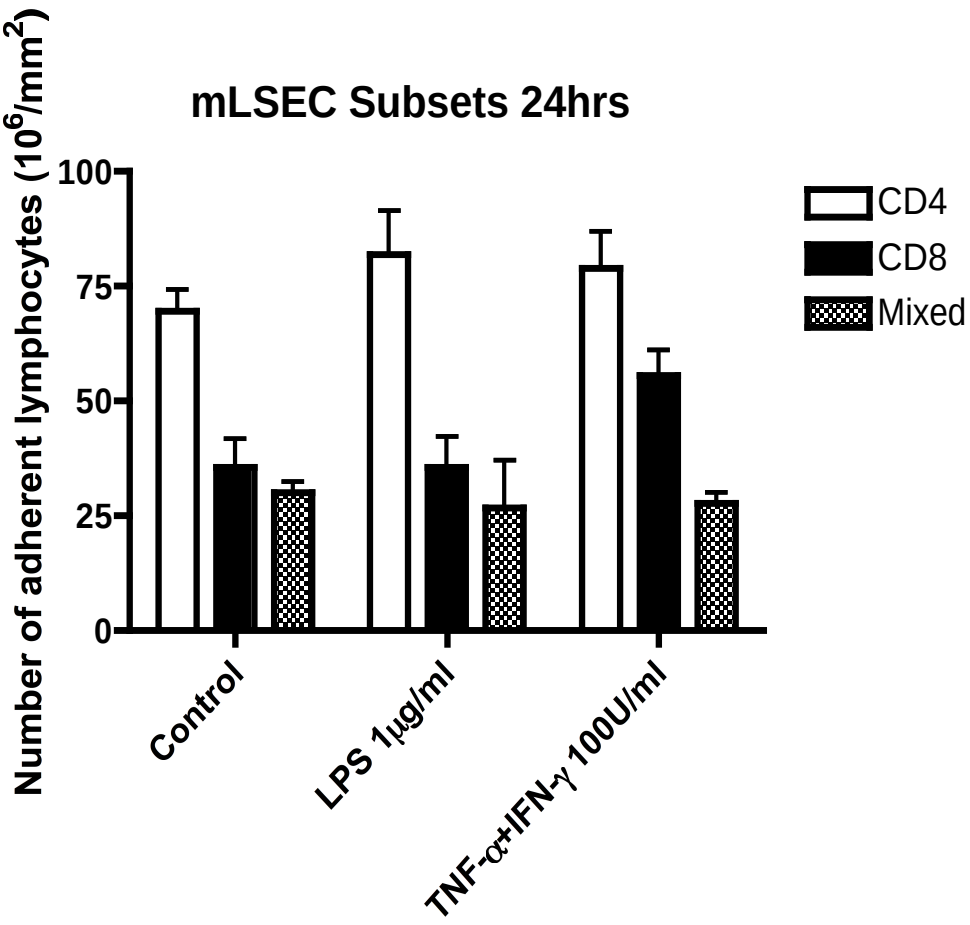
mLSEC Subsets 24hrs
Number of adherent lymphocytes (10^6/mm^2)
100
75
50
25
0
CD4
CD8
Mixed
Control
LPS 1μg/ml
TNF-α+IFN-γ 100U/ml

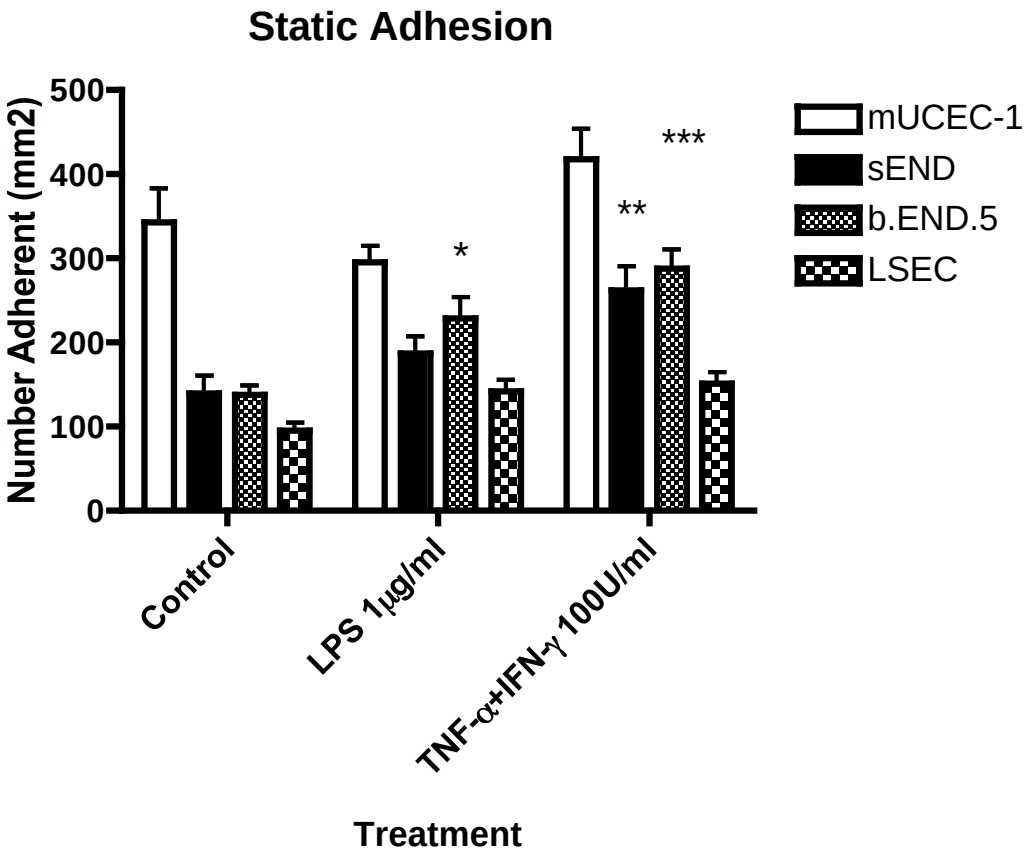
Static Adhesion
Number Adherent (mm2)
500
400
300
200
100
0
*
**
***
mUCEC-1
sEND
b.END.5
LSEC
Control
LPS 1μg/ml
TNF-α+IFN-γ 100U/ml
Treatment

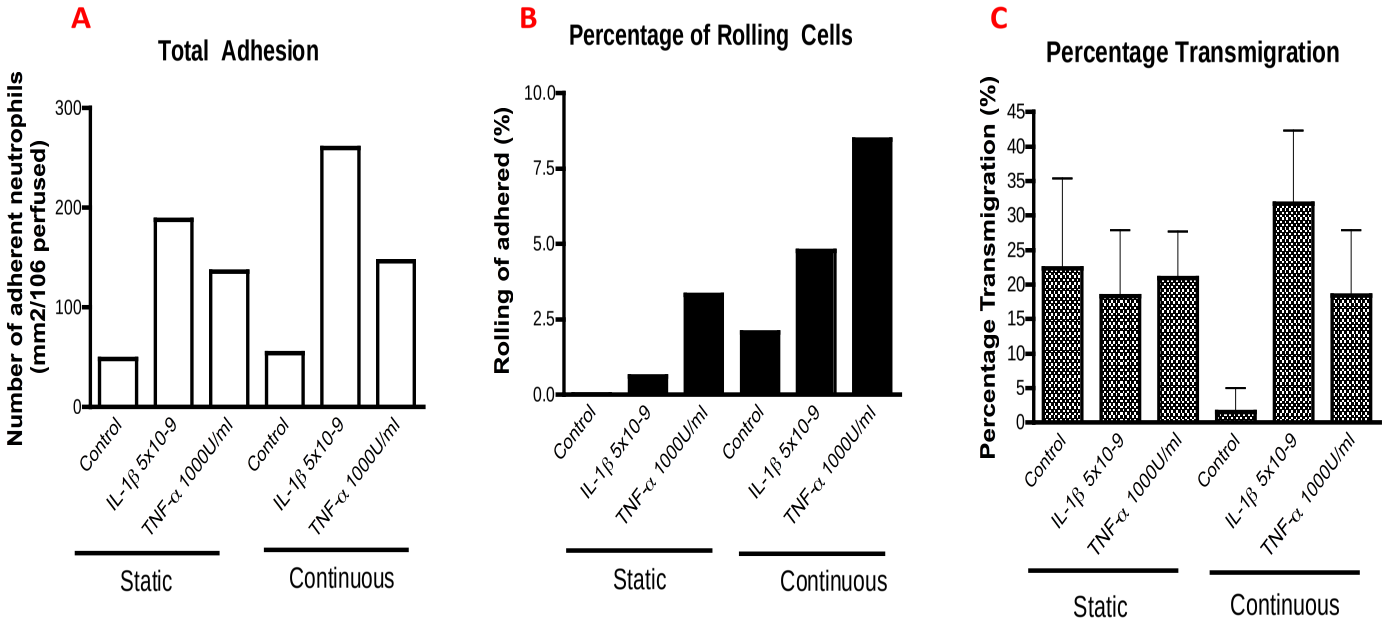
A
Total Adhesion
Number of adherent neutrophils (mm2/106 perfused)
300
200
100
0
Control
IL-1β 5x10-9
TNF-α 1000U/ml
Control
IL-1β 5x10-9
TNF-α 1000U/ml
Static
Continuous
B
Percentage of Rolling Cells
Rolling of adhered (%)
10.0
7.5
5.0
2.5
0.0
Control
IL-1β 5x10-9
TNF-α 1000U/ml
Control
IL-1β 5x10-9
TNF-α 1000U/ml
Static
Continuous
C
Percentage Transmigration
Percentage Transmigration (%)
45
40
35
30
25
20
15
10
5
0
Control
IL-1β 5x10-9
TNF-α 1000U/ml
Control
IL-1β 5x10-9
TNF-α 1000U/ml
Static
Continuous

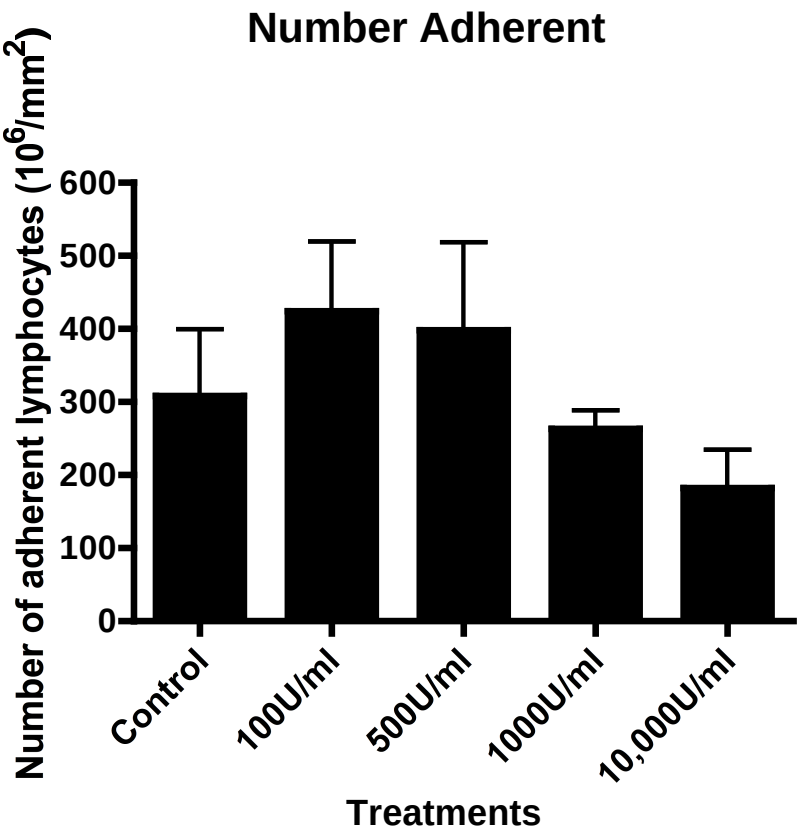
Number Adherent
Number of adherent lymphocytes (10^6/mm^2)
600
500
400
300
200
100
0
Control
100U/ml
500U/ml
1000U/ml
10,000U/ml
Treatments

A

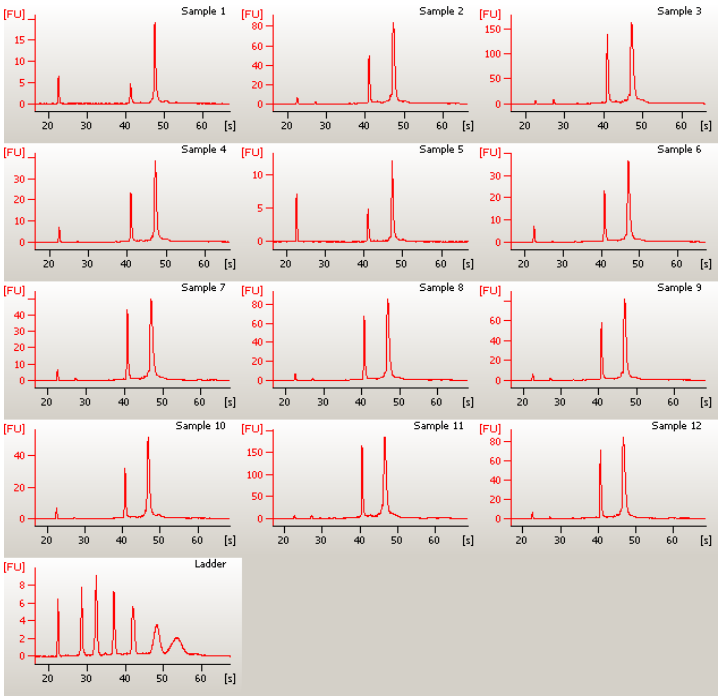

B

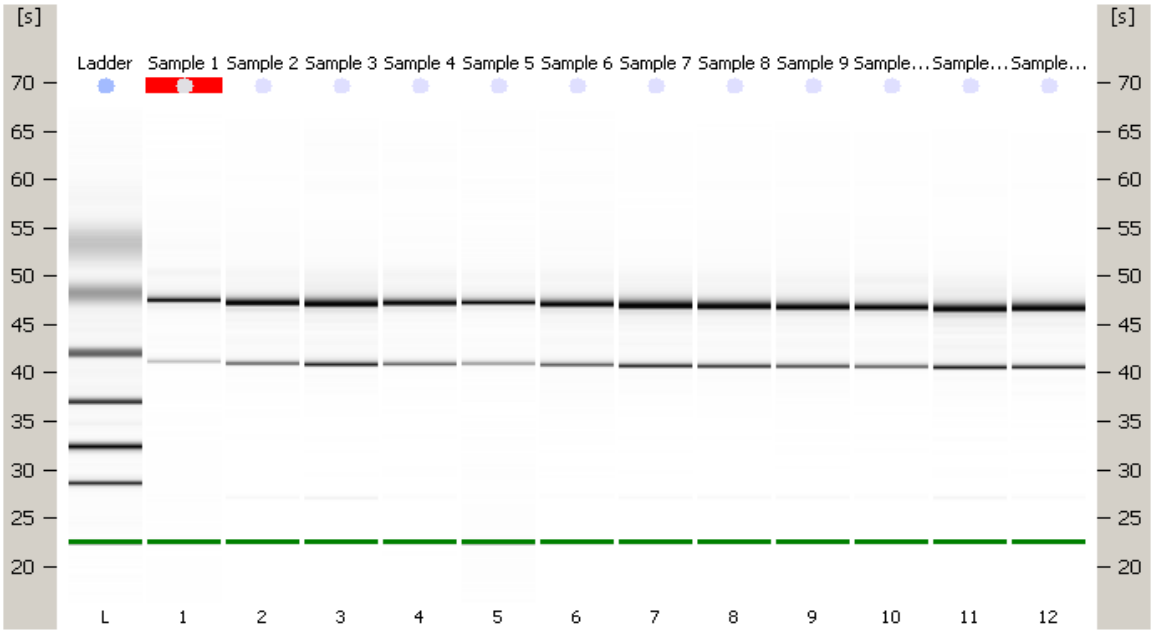

C

Sample Number	RIN Number
1	N/A
2	10
3	10
4	10
5	9.80
6	10
7	10
8	10
9	10
10	10
11	10
12	10

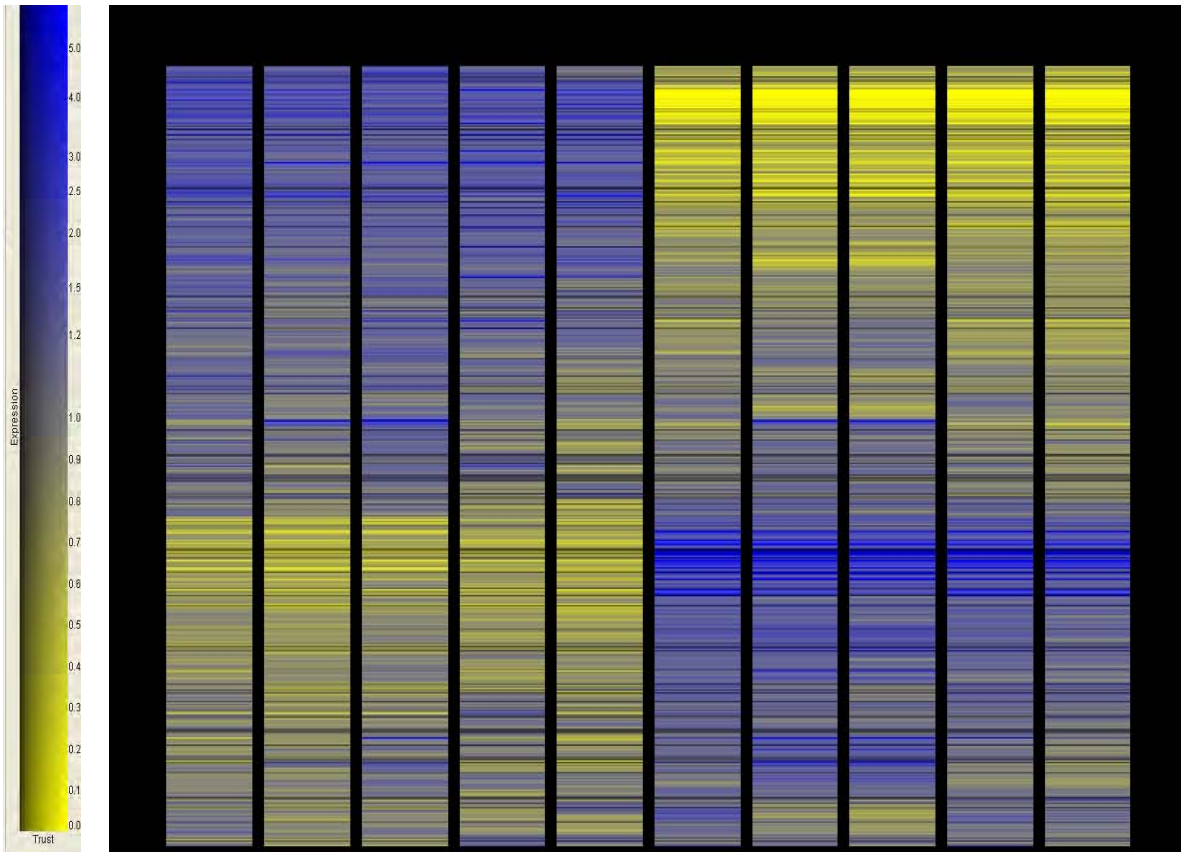
Expression
5.0
4.0
3.0
2.5
2.0
1.5
1.2
1.0
0.9
0.8
0.7
0.6
0.5
0.4
0.3
0.2
0.1
0.0
Trust
Control
IFN-γ
TNF-α + IFN-γ
LPS
TNF-α
Control
IFN-γ
TNF-α + IFN-γ
LPS
TNF-α
mUCEC-1
sEND

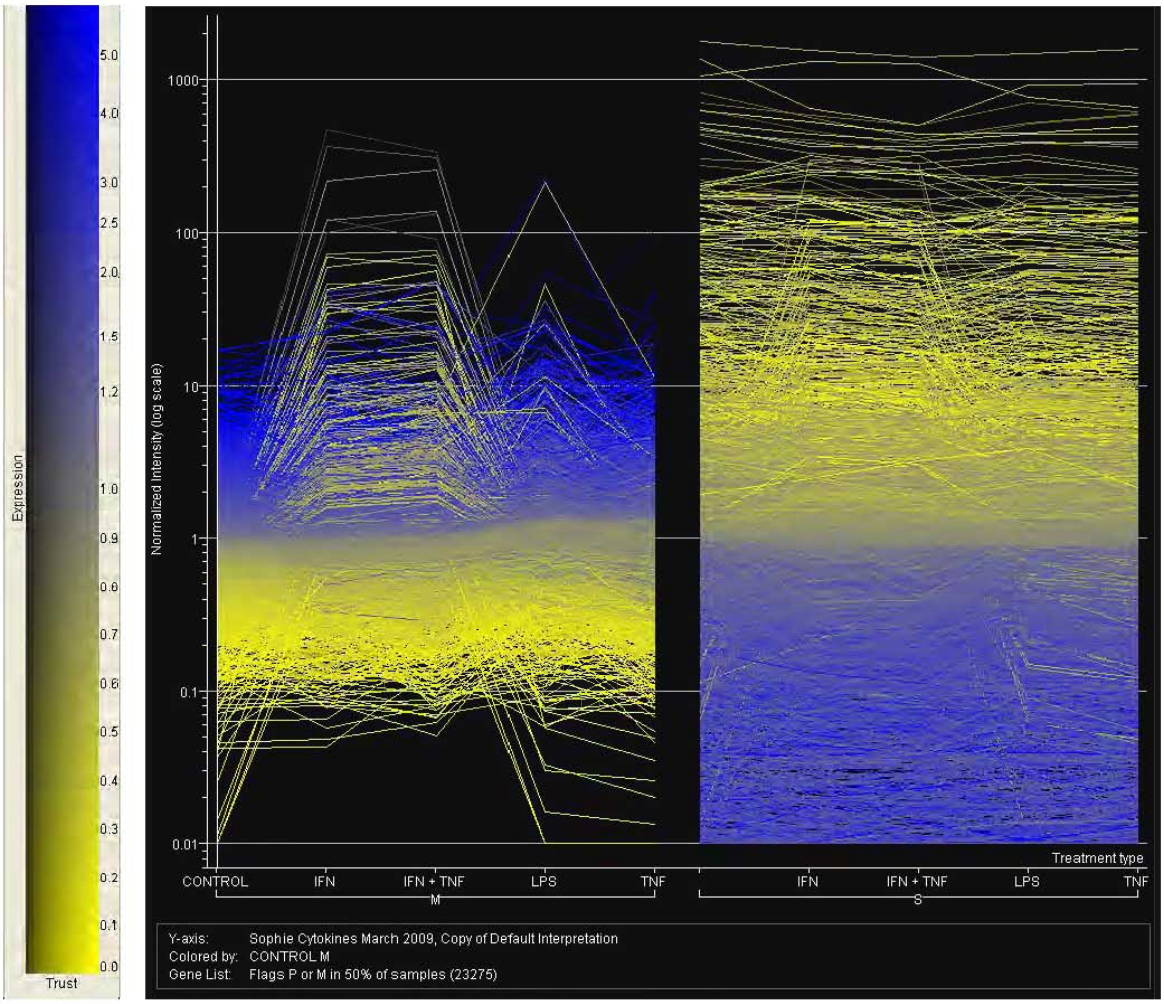
Expression
5.0
4.0
3.0
2.5
2.0
1.5
1.2
1.0
0.9
0.8
0.7
0.6
0.5
0.4
0.3
0.2
0.1
0.0
Trust
Normalized Intensity (log scale)
1000
100
10
1
0.1
0.01
Treatment type
CONTROL
IFN
IFN + TNF
LPS
TNF
IFN
IFN + TNF
LPS
TNF
M
S
Y-axis: Sophie Cytokines March 2009, Copy of Default Interpretation
Colored by: CONTROL M
Gene List: Flags P or M in 50% of samples (23275)

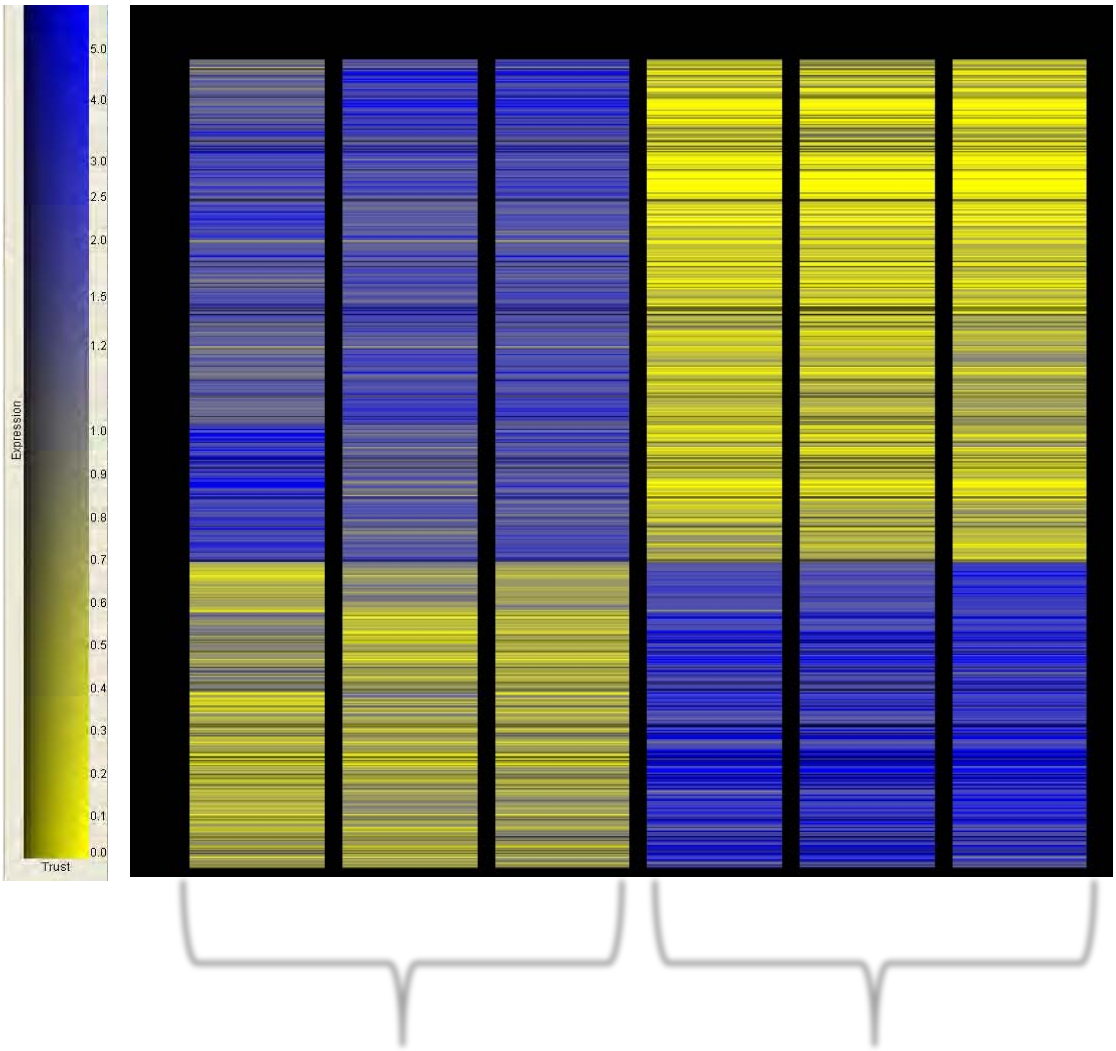
Expression
5.0
4.0
3.0
2.5
2.0
1.5
1.2
1.0
0.9
0.8
0.7
0.6
0.5
0.4
0.3
0.2
0.1
0.0
Trust
mUCEC-1
CONTROL
sEND
CONTROL

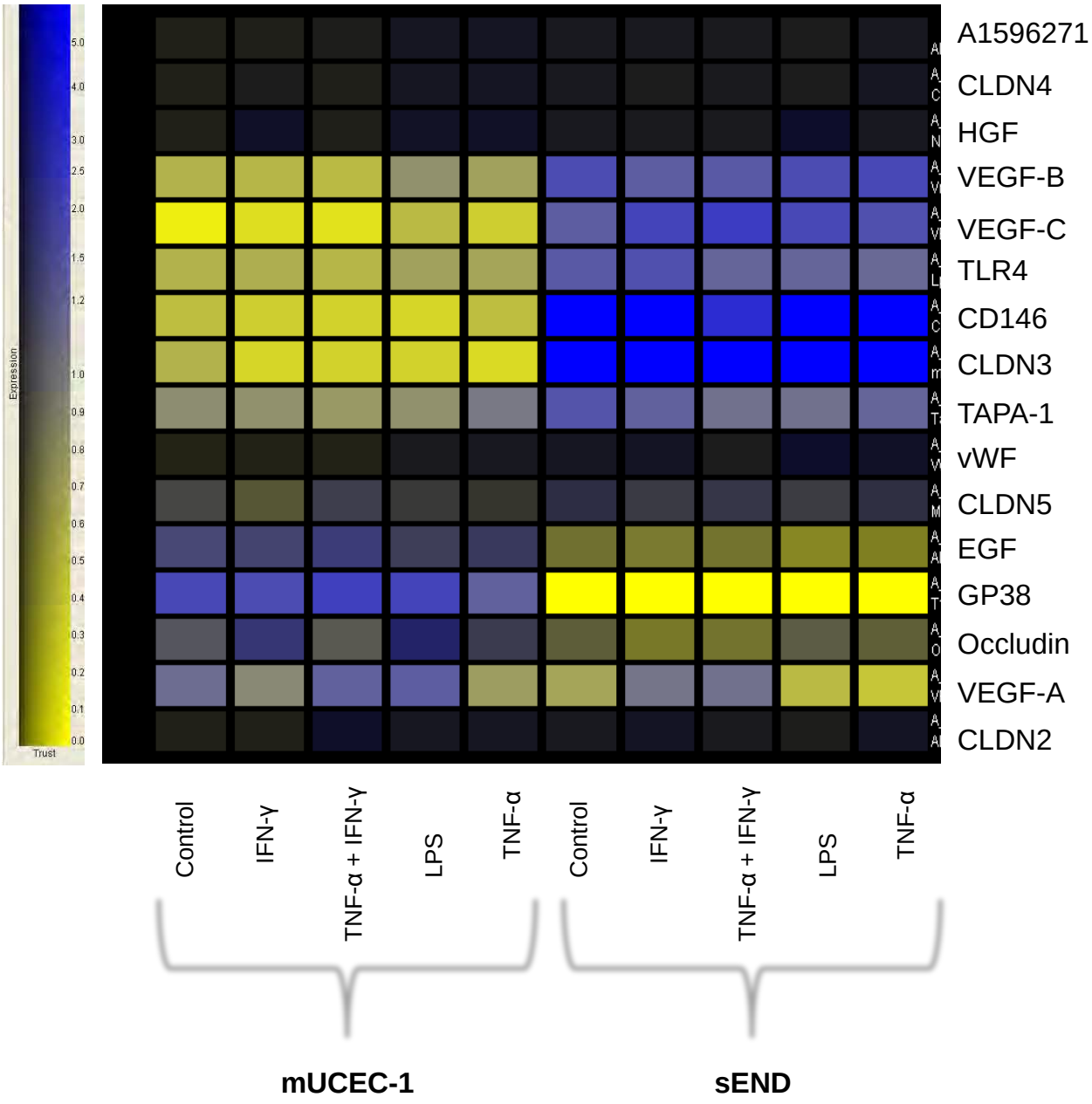
Expression
5.0
4.0
3.0
2.5
2.0
1.5
1.2
1.0
0.9
0.8
0.7
0.6
0.5
0.4
0.3
0.2
0.1
0.0
Trust
A1596271
CLDN4
HGF
VEGF-B
VEGF-C
TLR4
CD146
CLDN3
TAPA-1
vWF
CLDN5
EGF
GP38
Occludin
VEGF-A
CLDN2
Control
IFN-γ
TNF-α + IFN-γ
LPS
TNF-α
Control
IFN-γ
TNF-α + IFN-γ
LPS
TNF-α
mUCEC-1
sEND

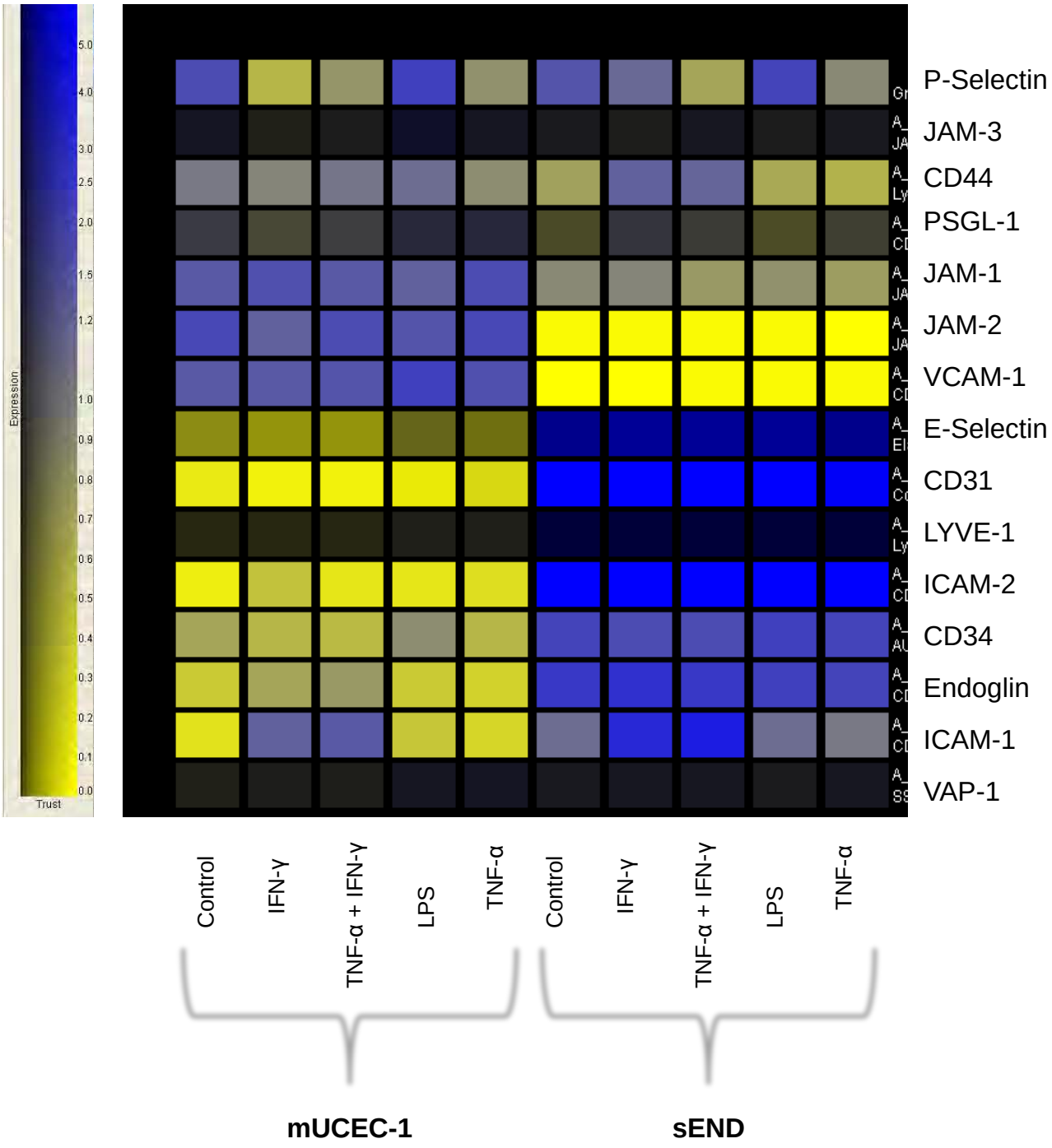
Expression
5.0
4.0
3.0
2.5
2.0
1.5
1.2
1.0
0.9
0.8
0.7
0.6
0.5
0.4
0.3
0.2
0.1
0.0
Trust
P-Selectin
JAM-3
CD44
PSGL-1
JAM-1
JAM-2
VCAM-1
E-Selectin
CD31
LYVE-1
ICAM-2
CD34
Endoglin
ICAM-1
VAP-1
Control
IFN-γ
TNF-α + IFN-γ
LPS
TNF-α
Control
IFN-γ
TNF-α + IFN-γ
LPS
TNF-α
mUCEC-1
sEND

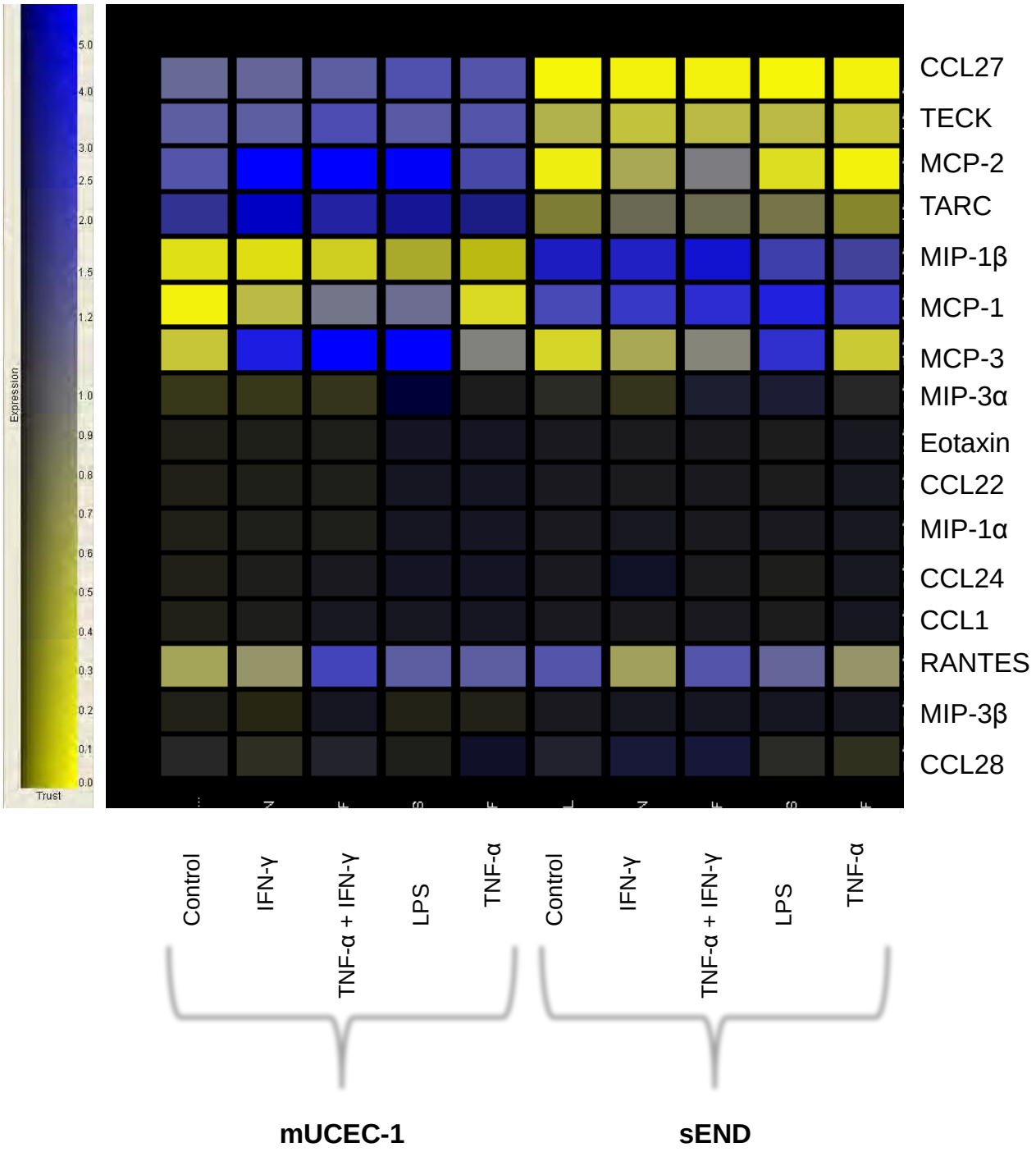
Expression
Trust
5.0
4.0
3.0
2.5
2.0
1.5
1.2
1.0
0.9
0.8
0.7
0.6
0.5
0.4
0.3
0.2
0.1
0.0
CCL27
TECK
MCP-2
TARC
MIP-1β
MCP-1
MCP-3
MIP-3α
Eotaxin
CCL22
MIP-1α
CCL24
CCL1
RANTES
MIP-3β
CCL28
Control
IFN-γ
TNF-α + IFN-γ
LPS
TNF-α
Control
IFN-γ
TNF-α + IFN-γ
LPS
TNF-α
mUCEC-1
sEND

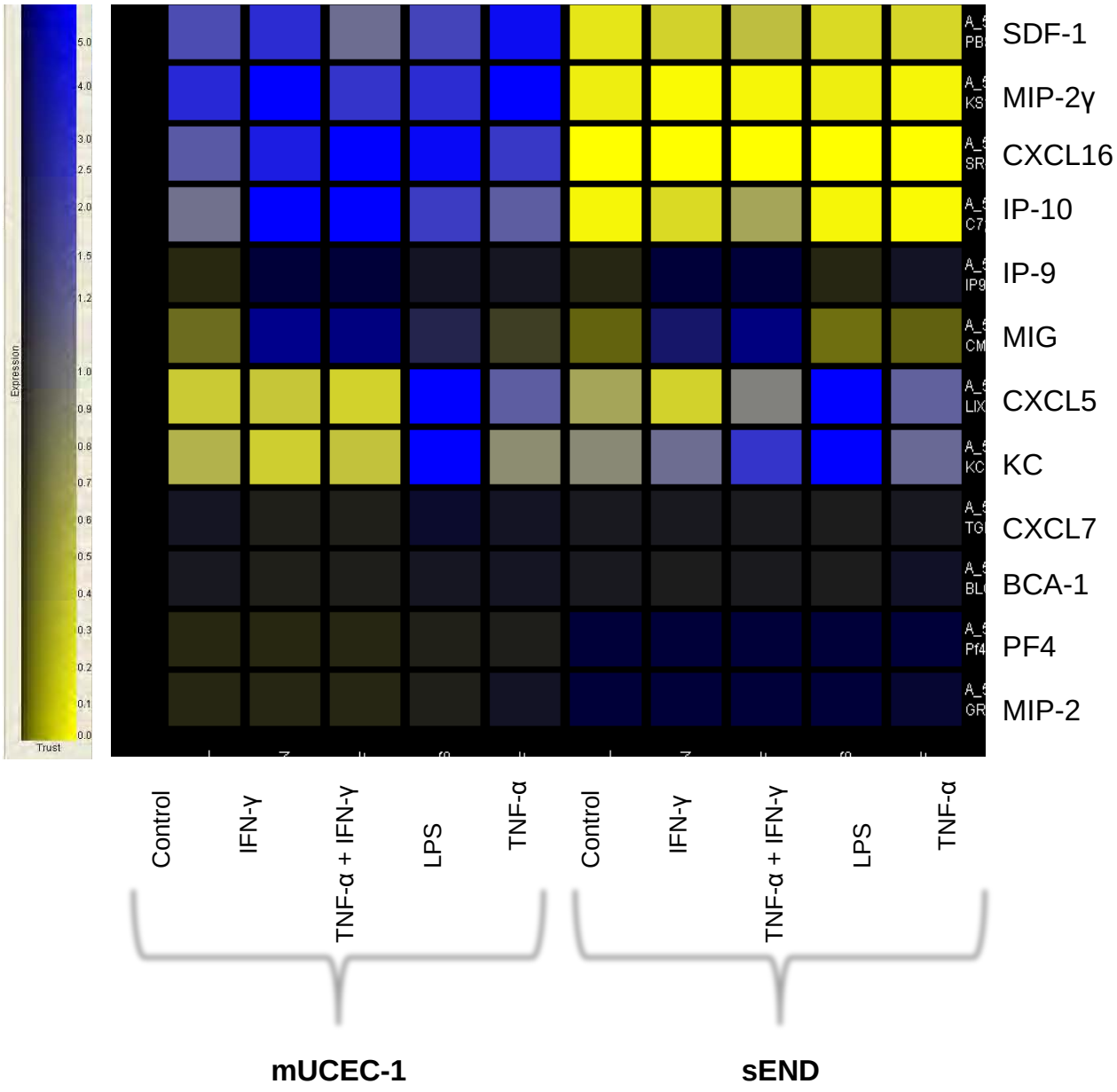
Expression
5.0
4.0
3.0
2.5
2.0
1.5
1.2
1.0
0.9
0.8
0.7
0.6
0.5
0.4
0.3
0.2
0.1
0.0
Trust
SDF-1
MIP-2γ
CXCL16
IP-10
IP-9
MIG
CXCL5
KC
CXCL7
BCA-1
PF4
MIP-2
Control
IFN-γ
TNF-α + IFN-γ
LPS
TNF-α
Control
IFN-γ
TNF-α + IFN-γ
LPS
TNF-α
mUCEC-1
sEND

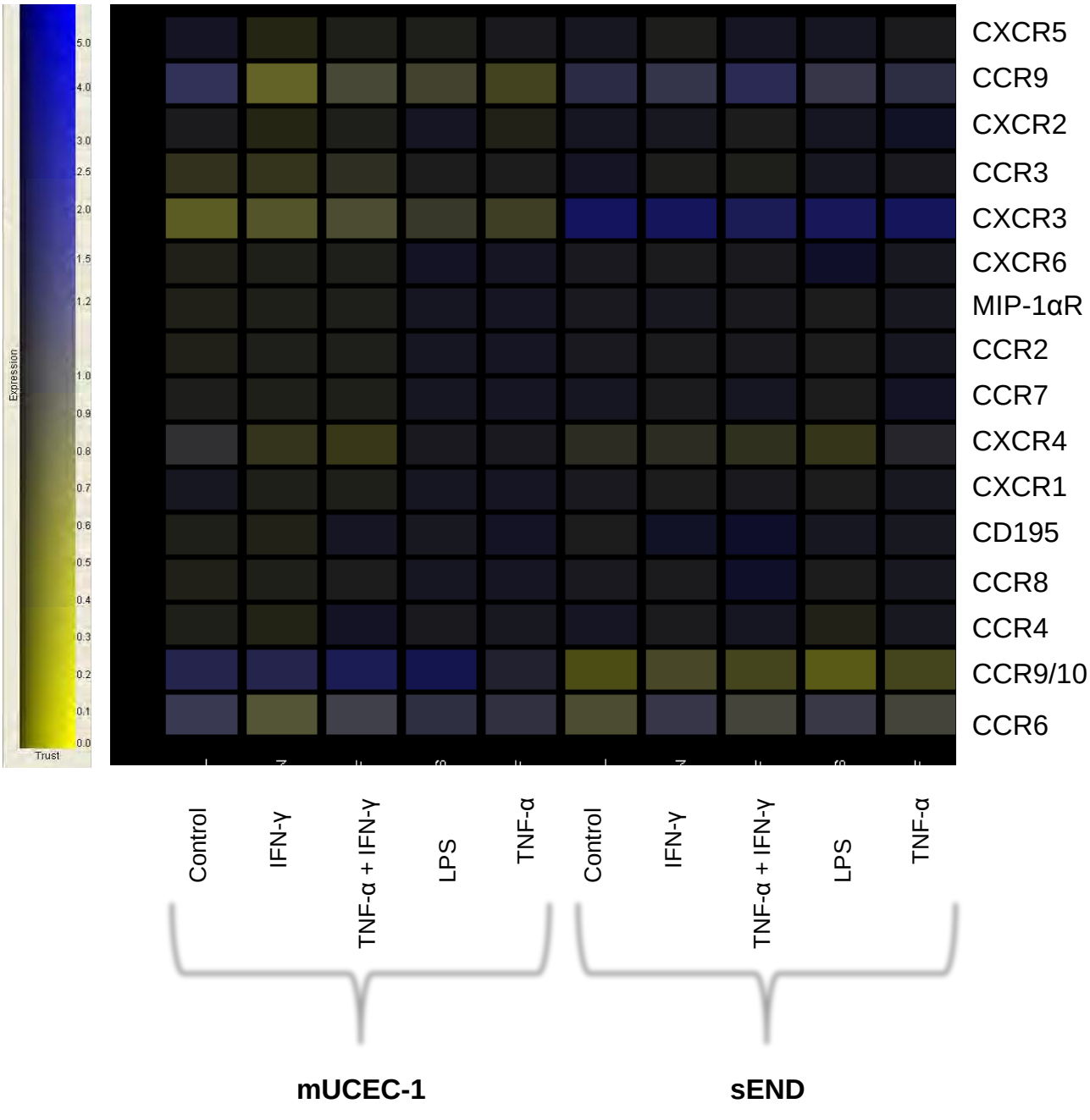
Expression
5.0
4.0
3.0
2.5
2.0
1.5
1.2
1.0
0.9
0.8
0.7
0.6
0.5
0.4
0.3
0.2
0.1
0.0
Trust
CXCR5
CCR9
CXCR2
CCR3
CXCR3
CXCR6
MIP-1αR
CCR2
CCR7
CXCR4
CXCR1
CD195
CCR8
CCR4
CCR9/10
CCR6
Control
IFN-γ
TNF-α + IFN-γ
LPS
TNF-α
Control
IFN-γ
TNF-α + IFN-γ
LPS
TNF-α
mUCEC-1
sEND

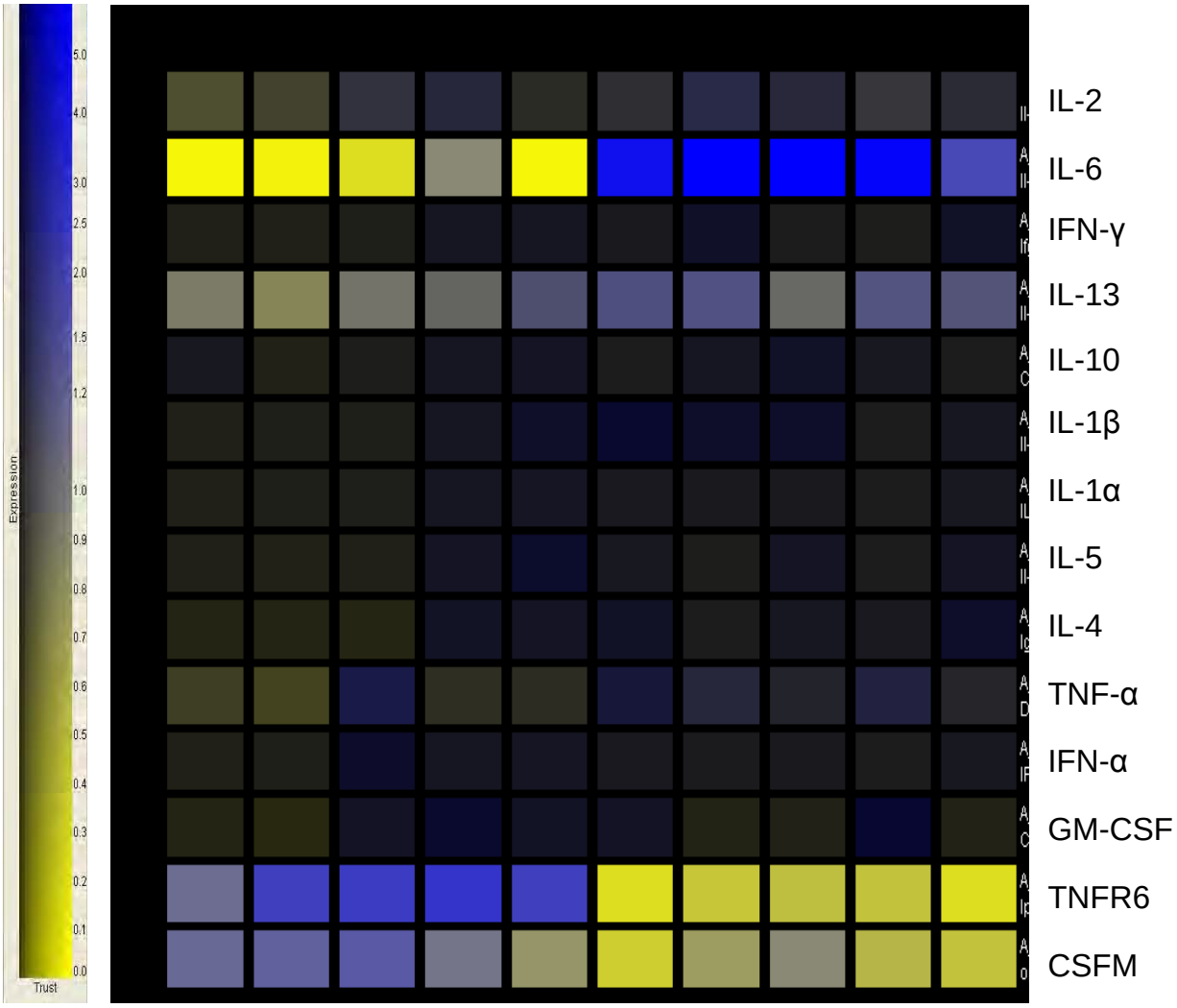
Expression
5.0
4.0
3.0
2.5
2.0
1.5
1.2
1.0
0.9
0.8
0.7
0.6
0.5
0.4
0.3
0.2
0.1
0.0
Trust
IL-2
IL-6
IFN-γ
IL-13
IL-10
IL-1β
IL-1α
IL-5
IL-4
TNF-α
IFN-α
GM-CSF
TNFR6
CSFM
Control
IFN-γ
TNF-α + IFN-γ
LPS
TNF-α
Control
IFN-γ
TNF-α + IFN-γ
LPS
TNF-α
mUCEC-1
sEND

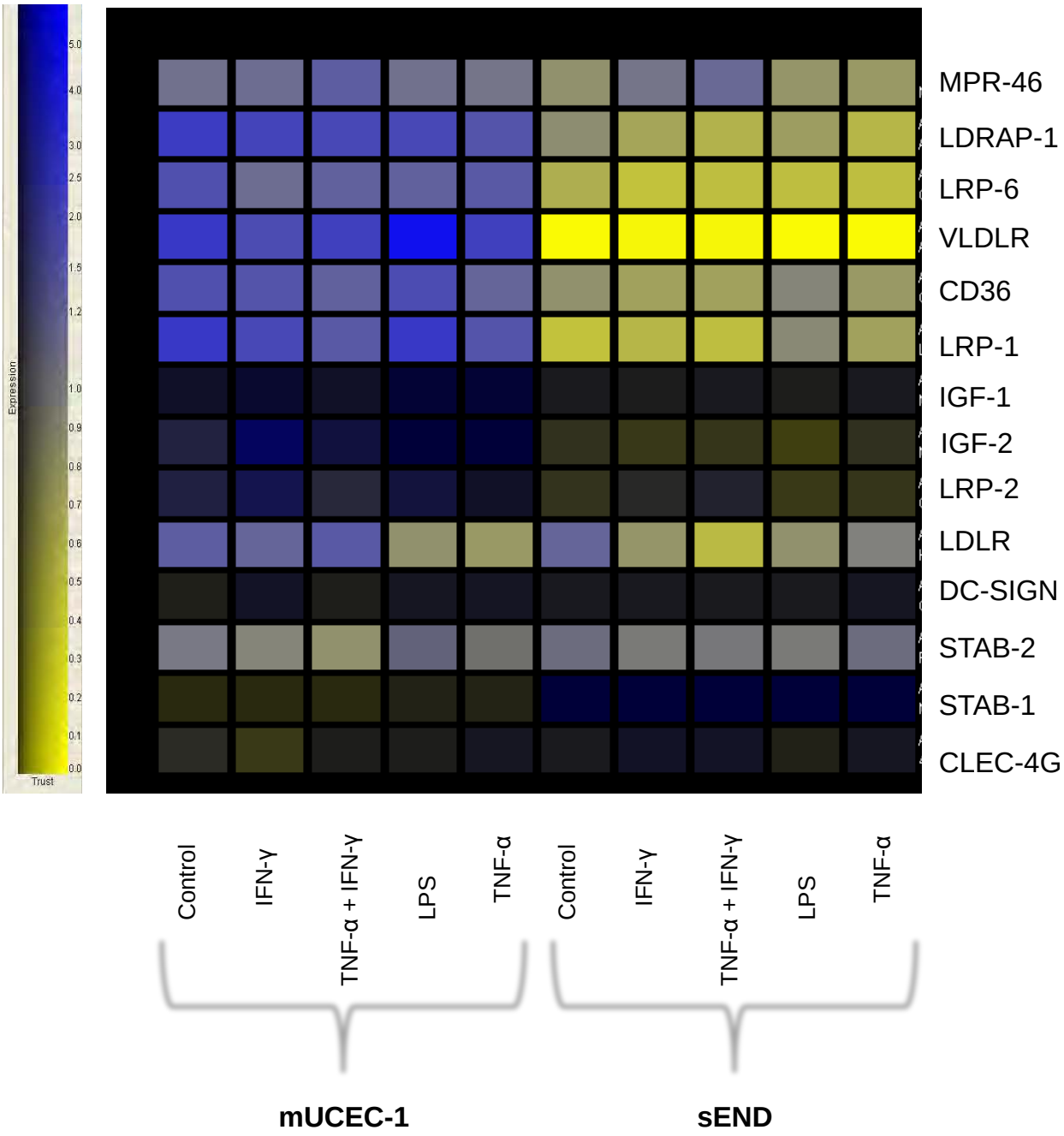
Expression
5.0
4.0
3.0
2.5
2.0
1.5
1.2
1.0
0.9
0.8
0.7
0.6
0.5
0.4
0.3
0.2
0.1
0.0
Trust
MPR-46
LDRAP-1
LRP-6
VLDLR
CD36
LRP-1
IGF-1
IGF-2
LRP-2
LDLR
DC-SIGN
STAB-2
STAB-1
CLEC-4G
Control
IFN-γ
TNF-α + IFN-γ
LPS
TNF-α
Control
IFN-γ
TNF-α + IFN-γ
LPS
TNF-α
mUCEC-1
sEND

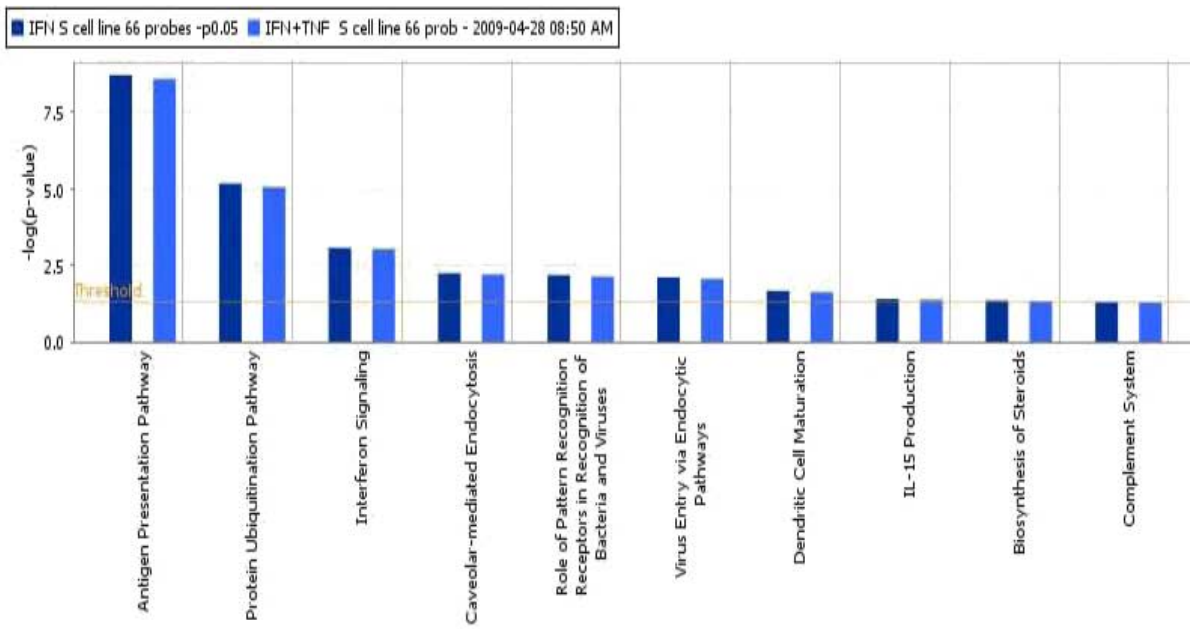

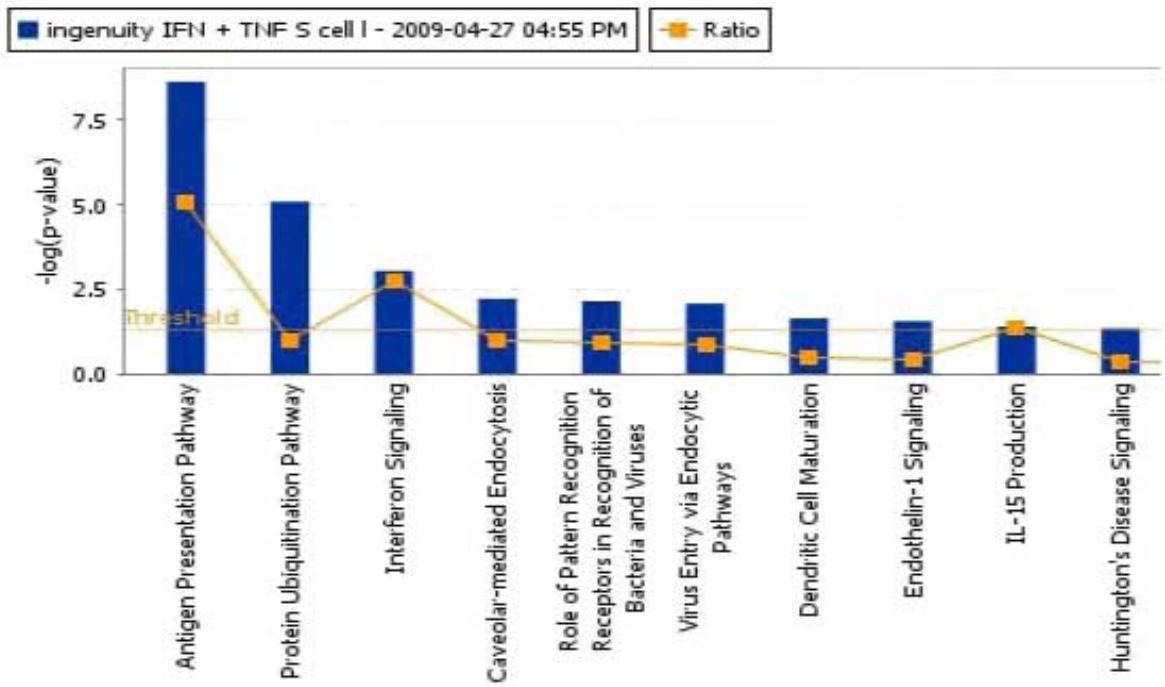

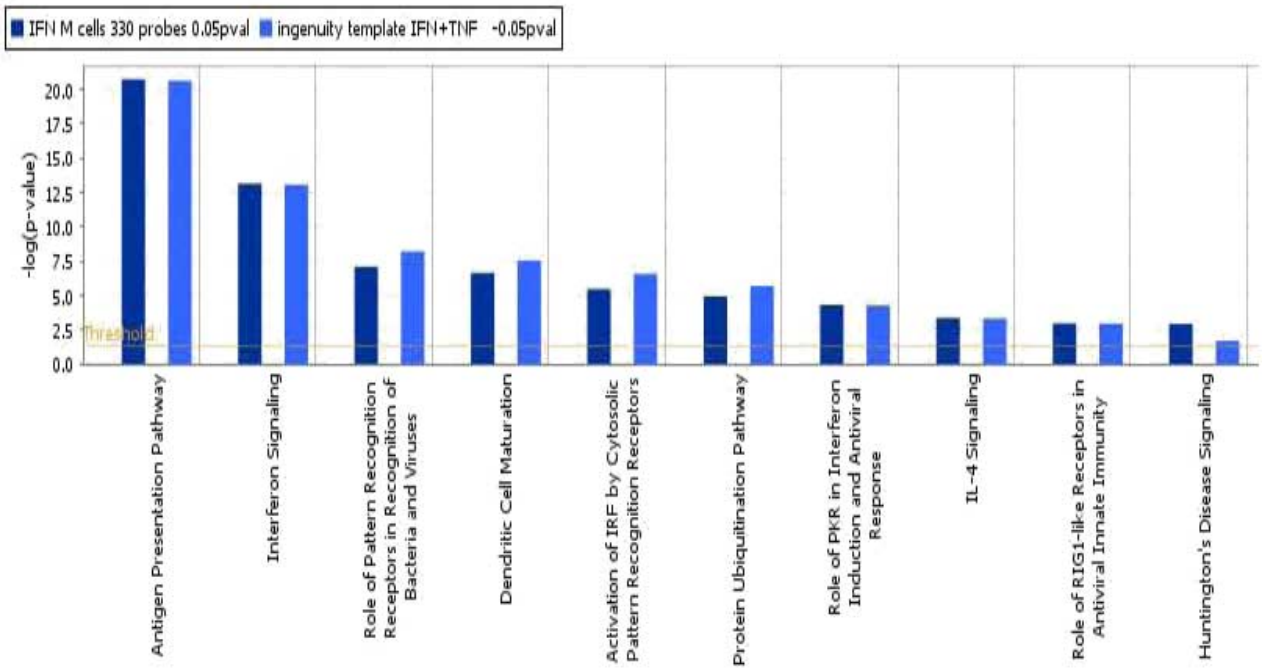

Analysis: ingenuity IFN + TNF M cell l - 2009-04-27 03:58 PM

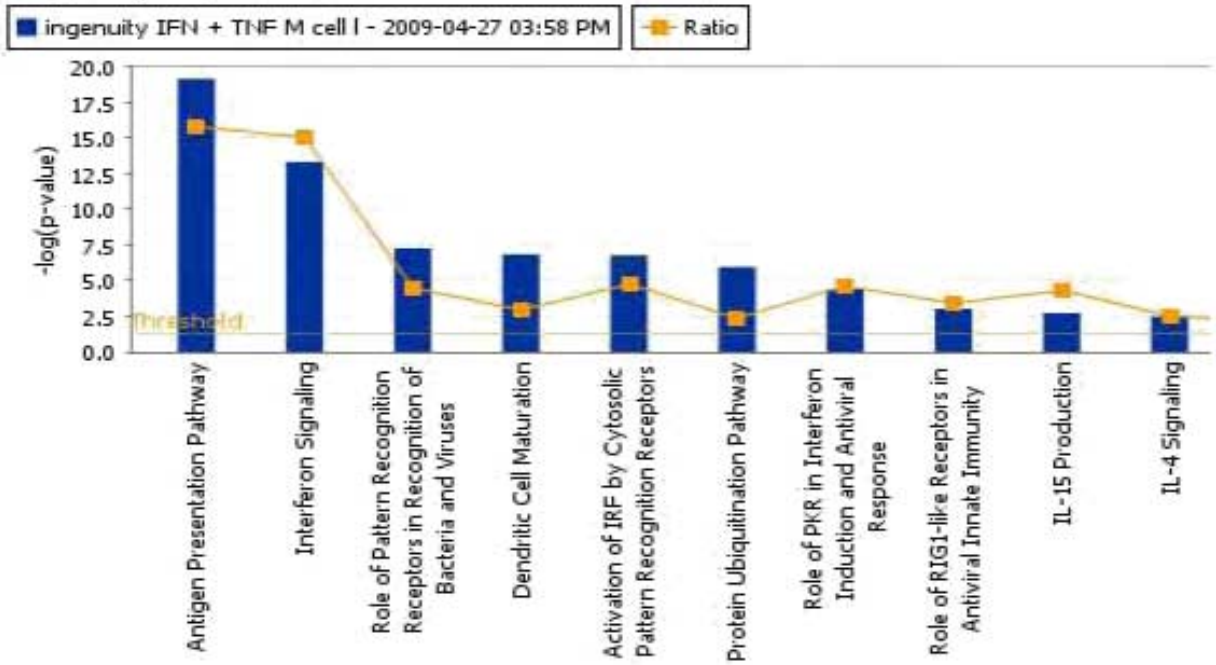

				ARRAY	RT-PCR	ARRAY	RT-PCR	ARRAY	RT-PCR
GenBank ID	Full Name	QT Primer	Common Name	IFN		TNF		TNF&IFN	
NM_009735	beta-2 microglobulin (B2m)	QT01149547	B2m	3.03	5.20	1.37	1.50	3.09	5.30
NM_008330	interferon gamma inducible protein 47 (Ifi47)	QT00116935	Ifi47	22.26	42.20	1.23	1.40	22.01	41.30
NM_008390	interferon regulatory factor 1 (Irf1)	QT00128989	Irf1	14.29	17.96	1.55	-1.20	18.63	21.60
NM_007955	protein tyrosine phosphatase, receptor type, V (Ptprv)	QT01070930	Ptprv	-2.99	-2.60	-1.26	1.30	-3.16	-2.50
NM_007393	actin, beta, cytoplasmic (Actb)	QT01136772	Actb	-1.01	1.00	-1.00	1.00	1.27	1.00
NM_009896	suppressor of cytokine signaling 1 (Socs1)	QT01059268	Socs1	20.09	891.40	1.24	30.60	21.28	691.40
NM_022032	PERP, TP53 apoptosis effector (Perp)	QT01065246	Perp	-2.11	-3.20	-1.47	-1.80	-1.74	-1.70
NM_001039647	similar to macrophage activation 2 (LOC634650)	QT01255142	LOC634650	114.10	119.40	-2.82	-1.60	152.60	42.20
NM_007669	cyclin-dependent kinase inhibitor 1A (P21) (Cdkn1a)	QT00137053	Cdkn1a	-2.56	-2.10	-1.31	-0.60	-1.76	-1.60
NM_021274	chemokine (C-X-C motif) ligand 10 (Cxcl10)	QT00093436	Cxcl10	17.54	35.90	1.25	-1.20	20.55	26.00
NM_009425	tumor necrosis factor (ligand) superfamily, member 10 (Tnfsf10)	QT00102970	Tnfsf10	57.66	54.40	2.50	1.50	48.56	37.60
NM_008620	macrophage activation 2 (Mpa2)	QT00174608	Mpa2	1075.00	2298.80	0.88	0.70	1416.00	1552.00
NM_017466	chemokine (C-C motif) receptor-like 2 (Ccrl2)	QT01040179	Ccrl2	11.13	14.60	1.26	1.60	16.78	23.70
NM_009283	signal transducer and activator of transcription 1 (Stat1)	QT01149519	Stat1	5.56	5.80	1.06	-1.50	5.66	5.70
NM_010531	interleukin 18 binding protein (Il18bp)	QT00257663	Il18bp	89.28	64.00	1.61	-1.00	95.16	62.60

				ARRAY	RT-PCR	ARRAY	RT-PCR	ARRAY	RT-PCR
GenBank ID	Full Name	QT Primer	Common Name	IFN		TNF		TNF&IFN	
NM_009735	beta-2 microglobulin (B2m)	QT01149547	B2m	2.588	3.1	-1.17096	1.3	2.443	2.7
NM_008330	interferon gamma inducible protein 47 (Ifi47)	QT00116935	Ifi47	12.44	12.7	-1.48148	-1.1	14.56	12.4
NM_008390	interferon regulatory factor 1 (Irf1)	QT00128989	Irf1	15.85	12.2	-1.07411	-1.6	16.67	16.4
NM_007955	protein tyrosine phosphatase, receptor type, V (Ptprv)	QT01070930	Ptprv	-1.644737	-3.2	-1.07527	-2	-1.61031	-1.5
NM_007393	actin, beta, cytoplasmic (Actb)	QT01136772	Actb	1.019	1	-1.0142	1	-1.19617	1
NM_009896	suppressor of cytokine signaling 1 (Socs1)	QT01059268	Socs1	11.04	7.5	-1.11359	-1.4	12.1	7.3
NM_022032	PERP, TP53 apoptosis effector (Perp)	QT01065246	Perp						
NM_001039647	similar to macrophage activation 2 (LOC634650)	QT01255142	LOC634650	333	280.8	-1.65289	3	273	330
NM_007669	cyclin-dependent kinase inhibitor 1A (P21) (Cdkn1a)	QT00137053	Cdkn1a	1.135	1	-1.37174	7.5	1.077	-1
NM_021274	chemokine (C-X-C motif) ligand 10 (Cxcl10)	QT00093436	Cxcl10	5.682	4.5	-1.38313	2.1	14.5	9.6
NM_009425	tumor necrosis factor (ligand) superfamily, member 10 (Tnfsf10)	QT00102970	Tnfsf10	7.158	7	-1.14679	-1.1	9.269	6.2
NM_008620	macrophage activation 2 (Mpa2)	QT00174608	Mpa2	73.24	88.4	-1.44509	1.1	67.94	65.5
NM_017466	chemokine (C-C motif) receptor-like 2 (Ccrl2)	QT01040179	Ccrl2	8.398	12.1	-1.63132	-1.6	9.492	10.3
NM_009283	signal transducer and activator of transcription 1 (Stat1)	QT01149519	Stat1	4.091	4	-1.25471	1.3	4.269	3.4
NM_010531	interleukin 18 binding protein (Il18bp)	QT00257663	Il18bp	37.08	40.3	-1.76678	1.2	34.72	35.1

Normal Whole liver specimens

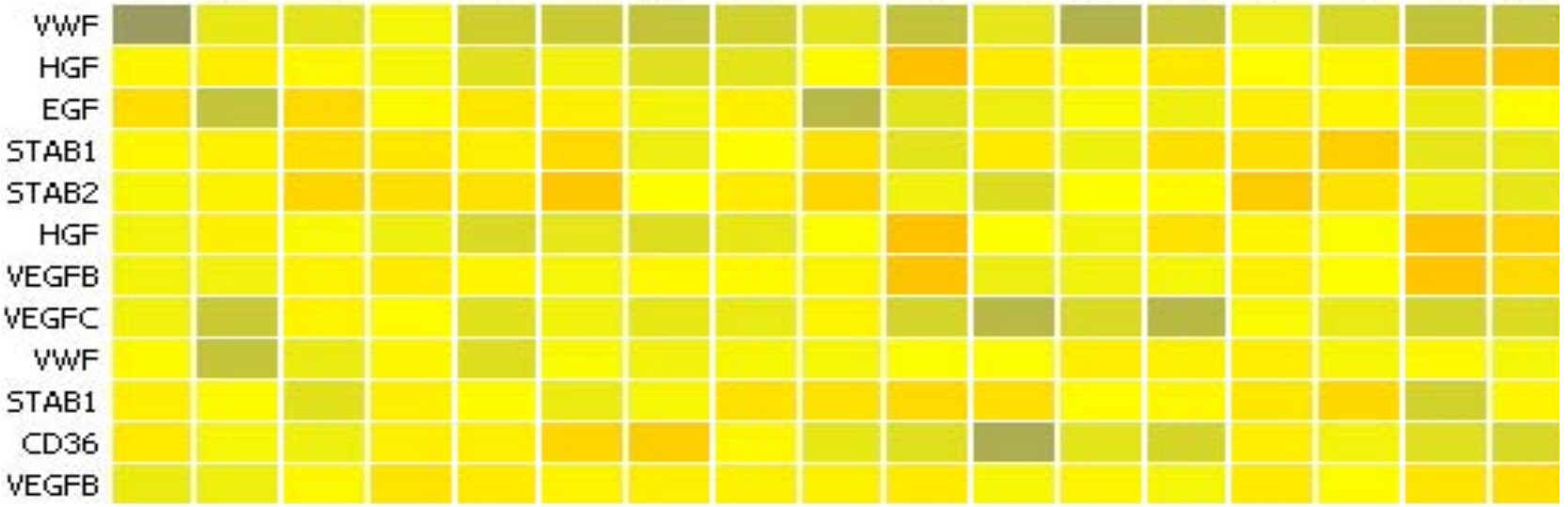

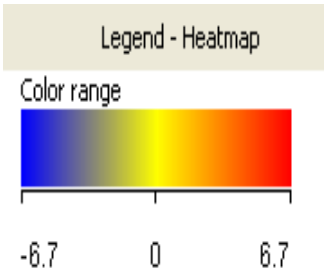

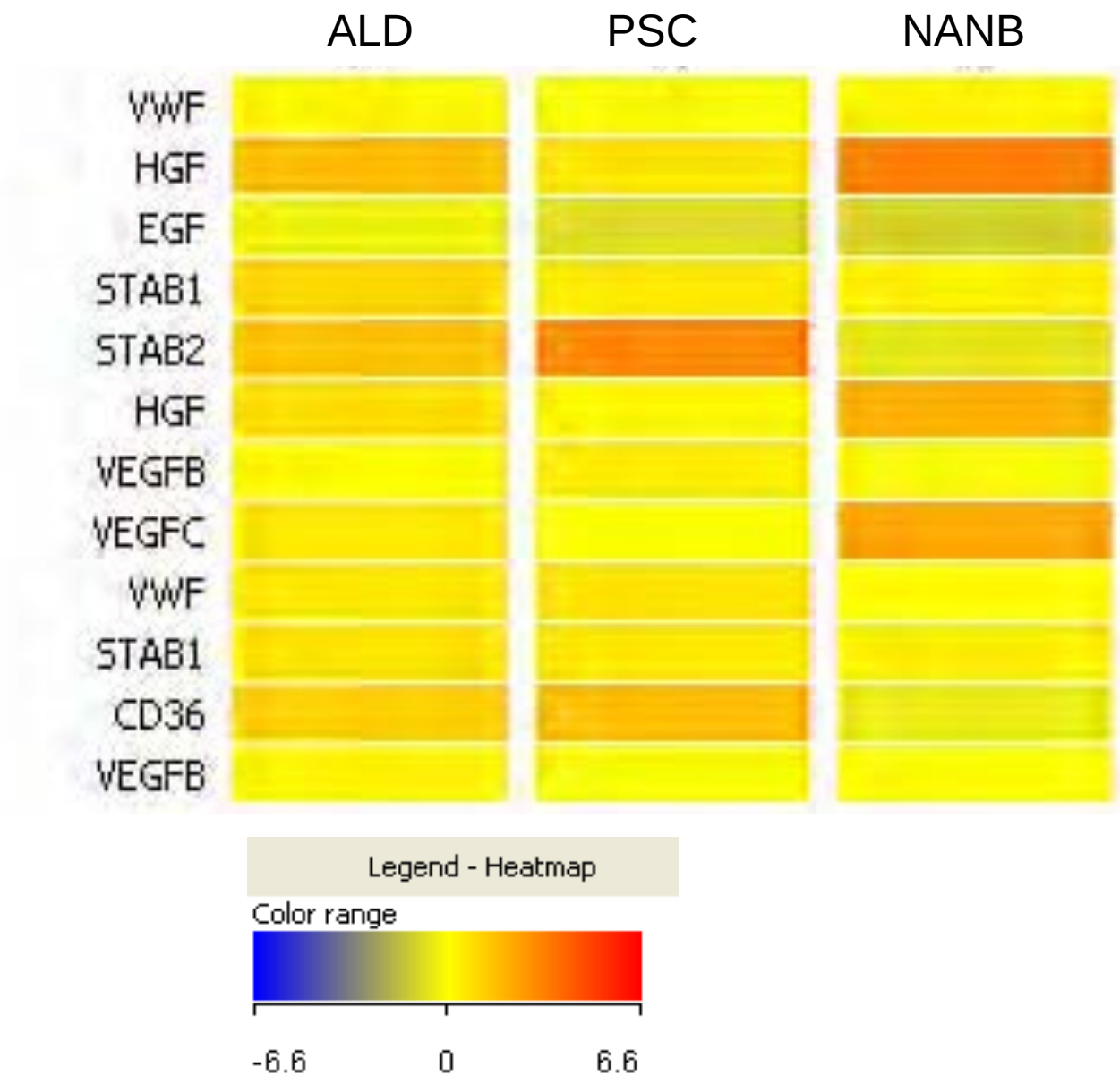
ALD
PSC
NANB
VWF
HGF
EGF
STAB1
STAB2
HGF
VEGFB
VEGFC
VWF
STAB1
CD36
VEGFB
Legend - Heatmap
Color range
-6.6
0
6.6